TLR4 SIGNALING MODULATES LIPOLYSIS IN DAIRY COWS' ADIPOSE TISSUES

By

Miguel Leonardo Chirivi

A DISSERTATION

Submitted to
Michigan State University
in partial fulfillment of the requirements
for the degree of

Comparative Medicine and Integrative Biology – Doctor of Philosophy

2023

ABSTRACT

Excessive lipolysis from adipose tissue (AT) is considered a major risk factor of postpartum metabolic disease in dairy cows. Among those, clinical ketosis occurs when dysregulated lipolysis provides abundant fatty acids for ketone body synthesis. Since excessive and protracted lipolysis increases the risk for disease, limiting lipolysis becomes crucial to mitigate excessive fat mobilization and consequently disease risk. However, the mechanisms behind AT dysregulated lipolysis and how to inhibit it are not fully understood. Additionally, periparturient dairy cows often present inflammatory conditions such as coliform mastitis, metritis, pneumonia, and leaky gut, which result in circulating free endotoxin. Endotoxins, which are the outer component of gram-negative bacteria, can activate TLR4 in cells. Once TLR4 is activated, it leads to various effects including cytokine production, increased metabolic stress, and altered cellular metabolism. However, there is a lack of comprehensive understanding regarding the effects of endotoxins on AT in dairy cows. This work proposes that endotoxin plays a determinant role during the development of metabolic and inflammatory/infectious comorbidities around parturition through the exacerbation of lipolytic responses in AT and reduction of insulin sensitivity. Although some studies have examined the impact of endotoxemia on the metabolism of lipids, the molecular mechanisms underlying the interactions between endotoxins and AT remain poorly characterized. To address this gap, we first studied clinical ketosis, the most representative disease during AT lipolysis dysregulation. We found that cows with clinical ketosis had elevated plasma endotoxin and inflammatory markers. A randomized clinical trial was conducted to investigate the effectiveness of niacin and flunixin as inhibitors of lipolysis during clinical ketosis. Furthermore, given that the physiological role of AT is not fully understood during ketosis, we evaluated the AT function, and we characterize the AT macrophage phenotype

involved in CK. We identified that endotoxins and inflammation were playing a determinant role during clinical ketosis and its recovery. Therefore, we developed an ex vivo model of AT inflammation to determine how endotoxins influence lipolytic and inflammatory markers. We found that endotoxin LPS triggers lipolysis and insulin resistance in AT from non-lactating and postpartum dairy cows. Among the pathways involved ERK1/2 was observed as a mediator of activation of lipases HLS and ATGL. To further characterize endotoxin-induced lipolysis, an in vitro cell culture model was developed to assess the mechanisms behind lipolysis in bovine adipocytes exposed to LPS. In our bovine adipocyte inflammation model, endotoxin depends upon the presence of TLR4 to activate lipolysis and inflammation. Adipocytes were also treated with lipolysis inhibitors niacin and flunixin meglumine and then exposed to endotoxin. Flunixin meglumine inhibits lipolysis in adipocytes and improves insulin sensitivity. This work suggests that inflammation is involved in lipolysis dysregulation in dairy cows with clinical ketosis. Our data also provides evidence for the novel therapy for inhibiting lipolysis with faster hyperketonemia recovery, lower lipolytic rates and reduced inflammation. Hence, treating cows with flunixin meglumine reduces inflammation and improves AT function during clinical ketosis. Additionally, our data suggests that TLR4 is mediating lipolysis and inflammation in bovine adipocytes. Therefore, if endotoxins are involved in lipolysis dysregulation, it is important to acknowledge the potential impact of endotoxin on metabolic diseases in dairy cows. Establishing the relationship between low-grade endotoxemia and AT effects, both in the short and long term, should be the focus of future studies. Moreover, future work should be based on further characterizing the mechanisms by which TLR4 activation impacts other adipose tissue functions, such as lipid accumulation.

I would like to dedicate this dissertation to my beloved parents Patricia and German who taught me perseverance, kindness, and gratitude in my life. To my adored siblings Catalina, David and Jeronimo. It is dedicated to my inamorata Susana who never faltered in her support. It is also dedicated to my mentor Dr. Andres Contreras, who provided me with the best guidance throughout my entire educational journey. Finally, to my family and friends, who from a distance carried me in their prayers. Thank you.

ACKNOWLEDGEMENTS

I would like to acknowledge the amazing people I was lucky enough to be mentored by. During my DVM, Dr. Claudia Jimenez saw in me the potential for higher goals in my life. Dr. Andres Contreras mentored me through my Ph.D. program with wisdom and helped me growth in confidence as a scientist. I give many thanks to my other guidance committee members: Dr. Adam Lock, Dr. Adam Moeser and Dr. Daniel Langlois. I would also like to thank the leaders of the Comparative Medicine and Integrative Biology program at Michigan State University, especially Dr. Hegg Colleen for their continued support and hard work. I would like to thank the following entities for supporting this work: the USDA-National Institute of Food and Agriculture (Washington, DC; competitive grant 2019-67015-29443 and 2021-67015-34563), Michigan Alliance for Animal Agriculture award (East Lansing, MI; Awards AA18–003, AA 21-154, AA 22-055), Department of Large Animal Clinical Sciences (East Lansing, MI), Office of the Associate Dean for Research and Graduate Studies of the College of Veterinary Medicine (East Lansing, MI), the College of Veterinary Medicine Endowed Research Funds 2020 (East Lansing, MI). Graduate Office Fellowship (GOF) Spring 2023. Michigan State University. Dissertation Completion Fellowship Summer 2023. Michigan State University Thank you to Applegate Dairy Farm and staff for allowing access to their animals and facilities where part of this research was conducted. Thank you to the staff at the Michigan State University Dairy Teaching and Research Center (East Lansing, MI). Finally, I could not enjoy this program without my laboratory colleagues, who also became my dear friends, Thank to them for the laughs and the nice moments.

TABLE OF CONTENTS

LIST OF TABLES

LIST OF FIGURES

LIST OF ABBREVIATIONS

ABDH5	B-hydrolase domain containing 5
Akt	Protein kinase B
APP	Acute phase proteins
AT	Adipose tissue
ATF6	Transcription factor 6
ATGL	Adipose triglyceride lipase
ATIR	Adipose tissue insulin resistance
ATM	Adipose tissue macrophages
ATP	Adenosine triphosphate
BHB	B-hydroxybutyrate
cAMP	Cyclic AMP
CCL2	Chemokine (C-C motif) ligand 2
CD	Clusters of differentiation
CD204	Cluster of differentiation 204
CK	Clinical ketosis
CLS	Crow-like structures
COX	Cyclooxygenase
CPT1	Carnitine palmitoyl transferase 1
DA	Displaced abomasum
DG	Diacylglycerol
DGAT1	Diacylglycerol O-acyltransferase-1

DIM	Days in milk
DNA	Deoxyribonucleic acid
EIF3K	Eukaryotic translation initiation factor 3 subunit K
eNOS	Endothelial Nitric oxide synthase
ER	Endoplasmic reticulum
ET	Endotoxin
EU	Endotoxin units
FA	Fatty acid
FABP4	Fatty acid binding transport
FFA	Free fatty acids
FM	Flunixin meglumine
FMO	Fluorescence minus one
GPR109A	G protein-coupled receptor 109A
GRP94	Glucose-regulated protein 94
HC	Healthy cows
HDL	High density lipoproteins
HIF-1α	Hypoxia-inducible-factor-1α
Hp	Haptoglobin
HSL	Hormone sensitive lipase
IFNγ	Interferon-gamma
IL-10	Interleukin 10
IL-12	Interleukin 12

IL-17A	Interleukin 17A
IL-18	Interleukin 18
IL-1α	Interleukin-1 alpha
IL-1β	Interleukin 1-β
IL-23	Interleukin 23
IL-36RA	Interleukin 36 receptor antagonist
IL-4	Interleukin 4
IL-6	Interleukin 6
IL-8	Interleukin 8
iNOS	Inducible Nitric oxide synthase
IP-10	Interferon gamma-induced protein 10
IR	Insulin resistance
IRAK1	Interleukin-1 receptor-associated kinase 1
IRAK4	Interleukin-1 receptor-associated kinase 4
IREA1	Inositol-requiring protein 1
IRS1	Insulin receptor substrate 1
ISO	Isoproterenol
ISO+IN	Isoproterenol + insulin
JNK	C-Jun N-terminal kinase
KRBH	Krebs-ringer bicarbonate hepes buffer
LAL	Limulus amebocyte lysate
LBP	Lipopolysaccharide-binding protein

LD	Limit of detection
LIPE	Gene encoding hormone-sensitive lipase
LOC527744	Gene encoding BHB receptor
LPIN1	Phosphatidic acid phosphodiesterase lipin1
LPL	Lipoprotein lipase
LPS	Lipopolysaccharide
LRW	LAL reagent water
M1	Macrophages type 1
M2	Macrophages type 2
MAG	Monoacylglycerol
MAK	Mitogen activated kinase
MAPK	Mitogen activated protein kinase
MCP-1	Monocyte chemotactic protein 1
MDP	Muramyl dipeptide
meso-DAP	D-glutamyl-meso-diaminopimelic acid
MFI	Median fluorescent intensity
MGL	Monoglyceride lipase
MHCII	Major histocompatibility complex II
MIP-1α	Macrophage inflammatory protein 1-alpha
MIP-1β	Macrophage inflammatory protein 1-beta
MYD88	Myeloid differentiation primary response 88
NA	Noradrenaline

NEB	Negative energy balance
NEFA	Non-esterified fatty acid
NF-κB	Nuclear factor-kappa
NIA	Niacin
NL	Non-lactating
nNOS	Neuronal Nitric oxide synthase
NO	Nitric oxide
NOD1	Nucleotide oligomerization domain 1
NOS	Nitric oxide synthase
NSAID	Non-steroidal anti-inflammatory drug
NTC	Non-template control
OP	Oxidative phosphorylation
OR	Odds ratio
pAkt	Phosphorylated protein kinase B (Akt)
PAMP	Pathogen-associated molecular pattern
PDE3B	Phosphodiesterase 3B
PDK1	Phosphoinositide-dependent kinase 1
PERK	Protein kinase RNA-like ER kinase
PG	Propylene glycol
PGE2	Prostaglandin E2
PGN	Peptidoglycan
PGNIA	Propylene glycol + Niacin

PGNIAFM	Propylene glycol + Niacin + Flunixin Meglumine
pHSL	Phosphorylated hormone sensitive lipase
PI3K	Phosphatidylinositol 3-kinase
PKA	Protein kinase A
PKCδ	Protein kinase C-delta
PP	Periparturient
PPARα	Proliferator-activated receptor alpha
PPARγ	Peroxisome proliferator- activated receptor gamma
QC	Quality control
RNA	Ribonucleic acid
RNS	Reactive nitrogen species
ROC	Receiver operating characteristics
ROS	Reactive oxygen species
RPLP0	Ribosomal protein Lateral Stalk Subunit P0
RPS9	Ribosomal protein 9
RT	Room temperature
SAA	Serum amyloid A
SARA	Subacute ruminal acidosis
SCAT	Subcutaneous adipose tissue
siRNA	Small interference RNA
SIRPA	Signal regulatory protein alpha
siTLR4	Small interference TLR4

SLC2A4	Solute carrier family 2 member 4
SOCS1	Suppressor of cytokine signaling 1
SP	Substance P
SPP1	Osteopontin
SR-BI	Scavenger receptor of the class B type I
STAT1	Signal transducer and activator of transcription 1
STAT3	Signal transducer and activator of transcription 3
SVF	Stromal vascular fraction
TCA	Tricarboxylic acid
TG	Triglycerides
TLR4	Toll-like receptor 4
TNF	Tumor necrosis factor
TREM2	Triggering receptor expressed on myeloid cells 2
TRIF	TIR-domain-containing adapter-inducing interferon-β
UPR	Unfolded protein response
VEGF-A	Vascular endothelial growth factor A
VLDL	Very low-density lipoproteins
β-ARs	B-adrenergic receptors

INTRODUCTION

Inflammatory and metabolic diseases in periparturient dairy cows result in welfare issues and economic losses associated with reduced milk yield, cost of treatment, and high culling rates. One of the significant risk factors for disease susceptibility in periparturient cows is lipolysis dysregulation (Ospina et al., 2013) which is defined as an impaired response of adipose tissue (**AT**) to the antilipolytic and pro-lipogenic effects of insulin (Contreras et al., 2017b). Simultaneously, periparturient dairy cows exhibit a rise in circulating bacterial endotoxin, derived from bacterial diseases or leaky gut syndrome (Eckel and Ametaj, 2020). Therefore, the understanding of metabolic alterations in AT after endotoxin exposure becomes crucial to implementing health programs that include prophylactic and therapeutic measures to prevent periparturient diseases that cause losses of more than $1.3 billion per year to the US dairy industry (Foreign Agriculture Service, 2011).

Lipolysis is defined as the hydrolysis of triglycerides to release non-esterified fatty acids (**NEFA**) and glycerol. Lipolysis within the AT occurs during the periparturient period as an adaptation mechanism to fulfill energy demands required by the onset of lactation, and the reduced dry matter intake which leads the cows into negative energy balance (**NEB**). High lipolysis rates are reflected in elevated concentrations of NEFA in blood. When excessive, lipolysis overwhelms the liver's capacity to process FA to fatty acyl-CoA and triglycerides, predisposing cows to ketosis, fatty liver, and displaced abomasum (Ospina et al., 2010c, Ospina et al., 2013). The primary reason behind excessive lipolysis is the loss of the AT insulin sensitivity, which is mainly attributed to inflammation (de Luca and Olefsky, 2008). Various conditions such as high body condition score are known to contribute to AT inflammation and excessive lipolysis (Zhang et al., 2019), however the impact of inflammatory mediators, such as bacterial endotoxins, on AT lipolysis remains

poorly understood.

One of the possible factors behind the presentation of metabolic and infectious disease complexes in periparturient dairy cows is the increase in circulating endotoxins. Remarkably, common periparturient diseases such as mastitis, metritis, pneumonia, and metabolic events such as subacute ruminal acidosis (**SARA**), heat stress, and parturition, often result in endotoxemia (Dickson et al., 2019a). Although the inflammatory response induced by endotoxins impairs the metabolic function of AT (Mehta et al., 2010) the mechanisms remain unknown in dairy cows. Endotoxins can trigger several changes in AT including canonical and inflammatory lipolysis, inflammation, mitochondrial dysfunction, endoplasmic reticulum (**ER**) stress, and alterations in lipid storage that are reviewed in Chapter 1. In the AT, inflammatory responses are characterized by the production of proinflammatory cytokines and macrophage infiltration. Inflammatory products are the main mediators of adipocyte dysfunction including uncontrolled lipolysis, and insulin resistance. The available data on lipolysis and AT dysfunction in dairy cows fails to consider endotoxin as a potential trigger of lipolysis dysregulation. To address this gap, we studied the systemic inflammatory status of cows with clinical ketosis, which is a disease model of dysregulated lipolysis. Cows were treated with inhibitors of lipolysis including the use of niacin to target canonical lipolysis and a non-steroidal anti-inflammatory drug (**NSAID**) flunixin meglumine (**FM**) to inhibit inflammatory-induced lipolysis. In Chapter 2 we demonstrated that lipolysis dysregulation during clinical ketosis is highly correlated with inflammatory markers including endotoxin and the use of FM was beneficial to reduce excessive lipolysis. Similarly, in Chapter 3 we characterize the AT function of the cows enrolled in the clinical trial before and after treatment with lipolysis inhibitors. For the first time we demonstrated that cows with lipolysis dysregulation during clinical ketosis are presenting AT insulin resistance that is recovered after

FM treatment.

Although cows with clinical ketosis exhibited endotoxemia, it is still unclear whether endotoxins can cause dysregulation of adipose tissue lipolysis. To establish this, AT explants were exposed ex-vivo to endotoxin, LPS. As outlined in Chapter 4, we demonstrated that endotoxin triggers lipolysis and AT insulin resistance possibly by amplification of inflammatory mediators. To understand the cellular pathways involved in endotoxin-induced lipolysis, Chapter 5 describes a reductionist approach using primary isolated bovine adipocytes exposed to endotoxin. Using gene silencing approaches, we demonstrate that TLR4 is the key regulator of endotoxin-induced lipolysis. This study is not just the first investigating the lipolytic effect of endotoxin, but it also demonstrates that FM may reduce adipocyte lipolysis and inflammation.

We hypothesized that toll-like receptor 4 activation promotes lipolysis and insulin resistance in AT dairy cows, which are reduced by inhibiting canonical and inflammatory lipolytic pathways. This hypothesis was tested across specific aims using in-vivo, ex-vivo, and in-vitro studies that will evaluate the functional and metabolic effects of endotoxin and the effects of inhibitors of canonical and inflammatory lipolytic pathways. (1) To determine the role of endotoxin during lipolysis dysregulation in dairy cows and the capacity of lipolysis inhibitors to reduce lipolysis. (2): To characterize the AT function during lipolysis dysregulation. (3) To define the lipolytic response and development of insulin resistance in bovine AT after ET exposure. (4) To determine the mechanisms by which endotoxins modulate lipolytic responses in bovine adipocytes.

CHAPTER 1: ENDOTOXIN-INDUCED MODULATION OF ADIPOSE TISSUE FUNCTION IN DAIRY COWS: A COMPREHENSIVE REVIEW

ABSTRACT

Bovine adipose tissue (**AT**) is the central regulator of energy metabolism, and its dysfunction has been associated with pathological conditions. Bacterial endotoxin may mediate dysfunctional AT, including excessive lipolysis, inflammation, immune cell infiltration, mitochondrial dysfunction, and insulin resistance. Endotoxins are the outer component of the cell wall of Gram-negative bacteria and have been implicated in various metabolic disorders in humans and animals. In this review, we summarize the current understanding of the effects of endotoxins on bovine AT.

Endotoxins are likely to reach the blood circulation (i.e., endotoxemia) in postpartum dairy cows producing a pro-inflammatory response in bovine AT including the polarization of macrophages and the upregulation of various inflammatory mediators such as interleukin-6 and tumor necrosis factor-alpha. This inflammatory response is thought to contribute to the development of insulin resistance, as well as other metabolic disorders. Additionally, endotoxin stimulates lipolysis in bovine AT, leading to the release of free fatty acids into the bloodstream. The increased endotoxin-induced lipolysis can contribute to the development of insulin resistance by impairing insulin signaling and glucose uptake. Endotoxin exposure can also induce oxidative stress, which can impair the function of key lipogenic enzymes. The AT oxidative stress is caused by the production of reactive oxygen species by inflammatory cells in response to endotoxin and it can greatly contribute to the development of insulin resistance.

In conclusion, endotoxemia can have a significant impact on bovine AT, inducing inflammation, stimulating lipolysis, reducing adipocyte differentiation, and inducing oxidative stress. These effects are thought to lead to the development of insulin resistance and other

metabolic disorders in cows. Further research is needed to fully understand the mechanisms underlying these effects and to develop effective interventions to prevent or treat these conditions.

INTRODUCTION

In mammals, adipose tissue **(AT)** is the largest organ for storing energy in the form of lipids. During positive energy balance, higher glucose availability enhances the release of anabolic hormones such as insulin, which results in enhanced deposition of triglycerides (**TG**) within the AT (i.e., lipogenesis). In contrast, during negative energy balance lipid reserves are released to supply energy demands (i.e., lipolysis) (Saponaro et al., 2015). The AT is also an endocrine organ with the capacity to regulate biological functions including immune function, angiogenesis, glucose homeostasis, food intake, blood pressure, and reproduction (Contreras et al., 2017c). Importantly, systemic metabolism is regulated by AT, hence any disruption in its normal function is associated with multiple metabolic disorders including metabolic syndrome, obesity, diabetes, insulin resistance (**IR**), ketosis, and fatty liver disease (Mancuso, 2016).

The term metabolic syndrome is used to define the complex metabolic and physiological risk factors associated with elevated metabolic disease risk, where AT is the key driver of this syndrome (Ordovas and Corella, 2008). In humans, the metabolic syndrome is characterized by obesity, muscular and AT insulin resistance (**ATIR**), multiple defects in glucose metabolism, and inflammation (Hruby and Hu, 2015). In veterinary medicine, the equine metabolic syndrome is characterized by horses with obesity, IR, laminitis, and/or infertility (Johnson et al., 2009). Similarly, metabolic syndrome in canines is associated with obesity, IR, and mild hypertension (Tvarijonaviciute et al., 2012). Although the term metabolic syndrome is not defined in bovine medicine, the cow fat syndrome was proposed in the 70s to characterize the metabolic alterations in over conditioned dairy cows that present a high morbidity and mortality due to postpartum disease (Morrow, 1976). Although fat cow syndrome is not used any more in the literature, different metabolic diseases in dairy cows have been associated with over-conditioned cows and

AT dysfunction, including ketosis, fatty liver disease, and displaced abomasum (Vanholder et al., 2015). Among the several reasons proposed to explain the origin of AT dysfunction during the different metabolic syndromes, inflammation has been implicated as a major factor in the initiation of metabolic alterations and the pathophysiological consequences across the mentioned species (Wisse, 2004, Kunz et al., 2021).

The AT can become inflamed through a complex interplay of various endogenous and exogenous factors including endotoxemia (Mehta et al., 2010). Endotoxemia occurs when lipopolysaccharides (**LPS**), which are components of the cell wall of gram-negative bacteria, enter the bloodstream. Gram-positive bacteria in the other hand, have peptidoglycans and lipoteichoic acid that are responsible for the endotoxin-like properties. This can occur due to several reasons including bacterial infections, leaky gut syndrome and consumption of high fat diets in humans (Mehta et al., 2010, Moreira et al., 2012). Endotoxemia can have several effects on AT, including inflammation, lipolysis dysregulation, oxidative stress, IR, and changes in adipokine secretion that may lead to often called low grade chronic inflammation or 'meta-inflammation,' which are associated with higher risk of disease.

This review seeks to provide an overview of the current knowledge on the AT metabolic alterations induced by endotoxemia in mammals, with particular emphasis on dairy cows. Specifically, the review focuses on how endotoxins directly impact the lipolysis and lipogenesis pathways in AT, as well as how the inflammatory response plays a crucial role in the development and severity of AT dysfunction through the upregulation of cytokines, oxidative stress, and IR. In this this review, the terms endotoxin and LPS will be used interchangeably as they are commonly considered synonymous.

ENDOTOXEMIA

Definition

The term endotoxemia refers to the presence of endotoxins in blood, which is usually associated with the presence of bacteremia or septicemia (Cani et al., 2007, Munford, 2016). Endotoxin or LPS is the principal component of the outer membrane of gram-negative bacteria (Hurley, 1995). It is a heat-stable and glycolipid component, containing a pathogen-associated molecular pattern **(PAMP)**, lipid A, which is the major antigenic compound of the bacteria. Upon binding to its pattern recognition receptor, toll-like receptor 4 **(TLR4)**, endotoxin triggers a complex signaling cascade resulting in local or systemic activation of proinflammatory mediators and increases the oxidative stress (Bannerman and Goldblum, 1999, Chow et al., 1999, Ryan et al., 2004, Cani et al., 2007). A second pathogen component involved in immune activation is the bacterial peptidoglycan **(PGN)** which is detected by nucleotide oligomerization domain 1 **(NOD1)** by sensing the D-glutamyl-meso-diaminopimelic acid (**meso-DAP**) found in PGN of Gram-negative bacteria and NOD2 that detects muramyl dipeptide **(MDP)** present in in Gram-positive bacteria (Carneiro et al., 2004).

In healthy dairy cows, the prevalence of endotoxemia has been estimated at 50% (Wittek et al., 2004). Recently, our group demonstrated that 33.3% of healthy postpartum dairy cows had detectable blood levels of endotoxin units (**EU**>0.05) with no signs of disease. Whereas 72.2% of the cows diagnosed with clinical ketosis presented endotoxemia (Chirivi et al., 2023b). The above highlights endotoxin as an active player during metabolic disease as occurs in humans with obesity and IR. Cani et al. (2007) proposed the term metabolic endotoxemia to describe a condition of chronically elevated endotoxin in plasma at levels 10-50 times lower than values during septic shock. Metabolic endotoxemia status was reached after a 4-week high-fat diet in C57bl6/J mice,

who despite looking healthy, the low and chronic levels of endotoxin increased fat deposition, pro-inflammatory and oxidative pathways, and IR (Cani et al., 2007). Given that dairy cows that develop clinical ketosis are found with endotoxemia with no evidence of septic shock or disease during the pre-partum period (Abuajamieh et al., 2016), we speculate that dairy cows may be silently suffering metabolic endotoxemia and AT alterations prior to the development of metabolic disease.

Sources of endotoxin

The main cause of endotoxemia is endotoxin translocation due to increased permeability of the intestine (Abuajamieh, 2015, Aileen et al., 2015). Dairy cattle have complex mechanisms to maintain a balanced metabolic function and interaction with the gut microbiome, and have developed mechanisms to maintain gut homeostasis, including secretory antibodies, intestinal alkaline phosphatase, bile acids secretion and antimicrobial peptides (Porter et al., 1972, Ji et al., 2020, Wang et al., 2021). However, any disturbances to the regulatory mechanism may result in reduced regulation of gut endotoxins.

The mechanisms behind intestinal translocation of endotoxin lies mainly in the gut microbiome composition. An alteration in the microbiome's composition is linked with rise in the concentrations of endotoxin in the bloodstream (Cani et al., 2007, Wang et al., 2019). Research in germ-free mice has revealed the significant role of the gut microbiome in regulating body weight and endotoxin translocation. When fed a high-fat and sugar-rich diet, germ-free mice do not become obese, but they do gain weight when colonized with bacteria from cecum of wild-type mice (Bäckhed et al., 2004, Bäckhed et al., 2007). A recent study in dairy cows also demonstrates the role of gut microbiome in translocation of endotoxin and AT function, observing that at least 14 species of bacteria contribute to lipolysis-linked microbiome (Gu et al., 2023). Postpartum dairy

cows are highly vulnerable to endotoxemia, since the intestinal and ruminal microbiomes of these cows are influenced by several factors that occur simultaneously during this period. Factors affecting microbiome include ruminal acidosis (McCann et al., 2016), the duration of feeding grain-rich diets (Plaizier et al., 2020), heat stress (Chen et al., 2018), lameness (Zinicola et al., 2015), and mastitis (Hoque et al., 2020). Therefore, endotoxins are expected to have more pronounced effects on AT during the peripartum period when the tissue is more metabolically active.

The reduction in the ruminal and intestinal pH during subacute ruminal acidosis (**SARA**) is associated with alterations in the microbiome composition and disturbed intestinal epithelium (McCann et al., 2016), which result in translocation of endotoxin into the bloodstream. SARA increases ruminal endotoxin in mild lactation cows from 24,547 EU/mL to 128,825 EU/mL (Gozho et al., 2007) and in peak lactation animals from 28,184 to 107,152 EU/mL (Khafipour et al., 2009). Animals with SARA also presented an increased in plasma endotoxin from <0.05 to 0.52 EU/mL (Khafipour et al., 2009). Similarly, heat stress reduces blood flow to the visceral organs, resulting in hypoxia and death of enterocytes and an increase in intestinal permeability (Hall et al., 1999). The higher permeability of humans under heat stress is associated with endotoxemia (Graber et al., 1971). Remarkably, animals under heat stress may share many metabolic and physiologic alterations with animals under endotoxemia (Lim et al., 2007).

Postpartum diseases such as mastitis, metritis, or pneumonia are also important sources of circulating endotoxin in dairy cows (Mani et al., 2017, Dickson et al., 2019a). Cows with naturally occurring mastitis had 18-fold greater plasma endotoxin levels than control cows (Hakogi et al., 1989). Similarly, experimentally induced mastitis increased plasma endotoxin levels up to 10-fold (Dosogne et al., 2002). Uterine inflammation is another source of endotoxin during the

periparturient period. Endotoxin was detected qualitatively in the plasma of cows that underwent intrauterine infusion of 5 µg/kg of BW of E. coli, whereas control cows consistently tested negative for LPS (Peter et al., 1990). In cases of spontaneous endometritis, endotoxin was found to be present in the plasma, depending upon the severity of the disease. Specifically, 17% of cows with mild endometritis (mucopurulent lochia) presented with endotoxemia, while 100% of cows with severe endometritis (sanguine-purulent lochia) had endotoxemia (Mateus et al., 2003).

How endotoxins reach the AT

Endotoxins in dairy cattle primarily translocate from the lumen in the gastrointestinal tract, mammary gland, and uterus, however, there are additional routes by which endotoxins may enter the bloodstream in smaller amounts including respiratory tract and lesions on the skin (Nishi et al., 2019). There are no studies in ruminants about the molecular absorption of endotoxin and most of the information available is from studies conducted in murine intestinal models, therefore the mechanisms of endotoxin translocation into the circulation remains speculative.

The first mechanism is the passive diffusion by increased paracellular permeability or "leaky gut." The paracellular transport of endotoxins includes the alteration of tight junctions, which regulate paracellular permeability (Camilleri, 2019). Therefore, endotoxins may enter through the paracellular pathway in the presence of mucosal injury (Drewe et al., 2001). The molecular pathways involved in paracellular and tight junction disfunction was recently reviewed by Horowitz et al. (2023). The second proposed mechanism is the active transport of endotoxin or transcellular pathway (Nolan et al., 1977). Different studies using electron microscopy suggest that either in vitro (Beatty et al., 1999) or in vivo (Laugerette et al., 2012), endotoxin is internalized by enterocytes and crosses the basal epithelium by endocytic pathways (Figure 1). The internalization of endotoxin by enterocytes involves lipid transport mechanisms including TLR4

with MD-2-dependent pathways (Neal et al., 2006) and scavenger receptor of the class B type I (**SR-BI**), and fatty acid translocase CD36 (Vishnyakova et al., 2003, Akiba et al., 2020). Using a mouse line with a mutation in TLR4, it was demonstrated that TLR4 is necessary for enterocyte phagocytosis. In this model, the internalization of endotoxin did not occur (Neal et al., 2006)

Inside the enterocytes, endotoxin is transported to the endoplasmic reticulum and then transported to the Golgi apparatus to be part of mature chylomicrons (Ghoshal et al., 2009). Chylomicrons synthesis is essential for endotoxin transport into the lymph (Akiba et al., 2020). That explains why healthy subjects may experiment endotoxemia after fat intake, because fat is a more efficient transporter for bacterial endotoxin (Amar et al., 2008). Endotoxins are preferentially transferred from the surface of chylomicrons to high density lipoproteins (**HDL**) and other lipoproteins that are transported into the circulation by transcytosis (Nordestgaard et al., 1990). Transcytosis is the vesicular transport from one side of the cell to the other, involving apical endocytosis of macromolecules following by trafficking across the cytoplasm and exocytosis (Tuma and Hubbard, 2003). After entering the bloodstream, approximately 60% of endotoxin gets attached to HDL, while the remaining portion binds to LBP and soluble CD14 (Levels et al., 2001). The interaction between endotoxin and HDL is crucial for innate immune functions, as HDL transports endotoxin to the liver for elimination (Yao et al., 2016). Human and mouse models have demonstrated that HDL reduced inflammation during endotoxin challenges (Ramírez et al., 2004, Birjmohun et al., 2007). In dairy cows, HDL accounted for up to 75.7% of the lipoproteins (Duran et al., 2021), which may influence the particular resistance of cows to endotoxemia when compared to other species.

SR-BI and CD36 receptors are responsible for facilitating the passage of HDL-endotoxin associated molecules from the bloodstream to endothelial cells. (Rohrer et al., 2009, Brundert et

al., 2011). Importantly, caveolin and cavin family proteins, known to be involved in various physiological functions such as cell signaling, and endocytosis are significantly colocalized with SR-BI and CD36 (Babitt et al., 1997). Remarkably, caveolae constitute up to 50% of the plasma membrane surface in both adipocytes and endothelial cells (Parton and del Pozo, 2013). The above statement suggests that the binding of HDL-endotoxin to SR-BI or CD36 may lead to an elevated transportation of endotoxin into the adipocytes. Importantly, AT is considered as a site of accumulation of several toxins, which occurs through lipoprotein transport (Jackson et al., 2017). However, less is known about the dynamics and accumulation of endotoxin in AT of ruminants.

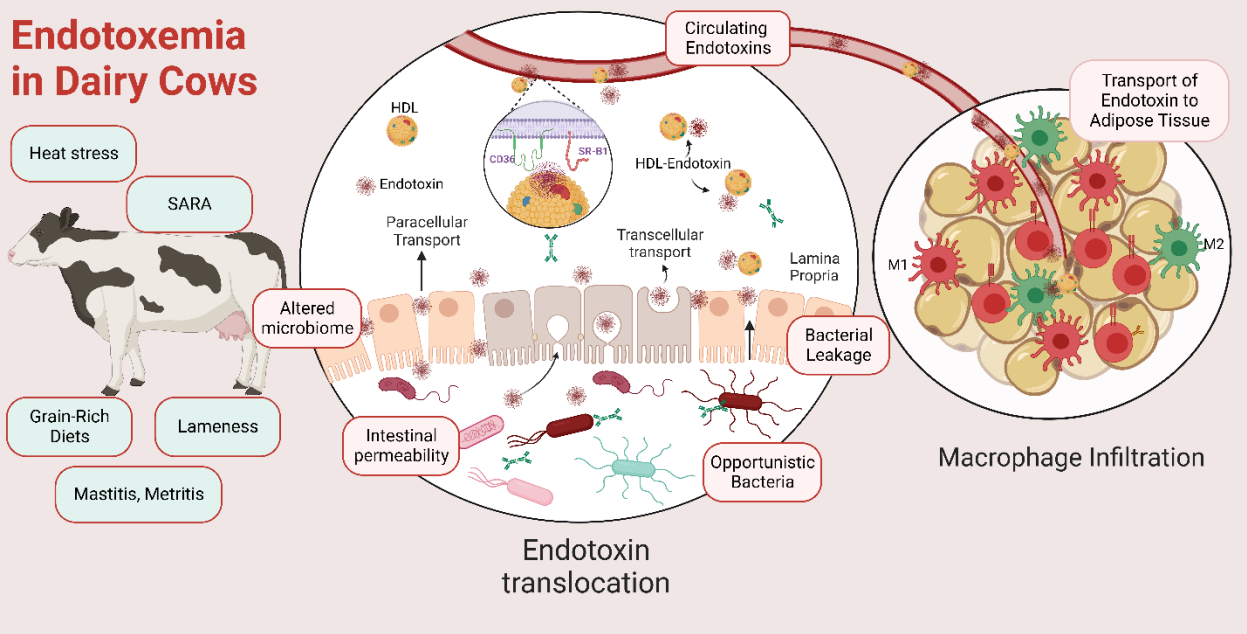

Figure 1. Sources of endotoxemia in dairy cows and transport to the adipose tissue. Created with BioRender.com.

AT STRESS RESPONSES DURING ENDOTOXEMIA

Inflammation

Endotoxemia results in profound systemic inflammation that is associated with marked alterations in lipid, protein, and carbohydrate metabolism (Cani et al., 2007). The activation of inflammatory mediators by endotoxemia may cause a cascade of changes in multiple organ

systems, leading to organ failure, or even death. Among the mediators activated, cytokines have a key role in regulating host responses to sepsis. Some cytokines have a direct effect over AT metabolism or via the release of metabolic active hormones like catecholamines, cortisol, glucagon, and adrenocorticotropin (Cani et al., 2007). However, AT is also a target of direct activation by endotoxin via TLR (Zu et al., 2009a, Rogero and Calder, 2018).

TLR4 is importantly implicated during AT inflammation either by MYD88-dependent or -independent pathway (Li et al., 2010). The MYD88-dependent pathway signaling results in early activation of transcription factor nuclear factor-kappaB **(NF-κB)** which leads to the production of inflammatory cytokines. The TRIF-dependent pathway (MYD88-independent) activation concludes with a late phase of NF-κB activity (Yamamoto et al., 2003). Both MYD88 and TRIF pathways are essential for inflammation signaling in AT and macrophage polarization following LPS stimulation (Griffin et al., 2018). The activation of NF-κB is essential for cytokine production, since NF-κB inhibition resulted in reduced IL-6 and IL-8 expression in adipocytes (Zu et al., 2009a). AT explants from dairy cows are immunologically responsive to 20 μg/ml of LPS during 2 h, resulting in higher transcription of IL-6 and tumor necrosis factor **(TNF),** especially in mesenteric AT (Mukesh et al., 2010). Equally, our group demonstrated that the same dose of LPS increases the mRNA expression of proinflammatory cytokines (CCL2, CD204, IL-6, IL-8, SOCS1) after 3 h of challenge and reduce the transcription of anti-inflammatory mediators (IL-10, STAT3) after 7 h of exposure in subcutaneous AT explants from non-lactating dairy cows (Chirivi et al., 2022). Similarly, the NOD1 ligand activation by PGN in AT and adipocytes might result in increased proinflammatory profile (IL-1β, IL-18, IL-6, TNF) mediated by PKCδ, IRAK1/4 and of NF-κB activation (Zhao et al., 2011, Sharma et al., 2019). The AT is a complex organ composed of diverse types of cells that present variations in inflammatory response to LPS. For example,

adipocytes might not initiate a potent inflammatory response to LPS as macrophages do (McKernan et al., 2020). These differences are related with higher density of receptors in macrophages compared to adipocytes.

AT Macrophages Infiltration

Macrophages are the most abundant and important immune cell within the AT due to their role as modulators of immune response, energy metabolism, and mitochondrial function. The AT macrophages (**ATM**) are derived from both circulating monocytes and resident macrophages derived from chemotactic protein 1 (**MCP-1**) activity. ATM were initially classified in M1 (classically activated) with proinflammatory characteristics and M2 (alternatively activated) which exhibited anti-inflammatory properties. A comprehensive review on macrophage phenotypes was made by Caslin et al. (2020). LPS polarizes macrophages toward the M1 phenotype, through TLR4/MYD88 independent pathway and STAT1-alpha-betha (Toshchakov et al., 2002), resulting in secretion of proinflammatory mediators such as IL-1β, TNF, IL-12, IL-18, and IL-23. During endotoxemia, Caesar and collaborators demonstrated the gut derived LPS promoted M1 polarization in AT of mice (Caesar et al., 2012). Given that endotoxemia is linked with metabolic syndrome, the infiltration of ATM population with M1 phenotype is frequently observed in obese animals and humans with IR (Weisberg et al., 2003), forming typical "crow-like structures (**CLS**)" around adipocytes with hypertrophy, necrosis, and cellular or extracellular components that need to be resorbed (Murano et al., 2008). M1 polarization has been similarly found in the course of disease, in omental AT from dairy cows during naturally occurring cases of displaced abomasum (Contreras et al., 2015). Recently, glucose-regulated protein 94 (**GRP94**), a endoplasmic reticulum chaperone, was discovered a novel regulator of M1 macrophages in AT from mice (Song et al., 2020), since the specific deletion of GRP94 resulted in low number of M1 and increased insulin

sensitivity. In healthy AT, M2 macrophages are prevalent compared to M1 and the ratio of M2 to M1 macrophages is 4:1. However, during low grade inflammation the proportion of M1 is enhanced resulting in an enhanced ratio of 1.2:1.

Endoplasmic reticulum stress

The endoplasmic reticulum (**ER**) is essential for lipid synthesis, calcium Ca^{2+} storage, protein synthesis and folding, and it participates in inflammation, insulin signaling, cell death and proliferation. Under cellular process that breaks ER homeostasis such as pathogens, inflammation, and oxidative stress, ER develops stress leading to the activation of the unfolded protein response (**UPR**) signaling. The elements of the UPR/ER stress response include inositol-requiring protein 1 (**IRE1**), activating transcription factor 6 (**ATF6**), and protein kinase RNA-like ER kinase (**PERK**). Although the UPR is considered a mechanism to re-establish cellular homeostasis, the continued stress may result in cell death. In adipocytes, the activation of TLR4 is linked with ER stress and downstream activation of inflammation (Alhusaini et al., 2010, Li, 2018). The activation of IRE1 leads to upregulation of c-Jun N-terminal kinase (**JNK**) and NF-κB which results in transcription of inflammatory genes, increased oxidative stress and apoptosis dependent of caspase activation. In AT, the induction of ER stress is associated to obesity, IR, type II diabetes, and low adiponectin synthesis (Ozcan et al., 2004, Torre-Villalvazo et al., 2018). The last is correlated with low insulin response in dairy cows (De Koster et al., 2017). Very little is understood about the mechanism by which ER stress impairs adiponectin production. An approach in bovine adipocytes investigated the role of ER chaperones on post transcriptional modifications of adiponectin mRNA (Krumm et al., 2018). Although the ER stress in AT dairy cows has been poorly studied, the alteration in ER homeostasis is linked with liver damage and clinical ketosis (Shi et al., 2021). Researchers also demonstrated that cows with high levels of FA presented ER stress in hepatocytes

and it is linked to fatty liver disease (Zhu et al., 2019).

Mitochondrial dysfunction

Using the electron transport chain, mitochondria are the main source of ATP through the activity of tricarboxylic acid (**TCA**) cycle and oxidative phosphorylation (**OP**). In addition, mitochondria regulate progenitor cell differentiation, lipid homeostasis, insulin sensitivity, and oxidative capacity in AT (Boudina and Graham, 2014). Mitochondria are involved in several cellular events including apoptosis, innate immunity, production of essential metabolites for cytosolic function, amino acid metabolism, urea cycle, formation of reactive oxygen-nitrogen species (**ROS**/**RNS**) and ketone bodies production (Kusminski and Scherer, 2012, Boudina and Graham, 2014). The activation of TLR4, NOD1, and NOD2 in adipocytes induce stress signals including reduced OP and electron transport chain activity, leading to reduced ATP and increased anaerobic oxidation, evidenced with higher levels of glycolysis and lactate (Bae et al., 2014). Those alterations in cellular oxygen supply have been described as well during obesity in humans (Cao, 2013) and over conditioned dairy cows (Laubenthal et al., 2017). The expansion of AT leads to decreased blood flow and low oxygen availability in the cells, leading to increased mitochondrial DNA copies, and higher transcription of angiogenic factors such as hypoxia-inducible-factor-1α (**HIF-1α**) which leads to inflammation and cell death in AT of nonlactating dairy cows (Laubenthal et al., 2017). Moderate production of ROS maintains cellular homeostasis, for example innate immune activation is mediated by ROS, and peroxisome proliferator- activated receptor gamma (**PPARγ**) depends on H_2O_2 activity to transcript factors that induce adipocyte differentiation (Loh et al., 2009). In contrast, cellular damage is undoubtedly a consequence of the loss of redox homeostasis and high ROS production as take place during LPS exposure in adipocytes (Ji et al., 2020), which can damage protein, lipids, nuclear DNA but particularly

mitochondrial DNA (Richter et al., 1988).

Redox Signaling Alteration

Endotoxemia and sepsis are processes accompanied by high expression of free radicals. All the cellular components of AT are sources of free radicals. Nitric oxide (**NO**) is synthesized by nitric oxide synthases (**NOS**). Three different NOS have been isolated, one in endothelial cells (**eNOS**), a second one in neuronal cells (**nNOS**) and the third isoform is inducible by LPS and cytokines (**iNOS**) (Förstermann et al., 1994). AT from male Sprague-Dawley rats produce higher amounts of iNOS after i.p injection of 4 mg/kg of LPS (Ribiere et al., 1996). The role of NO in modulating lipolysis was evaluated in AT explants during LPS challenge using specific inhibitors of NOS (Penfornis and Marette, 2005). The lower NO production did not reduce the lipolysis induced by LPS, in contrast iNOS inhibition further increased lipolysis by 30%. Those findings suggest that NO confines lipolysis in AT under inflammatory conditions and researchers also demonstrated that NO-mediated reduced lipolysis is facilitated by reduction of cAMP/PKA products (Penfornis and Marette, 2005). The activation of lipolysis modulates the synthesis of proinflammatory oxylipids, facilitated by the high content of ROS and RNS given the pro-oxidative environment in the AT of dairy cows during the postpartum period (Contreras et al., 2020).

ENDOTOXEMIA ALTERS LIPID METABOLISM

Lipolysis

Upon high energy demand, triglycerides stored in the AT are hydrolyzed to release non-esterified fatty acids (**NEFA**s). The breakdown of the ester bonds between the fatty acids and the glycerol backbone is determined by 3 specific lipases (Vaughan et al., 1964, Holm, 2003, Lass et al., 2006); 1. adipose triglyceride lipase (**ATGL**), hydrolyzes TG to generate NEFA and

diacylglycerol (**DG**) (Zimmermann et al., 2004b), 2. hormone sensitive lipase (**HSL**) is a more versatile enzyme competent to hydrolyze TG, DG, and monoacylglycerol (**MAG**) (Holm, 2003), and finally 3. monoglyceride lipase (**MGL**) that hydrolyzes MAG into NEFA and glycerol in AT (Vaughan et al., 1964). Basal lipolysis is conditioned specially by adipocyte size and TAG in human, bovine and rodent AT (Kosteli et al., 2010, De Koster et al., 2016, Magkos et al., 2016), however additional factors such as sex, age, physical activity and fat location have been reviewed to influence the lipolytic activity (Wahrenberg et al., 1989, Lange et al., 2002). During stimulated lipolysis, β- adrenergic receptors are activated by catecholamines, which results in stimulation of cAMP and subsequent activation of protein kinase A (**PKA**). The last phosphorylates HSL and perilipin causing the TG breakdown (Egan et al., 1992).

The initial evidence of activation of AT lipolysis mediated by inflammation, reported in vitro lipolysis mediated by increased cAMP in of human and non-humane primate adipocytes exposed to 0.16 µg/ml of endotoxin (Hikawyj-Yevich and Spitzer, 1977). In addition, endotoxin enhanced norepinephrine-stimulated lipolysis. Later a study found that AT surrounding lymph nodes enhanced lipolysis in presence of lymphoid cells stimulated with 50 µg/mL of LPS (Pond and Mattacks, 1995). The same study showed that AT located near to eight lymphatic nodes presented a higher lipolysis compared to fat depots collected in any other area. Those findings were later confirmed in vivo with spontaneous lipolysis in the adipocytes surrounding the popliteal lymph node of guinea pigs after subcutaneous injection of LPS (1µg/100 g body mass) (Pond and Mattacks, 1998). This study found a peak of lipolysis after 6-9 h of challenge that decline after 24 h. Following experiments confirmed that LPS at a dose of 0.3 µg/Kg in rabbits increased the release of FFA into the bloodstream (Szewczenko-Pawlikowski and Kozak, 2000). In addition, this research evidenced changes in monocyte membrane fluidity due to accumulation of lipid rich

in double bounds because of higher availability of very low-density lipoproteins (**VLDL**) after LPS challenge. The authors noticed that the change in mononuclear phagocyte membrane is accompanied by a process of endotoxin tolerance. The last is proposed as an adaptation to repeated exposure to endotoxin. Those findings point to the importance of lipid mobilization as an immunomodulatory process against endotoxin. In fact, Kitchens et al. (2003) confirmed that lipoproteins play an important role neutralizing the bioactivity of LPS.

Canonical pathway

The canonical pathway of lipolysis refers to the cellular mechanism described above during hormonal stimulation. LPS did not increase lipolysis either in vivo or in vitro in TLR4 knockdown mice, demonstrating the importance of TLR4 in the activation of lipolysis (Zu et al., 2009a). Mice and human adipocytes exposed to LPS from 0.01 up to 10 µg/mL, increase lipolysis in dose dependent manner (Zu et al., 2009a, Grisouard et al., 2010). The incubation of human's adipocytes with inhibitors of the canonical lipolytic pathway such as PKA (H-89) or HSL (CAY10499) followed by stimulation with 100 ng/mL of LPS during 24 h, resulted in inhibition of lipolysis (Grisouard et al., 2010). Similarly, PGN (10 µg/mL) is a lipolytic agent by NOD1 ligand and PKA/HSL dependent activity (Chi et al., 2014).

Inflammatory pathway

The addition of 1 µg/ml of LPS in mice adipocytes resulted in higher phosphorylation of the Raf-1, an important kinase in the mitogen activated protein kinase (**MAPK**) pathway. In addition, LPS induced the phosphorylation of MEK1/2 (ERK1/2 MAPK Kinase) (Zu et al., 2009a). To demonstrate the dependency of this pathway on lipolysis, the inhibition of MEK-ERK1/2 with either PD98059 or U0126, resulted in inhibition of glycerol release following LPS stimulation. Similar findings were reported in adipocytes stimulated with PGN (10 µg/ml), where ERK

activation is partially involved in lipolysis (Chi et al., 2014). In align with those facts, our group showed that AT of dairy cows exposed to LPS during 7 h, increase the phosphorylation of ERK1/2 parallelly with lipolysis activation (Chirivi et al., 2022). New evidence has demonstrated that ERK1/2 promoted serine phosphorylation of the beta3 adrenoreceptor and enhanced lipolysis (Hong et al., 2018). A second inflammatory pathway was described only in human adipocytes treated with 100 ng/ml of LPS for 24 h. The inhibitors of IKKβ (sc-514) and NF-κB (PDTC) abolished LPS induced lipolysis, indicating that NF-κB is similarly involved in lipolysis (Grisouard et al., 2010). In contrast, the inhibition of NF-κB resulted in partial reduction of lipolysis induced by PGN, suggesting that NF-κB is involved in at least part of lipolysis in mouse adipocytes (Chi et al., 2014).

The mechanisms of both ERK1/2 and NF-κB-induced lipolysis depends on the downstream activation of TNF-α. LPS can induce activation of ERK1/2, JNK, and p38. The activation of P38 es necessary for TNF-α production in human adipocytes (Hoareau et al., 2010). The studied mechanisms of TNF-α-induced lipolysis include first; downregulation of phosphodiesterase 3B (**PDE3B**) which is an enzyme that reduces the activity of cAMP (Rahn Landström et al., 2000). The second suggested processes include both downregulation and phosphorylation of perilipins in human and mice adipocytes (Rydén et al., 2004, Zu et al., 2009a), which results in uncoated lipid droplets, thus facilitating the access of lipases and then concluding in lipolysis. A third mechanism involves the downregulation of GTP binding protein Gα by TNF-α, which results in increased concentrations of cAMP (Gasic et al., 1999). Furthermore, as TNF-α also is produced by inflammatory cells in the AT during endotoxemia, the paracrine effect of TNF-α on adipocytes requires NF-κB pathway to induce lipolysis, which in turn results in reduced levels of PLIN (Jurga et al., 2007) without altering HSL levels (Green et al., 1994). However, it is important to note that

the mechanism of lipolysis mediated by TNF-α is dependent on time since it takes approximately 6-12 h before reach a quantifiable state (Green et al., 1994).

The pharmacological induction of ER stress in adipocytes developed activation of lipolysis by activation of cAMP/PKA and ERK1/2 pathways accompanied by higher perilipin phosphorylation (Deng et al., 2012). However, the distinction between lipolysis induced by immune responses and hormone/adrenergic signals was just recently uncovered. It was unclear if inflammation uses a specific kinase or shares hormonal pathways to activate lipolysis mediated by ERK1/2/PKA/Lipases. The study analyzed different inflammatory effectors such as LPS, PGN, and TNF-α, and it demonstrated that lipolysis by inflammatory agents is mediated by ER stress (Foley et al., 2021). The activation of IREA-1 is indispensable for immune but not for hormonal lipolysis.

Conflicting reports in dairy cows have shown that IV. Infusion of LPS activates lipolysis, leading to elevated levels of NEFA in plasma. Waldron et al. (2003) observed a peak of NEFA 2 h after infusing 1 μg/kg of LPS in mild lactation cows (150 -220 DIM). Similarly, in non-pregnant lactating cows (169 ± 20 DIM), circulating NEFA also increased during continuous LPS (up to 0.148 μg/kg) infusion for 8 d (Horst et al., 2019a). In contrast, periparturient dairy cows receiving intermittent infusion of LPS before parturition (-14 and -10 d) and after calving (d 3 and d 7) did not present changes in plasma NEFA. The contrasting evidence on the lipolytic effects of LPS on dairy cows may obey to varied reasons including the type of LPS used and specially the different metabolic status of those animals. More evidence in humans highlights that endotoxin effects vary depending upon the metabolic status of the subject. In healthy patients, endotoxin activated gene and protein expression of lipases including LPL and HSL. However, patients with type II diabetes are resistant to LPS induced increases in lipases expression (Mathur et al., 2012). It is possible that

previous metabolic endotoxemia may induce endotoxin tolerance and lipase activation in patients with type II diabetes.

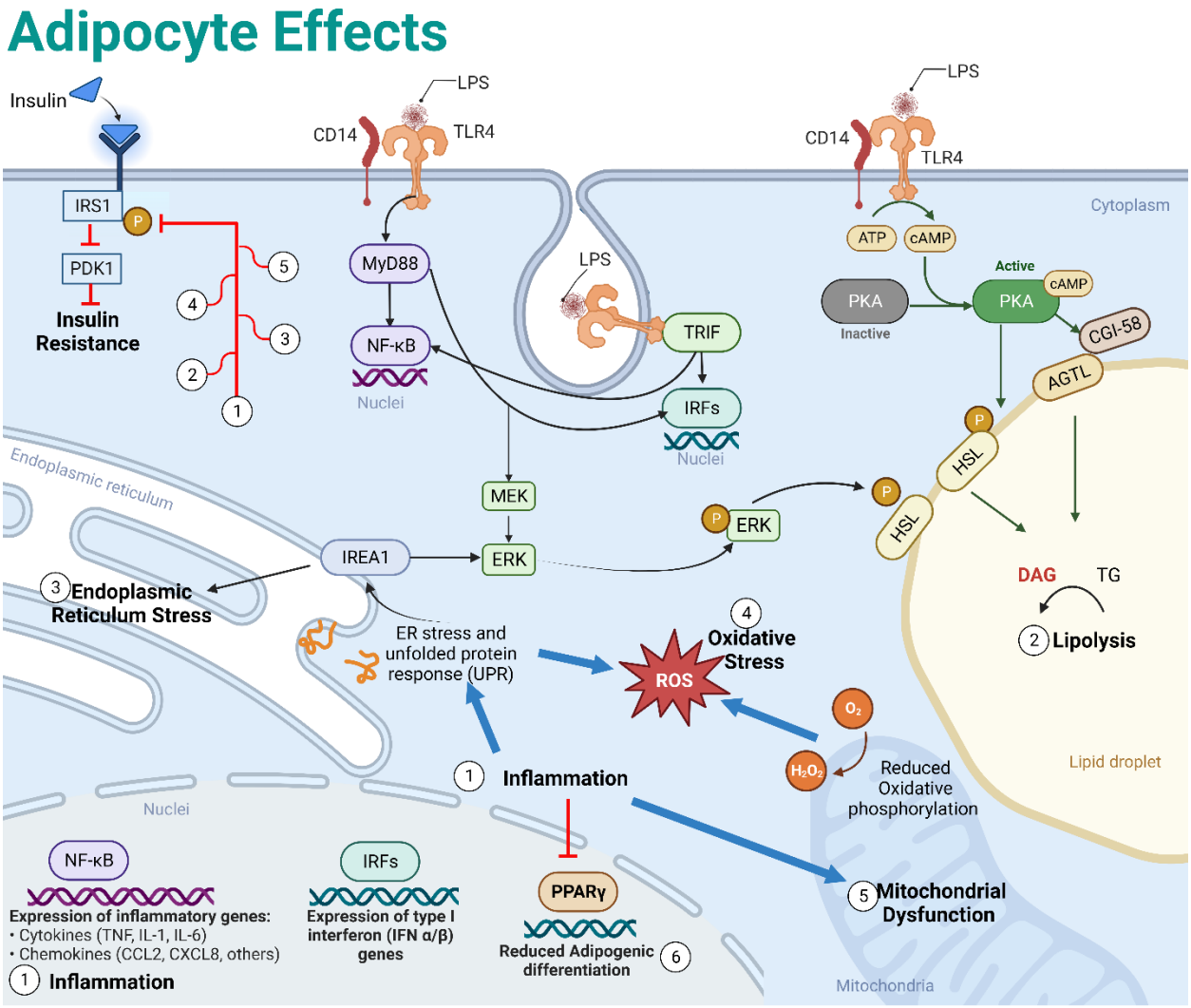

Figure 2. Endotoxin effects on adipocytes. Created with BioRender.com.

Lipid Accumulation

The changes in lipid accumulation that occurs during endotoxemia depend upon the amount and duration of exposure to endotoxin. In humans, higher levels of endotoxin during obesity has been linked with reduced lipid accumulation markers (Clemente-Postigo et al., 2019). Adipocyte hyperplasia (i.e., adipogenesis) refers to the process of recruiting new adipocytes from adipose progenitor cells. Hyperplasia of adipose cells results in an increase capacity to store lipids,

which is considered to play a beneficial role in the regulation of metabolism in humans (Kim et al., 2007, Kim et al., 2014). The reduction of adipocyte hyperplasia is a common characteristic during obesity in humans, while enhanced lipid accumulation (i.e., lipogenesis) results in hypertrophy of adipose cells (Kim et al., 2007, Jo et al., 2010). The literature presents conflicting evidence about the adipogenic potential of AT during endotoxemia. In vitro studies found that endotoxin ranging from 0.1 up to1 μg/mL of LPS reduces the adipogenic potential in primary SV cells isolated from mouse inguinal AT (Wang et al., 2013, Zhao and Chen, 2015). One potential mechanism for decreased adipogenesis is through the inhibition of AMPK phosphorylation, which can subsequently suppress the expression of important adipogenic factors, such as PPARγ. (Wang et al., 2013). Similarly, SVF cells treated with 10 and 25 ng/mL of LPS reduced triglyceride accumulation and adipocyte differentiation by reduction of PPARγ (Luche et al., 2013). In the other hand 3T3-L1 cells treated with 20 μg/mL of endotoxin increased cell proliferation and adipogenesis via JAK2/STAT and AMPK (Chang et al., 2019). An in vivo study induced metabolic endotoxemia in mice by infusing LPS for 4 weeks. Researchers observed that endotoxemia provoked adipocyte proliferation as observed by a higher counts of progenitor cells, however those cells exposed in vitro to LPS had a reduced adipogenic potential (Luche et al., 2013). The same study also evaluated the effects of metabolic endotoxemia on AT lipid storage over the time. After finishing the LPS infusion, mice were fed a high energy diet for 8 weeks. Compared to saline animals, mice previously treated with LPS had increased body weight, higher AT mRNA expression of TNF and glucose intolerance. Remarkably the increase in weight was specifically observed in the AT depots rather than in other organs. The above highlights the long-term effects of endotoxemia on AT function. Initially, adipocyte hyperplasia was enhanced, and subsequently, hypertrophy developed due to the increased energy availability. Unfortunately, there is lack of

research about the effects of endotoxemia on adipogenic potential in dairy cows. Over-conditioned cows during the dry period is a significant risk factor to develop numerous health problems during the transition period. However, most of the studies reviewed by Roche et al. (2009), evaluated how body fat composition (body condition score) affects disease incidence, however there is lack in research to understand the effects of endotoxin-related disease on fat accumulation.

Insulin resistance

IR within the AT occurs when a normal concentration of insulin induces a reduced biological effect (Ronald Kahn, 1978). A reduced insulin activity in AT results in reduced glucose uptake and lipogenesis and lack of inhibition of lipolysis (Brockman and Laarveld, 1986). It is widely recognized that IR can be induced by inflammation resulting from endotoxins mediated TLR4 activation, which can inhibit the transduction of insulin signaling. All the metabolic responses previously discussed in this review are fundamentally linked to the development of ATIR. For detailed molecular processes, the reader is directed to the reviews on this topic (de Luca and Olefsky, 2008, Piya et al., 2013, Khan and Wang, 2014, Petersen and Shulman, 2018)

Insulin signaling is a complex process involving two main cellular pathways. The phosphatidylinositol 3-kinase (**PI3K**)-Akt pathway mediates insulin's effects on glucose uptake and metabolic functions. The Ras-MAPK pathway, on the other hand, regulates gene expression and interacts with the PI3K-Akt pathway to control cell growth and differentiation (reviewed in (Taniguchi et al., 2006)). Insulin receptor substrate 1 (**IRS1**) is a common intermediate for the two pathways, and alternative phosphorylation of serine 307 on IRS1 can reduce downstream signaling (Aguirre et al., 2002). Inflammatory factors like TNF, JNK, and suppressor of cytokine signaling (**SOCS**) proteins negatively regulate IRS proteins, promoting their degradation and contributing to IR (Rui et al., 2002).

Reduced insulin signaling is primarily influenced by inflammatory mediators during endotoxemia. Murine adipocytes exposed to TNF presented a serine phosphorylation in the IRS1, which resulted in attenuated insulin signaling activation (Hotamisligil et al., 1996). TNF can also induce IR by reducing the expression of insulin receptor IRS1in 3T-L1 adipocytes. The elevated JNK activity by inflammation also contributes to IR, when mouse are JNK1 knockout, there was a reduced serine phosphorylation of the IRS1 and reduced development of IR (Hirosumi et al., 2002). Oxidative stress also leads to IR by the activity of iNOS. In skeletal muscle, the presence of iNOS resulted in degradation of IRS1 (Perreault and Marette, 2001). Similarly, higher abundance of NO can reduce Akt signaling by s-nitrosylation of a specific cysteine residue (Yasukawa et al., 2005). CCL2, also known as monocyte MCP-1 is a key player during IR in obese mice. The CCL2 knockout mice presented reduced ATM infiltration and improved insulin sensitivity. Another potential cause of IR is ER stress in AT. The induction of ER stress induces IR via JNK-mediated serine phosphorylation of IRS1. The detailed mechanisms of IR during ER were reviewed by Khan and Wang (2014).

CONCLUSIONS

Overall, the information presented in this review suggests that the AT function is strongly affected by endotoxin. The heightened susceptibility of AT to endotoxin entry is amplified by the capacity of HDL to transport and translocate endotoxins within adipocytes, primarily driven by increased expression levels of SR-BI and CD36 receptors. Activation of TLR4 by endotoxins triggers a broad range of stress responses within the AT. These stress responses include various mechanisms that affect AT function such as cytokine production, higher polarization of proinflammatory macrophages (M1), ER stress, mitochondrial dysfunction, and oxidative stress. The activation of stress responses is also responsible for affecting lipid metabolism in AT.

Remarkably, Endotoxin enhances lipolysis while adipogenic differentiation is impaired, which may play a significant role in the development of multiple periparturient diseases currently affecting the periparturient period. It is a need to continue expanding our knowledge of endotoxin and AT interactions in order to establish the necessary preventive measures that reduce the impact of endotoxins on dairy cows.

CHAPTER 2: LIPOLYSIS INHIBITION AS A TREATMENT OF CLINICAL KETOSIS IN DAIRY COWS, A RANDOMIZED CLINICAL TRIAL

Published in Journal of Dairy Science: M. Chirivi, D. Cortes-Beltran, A. Munsterman, A. O'Connor, G. A. Contreras. 2023. J. Dairy Sci. In press.

ABSTRACT

Excessive and protracted lipolysis in adipose tissues of dairy cows is a major risk factor for clinical ketosis (CK). This metabolic disease is common in postpartum cows when lipolysis provides fatty acids (FA) as an energy substrate to offset negative energy balance. Lipolysis in cows can be induced by the canonical (hormonally induced) and inflammatory pathways. Current treatments for CK focus on improving glucose in blood (i.e., oral propylene glycol (PG), or IV dextrose). However, these therapies do not inhibit the canonical and inflammatory lipolytic pathways. Niacin (NIA) can reduce activation of the canonical pathway. Blocking inflammatory responses with cyclooxygenase inhibitors such as flunixin meglumine (FM) can inhibit inflammatory lipolytic activity. The objective of this study was to determine the effects of including NIA and FM in the standard PG treatment for postpartum CK on circulating concentrations of ketone bodies. A 4-group, parallel, individually randomized trial was conducted in multiparous Jersey cows (n=80) from a commercial dairy in Michigan during a 7-month period. Eligible cows had CK symptoms (lethargy, depressed appetite, and milk yield) and hyperketonemia [blood β-hydroxybutyrate (BHB) ≥ 1.2 mmol/L]. Cows with CK were randomly assigned to one of three groups; T1) **PG**: 310 g oral once per day for 5 d; T2) **PG** for 5 d **+ NIA**: 24 g oral once per day for 3 d; T3) **PG** for 5 d **+ NIA** for 3 d **+ FM:** 1.1 mg/kg IV once per day for 3 d. The control group consisted of cows that were clinically healthy (**HC;** untreated; BHB < 1.2 mmol/L, n=27) matching for parity and DIM with T1, T2, and T3. Animals were sampled at enrollment (d0), d3, d7, and d14 to evaluate ketone bodies and circulating metabolic and

inflammatory biomarkers. Effects of treatment, sampling day, and their interactions were evaluated using mixed effects models. Logistic regression was used to calculate the odds ratio (OR) of returning to normoketonemia (BHB < 1.2 mmol/L). Compared to HC, enrolled CK cows exhibited higher blood concentrations of dyslipidemia markers, including non-esterified fatty acids (NEFA) and BHB, and lower glucose and insulin levels. Cows with CK also had increased levels of biomarkers of pain (substance P), inflammation, including LPS binding protein (LBP), haptoglobin (Hp), and serum amyloid A (SAA), and proinflammatory cytokines IL-4, MCP-1, MIP-1α, and TNFα. Importantly, 72.2% of CK cows presented endotoxemia and had higher circulating bacterial DNA compared to HC. By d7, the percentage of cows with normoketonemia were higher in PGNIAFM = 87.5%, compared to PG = 58.33%, and PGNIA = 62.5%. At d7 the OR for normoketonemia in PGNIAFM cows were 1.5 (95% CI, 1.03-2.17) and 1.4 (95% CI, 0.99-1.97) relative to PG and PGNIA, respectively. At d3, d7, and d14, PGNIAFM cows presented the lowest values of BHB (PG = 1.36; PGNIA = 1.24; PGNIAFM = 0.89 ± 0.13 mmol/L), NEFA (PG = 0.58; PGNIA = 0.59; PGNIAFM = 0.45 ± 0.02 mmol/L), and acute phase proteins. Cows in PGNIAFM also presented the highest blood glucose increment across time points and insulin by d7. These data provide evidence that bacteremia/endotoxemia, systemic inflammation, and pain may play a crucial role in CK pathogenesis. Additionally, targeting lipolysis and inflammation with NIA and FM during CK effectively reduces dyslipidemia biomarkers, improves glycemia, and improves overall clinical recovery.

INTRODUCTION

Periparturient diseases in dairy cows cost the US dairy industry $1.3 billion annually (Foreign Agriculture Service, 2011). Among these, ketosis or hyperketonemia predisposes cows to infectious and other metabolic diseases, alters their behavior, and increases their risk of death or being culled (McArt et al., 2012, McArt et al., 2015). Clinical Ketosis (**CK**) is characterized by reduced blood glucose concentrations, decreased appetite, and lethargy with plasma β-hydroxybutyrate (**BHB**) >1.2 mmol/L (Duffield, 2000, Dervishi et al., 2021). Additionally, CK increases the risk for displaced abomasum, laminitis, or early culling, and nearly 60% of CK cases co-occur with other periparturient health events (Probo et al., 2018). Therefore, improving CK therapeutics is paramount to maintaining periparturient cow health and well-being during the postpartum period and minimizing the negative impact of CK on lactation and reproductive efficiency.

Excessive fat mobilization from adipose tissues (**AT**) is a determining factor for CK's development, however, current CK therapies do not target lipolysis. Between approximately 3 weeks before parturition and 5 weeks postpartum, the rate of lipolysis in cows exceeds that of lipogenesis in AT. During this period, lipolysis is driven by hormonal changes associated with parturition and the onset of lactation. Lipolysis is also enhanced by energy deficits caused by high milk production and limited dry matter intake (Zachut and Contreras, 2022). Normally, as lactation progresses, AT lipolysis decreases, and lipogenesis begins to replenish adipocytes' triglyceride stores. However, when AT exhibits exacerbated inflammation and impaired responses to the anti-lipolytic effects of insulin, excessive lipolysis endures leading to CK.

Herdt and Emery (1992) proposed three pillars for the coherent treatment of CK: 1) reestablishing normal appetite; 2) restoring normal blood concentrations of glucose; 3) reducing

fatty acid (**FA**) availability for ketogenesis. Currently, the accepted treatment for CK is oral administration of propylene glycol [**PG**, (Gordon et al., 2013)]. Although PG provides glucose and stimulates gluconeogenesis, it does not have any effect on fat mobilization from AT. To inhibit lipolysis in dairy cattle it is necessary to target the two major lipolytic pathways: the canonical and the inflammatory (Chirivi et al., 2022). In the canonical pathway, catecholamines, growth hormone, and other pro-lipolytic hormones and peptides activate adipocyte membrane receptors that increase adenyl cyclase activity, which converts ATP to cAMP (Grisouard et al., 2010). The latter turns on protein kinase A that ultimately triggers hormone-sensitive lipase (**HSL)**, the enzyme with the highest lipolytic activity in AT around calving (De Koster et al., 2018a). The inflammatory pathway is triggered by the activation of the inflammatory signaling cascades MAPK and NFκB that stimulate protein kinase C that in turn, activates HSL (Chirivi et al., 2022).

Niacin (**NIA**) is a potent inhibitor of the canonical lipolytic pathway approved for use in lactating dairy cattle. Although NIA effectively reduces lipolysis (Pires et al., 2007), inhibiting the canonical lipolytic pathway alone may not suffice for effective CK treatment. Periparturient cows, especially those with CK, are in a proinflammatory state driven by physiological immune responses and by health events (e.g., heat stress, subacute ruminal acidosis, mastitis, metritis, retained placenta, lameness, pneumonia) that may lead to the entry of bacteria or endotoxins into the bloodstream. We recently showed that the endotoxin lipopolysaccharide (**LPS**) increases AT lipolysis by 70% compared to unstimulated conditions (Chirivi et al., 2022). These results suggested that inflammation may be a key modulator of lipolysis as it occurs during the early postpartum and CK. Given the proinflammatory environment in CK cows, a pharmacological approach using a cyclooxygenase (**COX**) inhibitor, such as flunixin meglumine (**FM**), could limit the activation of the lipolytic inflammatory pathway (Kovacevic et al., 2019, Inazumi et al., 2020).

However, whether the combination of NIA and FM exerts an inhibitory effect on lipolysis and improves CK recovery remains unknown. Using a randomized clinical trial, we tested the alternative hypothesis that the combination of PG, NIA, and FM improves the overall recovery of CK while reducing lipolysis and inflammatory biomarkers.

MATERIALS AND METHODS

Study Design

An individually randomized clinical trial was conducted on Jersey dairy cows in a single commercial dairy farm in Michigan, USA, from July 2021 until January 2022. We used a four-arm parallel controlled trial to assess the impact of three different interventions for the treatment of spontaneous CK in postpartum dairy cows and a negative control consisting of cows without ketosis who received no treatment. The study followed the animals for a period of 14 d after enrollment. All experimental procedures were approved by the Institutional Animal Care and Use Committee at Michigan State University (AUF:202100139). This report followed the guidelines of the REFLECT statement for reporting controlled clinical trials in livestock (Sargeant et al., 2010).

Animals

The farm was selected by convenience, given the voluntary willingness to participate in the study. The dairy had an average of 2645 lactating cows milked twice daily in a double 25 parallel herringbone parlor with an average of 25 kg of milk per cow per day. Animals were housed in free stalls with recycled manure solids as bedding. At this dairy, postpartum cows are screened multiple times throughout the day by two experienced farm staff members. These screenings aim to identify any signs of clinical disease. The study animals were selected from the population of postpartum dairy cows during a period of 7 months (n = 1250; Figure 3).

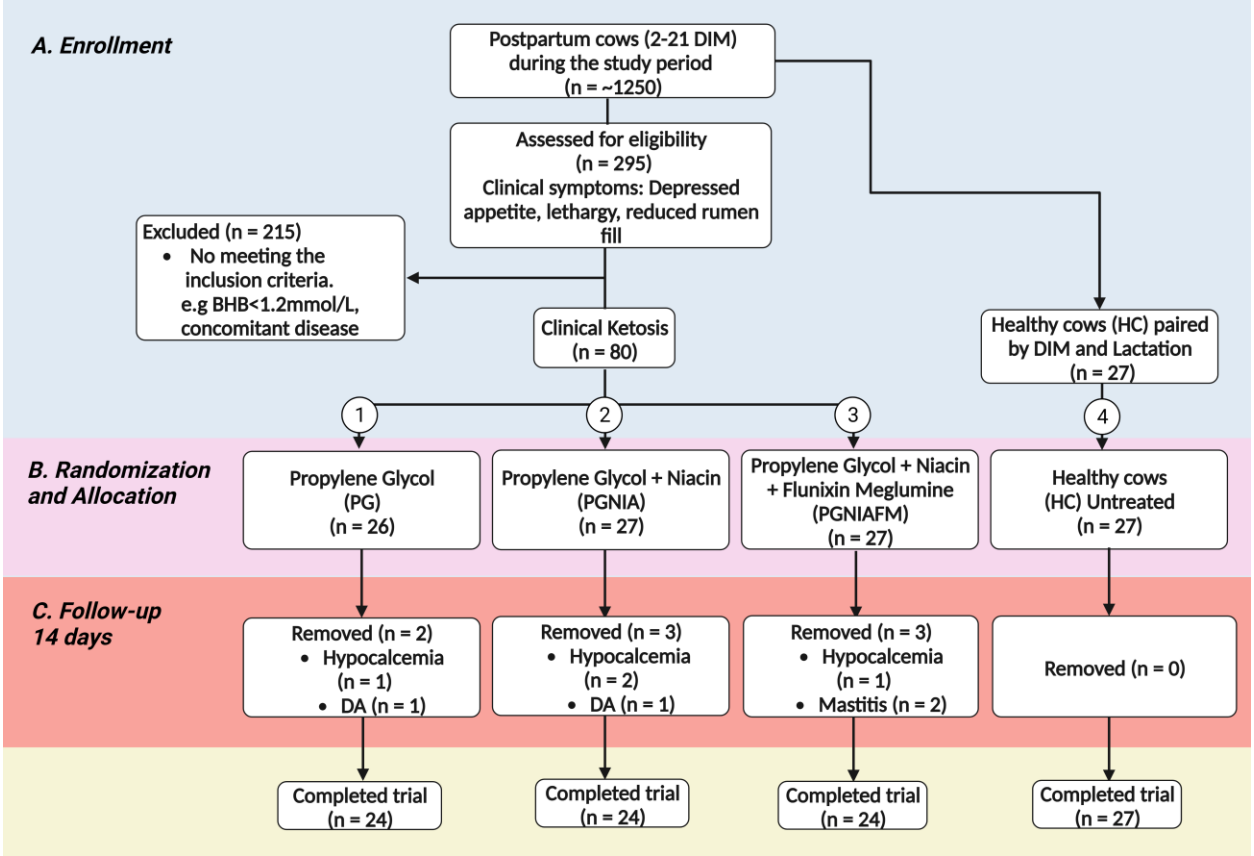

Figure 3. Clinical ketosis treatment randomized clinical trial flowchart. A) Enrollment: From a group of 1,250 dairy cows, 80 cows exhibiting symptoms of clinical ketosis were selected based on inclusion criteria (lethargy, depressed appetite, reduced milk yield and BHB>1.2 mmol/L). A group of healthy cows (HC) was selected based on matching CK cows' days in milk (DIM) and lactation number. B) Randomization Allocation: Selected CK cows were randomly assigned to 1 of 3 treatments for CK. C) Follow-up period was 14 d. During this time, a total of 8 cows were removed based on exclusion criteria. Created with Biorender**.**

Inclusion criteria for CK cases: multiparous dairy cows with 2-21 DIM presenting all the following findings: depressed appetite, reduced rumen fill, and lethargy. Only cows showing the above clinical signs (n = 295) were tested for hyperketonemia using the Precision Xtra® meter following manufacturer instructions and as described by Iwersen et al. (2009). *Clinical ketosis definition*: Cows with depressed appetite, reduced rumen fill, lethargy, and blood BHB > 1.2 mmol/L (hyperketonemia). Only cows matching CK definition were enrolled. Animals were assessed for eligibility without knowledge of allocation (Figure 3)

Exclusion criteria: having at least one concomitant disease at the time of enrollment,

including displaced abomasum, retained placenta, lameness, metritis, pneumonia, or clinical mastitis. Any animal that presented any of these diseases within 14 days after enrollment (follow-up) was removed from the trial (Figure 3).

Inclusion criteria for the healthy control cows (HC) group included: clinically healthy cows with no signs of disease and normoketonemia (blood BHB < 1.2 mmol/L). The HC animals were paired with CK cows based on their date of calving (± 2 days) and parity. BHB levels in HC were measured at the moment of recruitment and subsequently at the same time points as CK cows. Cows in the HC group were used to establish a baseline for metabolic and inflammatory biomarkers in non-ketotic animals on the farm. HC cows that presented any clinical disease within 14 days after enrollment were removed from the trial.

Treatments

All treatments started immediately after enrollment and randomization.

- **PG:** 310 g (300 mL) of oral propylene glycol [(**PG**) Propylene Glycol, USP Kosher, Interstate chemical company, Inc, USA] once per day for 5 days.
- **PGNIA:** PG for 5 days and 24 g of oral niacin [(**NIA**), NiaShure^{TM}, rumen-protected niacin, Balchem, USA] once per day for 3 days.
- **PGNIAFM:** PG for 5 days, NIA for 3 days, and 1.1 mg/Kg of BW of intravenous flunixin meglumine [(**FM**) Banamine ® Merck Animal Health, USA] once per day for 3 days.
- **HC:** healthy animals with normoketonemia did not receive any treatment.

Treatments were administered at ~ 11:00 am each day. Drugs within each treatment were given as follows:

Propylene glycol: (PG) was administered in a single bolus using a cattle drench gun after animal restraint. Niacin: Two gelatin capsules (Size 10 Torpac®) containing 12 g of NIA each were given

orally using a cattle bolus gun. Flunixin meglumine was injected in the jugular vein following a site preparation that included skin disinfection with 70% ethanol. Milk from cows treated with FM was discarded for at least 36 hours after the last injection.

All enrolled cows were examined daily during the study. The commercial dairy's cow health and welfare guidelines did not allow the inclusion of an untreated CK control; therefore, all animals received treatment. The study was designed to demonstrate the superiority of at least one CK treatment.

Objectives

The primary objective of this study was to investigate the effect of PG, PGNIA, and PGNIAFM treatment on circulating concentrations of ketone bodies defined as blood BHB concentration, and lipolysis markers in multiparous dairy cows with CK. A secondary objective was to characterize CK by comparing the metabolites of enrolled cows with a group HC, and the effect of treatments on the dynamics of blood inflammatory markers. The null hypothesis is that the concentrations of BHB are not reduced in cows with spontaneous CK after receiving the proposed treatments.

Outcomes

The primary outcome was blood BHB (mmol/L) concentration during the study period. The secondary outcome was the recovery from hyperketonemia, defined as animals with BHB < 1.2 mmol/L (normoketonemia) at d3, d7, and d14 after enrollment. Additional secondary outcomes included the blood concentrations of albumin, blood urea nitrogen, calcium, cholesterol, glucose, magnesium, non-esterified fatty acids (**NEFA**), total protein, triglycerides, endotoxin, bacterial 16S rDNA gene, haptoglobin (**Hp**), lipopolysaccharide-binding protein (**LBP**), serum amyloid A (**SAA**), noradrenaline, substance P (**SP)**, and a panel of 15 cytokines that included: interferon-

gamma (**IFNγ**), interleukin-1 alpha (**IL-1α**), interleukin-1 beta (**IL-1β**), interleukin-4 (**IL-4**), interleukin-6 (**IL-6**), interleukin-8 (**IL-8**), interleukin-10 (**IL-10**), interleukin-17A (**IL-17A**), interleukin 36 receptor antagonist (**IL-36RA**), interferon gamma-induced protein 10 (**IP-10/CXCL10**), monocyte chemoattractant protein-1 (**MCP-1/CCL2**), macrophage inflammatory protein 1-alpha (**MIP-1α/CCL3**), macrophage inflammatory protein 1-beta (**MIP-1β/CCL4**), tumor necrosis factor-alpha (**TNFα**), and vascular endothelial growth factor A (**VEGF-A**). Clinical and production data were recorded in the dairy management software Dairy Comp 305 (DC 305; Valley Agricultural Software, Tulare, CA).

Milk production was recorded and presented as descriptive findings. The evaluation of productive and reproductive parameters was outside the scope of this study.

Sample Size Determination

The sample size was calculated based on the guidelines for superiority trials in a four-arm randomized trial with a continuous variable reported by Zhong (2009). Using the formula $N = 4 \times \left(\frac{z_{1-\frac{\alpha}{2}+z_{1-\beta}}}{\delta}\right) \times s^2$ where Z is the critical value assuming a confidence level of 95% (alpha of 5%), a power of 80%, a minimum difference δ = 0.9 and a standard deviation S = 0.77 mmol/L of BHB among treatments, the sample size required was 23 cows per treatment. We aimed to enroll 25 to 27 cows per treatment, as we expected a 2-3% attrition.

Randomization -Sequence Generation

After a cow with CK was determined eligible, she was allocated to one of the three treatments using a sequence generated with an online random sequence generator (random.org) by a research team member not involved in the farm work. To recruit HC cows, a list of eligible healthy cows was generated using the calving date (±2 days) of three consecutive CK cows already enrolled. Each cow on the list was examined to determine their eligibility for inclusion in the HC

group.

Randomization -Allocation Concealment and Implementation

Randomization sequences were generated before starting the trial and given to the veterinarian leading the study at the farm. The treatment allocation was concealed until after the animals were determined eligible. Once eligibility was confirmed, the veterinary practitioner disclosed the treatment assigned to the farm staff.

Blinding of Intervention Delivery and Caregiving

Treatments were administered by farm personnel following cow ID and medication verification by the veterinarian conducting the trial at enrollment and daily until therapy was finished. Farm staff could not be blinded to the treatment group during the administration of the treatment or the study due to the different administration routes.

Outcome Measurement

Prior to treatment administration, blood samples were collected aseptically from coccygeal vessels by venipuncture on day 0 (i.e., enrollment, **d0**), 3 (**d3**), 7 (**d7**), and 14 (**d14**) relative to enrollment. Blood was collected in sterile 10-mL vacuum tubes with sodium heparin (BD Vacutainer® SST II Advance, BD Plymouth, UK) and clot activator (BD Vacutainer® SST Serum separation tubes: Hemogard, BD Plymouth, UK). Plasma samples were obtained after blood centrifugation at 2,500 × *g* for 10 min, and serum sample tubes were allowed to clot at RT for 30 min and centrifugated at 2,500 × *g* for 10 min. Samples were immediately frozen at -20 °C and transported to the laboratory to be stored at -80 °C, until further analysis.

Evaluation of Metabolic Parameters

Plasma concentrations of metabolites were quantified in duplicates in the small-scale biochemistry fully automated analyzer CataChemWell-T (Catachem Inc., Oxford, CT). Reagents

were obtained from the same manufacturer for albumin (V244-12), BHB (V444-0B), blood urea nitrogen (BUN) (V264-12), calcium (V294-12), cholesterol (V104-12), glucose (C124-12), magnesium (V322-12), NEFA (V514-0B), total protein (V254-12), and triglycerides (V114-12). The analyzer was calibrated every week using Catachem's calibrators Catacal^{TM}, Beta (β)-Hydroxybutyrate, and NEFA calibrator and 2 control level material (Catatrol^{TM} I, Catatrol^{TM} II, Beta (β)-Hydroxybutyrate Control I, Beta (β)-Hydroxybutyrate Control II, NEFA Control I and NEFA Control II, Catachem Inc.). The mean intra-assay coefficients of variation (**CV**) were 2.61%, 2.99%, 250%, 2.98%, 2.81%, 2.60%, 2.11%, 4.81%, 2.45%, and 3.29% for albumin, BHB, BUN, calcium, cholesterol, glucose, magnesium, NEFA, total protein, and triglycerides, respectively. The mean inter-assay CV were 7.68%, 8.75%, 9.28%, 8.50%, 8.75%, 8.65%, 8.60%, 8.15%, 8.75%, and 9.15%, respectively. A commercial enzyme-linked immunosorbent assay (**ELISA**) kit was used to determine plasma insulin (10-1201-01, Mercodia AB, Uppsala, Sweden) at d0 and d7. The assay was carried out using 96-well plates. Standards, samples, and low and medium control concentrations were run in duplicates. The intra- and inter-assay coefficients of variation were 2.99% and 7.58%, respectively.

Plasma Endotoxin Detection

Endotoxin units (**EU**) per mL of plasma were measured using the advanced recombinant Limulus amebocyte lysate (**LAL**) PyroSmart NextGen® (Associates of Cape Cod, Inc. East Falmouth, MA, USA). Recombinant LAL does not have factor G, which eliminates the potential 1,3-β-D-glucans cross reactivity present in other commercially available natural LAL kits (Stevens et al., 2022). The protocol was performed aseptically using endotoxin-free supplies and following manufacturer instructions. Before proceeding, samples were diluted (1:10, 1:20, 1:40, 1:80) in LAL Reagent Water (**LRW**) and incubated for 10 min at 75 °C. The percent of endotoxin recovery

was tested by spiking diluted samples with 5 µL of endotoxin standard (5 EU/mL). Dilution was considered optimal and free from interfering factors when the endotoxin recovery was within 50 – 200% (Stevens et al., 2022). Fifty (50) µL of standard, negative control (LRW) and sample (1:10 dilution) were loaded in 96 well plates. Next, LAL Recombinant reagent was reconstituted and 50 µL were added to each well. Immediately, kinetic absorbance was recorded every 30 sec for 1 hour at 405 nm. The reaction time (sec) needed to reach an absorbance threshold is used to construct the log converted onset time against the standard concentration. The range of detection was from 0.005 to 50 EU/mL. Measures were considered valid with an R value higher than 0.98 in the standards and CV lower than 15% within duplicate samples. The intra- and inter-assay coefficients of variation were 5.96% and 11.51%, respectively.

Bacterial DNA Quantification in Plasma

The amount of bacterial 16S rDNA gene in the blood is a marker of bacterial translocation and loss of gastrointestinal barrier function in different human diseases and animal models (Kramski et al., 2011, Vrakas et al., 2017, Whitfield-Cargile et al., 2021). The 16S ribosomal subunit is a pan-bacterial conserved region that allows the examination of bacterial translocation. We randomly selected a subset of fifteen plasma samples from each treatment group. The circulating free DNA was extracted from 1.5 mL of plasma from CK or HC at d0 and d7 using a commercial cfDNA isolation kit (Mag-Bind® cfDNA, Omega mBio-Tek, Inc, Norcross, GA, USA) following manufacturer instructions. The relative abundance of 16S rDNA was quantified using TaqMan gene expression assay (BA04930791_s1, Applied Biosystems, Waltham, MA, USA) targeting the 16S gene. Each 20 µL of reaction contains 10 µL of TaqMan Multiplex Master Mix (4461881, Applied Biosystems, Waltham, MA, USA), 1X of TaqMan gene expression, and 6 ng of DNA. All qPCR reactions were performed in duplicates, and no-template controls (**NTC**)

were included on each plate. Internal control for 16S amplification was included using purified bacterial DNA. Total DNA extracted from a pool of multiple bacteria was generously provided by the department of Microbiology and Molecular Genetics at Michigan State University. Purified bacterial DNA was serially diluted from 0 to 6 ng/µL to generate a standard curve (R^2=0.99) of amplification in the qPCR. Linear regression was used to estimate the relative bacterial DNA (ng/µL) in the blood samples.

Acute Phase Proteins (APP) and Pain Biomarkers

At d0 and d7, the plasma APP were quantified in a randomly selected subset of fifteen cows per treatment. Haptoglobin (**Hp**) was measured using a commercial colorimetric assay kit (Tridelta Development Ltd., Kildare, Ireland). Plasma lipopolysaccharide-binding protein (**LBP**) and serum amyloid A (**SAA**) were quantified using commercial ELISA kits (LBP: Cell Sciences InC., Newburyport MA, USA, and SAA: Tridelta Development Ltd., Kildare, Ireland). Procedures were performed following the manufacturer's instructions. The pain biomarkers noradrenaline (**NA**) and substance P (**SP**) were determined using commercial ELISA kits (NA: EkF57994 Biomatik Corporation. Kitchener, ON, Canada, SP: ADI-900-018A, ENZO Life Sciences. Farmingdale, NY, USA). Standards, internal quality controls, and samples were loaded in duplicate. Plasma samples were diluted in their respective assays buffer 1:2, 1:50, 1:500, and 1:10 for Hp, LBP, SAA, and SP, respectively. Absorbance readings were performed on an automatic microplate reader (Synergy^{TM} H1 Hybrid multi-mode, Biotek Instruments, Inc., Winooski, VT, USA). The mean intra-assay CV was 2.86, 2.4, 4.2, 3.01, and 3.42% for Hp, LBP, SAA, SP, and NA, respectively. The mean inter-assay CV was 8.32, 4.96, 7.8, and 9.7 % for SP, Hp, LBP, and SAA, respectively.

Bead-Based Multiplex Assay for Cytokine Detection

Cytokines were measured at d0 and d7 in the serum from ten cows randomly selected from each treatment. A commercially available multiplex immunoassay kit (Milliplex® Bovine Cytokine/Chemokine Magnetic Bead Kit, BCYT1-33K; Millipore, Sigma) was used following manufacturer instructions. The standard provided in the kit was serially diluted 6 times and samples were diluted 1:2 in the assay buffer. Twenty-five (25) µL of standards, samples, and low- and high-quality controls (**QC**) were added to a 96-well plate. Standards and QC were run in duplicate, while samples were run individually. Samples were incubated overnight at 4 °C with 25 µL of premixed 15-plex beads solution containing antibodies against bovine IFNγ, IL-1α, IL-1β, IL-4, IL-6, IL-8, IL-10, IL-17A, IL-36RA, IP-10/CXCL10, MCP-1/CCL2, MIP-1α/CCL3, MIP-1β/CCL4, TNFα, VEGF-A. After washing the plate 3 times, beads samples were incubated with antibody detection solution for 1 hour at room temperature (**RT**) and beads were incubated with streptavidin-phycoerythrin for 30 min at RT. Next, beads were washed and resuspended in sheath fluid and the *median fluorescent intensity (**MFI**)* of each well was acquired using the Luminex^{TM} 200^{TM} instrument system and processed with the Milliplex Analyst software. For each cytokine, the results were accepted if the control was between 75 and 125% of the expected values. IL-8 results were not considered valid since the MIF values of the samples fell over the higher limit of detection. The average intra-assay CV was 5.56%. Cytokine concentrations (reported in pg/mL) were calculated using the 5-parameter logistic regression fitting model.

Statistical Analysis

To evaluate the effect of the treatments, only animals that completed the 14-d sampling period without a secondary disease were included in the analysis (Figure 3). Statistical analyses were performed using JMP Pro16 (SAS Inst., Inc., Cary NC). To characterize CK cows, an

unpaired t-test was used to assess differences at enrolment between CK and HC cows in the continuous variables: plasma metabolites, days in milk (DIM), dry days in the previous lactation, and open days in the previous lactation. Results are presented as mean ± SEM. To assess possible differences between treatment groups at the time of enrollment (d0), a nominal logistic model was used to evaluate the parity effect. Residuals for the BHB, NEFA, albumin, total protein, endotoxin, LBP, Hp, and SAA were not normally distributed. These variables were $\log_{10}$ transformed for statistical analysis, and model fit was reassessed.

A generalized linear mixed model assessed the treatment effect on BHB concentrations and secondary continuous outcomes (albumin, BUN, calcium, cholesterol, glucose, magnesium, NEFA, total protein, and triglycerides). The outcome models accounted for the random effect of cow, the fixed effect of treatment, and time and the interaction of treatment and time. Days after treatment (d3, d7, and d14) were included as repeated measures. One-way ANOVA analysis was performed to evaluate differences between treatments for secondary outcomes at d7 (insulin, Hp, LBP, SAA, Endotoxin, 16S bacterial DNA, cytokines, SP, and NA). Tukey's post hoc adjustment test was used for pairwise comparisons. Data are presented as means and SEM unless otherwise indicated. Effects were considered significant if $P<0.05$. Non-significant ($P>0.05$) two-way interactions were removed from the model.

Hyperketonemia recovery. Animals with normoketonemia (BHB < 1.2 mmol/L) at d3, d7, and d14 were considered recovered for this study. The difference in hyperketonemia recovery between treatments was tested by a nominal logistic model using the Cochran Mantel Haenszel method adjusted by lactation. The odds ratio (**OR**) for having normoketonemia and 95% CI were calculated and all pairwise comparisons are Wald test based.

Endotoxin values below the limit of detection (**LD**) <0.05 EU/mL, were substituted with a

constant value (0.05/square root of 2). A secondary analysis was performed to estimate the percentage of animals with detectable endotoxin during CK. As previously described, endotoxin values were classified as categorical variables (Wittek et al., 2004). Animals with endotoxin values below the LD were cataloged as negative, while those above the LD were considered *positive for endotoxemia*. Nominal logistic analysis was performed, and Chi-square was used to estimate differences among groups and the OR of being positive for endotoxemia.

Ancillary analysis: Statistical analyses also calculated associations between BHB concentrations of CK cows at d0 and the secondary outcomes measured in plasma. Pearson correlation coefficients were calculated for all plasma metabolites. This exploratory analysis evaluated the relationship between hyperketonemia and inflammatory markers. Additionally, we estimated correlation coefficients for BHB values measured with the Precision Xtra® handheld device and colorimetric-based BHB detection to confirm the accuracy of the portable device in enrolling CK cows in our study. We used a nominal logistic model to obtain receiver operating characteristics (ROC) and evaluated the sensitivity and specificity of the cow-side device for hyperketonemia detection (>1.2 mmol/L) compared to the laboratory-based plasma evaluation.

RESULTS

From a total of 1058 cows eligible to be enrolled during this study, 80 fulfilled the CK inclusion criteria. From the latter, 8 were removed because they developed a concomitant disease. Two cows in the PG and three in the PGNIA group presented hypocalcemia and displaced abomasum, and 3 cows in the PGNIAFM developed hypocalcemia and mastitis during the sampling period (Figure 3). Descriptive statistics of the study population are summarized in Table 1. At enrollment, DIM, parity, number of cows allocated, and previous lactation days dry were equally distributed among treatments, including the HC group (Table 1). As expected, blood BHB

(precision Xtra®) was higher in CK cows compared with the HC group (Table 1; *P*<.0001). The BHB values obtained with the precision Xtra® handheld device had a high correlation with the colorimetric-based BHB detection used in the laboratory (R^2 = 0.91). The sensitivity and specificity of the precision Xtra® device for hyperketonemia detection (BHB>1.2 mmol/L) were 97% (CI: 92.93%-99.64%) and 100% (CI: 96.26%-100%), respectively.

Table 1. Baseline characteristics of treatment allocation groups.

Parameter	Treatment allocation groups CK[1]			HC[2]	*P value*
	PG	PGNIA	PGNIAFM		
Days in milk (SD)	6.37 (3.09)	7.33 (3.79)	7.45 (3.93)	7.03 (4.47)	0.89
Parity mode and range	Mo=3 R=2-5	Mo=3 R=2-5	Mo=3 R=2-5	Mo=3 R=2-5	0.85
Previous dry days (SD)	59.79 (13.72)	60.37 (20.23)	58.13 (12.20)	54.01 (6.01)	0.65
BHB enrollment[3] (SD)	2.35 (1.07)[a]	2.15 (0.85)[a]	2.57 (1.26)[a]	0.70 (0.18)[b]	<0.0001
Milk kg/day[4]					
Day 0 (SD)	20.64 (7.37)	22.22 (8.38)	18.99 (7.53)	23.53 (8.43)	N/A[5]
Day 7 (SD)	23.81 (8.94)	24.38 (7.72)	22.01 (8.26)	26.54 (7.03)	N/A
Day 14 (SD)	25.85 (8.01)	29.35 (6.23)	25.58 (8.85)	30.67 (6.23)	N/A

[1]Treatments allocation for clinical ketosis (CK) cows with BHB>1.2 mmol/L at d0: PG = Propylene Glycol, PGNIA = PG + Niacin, PGNIAFM = PGNIA + flunixin meglumine.
[2]HC = Healthy cows with no sign of disease and BHB<1.2 at d0.
[3]BHB = Beta-hydroxybutyrate measured with cow-side Precision Xtra device. SD = standard deviation.
[4]Milk production: Data are mean values from enrollment day (d0). The evaluation of milk yield was outside the scope of this study.
[5]N/A = Not applicable.
[a-c]Mean values in the same row with different superscripts differ (*P*<0.05) by ANOVA analysis and adjusted by Tukey.

CK is Associated with Changes in Metabolic Function Biomarkers

At enrollment (i.e., d0), all CK cows exhibited higher plasma BHB and NEFA when compared to HC (Table 2; *P*<0.001). In contrast, CK cows presented lower plasma albumin,

cholesterol, glucose, insulin, and total protein than HC (Table 2; $P<0.01$). Importantly, there was no evidence of meaningful differences among cows assigned to the three treatment groups at enrollment in any of the blood metabolites analyzed, except for cows enrolled in PGNIAFM that presented lower cholesterol (mean = 56.21, SEM = 4.27 mg/dL) compared to cows in PG (mean = 62.5, SEM = 4.27) and PGNIA (mean = 68.62, SEM = 4.27; $P<0.05$). No differences were found at d0 between HC and all CK cows in plasma concentrations of BUN, calcium, magnesium, and triglycerides (Table 2). Complete results across d3 d7 and d14 are presented in appendix Table 11 Chirivi 2023).

Table 2. Baseline blood metabolites in dairy cows with or without clinical ketosis.

	CK[1]		HC[2]		
Parameter[3]	Mean[3]	SEM	Mean	SEM	*P*-Value[4]
Albumin g/dL	4.29	0.07	4.78	0.11	<0.0001
BHB mmol/L	2.24	0.09	0.67	0.15	<0.0001
BUN mg/dL	9.83	0.45	10.02	0.74	0.89
Calcium mg/dL	9.17	0.15	9.52	0.25	0.66
Cholesterol mg/dL	62.44	2.49	74.74	4.07	<0.01
Glucose mg/dL	56.86	1.38	70.56	2.25	<0.0001
Insulin µg/mL	0.12	0.04	0.47	0.07	<0.001
Magnesium mg/dL	2.77	0.06	2.67	0.10	0.51
NEFA mmol/L	0.67	0.03	0.39	0.05	<0.001
Total Protein g/dL	6.65	0.09	7.29	0.15	<0.001
Triglycerides mg/dL	10.09	0.62	9.48	1.01	0.50

[1]Clinical ketosis (CK) cows (n = 72) with hyperketonemia (BHB>1.2 mmol/L) at d0.
[2]HC = Healthy cows (n = 27) with no sign of disease and normoketonemia (BHB<1.2) at d0.
[3] Data are mean values from enrollment day (d0). Variables were measured with colorimetric method. BHB = Beta-hydroxybutyrate. BUN = blood urea nitrogen NEFA = non-esterified fatty acids.
[4]Significance from unpaired t-test. For statistical analyses albumin, BHB, NEFA, and total protein were $\log_{10}$ transformed.

CK Cows have Increased Biomarkers of Endotoxemia and Bacteremia

At enrollment, cows with CK presented higher plasma concentrations of endotoxin and bacterial DNA compared to HC group (Figure 4A-B; $P<0.05$). The percentage of cows positive for endotoxemia was higher in CK (72.2%) compared to HC (33.3%) $P<0.001$. Cows with CK

were more likely to present endotoxemia than HC (OR = 2.1 95% CI = 1.21-3.86). Similarly, APP including LBP, Hp, and SAA were higher in CK cows than HC (Figure 4 C-E).

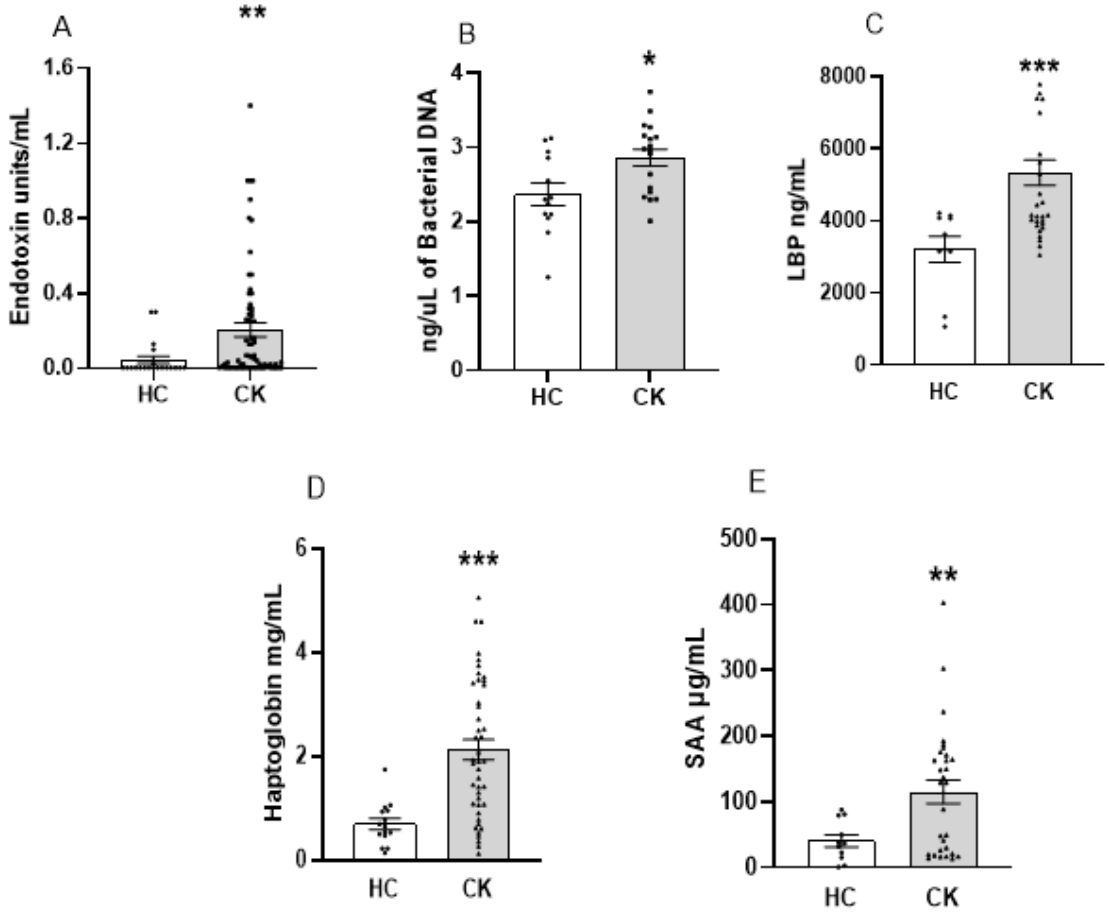

Figure 4. Endotoxin, bacterial DNA, and acute phase proteins are elevated in cows with clinical ketosis. Plasma concentrations at enrollment (day 0) of endotoxin **(A)**, bacterial DNA **(B)**, LPS binding protein (LBP) **(C)**, Haptoglobin **(D)**, and Serum amyloid A (SAA) **(E)**, in healthy (HC) and clinical ketosis (CK) cows. Error bars represent the SEM Bars with * differ (P<0.05) or ** (P<0.01) or *** (P<0.001). HC n=27, CK n=72 for (A); HC n=15, CK n=45 for (B-E). P values are from to log10 transformed data analysis in endotoxin, LBP, haptoglobin, and SAA.

Cytokine Profile and Pain Biomarkers in CK Cows

Serum concentrations of proinflammatory cytokines IL-4, IL-36RA, MCP-1, MIP-1α, and TNFα were elevated in CK cows (Table 3; *P*<0.05). Serum IFNγ, IL-1α, IL-1β, IL-6, IL-10, IL-17A, IP-10, MIP-1β, and VEGF-A were not different between CK and HC (Table 3). The circulating pain biomarker neuropeptide SP presented elevated concentrations in plasma from CK

animals compared to HC (Table 3; $P<0.01$). No differences between CK and HC were observed in noradrenaline/norepinephrine concentrations.

Table 3. Cytokine profile and pain biomarkers in dairy cows with or without clinical ketosis.

		CK[1]		HC[2]		
	Parameter pg/mL	Mean	SEM	Mean	SEM	*P*-Value[5]
Cytokine[3]	IFNγ	4.04	1.04	6.01	1.20	0.21
	IL-1α	43.94	7.16	31.06	12.40	0.37
	IL-1β	15.65	5.37	3.44	9.81	0.28
	IL-4	61.55	6.57	28.90	13.37	<0.05
	IL-6	1703.11	213.91	2037.58	414.23	0.47
	IL10	311.72	36.01	293.58	62.36	0.80
	IL17-A	2.62	0.51	3.57	1.03	0.41
	IL36-RA	637.17	51.26	480.31	68.78	<0.05
	IP-10	1937.72	179.07	1868.51	304.94	0.84
	MCP-1	1198.92	96.08	906.66	166.41	<0.05
	MIP-1α	486.28	53.18	326.76	62.10	<0.01
	MIP-1β	209.39	30.93	217.67	53.58	0.79
	TNF-α	4160.70	605.58	2574.10	648.90	<0.05
	VEGF-A	325.65	27.12	284.94	46.97	0.45
Pain biomarker[4]	SP	3894	198.1	2533	323.6	<0.01
	NA/NE	328.7	41.47	230.6	92.39	0.31

[1]Clinical ketosis (CK) cows (n = 30) with hyperketonemia (BHB>1.2 mmol/L) at d0.
[2]HC = Healthy cows (n = 10) with no sign of disease and normoketonemia (BHB<1.2) at d0.
[3] Data are mean values from enrollment day (d0). Cytokines were measured with Milliplex Bovine magnetic bead panel.
[4] Data are mean values from enrollment day (d0). SP = Substance P, NA/NE = noradrenaline/norepinephrine.
[5]Significance from unpaired t-test.

CK is Associated with Inflammation and Endotoxemia Biomarkers

Correlation coefficients were calculated for BHB, NEFA, albumin, cholesterol, glucose, insulin, total protein, endotoxin, and APP (Hp, LBP, and SAA) in CK cows at d0 (Figure 5). Parameters with non-significant correlations were removed from the matrix. BHB was negatively correlated with concentrations of albumin (-0.37), cholesterol (-0.45), glucose (-0.63), insulin (-0.26), and total protein (-0.31) and positively correlated with NEFA (0.33). Surprisingly, plasma BHB concentrations were positively associated with endotoxin (0.29), Hp (0.26), and LBP (0.43).

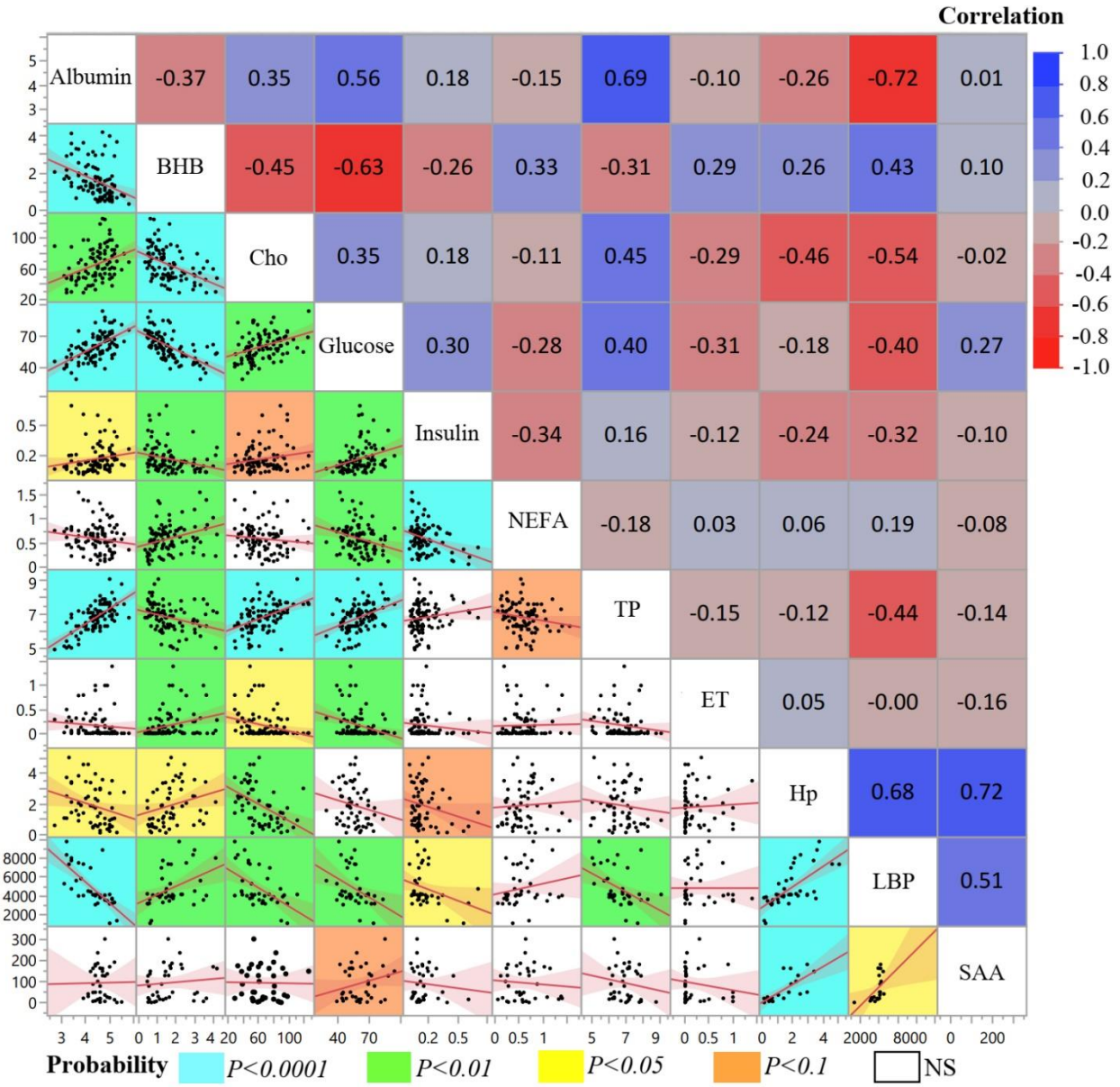

Figure 5. Pearson correlation coefficients for plasma metabolic analytes in dairy cows with clinical ketosis. Albumin g/dL, BHB = β-hydroxybutyrate mmol/L, Cho = Cholesterol mg/dL, Insulin µg/mL, Glucose mg/mL, NEFA = non-esterified fatty acids mmol/L, TP = Total Protein g/dL, ET = Endotoxin EU/mL, Hp = Haptoglobin mg/mL, LBP = LPS binding protein ng/mL, SAA = Serum amyloid A µg/mL. Correlation values R are presented in the top-right (Red = -1, gray = 0, blue = 1) of the matrix while scatterplots matrix is in the left button. P values are represented as the scatter plot background color (Cyan = *P*<0.0001; Neon = *P*<0.01; Yellow = *P*<0.05; Light salmon = *P<0.1:* White = non-significant (NS) n=72.

Similarly, NEFA was negatively correlated with glucose (-0.28) and insulin (-0.34) but not associated with Hp, LBP, and SAA levels. Plasma insulin values were positively associated with glucose (0.29) and albumin (0.18). Likewise, the abundance of Hp, LBP, and SAA were strongly

correlated. Finally, cholesterol levels were negatively associated with endotoxin, Hp, and LBP. The total list of correlation values is presented in Figure 5.

PGNIAFM Improved Biomarkers of Dyslipidemia in CK Cows

Independent of the treatment used, by d3, d7, and d14, plasma BHB was reduced compared to d0 in CK cows (Table 11). However, PGNIAFM cows had the lowest BHB values and were similar to those observed in HC across the study (Table 4; $P<0.0001$). By d3, the percentage of CK cows with normoketonemia (BHB<1.2 mmol/L) was not different among groups (PG = 58.33%; PGNIA = 66.71%; PGNIAFM = 79.17%; Table 5). Nevertheless, by d7, 87.5% of PGNIAFM cows had normoketonemia compared to 58.33% of PG and 62.5% of PGNIA. Therefore, by d7 PGNIAFM cows were 1.5 and 1.4 times more likely to have normoketonemia than PG and PGNIA, respectively (Table 5; $P<0.05$). By d14 the percentage of CK cows with normoketonemia was not different among groups (PG = 70.83%; PGNIA = 79.17%; PGNIAFM = 91.67%; Table 5).

PGNIAFM reduced plasma NEFA compared to other treatments at d3, d7, and d14 ($P=0.05$; Table 4). During the study, treatment did not affect plasma albumin and total protein levels. However, CK cows remained with low levels of albumin and low total protein content compared to those in the HC group (Table 4). Cholesterol remained low in CK cows compared to HC (Table 4). Cholesterol presented a linear increase ($P<0.001$) across time in both CK and HC, with a daily average rise of 2.57 ± 0.44, 2.63 ± 0.65, and 2.19 ± 0.56 mg/dL in PG, PGNIA, and PGNIAFM, respectively. Nonetheless, cholesterol in HC cows increased more rapidly compared to CK, exhibiting a daily increment of 4.03 ±0.45 mg/dL. Glucose levels did not present changes in PG and PGNIA treatments compared to enrolment, however, cows that received PGNIAFM presented a sudden glycemic surge at d3 that persisted through d7 and d14 (Table 4; $P<0.001$). By

d7, insulin concentrations improved in PGNIAFM cows compared to other treatments (Table 4; $P<0.01$). Treatment did not affect BUN, calcium, magnesium, and triglyceride plasma levels (Table 4).

Table 4. Blood metabolites were positively influenced by PGNIAFM in dairy cows with ketosis on d3, d7 and d14.

Metabolite[2]	Treatment group[1]					P [3]
	PG	PGNIA	PGNIAFM	HC	SEM	Treatment
BHB mmol/L	1.36[a]	1.24[ab]	0.89[b]	0.63[bc]	0.13	<0.0001
Cho mg/dL	82.61[b]	81.67[b]	78.71[b]	106.09[a]	3.1	<0.001
Glucose mg/dL	60.65[b]	60.57[b]	66.17[a]	71.32[a]	1.39	<0.0001
Albumin g/dL	4.31[b]	4.20[b]	4.17[b]	4.82[a]	0.11	<0.0001
BUN mg/dL	9.67	10.11	9.15	10.39	0.58	0.43
Ca^{+} mg/dL	9.02	8.98	9.15	9.23	0.21	0.52
Insulin µg/mL	0.14[b]	0.13[b]	0.23[a]	0.26[a]	0.03	<0.01
Mg^{+} mg/dL	3.01	2.96	2.93	2.75	0.09	0.24
NEFA mmol/L	0.58[a]	0.59[a]	0.45[b]	0.38[c]	0.002	0.05
TP g/dL	6.75[b]	7.11[b]	6.95[b]	7.65[a]	0.15	0.002
TG mg/dL	8.79	8.95	7.98	8.84	0.88	0.82

[1]Treatments for clinical ketosis (CK) cows with BHB>1.2 mmol/L: PG = Propylene Glycol, PGNIA = PG + Niacin, PGNIAFM = PGNIA + flunixin meglumine. HC = Healthy cows with no sign of disease and BHB<1.2 at d0.

[2] Data are mean values from d3, d7, and d14 after enrollment. BHB = Beta-hydroxybutyrate. Cho = Cholesterol. BUN = blood urea nitrogen. Ca^{+} = Calcium. Mg^{+} = Magnesium. NEFA = non-esterified fatty acids. TP = Total protein. TG = triglycerides measured with colorimetric method.

[3]*P* values are from one-way ANOVA analysis. For statistical analysis albumin, BHB, NEFA, and total protein were $\log_{10}$ transformed.

[a-c]Mean values in the same row with different superscripts differ ($P<0.05$) adjusted by Tukey.

Table 5. Recovery rate at day 3, 7 and 14 for a randomized controlled trial comparing PG, PGNIA and PGNIAFM.

Parameter			Numerator treatment group[1]		
			PG n = 24	PGNIA n = 24	PGNIAFM n = 24
No. Cows Recovered [2]					
	Day 3		14 (58.33%)	16 (66.71%)	19 (79.17%)
	Day 7		14 (58.33%)	15 (62.5%)	21 (87.5%)
	Day 14		17 (70.83%)	19 (79.17%)	22 (91.67%)
Pairwise Odds Ratio (95%CI)[3]					
Reference Treatment	d3	PG	N/A	1.42 (0.44-2.60) *P* = 0.55	2.7 (0.75-5.41) *P* = 0.12
		PGNIA	0.70 (0.23-2.21) *P* = 0.55	N/A	1.9 (0.51-4.91) *P* = 0.33
		PGNIAFM	0.36 (0.10-1.32) *P* = 0.12	0.52 (0.14-1.73) *P* = 0.33	N/A
Reference Treatment	d7	PG	N/A	1.19 (0.37-3.79) *P* = 0.76	1.5 (1.03-2.17) *P* = 0.02*
		PGNIA	0.84 (0.26-2.5) *P* = 0.76	N/A	1.4 (0.99-1.97) *P* = 0.04*
		PGNIAFM	0.2 (0.04-0.81) *P* = 0.02*	0.23 (0.05-0.96) *P* = 0.04*	N/A
Reference Treatment	d14	PG	N/A	1.5 (0.40-2.55) *P* = 0.50	1.49 (0.97-1.71) *P* = 0.06
		PGNIA	0.63 (0.17-2.35) *P* = 0.50	N/A	1.15 (0.91-1.46) *P* = 0.23
		PGNIAFM	0.22 (0.04-1.20) *P* = 0.06	0.34 (0.05-1.95) *P* = 0.23	N/A

[1]Treatments for clinical ketosis (CK) cows with BHB>1.2 mmol/L: PG = Propylene Glycol, PGNIA = PG + Niacin, PGNIAFM = PGNIA + flunixin meglumine.
[2]Recovery was defined as animals with normoketonemia (BHB < 1.2 mmol/L) at d3, d7, and d14.
[3]The odds ratio (OR) for having normoketonemia and *P* value and 95 % confidence interval (95%CI) are Wald test based.
No. = Number, BHB = Beta-hydroxybutyrate measured with colorimetric based method, N/A = not applicable.

PGNIAFM Reduced Inflammation in CK Cows

Blood markers of inflammation at d7 are summarized in Table 6. Cows treated with PGNIAFM presented lower Hp, and SAA than PGNIA and PG ($P<0.05$). Endotoxin, bacterial DNA, LBP, and SP were not affected by treatment. However, the percentage of cows positive for

endotoxemia was still higher in CK-treated cows compared to HC (PG = 62.5%, PGNIA = 62.2%, PGNIAFM = 66.7%, and HC = 25%; $P<0.05$). The concentrations of MIP-1α and TNF-α that were more abundant at d0 in CK cows presented a reduction at d7 in all three treatments. Animals treated with PGNIAFM had lower concentrations of IL-6 compared to PG or PGNIA at d7. But only PGNIA and PGNIAFM cows presented low concentrations of IL-17A. No differences were observed in serum concentrations of IFNγ, IL-1β, IL-4, IL-36A, IP-10, MIP-1β, and VEGF-A among CK-treated cows and HC after d7.

DISCUSSION

Ketosis is the most common metabolic disorder in dairy cows and is associated with increased risk for other diseases, poor animal welfare, reduced milk production, and impaired reproductive performance (McArt et al., 2015). Early studies indicated that excessive NEB and lipolysis are critical factors in the pathogenesis of the disease; therefore, an efficient CK treatment should reduce lipolysis and improve gluconeogenesis (Cote, 1971, Herdt and Emery, 1992). However, PG, the most widely used CK therapy, is effective only in 50% of the cases, and hyperketonemia relapse is common (Gordon et al., 2017). The limited efficacy of PG may be attributed to its minimal effects on reducing lipolysis and inflammation. The present study demonstrates that cows with CK exhibit dyslipidemia, systemic inflammation, and high circulating endotoxin and bacterial DNA levels. Thus, endotoxemia may be a determining factor in the development of CK during early lactation. Our results also demonstrate that using NIA and FM combined with PG reduced lipolysis and improved CK recovery.

Table 6. Inflammatory and pain biomarkers were influenced by PGNIAFM in dairy cows with ketosis.

Metabolite[2]	Treatment group[1]					*P* [3]
	PG	PGNIA	PGNIAFM	HC	SEM	Treatment
Endotoxin	0.16	0.22	0.18	0.04	0.06	0.11
16S rDNA	1.95	2.05	2.11	1.81	0.19	0.62
Hp	1.89[a]	1.56[a]	0.95[b]	1.51[a]	0.30	0.04
LBP	3891.13	3635.10	3641.38	3482.90	302.49	0.45
SAA	70.43[a]	65.88[a]	27.89[b]	27.45[b]	19.99	0.03
SP	2663.89	2860.48	2615.26	2665.84	255.55	0.28
IFNγ	4.97	5.53	4.18	7.47	1.10	0.23
IL-1α	32.61[a]	34.80[a]	33.64[a]	19.06[b]	5.31	0.07
IL-1β	10.73	13.49	12.30	13.75	4.84	0.91
IL-4	53.59	44.33	47.76	48.65	4.78	0.59
IL-6	1033.66[a]	1005.55[ab]	826.00[b]	785.33[b]	51.13	<0.01
IL-10	287.29[a]	261.77[a]	257.76[a]	185.55[b]	30.91	0.08
IL-17A	19.62[a]	3.14[b]	6.09[b]	3.90[b]	3.70	0.04
IL36-RA	535.18	602.76	781.59	627.17	111.83	0.49
IP-10	1760.89	1875.68	1807.34	1648.00	171.10	0.84
MCP-1	1145.69[a]	1010.85[ab]	949.13[b]	723.53[b]	110.41	0.08
MIP-1α	380.33	395.21	384.09	295.74	31.25	0.27
MIP-1β	205.74	207.80	199.58	149.08	24.07	0.29
TNF-α	2922.80	3011.61	3250.00	2468.57	241.87	0.39
VEGF-A	339.34	279.12	289.18	354.12	40.23	0.48

[1]Treatments for clinical ketosis (CK) cows with BHB>1.2 mmol/L: PG = Propylene Glycol, PGNIA = PG + Niacin, PGNIAFM = PGNIA + flunixin meglumine. HC = Healthy cows with no sign of disease and BHB<1.2 at d0.
[2] Endotoxin = EU/mL, 16S rDNA = ng/mL, Hp= Haptoglobin mg/mL, LBP= LPS binding protein ng/mL, SAA= Serum amyloid A µg/mL, SP= Substance P pg/mL (IFNγ, IL-1α, IL-1β, IL-4, IL-6, IL-10, IL-17A, IL-36RA, IP-10, MCP-1, MIP-1α, MIP-1β, TNFα, VEGF-A) pg/mL.
[3]*P*-values refer to the main effect of treatment. *P* values are from to $\log_{10}$ transformed data analysis in endotoxin, LBP, Hp and SAA.
[a-c]Mean values in the same row with different superscripts differ (*P*<0.05) adjusted by Tukey. Data are mean values d7 after enrollment. n=10-15.

CK Cows Exhibit Dyslipidemia

CK is more common in animals in NEB, such as periparturient cows. Low energy levels activate metabolic adaptations favoring lipolysis in AT, leading to higher availability of NEFA for ketogenesis. As expected, CK cows in the present study showed hyperketonemia, high lipolysis rates (i.e., elevated blood NEFA), hypoglycemia, and hypoinsulinemia when compared to healthy

cows. Excessive lipolysis is one of CK's signature findings, mainly promoted by the impaired response of AT to the antilipolytic effects of insulin (Contreras et al., 2017b). Since lipolysis drives hepatic ketogenesis, limiting it is critical to reducing hyperketonemia. Remarkably, ketone bodies are potent inhibitors of gluconeogenesis (Zarrin et al., 2013). However, this inhibition could potentially worsen the hypoglycemic and lipolytic conditions commonly observed during CK.

Low plasma cholesterol levels are commonly reported in animals with ketosis (Djokovic et al., 2014), and CK cows enrolled in this study were no exception. Limited cholesterol biosynthesis during CK may be associated with a compromised export rate of cholesterol and possibly reduced hepatic function. Similar to cows experiencing hepatic steatosis, cows with CK exhibit an excessive influx of fatty acids into the liver, leading to a diminished ability to produce lipoproteins and enzymes essential for lipid transport. (Kessler et al., 2014). In contrast to blood cholesterol, we did not observe differences in triglyceride concentrations between HC and CK cows in the present study. These observations align with previous reports characterizing blood cholesterol in CK (Zhang et al., 2013). However, low concentrations of triglycerides are reported during subclinical ketosis (González et al., 2011). Gonzalez and colleagues hypothesized that hepatocytes accumulate triglycerides due to the reduced lipid export leading to hepatic lipidosis. In summary, our results demonstrate that CK coincides with lipid metabolism alterations in periparturient cows characterized by excessive circulating NEFA and BHB and limited cholesterol production that may impact the biosynthesis of lipid transporters and buffering proteins such as lipoproteins.

Systemic Inflammation in Cows Affected by CK

In dairy cows, systemic inflammation is a whole body response to external (pathogen-associated molecular patterns—PAMP e.g. bacterial endotoxins) and internal (damaged associated molecular pattern—DAMP) stimuli (Tang et al., 2012). This inflammatory response is

characterized by increased cytokine release, hypoalbuminemia, and enhanced hepatic production of Hp, SAA, LBP, ceruloplasmin, and C-reactive protein (Bradford et al., 2015). Several authors have documented elevated levels of plasma inflammatory markers such as LBP, SAA, Hp, IL-1, and IL-6 in cows suffering from CK (Abuajamieh et al., 2016, Zhang et al., 2016). Consistent with these findings, our current study revealed a heightened inflammatory response in CK cows.

APP are plasma proteins synthesized in the liver that can either increase (positive APP) or decrease (negative APP) in response to inflammation. In ruminants, the positive APP with the most significant response during inflammation are LBP, Hp, and SAA. In line with an inflammatory state, the present study observed a substantial increase in these APP at d0 in cows with CK when compared to HC cows. Notably, LBP plays a pivotal role in the innate immune response against bacterial infections. SAA is mainly produced in the liver following stimulation by cytokines such as TNFα, and it serves as a regulator of immune responses by promoting chemotaxis, cell migration, and opsonization of diverse bacteria (Uhlar and Whitehead, 1999). Hp is used as a marker of inflammation and a predictor of disease in dairy cows (Manimaran et al., 2016). Hp binds to free hemoglobin resulting in lower iron availability for bacteria, and it has anti-inflammatory properties (Ceciliani et al., 2012). A previous study demonstrated that cows with ketosis had increased positive APP even before hyperketonemia develops (Abuajamieh et al., 2016). The increased concentration of positive APP observed in the present study confirm that cows with CK present systemic inflammation.

CK cows presented low concentrations of albumin during the duration of the present study. This finding is in line with previous reports documenting similar findings in cows affected by CK (Ha et al., 2022). The mechanism by which albumin concentrations fall in inflammation is mainly due to reduced liver production (Moshage et al., 1987). However, as insulin is also required to

maintain hepatocytes' albumin synthesis (Chen et al., 2016), the low plasma insulin levels observed in CK cases during the present study may favor lipolysis and contribute to low albumin production.

We observed higher production of IFNγ, IL-4, IL-36RA, MIP-1α, MCP-1, and TNFα in CK cows. Cytokines, produced by T-helper cells and macrophages in response to pathogens, act as the initial alarm of inflammation, stimulating, recruiting, and activating immune cell proliferation (Zhang and An, 2007). To our knowledge, only one study reported elevated concentrations of cytokines (IL-6, IL-10, and TNFα) in cows with subclinical and CK (Brodzki et al., 2021). IL-4 is a proinflammatory cytokine, while IL-36RA inhibits proinflammatory activation of immune cells (Zhu et al., 2010, Queen et al., 2019). MCP-1 and MIP-1α are cytokines involved in the chemotaxis of phagocytic cells required for pathogen removal (Bhavsar et al., Deshmane et al., 2009). Alterations in CK cows' circulating cytokine profile suggest that CK cows exhibit an active systemic inflammatory response that may be dysregulated and thus require anti-inflammatory treatment. The findings of this study, which show higher levels of proinflammatory cytokines in CK cows, offer strong evidence for systemic inflammation in these animals. These results should not be interpreted as proof of a cause-and-effect relationship but rather as an indication of systemic inflammation in cows affected by CK.

Although the exact mechanism leading to inflammation during CK is unknown, previous research suggests increased gut permeability leading to bacteremia/endotoxemia as one of the possible etiological origins in dairy cows (Abuajamieh et al., 2016, Kvidera et al., 2017). The changes in APP and cytokines observed in the present study have also been reported during endotoxin immune activation (Abuajamieh et al., 2016, Brodzki et al., 2021). Most CK cows in the present study exhibited both endotoxemia and bacteremia. Although conjecture, the observed

systemic inflammation in CK cows during this study may be attributed to the detected endotoxemia and bacteremia. Previously, Kremer et al. (1993) showed a strong correlation between BHB levels and the severity of coliform mastitis in dairy cows. Although the source of endotoxin in the present study is unknown, a possible mechanism could be intestinal barrier dysfunction and bacterial translocation (Khafipour et al., 2009). In line with this, damaging intestinal barrier function with gamma-secretase inhibitor resulted in higher APP, and BHB in mid-lactation dairy cows (Kvidera et al., 2017). To our knowledge, this is the first study that provides evidence of endotoxemia during CK. Our findings further support that CK arises from a complex dysregulation of host responses to systemic inflammation, with endotoxin potentially acting as the underlying cause (Zhang and Ametaj, 2020). In summary, our findings suggest a link between clinical ketosis and systemic inflammation, indicating that clinical ketosis may be a consequence of systemic inflammation rather than a standalone metabolic disorder solely derived from negative energy balance (NEB).

In humans, 40-75% of ketoacidosis patients experience acute abdominal pain unrelated to hyperglycemia (Umpierrez and Freire, 2002). In lactating dairy cows, pain associated with metabolic diseases, especially CK, is suspected but poorly characterized. In the present study, CK cows had elevated concentrations of the stress marker SP. This protein is an objective biomarker of pain and recently emerged as a potential indicator of nociception in cattle as it is associated with the transmission and modulation of pain, inflammation, and anxiety (Tschoner and Feist, 2022). In painful conditions such as dehorning, castration, metritis, and lameness, circulating SP increases dramatically (Barragan et al., 2018, Rodriguez et al., 2018). To our knowledge, this is the first study describing increased SP in CK, highlighting pain and discomfort as possible factors contributing to poor cow well-being during metabolic diseases.

CK Treatments Responses

PG is widely used for CK treatment to restore gluconeogenesis; however, it does not target lipolysis dysregulation. Furthermore, PG rapidly reduces plasma ketone bodies that are potent anti-lipolytic agents (Taggart et al., 2005), possibly increasing the rate of lipolysis again and predisposing cows to CK relapse. In the present study, PG's efficacy in reducing BHB levels to <1.2 mmol/L was 58.3% at d7 and 70.8% at d14. Three recent randomized clinical trials report PG's efficacy to be 45-60% (Tatone et al., 2016, Gordon et al., 2017, Capel et al., 2021).

In the present study, including 24 g per day of NIA (PGNIA) reduced hyperketonemia by 62.5% at d7. However, we observed no differences in lipolysis rates or hyperketonemia recovery between PGNIA and PG. Although NIA is a well-characterized inhibitor of the canonical lipolytic pathway, its antilipolytic effect varies among studies in dairy cattle. In feed-restricted cows, abomasal infusion and rumen-protected NIA supplementation exhibited a dose-dependent antilipolytic effect, with a dosage of 26 g per day proving more effective. (Pires et al., 2007, Pescara et al., 2010). In the past, NIA has been proposed as CK treatment. Ruegsegger and Schultz (1986) used NIA (12g/PO/for 1 day) in conjunction with PG (125 mL) and found no effect of the combined treatment on reducing BHB levels or clinical signs of ketosis. However, Ruegsegger & Shult's study had a very small sample size, and the dosing of PG was too low for lactating dairy cattle. Although NIA is an effective inhibitor of the canonical lipolytic pathway in healthy cows, its anti-lipolytic effects might not suffice when lipolysis is driven by inflammatory pathways, such as in CK. Although this is the first study using a relatively high dose of NIA for treating CK, more research is needed to evaluate its pharmacokinetics and dosing during clinical disease.

To our knowledge, this is the first clinical trial evaluating the effect of PGNIAFM during CK. The positive responses to PGNIAFM treatment may be attributed either to the individual

effects of FM or the synergistic interaction between the mechanisms of action of NIA and FM. First, both drugs are potent inhibitors of lipolysis. NIA targets the canonical pathway of lipolysis mediated by PKA/HSL (Kenéz et al., 2014). FM inhibits COX activity resulting in lower activation of the inflammatory pathway of lipolysis that is mediated by ERK1/2-HSL and prostaglandin E2/HSL (Bashir et al., 2020, Inazumi et al., 2020). The second mechanism may be related to the capacity of FM to boost circulating insulin as observed on d7 in the present study. Insulin is a powerful antilipolytic hormone and a potent suppressor of ketogenesis (Gordon et al., 2013). COX inhibitors can increase insulin release from beta cells by inhibiting ATP-sensitive potassium channels (Li et al., 2007). In line with our findings, the use of NSAID (sodium salicylate) in postpartum dairy cows contributed to enhanced insulin activity (Montgomery et al., 2019). A possible third mechanism may be related to FM's capacity of reducing carnitine palmitoyl transferase 1 (CPT1) expression, which is responsible for the translocation of fatty acids from the cytosol into the mitochondria for later ketone production (de Souza et al., 2015). As lipolysis was reduced in PGNIAFM cows, ketogenesis and its inhibitory effect on gluconeogenesis were suppressed. Although inhibition of lipolysis may lead to a decrease in ketone synthesis, it is important to recognize that reducing ketone levels does not automatically indicate an improvement in the overall health status of the cow. Indeed, the comprehensive evaluation of other metabolites and inflammatory markers might represent a better understanding of the metabolic status of animals treated for CK.

Few studies have evaluated the use of non-steroidal anti-inflammatory (NSAID) drugs for dyslipidemia. Treatment of healthy postpartum dairy cows with FM had no effect on lipid mobilization parameters (Shwartz et al., 2009, Schmitt et al., 2022). However, the use of 3 mg/kg of ketoprofen for 3 d reduced circulating NEFA, BHB, and proinflammatory markers in

postpartum dairy cows (Kovacevic et al., 2019). Aligning with our results, a recent clinical trial demonstrated that a single FM dose (3.3 mg/kg) reduced BHB and inflammatory markers in postpartum cows diagnosed with inflammation [Hp>0.6 g/L, (Schmitt et al., 2022)].

In the present study, treating dairy cows with PGNIAFM reduced production of several proinflammatory biomarkers, including Hp, SAA, IL-6, and MCP-1. These findings coincide with a recent report demonstrating reduced Hp after a single dose of FM (Schmitt et al., 2022). By reducing PGE_2 biosynthesis, FM inhibits the production of proinflammatory cytokines (Siddiqui and Williams, 1989). Although PGNIAFM reduced most of the inflammatory markers by d7, CK cows persisted with elevated IL-1α and IL-10 circulating concentrations. This inflammatory status at d7 may have been caused by the continued endotoxemia observed in CK.

This study has limitations. First, the sample size is inadequate to draw conclusions related to reproductive and production parameters beyond the duration of this study. Additionally, the absence of treatments NIA, FM, and PGFM limits the assessment of FM and NIA effects on CK recovery. Including an FM alone treatment is particularly complex given the IV administration route and the milk and meat withdrawal times However, more studies assessing the inclusion of FM and other NSAIDS in the treatment of CK are required to determine potential benefits and limitations and estimate the economic implications of implementing CK treatments that include NIA and FM.

CONCLUSION

The present study demonstrates that cows with CK exhibit enhanced lipolysis, dyslipidemia, and increased markers of systemic inflammation and pain. Further research is needed to elucidate the exact mechanisms leading to CK and the consequences of pain during metabolic disease. Furthermore, the results of this study indicate a strong association between

endotoxemia, bacteremia, and CK in cows, suggesting a potential involvement of these findings in the development of the disease. Treating cows with the combination of PG, NIA, and FM is an alternative for CK management that targets lipolysis dysregulation and may limit inflammation.

CHAPTER 3: LIPOLYSIS INHIBITION AS A TREATMENT OF CLINICAL KETOSIS IN DAIRY COWS: FACTORING IN THE RESPONSE OF FAT

Under peer review in Journal of Dairy Science: M. Chirivi, D. Cortes-Beltran, C. J. Rendon, G. A. Contreras. 2023. Submitted July 2023.

ABSTRACT

Dairy cows with clinical ketosis (CK) exhibit excessive adipose tissue (AT) lipolysis and systemic inflammation. Lipolysis in cows can be induced by the canonical (hormonally induced) and inflammatory lipolytic pathways. The current treatment for CK is oral propylene glycol (PG), however, PG does not reduce lipolysis or inflammation. Niacin (NIA) can reduce the activation of canonical lipolysis, whereas cyclooxygenase inhibitors such as flunixin meglumine (FM) can limit inflammation and inhibit the inflammatory lipolytic pathway. The objective of this study was to determine the effects of including NIA and FM in the standard PG treatment for postpartum CK on AT function. Multiparous Jersey cows [n = 18; 7.1 (SD = 3.8) DIM] were selected from a commercial dairy. Inclusion criteria were CK symptoms (lethargy, depressed appetite, and drop in milk yield) and high blood levels of β-hydroxybutyrate (BHB ≥1.2 mmol/L). Cows with CK were randomly assigned to one of 3 treatments 1) **PG**: 310 g administered orally once per d for 5 d, 2) **PG+NIA**: 24 g administered orally oral once per d for 3 d, 3) **PG+NIA+FM:** 1.1 mg/kg administered IV once per day for 3 d. Healthy cows (HC; n=6) matched by lactation and DIM (±2 d) were sampled. Subcutaneous AT explants were collected at day 0 (d0) and 7 (d7) relative to enrollment. To assess AT insulin sensitivity, explants were treated with insulin (INS = 1 µL/L) during lipolysis stimulation with a β-adrenergic receptor agonist (isoproterenol, ISO = 1 µM). Lipolysis was quantified by glycerol release in the media. Lipid mobilization and inflammatory gene networks were evaluated using real-time qPCR. Protein biomarkers of lipolysis, insulin signaling, and AT inflammation including HSL, AKT, and ERK1/2 were quantified by capillary

immunoassays. Flow cytometry of AT cellular components was used to characterize macrophage inflammatory phenotypes. Statistical significance was determined by a non-parametric t-test when two groups were analyzed and an ANOVA test with Tukey adjustment when three paired groups were analyzed. At d0, AT from CK cows showed higher mRNA expression of lipolytic enzymes *ABHD5*, *LIPE*, and *LPL*, as well as increased phosphorylation of the lipase HSL (pHSL), compared to HC. At d0, INS reduced lipolysis by 41±8% in AT from HC, while CK cows were unresponsive (-2.9±4%). AT from CK cows exhibited reduced Akt phosphorylation compared to HC. CK had increased AT expression of inflammatory gene markers, including *CCL2, IL8*, *IL10*, *TLR4*, and *TNF*, along with ERK1/2 phosphorylation. AT from CK cows showed increased macrophage infiltration compared to HC. By d7, AT from PGNIAFM cows had a more robust response to INS, as evidenced by reduced glycerol release (36.5±8% compared to PG, 26.9±7%, and PGNIA, 7.4±8%), and enhanced phosphorylation of Akt. By d7, PGNIAFM cows presented lower inflammatory markers, including ERK1/2 phosphorylation and reduced macrophage infiltration compared to PG and PGNIA. These data suggest that including NIA and FM in CK treatment improves AT insulin sensitivity and reduces AT inflammation and macrophage infiltration.

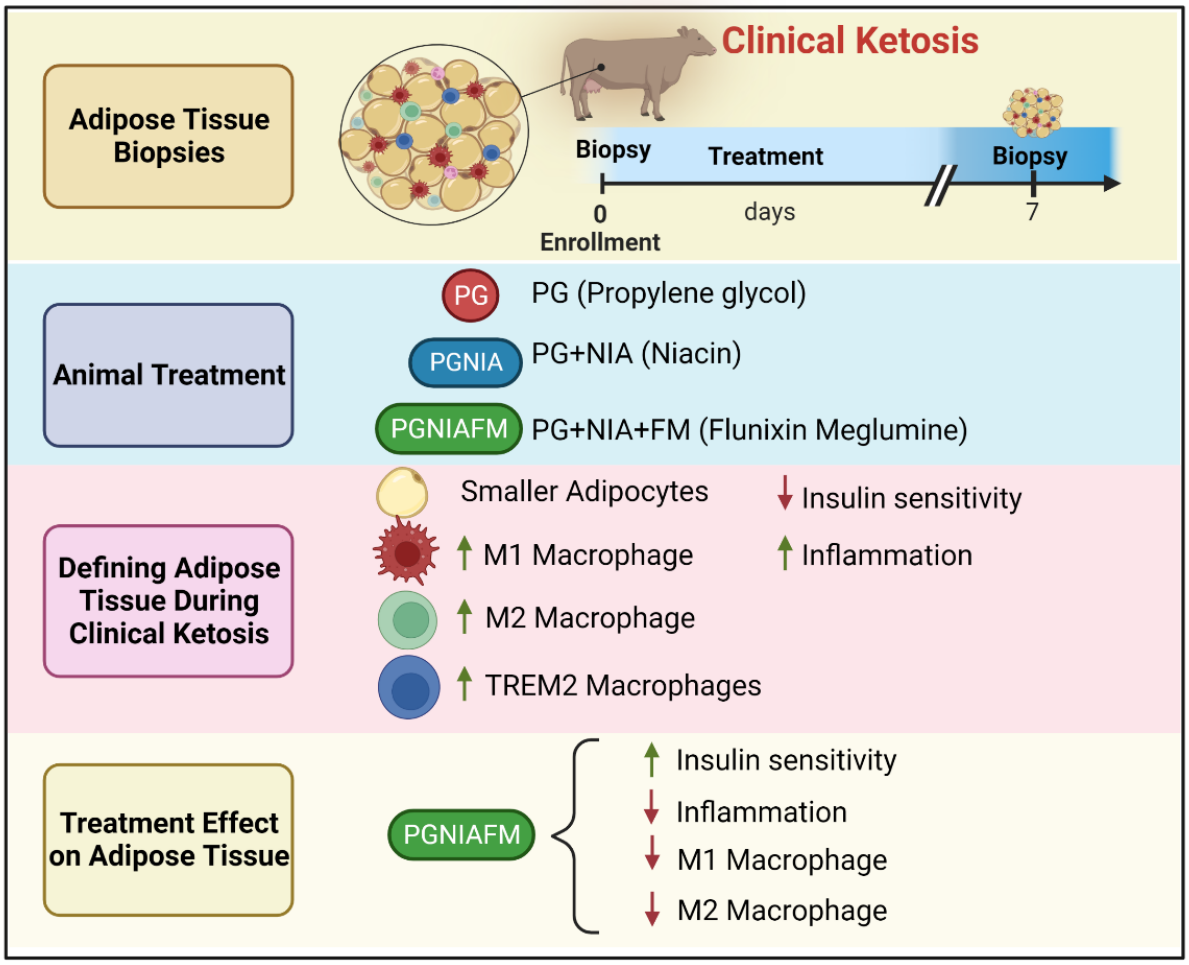

Figure 6. Graphical abstract. Adipose tissue function is affected during clinical ketosis, and it recovers when treated with PGNIAFM. Subcutaneous adipose tissue (SCAT) samples were collected from dairy cows with clinical ketosis (BHB>1.2 mmol/L) at enrollment and after 7 d . Cows were treated with: PG = Propylene Glycol, PGNIA = PG + Niacin, or PGNIAFM = PGNIA + flunixin meglumine. Created with Biorender.

INTRODUCTION

The postpartum period in dairy cows is the lactation stage associated with the highest risk for disease and culling. Despite progress in nutritional interventions, management, and preventive medicine programs, 30 to 50% of dairy cows still succumb to at least one disease during the early postpartum (LeBlanc, 2010). Among the numerous metabolic and inflammatory events associated with periparturient disease risk, lipolysis dysregulation in adipose tissues (**AT**) is well-recognized as a prominent predisposing factor (Ospina et al., 2010b, Zachut and Contreras, 2022). When dysregulated (i.e., intense and protracted), lipolysis rapidly overwhelms the liver's capacity to process the free fatty acids (**FA**) it releases, resulting in enhanced ketone body synthesis and development of ketosis. Clinical Ketosis (**CK**) is characterized by reduced appetite, drop in milk yield, and lethargy along with elevated plasma β-hydroxybutyrate [**BHB**, >1.2 mmol/L] and hypoglycemia [<2.0 mmol glucose/L] (Duffield, 2000, Dervishi et al., 2021). Although recent reports identified hepatic gene networks and circulating metabolic and proteomic profiles associated with CK (Wu et al., 2020), the pathogenesis of the disease is not entirely defined, and the role AT plays is poorly understood. Therefore, determining AT's metabolic and inflammatory responses before and after treatment of CK is important to advance our understanding of the mechanisms for the development and resolution of this disease.

Similar to other mammals, AT is the main energy-reserving organ in dairy cows. AT undergoes physiological adaptations around the time of calving to fulfill the energy requirements of periparturient cows (Contreras et al., 2017b). Among these adaptations, lipogenesis and re-esterification of FA are sharply reduced while lipolysis is upregulated (McNamara, 1991). These homeorhetic adaptations provide sufficient energy for pregnancy's final stages and the onset of lactation (Bauman and Currie, 1980). One critical mechanism that leads to intense lipolysis

postpartum is the reduction in circulating insulin levels. (Mann et al., 2016). Lipolysis is further intensified by decreased insulin sensitivity and heightened responses to β-adrenergic stimulation in AT (Contreras et al., 2017b). During pathologic conditions such as CK and displaced abomasum (**DA**), systemic insulin sensitivity is drastically reduced, resulting in excessive lipolysis (Pravettoni et al., 2004, De Koster and Opsomer, 2013). Despite the crucial role of AT in the pathophysiology of metabolic diseases, its specific contribution to the pathogenesis of CK remains poorly understood.

Within AT, lipolysis triggers an inflammatory response characterized by the infiltration of adipose tissue macrophages (ATM). Previous studies from our group showed that ATM infiltration is associated with heightened lipolysis during early lactation and dysregulated lipolysis during hyperketonemia and DA (Contreras et al., 2015, De Koster et al., 2018c). Dairy cows' ATM are characterized by the expression of clusters of differentiation (**CD**) markers, including CD14, CD68, and CD172a. ATMs are classified as M1 (classical) and M2 (alternative) depending on their phenotype and function. M1 ATM express CD14 and CD11c and secrete proinflammatory cytokines, including TNF-α and IL-6 (Lumeng et al., 2007). Remarkably, M1 is associated with intense lipolysis as it occurs during CK (Contreras et al., 2015). In contrast, M2 ATM express CD11b and CD163 and produce IL-10 which promotes the resolution of inflammation (Fujisaka et al., 2009, Ferrante Jr, 2013). Although several reports have described the use of flow cytometry in healthy or diseased cows (Contreras et al., 2015, Contreras et al., 2016b, Oliveira et al., 2020), no studies have characterized ATM phenotypes before and after treating cows with CK.

The optimal treatment for CK should focus on reestablishing appetite, promoting the return to normoglycemia, and reducing ketogenesis by limiting circulating FA availability (Herdt and Emery, 1992). Currently, oral administration of propylene glycol (**PG**) is accepted as the treatment

for CK in dairy practice due to its gluconeogenic properties (Gordon et al., 2013). However, PG does not reduce AT lipolysis. In dairy cows' AT, lipolysis is activated by the canonical and inflammatory pathways (Chirivi et al., 2022). The canonical pathway of lipolysis involves the activation (i.e., phosphorylation) of hormone-sensitive lipase (**HSL**) by protein kinase A (**PKA**). In the inflammatory pathway, mitogen-activated protein kinase/extracellular signal-regulated kinase (**MAK/ERK**) phosphorylates HSL, initiating lipolysis (Grisouard et al., 2010). Niacin (**NIA**) is a strong antilipolytic agent that inhibits PKA activation, resulting in reduced canonical lipolysis (Tunaru et al., 2003). However, as cows with CK are often in a proinflammatory state, inhibiting the canonical pathway alone may not be sufficient for reducing lipolysis. Therefore, curtailing inflammation with cyclooxygenase (**COX**) blockers such as flunixin meglumine (**FM**) could reduce stimulation of the inflammatory lipolytic pathway (Kovacevic et al., 2019, Inazumi et al., 2020). However, the effects of treating CK cows with NIA and FM on AT function remains unknown.

This work is part of a prospective cohort study that evaluated the effect of lipolysis inhibitors in treating CK (Chirivi et al., 2023b). In the present study, we characterized AT's functional and inflammatory profile during spontaneous cases of CK and determined the effects of PG, NIA, and FM treatment on AT function during the treatment of CK. The data presented herein demonstrate that CK cows exhibit inflammation and reduced insulin sensitivity in AT. We provide evidence that combined administration of PG, NIA, and FM improves AT's sensitivity to insulin and limits AT inflammatory responses, including ATM trafficking.

MATERIALS AND METHODS

Animals

All experimental procedures were approved by the Institutional Animal Care and Use

Committee at Michigan State University (IACUC:202100139). This study was conducted from July 2021 through January 2022 in a single commercial dairy farm in Michigan, USA. The farm was selected by convenience, given the owner's voluntary willingness to participate in the study. At the time, the dairy had ~2645 lactating cows milked twice daily in a double-25 parallel herringbone parlor that averaged 25 kg of milk per cow daily. Animals were housed in free stalls with recycled manure solids as bedding. Postpartum cows were examined daily by a trained veterinarian and two experienced members of the farm staff.

Animals from this study were part of a larger randomized clinical trial analyzing the effects of 1) propylene glycol (**PG**), 2) PG + niacin (**PGNIA**), or 3) PGNIA + flunixin meglumine (**PGNIAFM**) on BHB concentrations and lipolysis reduction during naturally occurring cases of CK in dairy cows. The full description of the study population is detailed in Chirivi et al. (2023b)

Inclusion criteria for **CK** cases included multiparous dairy cows 2-21 DIM with depressed appetite, reduced rumen fill, and lethargy. If animals fulfilled these criteria, blood BHB was measured with the Precision Xtra® meter following manufacturer instructions and as described by Iwersen et al. (2009). Only cows that presented hyperketonemia (BHB >1.2 mmol/L) were enrolled in the study.

Exclusion criteria: CK cows were excluded if they had at least one concurrent disease diagnosed by a trained veterinarian at enrollment, such as DA, retained placenta, lameness, metritis, pneumonia, or clinical mastitis. Animals that developed any of these diseases within 14 days after enrollment were subsequently removed from the trial.

*Inclusion criteria for cli*nically healthy control cows (HC; n = 6) included multiparous dairy cows 2-21 DIM without any signs of disease and blood BHB < 1.2 mmol/L. HC were selected by matching the CK cows by parity and ± 2 DIM. HC cows were used to establish a baseline of

AT function and inflammatory markers in non-ketotic animals within the farm.

Cows were assessed for eligibility without prior knowledge of their allocation. Randomization sequences were generated using an online random sequence generator (random.org) before the trial commenced, and the assigned sequences were provided to the veterinarian in charge of the trial at the farm. Once eligibility was determined, cows were moved to the chute for sampling. Subsequently, the treatment assignments were revealed.

Treatments

Treatments were assigned at the cow level as follows:

- **PG (n = 6)**: 310 g (~300 mL) of propylene glycol (PG) administered orally 1×/d for 5 d (Propylene Glycol, USP Kosher, Interstate chemical company, Inc, USA).
- **PGNIA (n = 6):** PG for 5 d and 24 g of niacin (NIA) administered orally 1×/d for 3 d (NiaShure^{TM}, rumen-protected niacin, Balchem, USA).
- **PGNIAFM (n = 6):** PG for 5 d, NIA for 3 d, and 1.1 mg/kg of BW of intravenous flunixin meglumine (FM) 1×/d for 3 d (Banamine®, Merck Animal Health, USA).
- **HC (n = 6):** healthy animals with normoketonemia did not receive any treatment.

Treatments were administered at ~ 11:00 AM each d as follows: 1) PG: after animal restraint, PG was administered in a single bolus using a cattle drench gun. 2) NIA: two gelatin capsules (size 10, Torpac®, Fairfield, NJ, USA) containing 12 g of NIA each were given orally using a bolus gun. 3) FM: following a site preparation that included skin disinfection with 70% ethanol, FM was injected into the jugular vein. Milk from cows treated with FM was discarded for at least 36 h after the last injection. The commercial dairy's cow health and welfare guidelines did not allow the inclusion of an untreated CK control; therefore, all animals received treatment.

Farm personnel administered the treatments based on cow identification and medication

verification performed by the veterinarian conducting the trial at enrollment. The administration of treatments occurred daily until their completion. Due to the treatments' different administration routes, it was not possible to blind the farm staff to the respective treatment groups.

Sampling

Before treatment administration (~11:00 AM), blood samples were collected on d0, d3, d7, and d14 for quantification of albumin, BHB, BUN, calcium, glucose, insulin, magnesium, NEFA, total protein, and inflammatory markers, including endotoxin and acute phase proteins [results reported in Chirivi et al. (2023b)]. Following blood collection, subcutaneous AT (SCAT) samples were obtained from the right flank on day 0 (**d0**). A second SCAT biopsy was collected on day 7 (**d7**) relative to enrollment. The surgical procedure was performed as described previously (Chirivi et al., 2022). Five grams of SCAT were collected, and the biopsy site was closed using a continuous interlocking suture with Braunamid (USP1, Aesculap, Center Valley, PA, USA). Sutures were removed 7-10 d after each procedure.

Immediately after harvesting, AT was divided into ~100 mg pieces. Lipolysis and flow cytometry samples were collected in Krebs Ringer Bicarbonate HEPES Buffer (KRBH, pH 7.4) and transported to the laboratory for experimental procedures. For histological studies, samples were immersed in 4% paraformaldehyde (Electron Microscopy Sciences, Hartfield, PA). For protein and gene expression analysis, samples were snap-frozen in liquid nitrogen and stored at -80 °C.

In Vitro Lipolysis Assay

AT lipolysis was assessed as described by Chirivi et al. (2022). Basal lipolysis was established without the addition of any reagent. Lipolysis was induced using the β-adrenergic receptor agonist isoproterenol (**ISO**, I6504, Millipore-Sigma, Burlington, MA) at 10^{-6} M

concentration. To evaluate the inhibitory effect of insulin on lipolysis, explants were pre-incubated (i.e., before ISO) for 1 h with 1 µg/L of insulin from bovine pancreas (I0516, Sigma-Aldrich, St. Louis, MO). After 3 h of incubation, AT explants and medium samples were collected, snap-frozen in liquid nitrogen, and stored at −80 °C until further analysis.

Following the procedure described by Chirivi et al. (2022), lipolysis quantification was performed using a free glycerol reagent (F6428, Millipore-Sigma) to determine the amount of glycerol released in the explant media. The intra-assay and inter-assay coefficients of variation were 3.9% and 6.8%, respectively. Glycerol release was normalized by the weight of the AT explant (nmol/mg), and the results are expressed as a percent of lipolysis reduction compared to ISO-induced lipolysis. All samples were run in duplicate.

RNA Extraction from Adipose Samples

RNA was extracted from SCAT samples using a TRIzol-based method as previously described by our group (Chirivi et al., 2022). RNA was stored at -80°C, and the concentration and integrity of total RNA were evaluated using a NanoDrop One^{C} spectrophotometer (Thermofisher Scientific, Waltham, MA, USA). All samples had a 260:280 nm ratio between 1.9 and 2.02. Reverse transcription was performed with 400 ng of RNA using 4 µL of the qScript cDNA SuperMix (95048 Quantabio, Beverly, MA, USA) for 5 minutes at 25°C, 30 minutes at 42°C, and 5 minutes at 85°C. cDNA was stored at -20°C.

Gene expression analysis

Transcriptional studies were performed using the QuantStudio^{TM} & Flex System (Applied Biosystems Inc., Waltham, MA). SYBR gene expression primers were used for qPCR assays and were either commercially available or designed from bovine sequences and synthesized (IDT, Integrated DNA Technologies, Inc., Coralville, IA). Samples were assayed in duplicate, each 10

µL PCR reaction contained 1X (5 µL) of SYBR™ Green PCR Master Mix (4309155, Applied Biosystems), 400 nM of primer assays (Appendix Table 12), and 5 ng of sample cDNA. A non-template control and non-reverse-transcriptase control monitored contamination and primer-dimer formation that could produce false-positive results and validated the absence of genomic DNA. The following cycling conditions were used: initial enzyme activation at 95 °C for 10 min, 40 cycles of denaturation at 95 °C for 15 sec, and annealing at 60 °C for 60 sec. Housekeeping genes with the lowest pairwise variation values including eukaryotic translation initiation factor 3 subunit K (*EIF3K*), ribosomal protein lateral stalk subunit P0 (*RPLP0),* and ribosomal protein S9 (*RPS9*) were used. Expression of genes of interest was normalized against the geometric mean of selected housekeeping genes' CT. Quantification cycle values were extrapolated using the $2^{-\Delta\Delta CT}$ method. Gene expression data are presented as geometric means ± 95% CI.

Protein analysis

Proteins were extracted from approximately 100 mg of snap-frozen SCAT samples as described previously (Chirivi et al., 2022). An optimal concentration of 0.75 mg/mL of protein was determined and used on all antibodies tested on 12–230 kDa Wes Separation Module capillary cartridges of the Simple Protein Wes system (SM-W004, ProteinSimple, Santa Clara, CA, USA) (Nelson et al., 2017). Rabbit monoclonal antibodies were obtained from Cell Signaling (Danvers, MA, USA). Akt [(1:50), Cat#9272 s], ERK1/2 [(1:50), Cat# 9102), phosphorylated (Ser563) HSL [(1:25) Cat#4139], phosphorylated (Ser473) Akt [(1:25), Cat#9271t], phosphorylated (Thr202/Tyr204) ERK1/2 [(1:50), Cat#9101]. HSL was obtained from ThermoFisher Scientific [1:25; Cat#PA5-17196]. The anti-rabbit detection module for the Wes (DM-001, ProteinSimple) kit included Luminol-S, Peroxide, antibody diluent 2, streptavidin-HRP, and anti-rabbit secondary antibody. Sample proteins were allowed to separate by microcapillary electrophoresis and the

chemiluminescence signal peaks were generated for analysis. These signal peaks were transformed into digital images depicting bands as observed in Western blot analysis. Using Compass software (ProteinSimple), the peak areas of proteins were estimated. The peak areas are directly proportional to the amount of target protein quantified. The normalized data are expressed as a ratio of phosphorylated protein over total protein ratio pHSL(Ser563):HSL, ratio pAkt:Akt, and ratio pERK1/2:ERK1/2). To validate protein detection, over-expression lysates were used as positive controls for Akt (LC401580, OriGene Technologies, Rockville, MD, USA), HSL (LC417354, OriGene Technologies), and ERK1/2 (042-488 ProteinSimple).

Flow Cytometry

SCAT samples were transported to the laboratory at 4°C in KRBH. Cells from SCAT's stromal vascular fraction (**SVF**) were obtained by collagenase digestion. Briefly, SCAT (1-2 g) was minced in 4% BSA dissolved in Hank's balanced salt solution, 10mM HEPES, and Liberase™ TL Research Grade (5401020001, Roche, Indianapolis IN) and incubated at 37°C for 60 min. Samples were then resuspended in 15 mL of 4% BSA solution, passed through 70µm (22363548, Fisherbrand, Pittsbrug PA) and 40µm (22363547, Fisherbrand, Pittsbrug PA) cell strainers, and centrifuged at 300 x g for 5 mins at 4°C. Next, the SVF pellet was resuspended and incubated in RBC lysis buffer (420301, Biolegend Inc, San Diego, CA) for 5 min at room temp and centrifuged 300 x g for 5 min at 4°C. The SVF pellet obtained was then resuspended and incubated for 30 mins at 4°C with 100 µg/mL of purified bovine IgG (Sigma-Aldrich) in 1X Dulbecco's PBS, 2% FBS, 2 mM EDTA, 10 mM HEPES as blocking reagent for non-specific antibody binding. To exclude dead cells, all samples were incubated with Biolegend Zombie NIR™ fixable viability dye (423106, Biolegend Inc, San Diego, CA) diluted 1:500 in FACS solution composed of 1X Dulbecco's PBS, 2% FBS, and 0.1% sodium azide (26628-22-8, ThermoFisher Scientific).

Afterward, SVF-derived cells were incubated with conjugated monoclonal primary antibodies for 30 minutes. Before conducting the experiments, the optimal concentrations of all primary antibodies were determined through titration (Antibodies list and dilutions described in Appendix Table 13). Following primary incubation, cells were washed, fixed with 2% paraformaldehyde in PBS, washed, and resuspended in Dulbecco's PBS, 2% FBS, 2 mM EDTA, and 10 mM HEPES.

In each experiment for gating selection, fluorescence minus one (**FMO**) control was made for all markers used using one sample. Compensation beads were used as single-stained control samples. Data acquisition and compensation were performed in Cytek® Aurora System (Cytek Biosciences, Fremont, CA) using the SpectroFlo® software (Cytek Biosciences) and analyzed in FCS express V.7 (DeNovo Software, Pasadena, CA). UltraComp eBeads™ compensation beads were used for compensation. A gate was drawn to allow the exclusion of aggregates/doublets and another to exclude cellular debris. (Chirivi et al., 2023a).

Hematopoietic cells ($CD45^+$) are reported as % of total SVF cells. ATM were selected from $CD45^+$ population cells and defined by the expression of CD172a and MHC class II (MHCII). Macrophage phenotype populations were defined as: M1 ($CD45^+, CD172a^+, MHCII^+, CD14^+$), M2 ($CD45^+$, $MHCII^+$, $CD11b^+$). TREM2 metabolically active ATM ($CD45^+$, $TREM2^+$). The results are expressed as the percentage of the specified population relative to the total hematopoietic cell count.

Histology

The SCAT biopsies were fixed in 4% paraformaldehyde, blocked in paraffin, and then sectioned into 4 µm slices by the Michigan State University Investigative Histopathology Laboratory (East Lansing, MI, USA). Following pretreatment protocol, standard micro-polymer staining was performed at room temperature on the IntelliPATH automated stainer (Biocare

Medical, Pacheco, CA). All staining steps were followed by rinses in TBS Auto-wash Buffer (Biocare Medical). Non-specific protein was blocked using Background Punisher (Biocare Medical) for 10 minutes. Primary antibody was diluted in Normal Antibody Diluent (Scytek Laboratories, Inc. Logan, UT); mouse monoclonal antibody to detect bovine CD172a (1:50; DH59B, Washington State University Monoclonal Antibody Center, Pullman, WA) and slides were incubated overnight at 4 °C. Sections were counterstained with CATHE Hematoxylin diluted 1:10 (Biocare Medical) as described previously (Abou-Rjeileh et al., 2023). Whole slide digital images were collected using the Olympus VS200 Research Slide (Olympus Corporation, Tokyo, Japan). The areas of adipocytes in 8 randomly selected fields per section were measured using the Adiposoft plugin (v. 1.15) for ImageJ Fiji (v. 2.0.0) as described in (Ferland et al., 2020). Adipocyte areas were divided into 7 bins ranging from smaller (< 1499 μm^2) to larger (> 9000 μm^2) adipocytes. CD172a signal intensity was measured in the same images using ImageJ as described in (Crowe and Yue, 2019). All image captures and signal quantification were conducted with the analyst blind to treatments.

Statistical analysis

The sample size was calculated on JMP Pro16 (SAS Inst., Inc., Cary NC) based on the percent of macrophage infiltration previously observed in studies by our laboratory (Contreras et al., 2015, De Koster et al., 2018c). Assuming a power of 80%, a confidence level of 95%, and a minumun defference of 18.5 % in ATM infiltration at d0 between CK and HC, a minimum sample size of 6 cows was calculated. All variables were analyzed in JMP Pro16. A non-parametric Wilcoxon matched-pairs signed rank test determined the statistical differences between CK and HC at d0. The protein expression data of the CK treatment at d0 was normalized by the HC data and is reported as “relative to HC” in the figures. Protein at d7 was normalized by the CK values at d0.

RNA data were transformed (Log10). Results are presented as mean ± SEM unless stated otherwise. Significance was declared at $P \leq 0.05$. At d7, treatment effects were evaluated by Friedman's two-way ANOVA test, and Tukey's post hoc adjustment was used for pairwise comparisons.

RESULTS

CK Increases AT Lipolytic Markers

On d0, CK cows had a higher level of blood NEFA (0.67±0.03 mmol/L) compared to HC cows (0.39±0.05 mmol/L), suggesting an increase in lipolysis (CHAPTER 2). Aligning with this observation, the transcription of AT neutral lipases, including β-hydrolase domain containing 5 (*ABDH5*), hormone-sensitive lipase *(LIPE),* and lipoprotein lipase (*LPL*), increased in CK cows compared to HC ($P < 0.01$; Figure 7A). Genes related to FA synthesis and transport including peroxisome proliferator-activated receptor alpha (*PPARA*) and gamma (*PPARG*) were upregulated in CK cows ($P < 0.0001$). In contrast, the expression of the mitochondrial FA transporter *CPT1* was not affected by CK (Figure 7A). To characterize AT lipolytic activity, we quantified HSL and its degree of phosphorylation (pHSL). At d0, pHSL:HSL in CK cows increased 4.03±1.38-fold compared to HC ($P = 0.08$; Figure 7B). Adipocyte size distribution is a proxy for lipolysis and triglyceride storage within the fat cells. As such, AT from CK presented a higher frequency of smaller adipocytes (< 1499 μm^2) compared to HC ($P < 0.05$; Figure 7C).

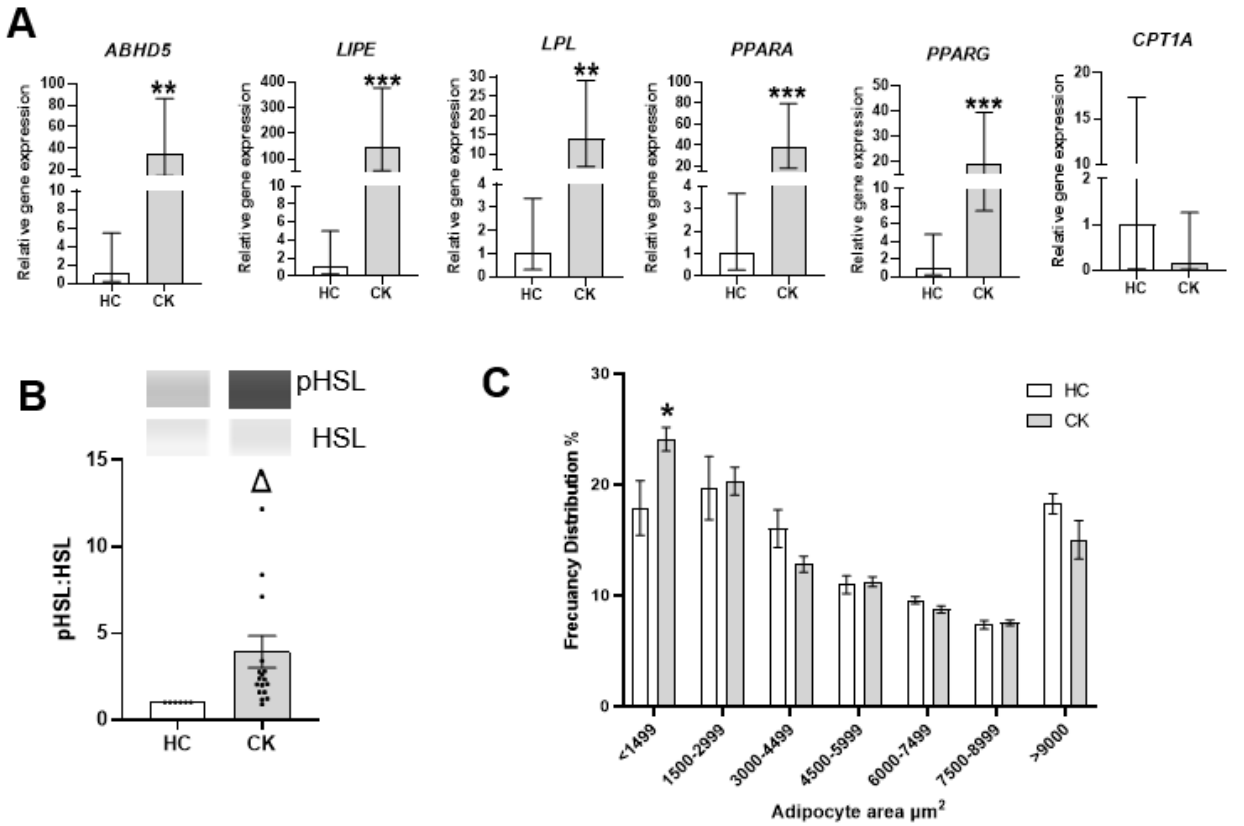

Figure 7. Cows with CK have increased lipolysis markers. Subcutaneous adipose tissue (SCAT) samples were collected at enrollment (d0) from postpartum cows that were healthy (HC) or with clinical ketosis (CK; BHB>1.2 mmol/L). **(A)** Fold change of *ABHD5*, *CPT1A*, *LIPE*, *LOCS527744*, *LPL*, *PPARA* and *PPARG* gene expression relative to HC ($2^{-\Delta\Delta CT}$). Gene expression was normalized to that of reference genes *EIF3K*, *RPL19*, and *RPS9*. **(B)** Protein abundance of HSL and phosphorylated HSL (pHSL, Ser563) relative to HC. Bands were detected at 81 kDa. **(C)** Frequency distribution of adipocyte area calculated in adipose tissue sections. Bars with Δ are different (*P*<0.1*)* or * (*P*<0.05) or ** (P<0.01) or *** *(P*<0.0001). Protein data are means of the ratio of pHSL:HSL ± SEM. Adipocyte area data are means ± SEM. Gene expression data are geometric means ± 95% CI. Each dot represents an individual animal. HC n = 6, CK n = 18.

AT Insulin Sensitivity is Reduced During CK

CK cows showed higher transcription of the genes encoding fatty acid transporter FA binding protein (*FABP4*) and triglyceride synthesis enzyme phosphatidic acid phosphodiesterase lipin1 (*LPIN1).* In contrast, solute carrier family 2 member 4 (*SLC2A4*) expression was reduced in CK compared to HC (*P* < 0.0001; Figure 8A). No changes were observed in the expression of insulin receptor substrate 1 (*IRS1*). To evaluate adipocyte insulin signaling activity we quantified Akt protein phosphorylation. At d0, pAkt:Akt was reduced by 60±6.4% in CK compared to HC

($P < 0.01$; Figure 8B). AT insulin sensitivity was also measured ex vivo by assessing the capacity of the pancreatic peptide to reduce adipocytes' lipolytic response upon β-adrenergic-stimulation (ISO). As expected, insulin reduced glycerol release by 41% in SCAT from HC ($P < 0.01$). In contrast, SCAT from CK cows were unresponsive to insulin (-9.5%; Figure 8C).

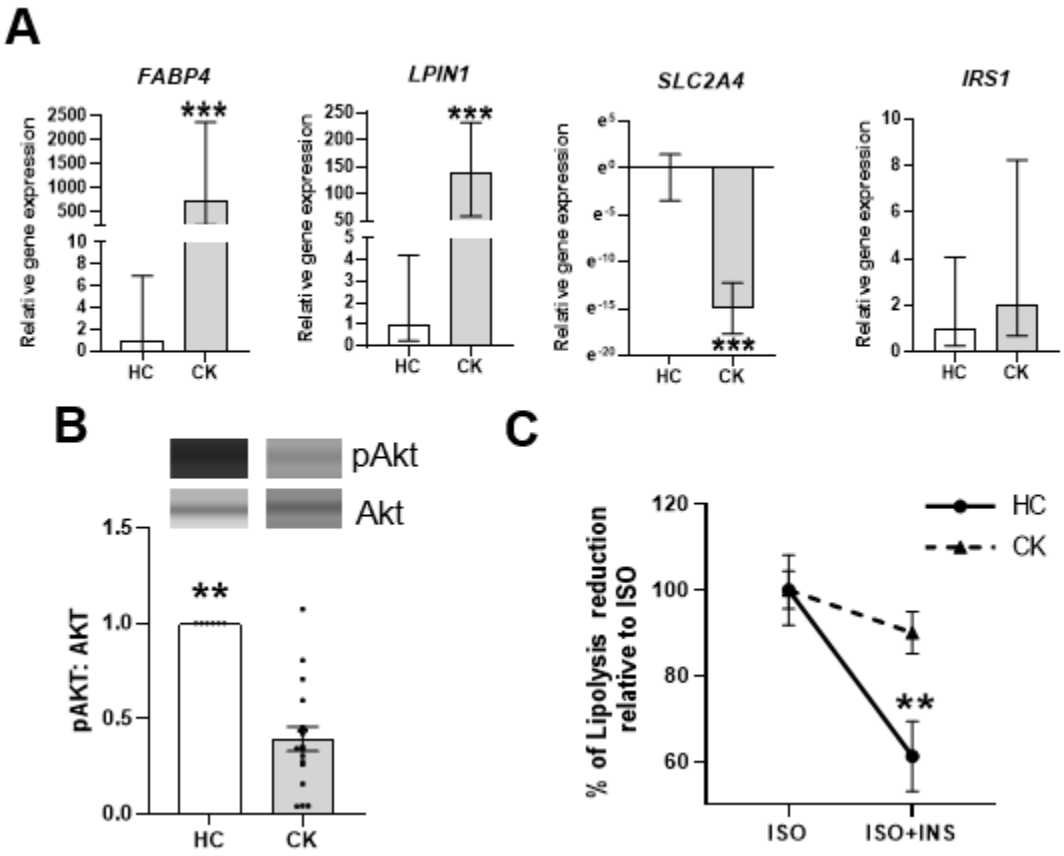

Figure 8. Cows with CK have reduced adipose tissue insulin sensitivity. Subcutaneous adipose tissue (SCAT) samples were collected at enrollment (day 0) from postpartum healthy dairy cows (HC) or with clinical ketosis (CK) (BHB>1.2 mmol/L). **(A)** Fold change of FABP4, LPIN1, SLC2A4, and IRS1 gene expression relative to HC (2- ΔΔCT). Gene expression was normalized by reference genes EIF3K, RPL19, and RPS9. **(B)** Protein abundance of Akt and phosphorylated Akt (pAkt) at Ser473 relative to HC. Bands were detected at 60 kDa. (C) Percentage of lipolysis reduction relative to isoproterenol (ISO; 1 µM) induced lipolysis in SCAT explants exposed to insulin (ISO+INS; 1 µg/L) for 3h. Bars with * are different (P<0.05) or ** (P<0.01) or *** (P<0.0001). Lipolysis reduction data are means ± SEM. Protein data are means of the ratio pAkt:Akt. Gene expression data are geometric means ± 95% CI. Each dot represents an individual animal. HC n = 6, CK n = 18**.**

CK Induces AT Inflammation

CK cows exhibited an upregulation of inflammatory gene markers such as interleukin 8 (*IL8*) and 10 (*IL10*), toll-like receptor 4 (*TLR4*), and tumor necrosis factor (*TNF*) compared to HC cows ($P < 0.05$; Figure 9A). Similarly, genes associated with macrophage chemotaxis including chemokine (C-C motif) ligand 2 (*CCL2*), and osteopontin (*SPP1*) were upregulated in CK ($P < 0.01$; Figure 9A). Moreover, the expression of signal regulatory protein alpha (*SIRPA*), which encodes for the macrophage marker CD172A protein was upregulated in AT from CK cows. The transcription of *LOC527744*, encoding the BHB receptor HCAR2, was upregulated in CK vs. HC ($P < 0.05$; Figure 9A). Unexpectedly, *IL6* was downregulated in CK cows compared to HC cows ($P < 0.001$; Figure 9A). We quantified pERK1/2:ERK1/2 protein content as a marker of inflammatory signaling in AT. At d0, AT's pERK1/2:ERK1/2 in CK cows was 1.6±0.42 fold higher than in HC ($P < 0.05$; Figure 9B).

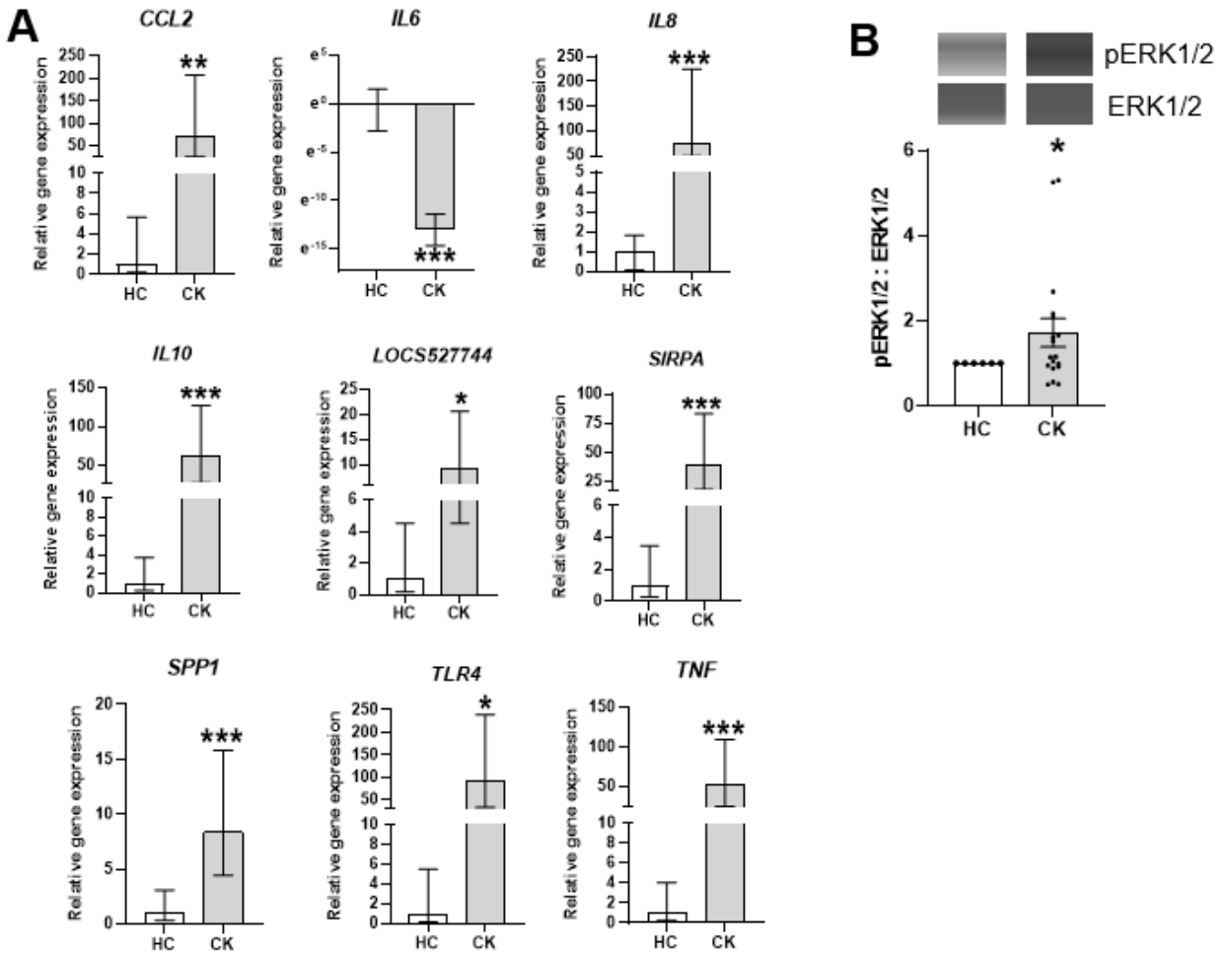

Figure 9. Cows with CK have increased adipose tissue inflammatory markers. Subcutaneous adipose tissue (SCAT) samples were collected at enrollment (d0) from postpartum healthy dairy cows (HC) or with clinical ketosis (CK) (BHB>1.2 mmol/L). **(A)** Fold change of *CCL2*, *IL6*, *IL8*, *IL10*, *SIRPA*, *SPP1*, *TLR4* and TNF gene expression relative to HC ($2^{-\Delta\Delta CT}$). Gene expression was normalized by reference genes *EIF3K*, *RPL19*, and *RPS9*. **(B)** Protein abundance of extracellular signal-regulated kinases 1/2 (ERK1/2) and phosphorylated ERK1/2 (pERK1/2) at Thr202/tyr204 relative to HC. Bands were detected at 44 kDa. Bars with * are different (P<0.05) or ** (P<0.01) or *** (P<0.0001). Protein data are means of the ratio pERK1/2:ERK1/2 ± SEM. Gene expression data are geometric means ± 95% CI. Each dot represents an individual animal HC n = 6, CK n = 18.

CK Increases ATM Infiltration

Flow cytometry of live SVF cells from SCAT showed no differences in the frequency of hematopoietic cells ($CD45^+$) between CK and HC at d0 (29.91% vs. 21.14%; P = 0.16) as a percentage of live SVF cells (Figure 10D). At d0, CK had a higher frequency of macrophages compared to HC (22.96% vs. 13.24%; P < 0.01; Figure 10E). At d0, M1 phenotype abundance

was higher in CK vs. HC (7.38% vs. 2.66%; $P < 0.05$; Figure 10F). Similarly, the percentage of M2 macrophages at d0 was elevated in CK vs. HC (6.3% vs. 2.4%; $P < 0.05$; Figure 10G). CK cows had fewer TREM2 anti-inflammatory metabolically active macrophages compared to HC (1.27% vs. 3.98%; $P < 0.05$; Figure 10H).

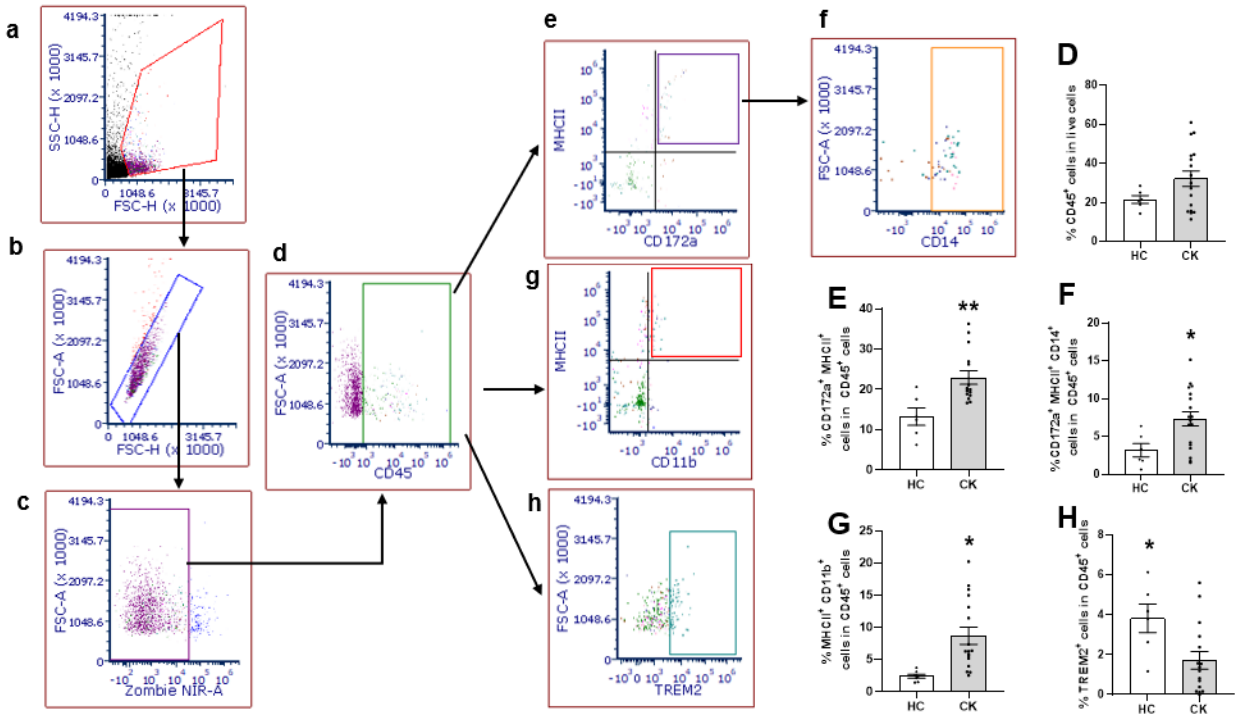

Figure 10. Cows with CK have increased adipose tissue macrophage trafficking. Frequency distribution of stromal vascular fraction (SVF) cells evaluated by flow cytometry from subcutaneous adipose tissue (SCAT) samples collected at enrollment (d0) from postpartum healthy dairy cows (HC) or with clinical ketosis (CK) (BHB>1.2 mmol/L). **(a-f)** Flow cytometry gating strategy used to define cell populations in stromal vascular fraction. Selection of cells without debris **(a)** and singlets **(b)**. Exclusion of dead cells with viability dye (Zombie NIR, Biolegend) **(c)**. Selection of hematopoietic cells ($CD45^+$) in total live SVF cells **(d, D)**. Selection of macrophages [$CD45^+$ $CD172a^+$, and MHC class II ($MHCII^+$)] in total hematopoietic cells **(e, E)**. Selection of classical activated (M1) macrophages (CD45+, CD172a+, MHCII+, CD14+) in total hematopoietic cells **(f, F)**. Selection of alternative activated (M2) macrophages (CD45+, MHCII+, CD11b+) in total hematopoietic cells **(g, G)**. Selection of foamy cells (CD45+, TREM2+) in total hematopoietic cells (h, H). Bars with * are different ($P<0.05$) or ** ($P<0.01$). Each dot represents an individual animal. Data means ± SEM. HC n = 6, CK n = 18.

ATM infiltration was evaluated by quantifying the HRP signal (CD172a+ cells) in SCAT sections. Compared to HC, CK cows had a 2.3-fold higher HRP signal. ($P < 0.05$; Figure 11-12).

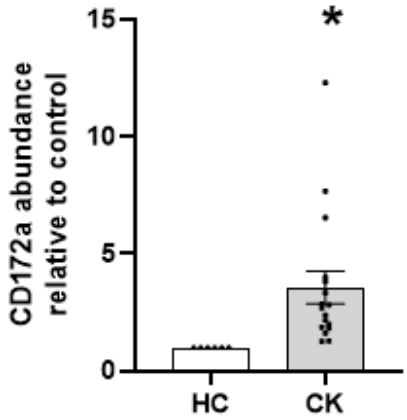

Figure 11. Cows with CK have increased macrophage infiltration in adipose tissue. Subcutaneous adipose tissue (SCAT) samples were collected at enrollment (d0) from postpartum healthy dairy cows (HC) or with clinical ketosis (CK) (BHB>1.2 mmol/L). Abundance of CD172a antibody signal in adipose tissue sections relative to HC. Bars with * are different ($P<0.05$). Each dot represents an individual animal. Bars are means ± SEM. HC n = 6, CK n = 18.

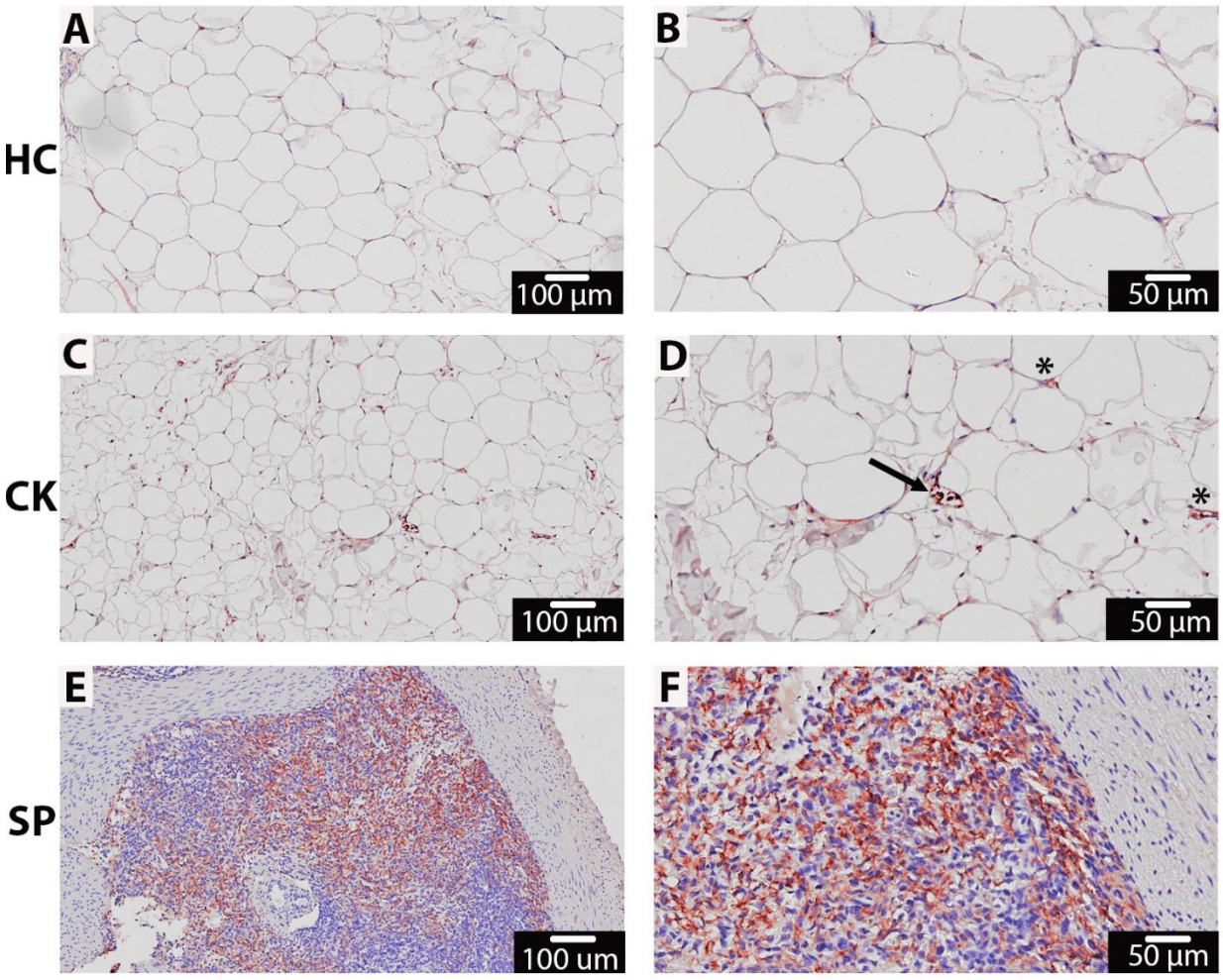

Figure 12. Representative images of tissue section after immunohistochemical staining using CD172a antibody to detect adipose tissue macrophages (ATM). (A-B) Healthy dairy cows HC or with **(C-D)** clinical ketosis (CK) (BHB>1.2 mmol/L). **(E-F)** Bovine spleen (SP) was used as positive control. Arrow points to crown-like structures and asterisks indicate a sole ATM throughout the tissue.

PGNIAFM Improves AT Insulin Sensitivity in CK Cows

To evaluate the impact of lipolysis inhibition on AT function, SCAT biopsies were collected at d7. On this day, AT from PGNIAFM showed 1.3- and 1.9-fold higher pAkt:Akt compared to PG or PGNIA respectively ($P < 0.05$; Figure 13A). In line with enhanced Akt signaling, lipolysis assays at d7 indicated that insulin reduced lipolysis by 36.5% in SCAT from PGNIAFM ($P < 0.05$; Figure 13B). In contrast, SCAT from PG and PGNIA remained unresponsive to the antilipolytic effect of insulin showing no lipolysis reduction (-16.97% and -

7.39% respectively; Figure 13B). By d7, PGNIAFM cows presented a higher distribution of large adipocytes (7499-8999 μm^2) and tended to have fewer small adipocytes (<1499 μm^2) vs. PG and PGNIA (Figure 13). No treatment effect was observed in the expression of genes related to insulin sensitivity and FA metabolism (Table 7). AT from PGNIAFM cows showed the lowest expression of the *LOCS527744* gene by d7 ($P < 0.05$; Table 7). *LPL* gene expression was reduced in AT from PGNIAFM vs. PG and PGNIA ($P < 0.05$; Table 7). The protein ratio content of pHSL:HSL was not affected by treatment (Figure 13D).

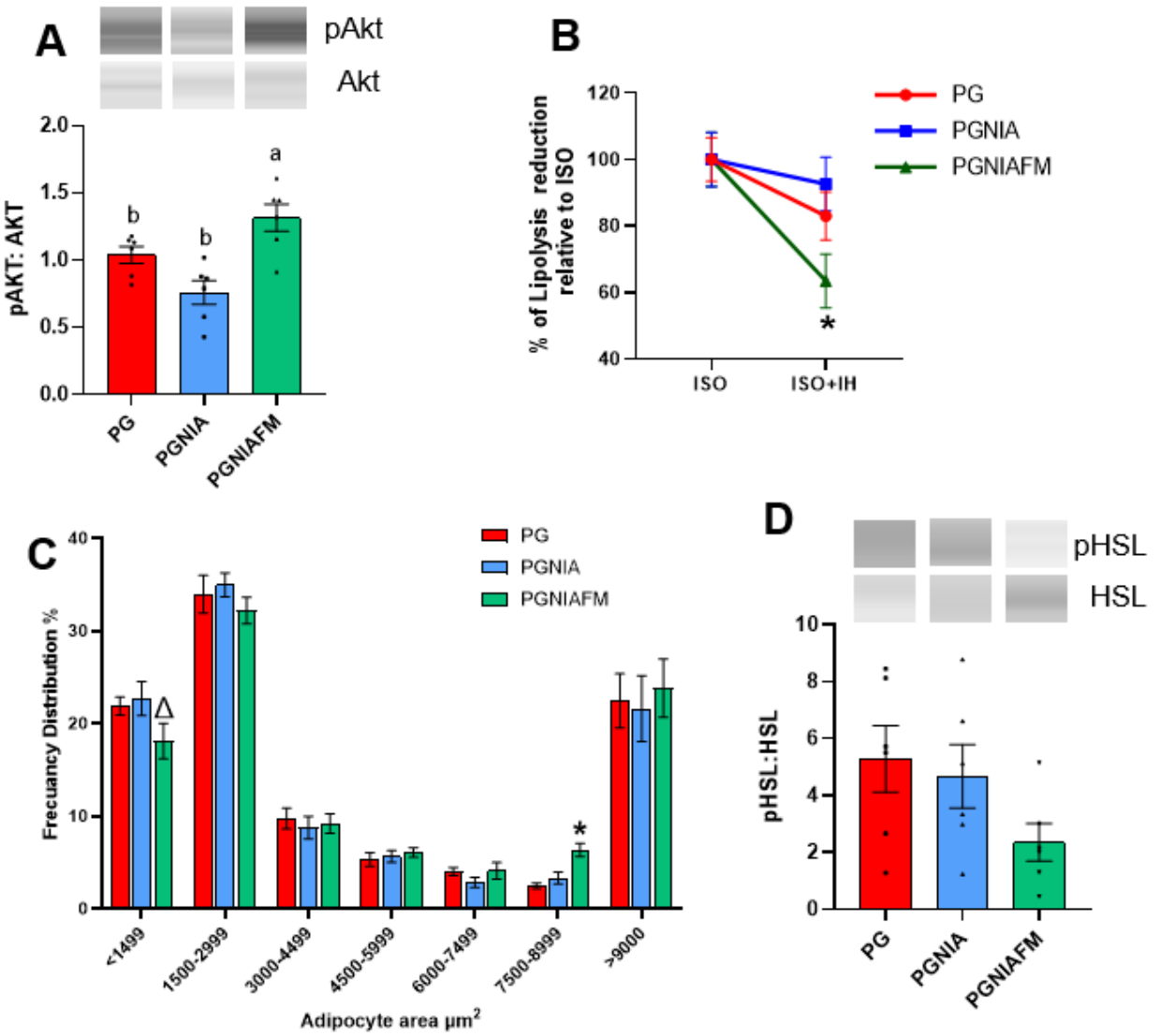

Figure 13. PGNIAFM treatment improves adipose tissue insulin sensitivity during clinical ketosis. Subcutaneous adipose tissue (SCAT) samples were collected from dairy cows with clinical ketosis (BHB>1.2 mmol/L) after 7 d of enrollment and treated with: PG = Propylene Glycol, PGNIA = PG + Niacin, or PGNIAFM = PGNIA + flunixin meglumine. **(A)** Protein abundance of HSL and phosphorylated HSL (pHSL) at Ser563 relative to HC. Bands were detected at 81 kDa. **(B)** Protein abundance of Akt and phosphorylated Akt (pAkt) at Ser473 relative to CK at d0. **(C)** Percentage of lipolysis reduction relative to isoproterenol (ISO; 1 µM) induced lipolysis in SCAT explants exposed to insulin (ISO+INS; 1 µg/L) for 3h. **(D)** Frequency distribution of adipocyte area calculated in adipose tissue sections. Bands were detected at 60 kDa. Bars with different letters (a-b) differ significantly ($P<0.05$). Bars with Δ are different ($P<0.1$) or * ($P<0.05$). Each dot represents an individual animal. Data are means ± SEM. Protein data are means of the ratio phosphorylated : total protein. n = 6.

Table 7. Relative expression of genes in subcutaneous adipose tissue from cows treated for clinical ketosis.

Gene Network	Gene	Treatment allocation[1]									
		PG			PGNIA			PGNIAFM			
		GM[2]	LCI	UCI	GM	LCI	UCI	GM	LCI	UCI	*P*-Value[3]
Lipid mobilization	*ABHD5*	0.59	0.14	2.49	0.63	0.15	2.66	0.32	0.06	1.70	0.79
	CPT1A	0.82	0.35	1.90	1.05	0.45	2.44	0.74	0.32	1.73	0.82
	LIPE	0.87	0.26	2.95	0.58	0.17	1.96	0.31	0.08	1.21	0.51
	LOCS527744	2.63[a]	0.79	8.68	0.71[b]	0.22	2.35	0.24[b]	0.06	0.92	0.03
	LPL	0.50[a]	0.16	1.56	0.11[ab]	0.03	0.33	0.06[b]	0.02	0.20	0.03
	PPARA	1.85	0.34	10.00	0.77	0.14	4.14	0.27	0.04	2.04	0.33
	PPARG	1.28[a]	0.49	3.36	0.39[ab]	0.14	1.07	0.28[b]	0.09	0.81	0.08
Insulin sensitivity	*FAB4*	0.06	0.01	0.54	0.08	0.01	0.76	0.09	0.01	0.89	0.94
	GLUT4	3.19	1.12	9.09	0.63	0.14	2.76	1.31	0.40	4.22	0.17
	IRS	0.18	0.02	1.54	0.42	0.07	2.50	0.07	0.01	0.53	0.41
	LPIN1	0.58	0.11	2.93	0.48	0.09	2.43	0.11	0.02	0.68	0.33
Inflammation	*CCL2*	2.39	0.73	7.83	2.97	0.91	9.72	0.88	0.27	2.86	0.29
	IL-6	0.17	0.06	0.51	0.34	0.10	1.13	0.21	0.07	0.61	0.68
	IL-8	0.45	0.08	2.46	0.66	0.12	3.57	0.43	0.07	2.86	0.92
	IL-10	0.65	0.07	5.94	1.11	0.12	10.09	1.09	0.12	9.90	0.92
	SIRPA	2.27	0.97	5.28	0.81	0.35	1.89	0.90	0.38	2.09	0.17
	SPP1	1.59	0.42	5.96	1.47	0.39	5.53	0.37	0.08	1.62	0.26
	TLR4	0.09	0.01	0.81	0.30	0.03	2.67	0.08	0.01	0.80	0.63
	TNFA	0.84	0.12	5.68	1.06	0.16	7.20	0.15	0.02	1.31	0.34

[1]Treatments for clinical ketosis (CK) cows (n = 6) with BHB>1.2 mmol/L at d7: PG = Propylene Glycol, PGNIA = PG + Niacin, PGNIAFM = PGNIA + flunixin meglumine.

[2]Geometric mean of Log_{10} transformed data. LCI-UCI = Lower and upper 95% CI. Gene expression values were calculated using $2^{-\Delta\Delta CT}$ method. $\Delta\Delta CT = \Delta CT_{\text{Calibrator sample}} - \Delta CT_{\text{Target sample.}}$ ΔCt values were normalized to the geometric mean of *EIF3K*, *RPLPO*, and *RPS9* housekeeping genes. HC samples were the calibrator for the calculation of the ΔΔCT.

[3]P-values refer to the main effect of treatment. P-values are from log10 transformed data analysis. n=24.

[a-c]Mean values in the same row with different superscripts differ (P<0.05) adjusted by Tukey.

PGNIAFM Reduces AT Inflammation and ATM Trafficking

Although treatments had no effect on the expression of genes encoding cytokines (Table 7), the pERK1/2:ERK1/2 in AT from PGNIAFM was reduced by 54.1% and 60.4±18% when compared to PG and PGNIA respectively ($P < 0.05$; Figure 14). There were no differences in the abundance of macrophages (CD172a+) in SCAT among treatment groups (Table 8). By d7, the flow cytometry analysis demonstrated no differences in the number of hematopoietic cells among the three treatment groups (Table 8). The frequency of macrophages ($CD45^+$, $CD172a^+$, $MHCII^+$) was reduced in SCAT from PGNIAFM cows, compared to PG and PGNIA groups (P=0.03; Table 8). The frequency of M1 macrophages ($CD45^+$, $CD172a^+$, $MHCII^+$, $CD14^+$) tended to be lower in PGNIAFM compared to PG and PGNIA cows (P=0.09; Table 8). Similarly, PGNIAFM had a lower frequency of M2 macrophages ($CD45^+$, $MHCII^+$, $CD11b^+$) compared to PG and PGNIA (P=0.01). Finally, there were no differences in the abundance of anti-inflammatory metabolically active macrophages ($CD45^+$, $TREM2^+$) among groups.

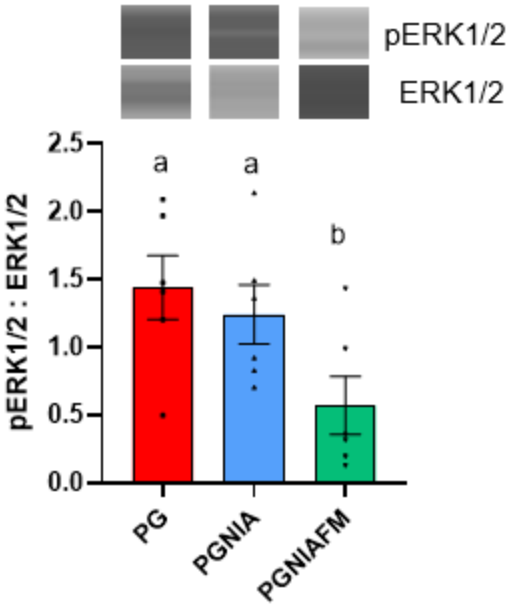

Figure 14. PGNIAFM treatment reduced adipose tissue inflammation. Subcutaneous adipose tissue (SCAT) samples were collected from dairy cows with clinical ketosis (BHB>1.2 mmol/L) after 7 d of enrollment and treated with: PG = Propylene Glycol, PGNIA = PG + Niacin, or PGNIAFM = PGNIA + flunixin meglumine. Protein abundance of extracellular signal-regulated kinases 1/2 (ERK1/2) and phosphorylated ERK1/2 (pERK1/2) at Thr202/tyr204 relative to HC. Bands were detected at 44 kDa. Bars with different letters (a-b) differ significantly ($P<0.05$). Each dot represents an individual animal. Bars are means ± SEM. Protein data are means of the ratio phosphorylated : total protein. n = 6.

Table 8. Macrophage quantification in subcutaneous adipose tissue in cows treated for clinical ketosis.

	Cell	Marker	Treatment allocation[1]				
			PG	PGNIA	PGNIAFM	SEM	P-value[2]
IHC[3]	Macrophages	CD172a	2.96	4.06	3.43	1.30	0.3
Flow cytometry[4]	Hematopoietic	$CD45^+$	59.04	47.97	58.33	8.97	0.9
	Macrophages	$CD45^+$ $CD172a^+$ $MHCII^+$	13.61[a]	17.55[a]	5.76[b]	2.63	0.03
	M1	$CD45^+$ $CD172a^+$ $MHCII^+$ $CD14^+$	9.76	11.06	3.55	2.70	0.09
	M2	$CD45^+$ $MHCII^+$ $CD11b^+$	7.86[a]	5.75[a]	1.64[b]	1.25	0.01
	TREM2	$CD45^+$ $TREM2^+$	4.40	7.14	1.43	2.70	0.4

[1]Treatments for clinical ketosis (CK) cows (n = 6) with BHB>1.2 mmol/L at d7: PG = Propylene Glycol, PGNIA = PG + Niacin, PGNIAFM = PGNIA + flunixin meglumine.
[2]*P*-values refer to the main effect of treatment.
[3]IHC = Immunohistochemistry. Data are means ± SEM of signal intensity of CD172a antibody in tissue sections.
[4]Data are the mean distribution (%) ± SEM of cells identified. Hematopoietic cells distribution is from the total of live stromal vascular cells. Macrophages, M1, M2 and TREM cells frequencies are from the total of hematopoietic cells. n=24
[a-b]Mean values in the same row with different superscripts differ ($P<0.05$) adjusted by Tukey.

DISCUSSION

Despite major advances in the management and prevention of CK, the effects of the disease on AT function are not completely understood and represent a major knowledge gap. Furthermore, PG, the most widely recommended treatment for CK, is not completely effective in controlling the disease having a resolution rate of 42% after 1 week of treatment (Gordon et al., 2017). The reasons behind this poor efficacy are likely associated with the minimal effect of PG on AT lipolysis and systemic inflammation, which are significant factors in CK pathogenesis. The present study demonstrates that cows with CK have impaired AT function, as evidenced by lipolysis dysregulation, inflammation, and insulin resistance. Our results also demonstrate that using the

lipolysis inhibitors NIA and FM combined with PG improved AT function by recovering insulin sensitivity and reducing inflammation.

AT Lipolysis During CK

During CK, AT lipolysis is dysregulated and becomes intense and protracted (Contreras et al., 2015). Accordingly, CK cows in the present study had higher adipocyte triglyceride hydrolysis, which was reflected in a higher frequency of smaller adipocytes (<1499 μm^2) and an increase in lipolysis biomarkers NEFA and BHB [described in detail in the companion paper (Chirivi et al., 2023b)]. Our findings are in line with the reduced adipocyte diameter observed in cows with DA and ketosis (Contreras et al., 2015). In the present study, we investigated the underlying mechanisms that contribute to lipolysis dysregulation in CK cows. Our findings demonstrate that this dysregulation is driven by enhanced activity of neutral lipases (e.g., HSL, ATGL), decreased utilization of FA as energy substrates in adipocytes, and AT inflammation and insulin resistance.

Lipolysis is regulated by the transcription of neutral lipases *LIPE, LPL,* and *PNPLA2*. Post-translationally, kinase activity (i.e., phosphorylation) on HSL and the activation of ATGL's coactivator CGI-58 (encoded by *ABHD5*) modulate lipolysis intensity (Grabner et al., 2021). In healthy cows during the early postpartum period, lipase gene transcription is reduced, but lipase activity remains high, as indicated by pHSL:HSL levels (Koltes and Spurlock, 2011, De Koster et al., 2018a). In the present study, lipase gene transcription was upregulated in CK cows, indicating that lipolysis dysregulation in these animals may originate at the transcriptional level. Likewise, dysregulated lipolysis at the transcriptional level has been observed in animal models of lipodystrophy, where the upregulation of *ABHD5* and *PNPLA2,* along with an increase in protein content of ATGL and HSL, is associated with intense lipolysis. (Dettlaff-Pokora et al., 2016).

In healthy periparturient cows, adipocytes adapt to increased release of FA by enhancing *CPT1A* and *CPT2* transcription (Elis et al., 2013). The proteins encoded by these genes facilitate FA transport into the mitochondria for oxidation. Our results provide evidence that CK affects adipocyte capacity to transport FA into mitochondria. Despite higher availability of FA, CK cows did not have changes in *CPT1A* transcription, suggesting an impaired capacity to oxidize excessive FA within AT. Our findings are consistent with AT transcriptomic data from cows with ketosis, indicating impaired FA oxidation during this condition (Ning et al., 2022).

Lipolysis products activate pro-lipogenic and adipogenic pathways, such as PPARs, in adipocytes. These pathways serve as negative feedback loops to limit the excessive depletion of triglyceride reserves (Mottillo et al., 2012). However, in the present study, we found that CK cows had increased transcription of PPAR genes, but the lipogenic responses triggered by these nuclear transcription factors were not activated. This suggests that PPAR pathways may be dysfunctional in CK cows. Further studies are required to evaluate the role of PPARs during CK.

AT Insulin Resistance During CK

The biological effects of insulin on AT are the suppression of lipolysis and the stimulation of lipogenesis and glucose uptake (Brockman and Laarveld, 1986). AT insulin resistance is a reduced biological response to the pancreatic peptide (Ronald Kahn, 1978). After insulin binds to its receptor, the effects on AT rely on the activation of protein kinase Akt (Degerman et al., 1998). To reduce lipolysis, Akt phosphorylation activates phosphodiesterase 3b, the enzyme involved in the degradation of cAMP, which consequently lowers HSL activity and lipolysis (Degerman et al., 1998). To the best of our knowledge, this study is the first to evaluate AT lipolytic responses in cows with CK. We report that CK cows had reduced Akt phosphorylation, which was evident in a diminished anti-lipolytic effect when AT was incubated with insulin. Our results are consistent

with previous AT proteomic analyses in cows with insulin resistance, which showed decreased Akt signaling and increased HSL and ERK/MAPK activity (Zachut, 2015).

The mechanisms leading to the development of AT insulin resistance appear to be multifactorial and likely involve a combination of lipid overflow, inflammation, adipokine dysregulation, genetic traits, and mitochondrial dysfunction (Li et al., 2022). We identified some of these factors in the present study. For example, we observed upregulation of *FABP4* and *LPIN1*, as well as downregulation of *SLC2A4* transcription, which have direct associations with insulin resistance in humans and rodents (Miranda et al., 2010, Trojnar et al., 2019). *FABP4*, encoding fatty acid-binding protein 4, is involved in intracellular FA transport and lipid oxidation. Its upregulation, observed in our study and triggered by AT inflammatory responses, has been linked to insulin resistance through suppression of Akt signaling and enhanced cyclooxygenase 2 activation (Trojnar et al., 2019). *LPIN1*, encoding phosphatidic acid phosphohydrolase 1, plays a role in triglyceride synthesis. As observed during CK, its upregulation during lipolysis is a regulatory mechanism that adjusts AT function by catalyzing triglyceride synthesis in the presence of abundant FA. Increased *LPIN1* expression is associated with reduced insulin function in dairy cows (Prodanović et al., 2022). *SLC2A4*, which encodes the glucose transporter type 4 protein (GLUT4), was downregulated in CK cows in the present study. This reflects impaired insulin response and aligns with limited *SLC2A4* transcription in AT from postpartum dairy cows classified with insulin resistance based on glucose tolerance tests (Jaakson et al., 2018). Our results suggest that in cows with CK, despite AT's increased capacity to transport and esterify fatty acids, the availability of energy for adipocyte function may be limited by reduced fatty acid oxidation and glucose uptake.

CK Increases AT Inflammation and ATM Infiltration

Our data indicate that CK coincides with AT inflammation. In this study, CK cows had increased transcription of proinflammatory cytokines (*CCL2, IL8, IL10, SIRPA, SPP1, TLR4, TNF)* in AT. This response may be triggered by the presence of lipolytic products in AT and endotoxemia. AT inflammation is characterized by the infiltration of myeloid immune cells, proliferation of resident immune cells, including ATM, and increased secretion of inflammatory mediators (Kawai et al., 2021). Lipolysis is another important trigger of AT inflammation, as it enhances the biosynthesis of lipid mediators of inflammation derived from linoleic and arachidonic acids (Contreras et al., 2017a). Therefore, the excessive AT inflammation observed in this study in CK cows is likely due to intense lipolysis during CK.

A second reported mechanism involved in AT inflammation is endotoxemia (Clemente-Postigo et al., 2019). In the companion paper, we report that over 70% of CK cows exhibited endotoxemia (Chirivi et al., 2023b), which aligns with the findings of the present study showing CK cows had increased transcription of TLR4 and heightened phosphorylation of ERK1/2 in AT. The ERK1/2 cascade plays a role in various cellular processes, including stress response, inflammation, and lipolysis. In humans and rodents with diabetes, ERK1/2 signaling has been associated with AT insulin resistance (Carlson et al., 2003). Despite limited research on AT function during CK, our findings align with previous proteomic analyses, indicating increased inflammatory signaling through the NFκB and ERK1/2 pathways, resulting in elevated cytokine expression in AT during ketosis. (Xu et al., 2019). Taken together, these results suggest that circulating LPS may potentially trigger metabolic dysfunction and inflammation in AT during CK.

In the present study, CK cows exhibited increased ATM infiltration, including cells of both M1 and M2 phenotypes. This finding coincides with previous reports in cows with DA and CK

(Contreras et al., 2015). Enhanced M1 polarization in CK cows may be due to TLR4 stimulation and TNF pathway activation. M1 ATM produce proinflammatory cytokines and chemokines that enhance the migration of monocytes (*CCL2, IL10, SPP1*), neutrophils, and basophils (*IL8, SIRPA*) into AT, resulting in enhanced phagocytic activity (Atri et al., 2018). To our knowledge, this is the first study identifying TREM2 ATM in postpartum cows. We observed a decrease in the frequency of TREM2 ATM during CK. TREM2 cells are specialized macrophages that contain lipids and have beneficial effects such as promoting the resolution of inflammation, lipid uptake, and removal of dying cells (Liebold et al., 2023). The reduction of TREM2 is associated with impaired macrophage ability to uptake oxidized lipids and cholesterol, which can lead to insulin resistance (Coats et al., 2017). While the decreased expression of TREM2 ATM during CK suggests a diminished capacity to clear excessive lipids, the specific role of TREM2 in metabolic inflammation in dairy cows remains to be determined. In summary, while AT inflammation serves a physiological purpose in tissue remodeling, dysregulated inflammation, as seen in CK, may initiate a deleterious cycle that links processes such as lipolysis, ATM infiltration, inflammation, and insulin resistance.

It is important to note that CK cows also show signs of inflammation resolution in the present study. For example, M2 ATM trafficking increased in CK cows suggesting an active inflammation resolution process within the AT. The M2 phenotype is responsible for resolving inflammation by increasing phagocytosis of apoptotic cells and producing angiogenic and chemotactic products that promote tissue repair (Fujisaka, 2021). This study's M2 polarization in CK cows may be associated with increased IL10 production, a cytokine known for activating anti-inflammatory M2 macrophages (Lopes et al., 2016). M2 polarization is also promoted by BHB in a STAT6-signaling pathway-dependent manner (Huang et al., 2022). Therefore, the increased

concentration of BHB during CK likely induces the M2 phenotype (as observed in the present study). Growing evidence suggests ketogenesis could be an endogenous protective mechanism to reduce inflammation and regulate macrophage activation. (Zhang et al., 2022).

In addition to M2 enhanced trafficking during CK, there was a downregulation of *IL6* in AT from CK cows. IL6 is a potent proinflammatory cytokine that increases leptin secretion in AT to mediate energy balance by suppressing food intake. Reduction of *IL6* is reported during chronic inflammation after using ketogenic diets (Pinto et al., 2018, Ciaffi et al., 2021). We also observed upregulation of *LOCS527744,* the gene encoding for the BHB receptor HCAR2 in CK cows. Previous reports indicate that HCAR2 mRNA was upregulated in SCAT from postpartum dairy cows , coinciding with the period of higher lipolysis (Lemor et al., 2009). BHB has several effects on AT, including anti-inflammatory effects and the inhibition of lipolysis by HCAR2 signaling (Kenéz et al., 2014, Mielenz, 2016). In rodents, HCAR2 activation enhances AMPK/Nrf2-mediated autophagy, reducing SCAT inflammation (Guo et al., 2021). HCAR2's antilipolytic effect is mediated by PKA/HSL signaling (Kenéz et al., 2014). Although the role of the BHB receptor is not clear in AT during hyperketonemia, our data suggest that the upregulation of this receptor may be a response to inflammation or an attempt to mitigate excessive lipolysis during CK. More research is needed to understand the physiological role of HCAR2 and its ligands during CK in cows.

PGNIAFM Improves AT Function in CK Cows

In the larger randomized clinical trial (Chirivi et al., 2023b), cows treated with PGNIAFM recovered from hyperketonemia and had reduced lipolysis and systemic inflammation. Aligning with the clinical observations, the subset of cows treated with PGNIAFM reported in the present study, had improved AT insulin sensitivity and reduced AT inflammation. In contrast, treatment

with PG alone did not improve AT insulin sensitivity. This finding may account for the higher lipolysis rates observed in cows treated with PG compared to PGNIAFM-treated ones. While PG increases blood glucose levels in cattle and limits the utilization of BHB and NEFA as energy sources, it does not seem to have an impact on lipolysis or AT function. In a study by Bjerre-Harpøth et al. (2015) that focused on periparturient over-conditioned cows, supplementation of 500 g/day of PG during the first four weeks postpartum did not result in any changes in AT proteome when compared to the placebo group. Although research investigating the effects of PG on AT function during ketosis is limited, it was demonstrated that even prolonged periods of PG supplementation do not improve AT function in cows at a high risk of dysregulated lipolysis (Bjerre-Harpøth et al., 2015).

In the present study, combining PG and 24 g of NIA for 3 days (PGNIA) did not improve AT insulin sensitivity. This finding suggests that inhibiting the canonical pathway with NIA alone was insufficient in controlling the dysregulation of lipolysis and insulin resistance in AT from cows with CK. Although the mechanisms by which NIA inhibits canonical lipolysis are well described (Tunaru et al., 2003, Hristovska et al., 2017), its effects on insulin sensitivity in healthy cows vary across studies. For example, a study supplementing 120 g/d of unprotected NIA (equivalent to ~ 12g/day of absorbed NIA) to dairy cows starting 14 d before expected calving date until 14 d after parturition, reported improved systemic insulin sensitivity, as measured by the RQUICKI insulin sensitivity index (Hristovska et al., 2017). However, another study supplementing 24 g/d of unprotected NIA during 21 days before and 21 days after parturition did not alter the expression of proteins related to insulin signaling in AT (Kinoshita et al., 2016).

In the present study, we observed that PGNIAFM promoted the recovery of AT insulin sensitivity by enhancing the phosphorylation of Akt. Consequently, PGNIAFM-treated cows

mobilized less fat from AT, resulting in a higher frequency of large adipocytes and a tendency for a reduced number of small adipocytes (<1400 microns). These results, align with the reduction in lipolysis and hyperketonemia described in the companion paper (Chirivi et al., 2023b). Combining NIA and FM in PGNIAFM simultaneously blocks the canonical and inflammatory lipolytic pathways. FM inhibits the activity of COX, which in turn suppresses the synthesis of prostaglandin E2 (PGE2), a known lipolytic agent, that enhances the activity of ERK1/2 (Bashir et al., 2020, Inazumi et al., 2020). Therefore, it is plausible to speculate that the observed reduction in lipolysis in PGNIAFM-treated cows can be attributed to the downregulation of ERK1/2 expression, likely resulting from the decreased synthesis of prostaglandins.

To our knowledge, this is the first trial studying the effect of lipolysis inhibitors such as NIA and FM on AT function in cows with CK. Previous reports suggest that the administration of FM for the first 3 DIM in postpartum cows is detrimental to feed intake and milk production (Shwartz et al., 2009). In contrast, a single dose of FM benefits healthy cows by reducing inflammatory markers (Schmitt et al., 2022), suggesting that prolonged administration of inflammatory therapy dampens metabolic adaptations in early lactation cows. The only study evaluating AT function during NSAID therapy demonstrated increased transcription of proinflammatory cytokines in AT after administration of carprofen at 1.3 mg/kg for 3 d in early (1, 3, and 5 d postpartum) postpartum dairy cows (Vailati Riboni et al., 2015). While ample evidence exists regarding the beneficial effects of various natural and synthetic anti-inflammatory agents in modulating AT inflammation and ATM infiltration in humans and rodents (da Cruz Nascimento et al., 2022), further research is needed to explore the use of anti-inflammatory therapies during metabolic diseases and its implications for AT function during metabolic diseases.

This study has limitations, including the lack of a PGFM treatment that limits our capacity

to differentiate the individual contribution of FM to CK therapy. We also did not evaluate systemic insulin sensitivity and only focused on the responses of AT to insulin. However, results from the ex-vivo lipolysis model used in the present work provide essential information for future studies evaluating systemic insulin responses using glucose clamp techniques.

CONCLUSION

The present study demonstrates that cows with CK exhibit increased AT inflammation, characterized by increased ATM infiltration of both M1 and M2 phenotypes and activation of the ERK1/2 inflammatory pathway. CK is also associated with reduced insulin sensitivity in AT. Treatment of CK with a combination of PG, NIA, and FM leads to a reduction in AT inflammatory markers and an improvement in AT insulin sensitivity.

CHAPTER 4: LIPOPOLYSACCHARIDE INDUCES LIPOLYSIS AND INSULIN RESISTANCE IN ADIPOSE TISSUE FROM DAIRY COWS

Published in Journal of Dairy Science: M. Chirivi, C. J. Rendon, M. N. Myers, C. M. Prom, S. Roy, A. Sen, A. L. Lock, and G. A. Contreras. 2021. J. Dairy. Sci. Jan; 105(1):842-855. doi: 10.3168/jds.2021-20855.

ABSTRACT

Intense and protracted adipose tissue (AT) fat mobilization increases the risk of metabolic and inflammatory periparturient diseases in dairy cows. This vulnerability increases when cows have endotoxemia—common during periparturient diseases such as mastitis, metritis, and pneumonia—but the mechanisms are unknown. Fat mobilization intensity is determined by the balance between lipolysis and lipogenesis. Around parturition, the rate of lipolysis surpasses that of lipogenesis leading to enhanced FFA release into the circulation. We hypothesized that exposure to endotoxin (ET) increases AT lipolysis by activation of canonical and inflammatory lipolytic pathways and reduction of insulin sensitivity. In experiment 1, Subcutaneous AT (SCAT) explants were collected from periparturient (PP; n=12) Holstein cows at 11±3.6 d before calving (PreP) and 6±1 d (PP1) and 13±1.4 d (PP2) after parturition. Explants were treated with the ET lipopolysaccharide (LPS=20 µg/ml; Basal=0 µg/ml) for 3 h. The effect of LPS on lipolysis was assessed in the presence of the beta-adrenergic agonist and promoter of lipolysis isoproterenol (ISO=1 µM; LPS+ISO). In experiment 2, SCAT explants were harvested from 24 non-lactating, non-gestating multiparous Holstein dairy cows (NL) and exposed to the same treatments as in experiment 1 for 3 and 7 h. The impact of LPS on the anti-lipolytic responses induced by insulin (INS=1 µL/L, LPS+INS) was established during ISO stimulation [ISO+INS, LPS+ISO+INS]. The characterization of lipolysis included the quantification of glycerol release and the assessment of markers of lipase activity [adipose triglyceride lipase (ATGL), hormone-sensitive lipase (HSL), and pHSL (Ser563)], and insulin pathway activation (AKT, pAKT) using capillary electrophoresis.

Inflammatory gene networks were evaluated by RT-qPCR. In PP cows, LPS increased AT lipolysis by 67±12% at 3 h across all time points (i.e., PreP, PP1, and PP2) compared to Basal. In NL cows, LPS was an effective lipolytic agent at 3 h and 7 h, increasing glycerol release by 115±18% and 68.7±16%, respectively, relative to Basal. In experiment 2, LPS enhanced ATGL activity with minimal HSL activation at 3 h. In contrast, at 7 h, LPS increased HSL phosphorylation (i.e., HSL activity) by 123±11%. LPS-induced HSL lipolytic activity at 7 h coincided with the activation of the MEK/ERK inflammatory pathway. In experiment 2, INS reduced the lipolytic effect of ISO (ISO+INS -63±18%) and LPS (LPS+INS -45.2±18%) at 3 h. However, INS's antilipolytic effect was lost in the presence of LPS at 7 h (LPS+INS -16.3±16%) and LPS+ISO+INS at 3 h and 7 h (-3.84±23.6% and -21.2±14.6). Accordingly, LPS reduced pAKT:AKT (0.11± 0.07) compared to Basal (0.18±0.05) at 7 h. Our results indicate that exposure to LPS activates the canonical and inflammatory lipolytic pathways and reduces insulin sensitivity in SCAT. These data provide evidence that, during endotoxemia, dairy cows may be more susceptible to lipolysis dysregulation and loss of adipocyte sensitivity to the antilipolytic action of insulin.

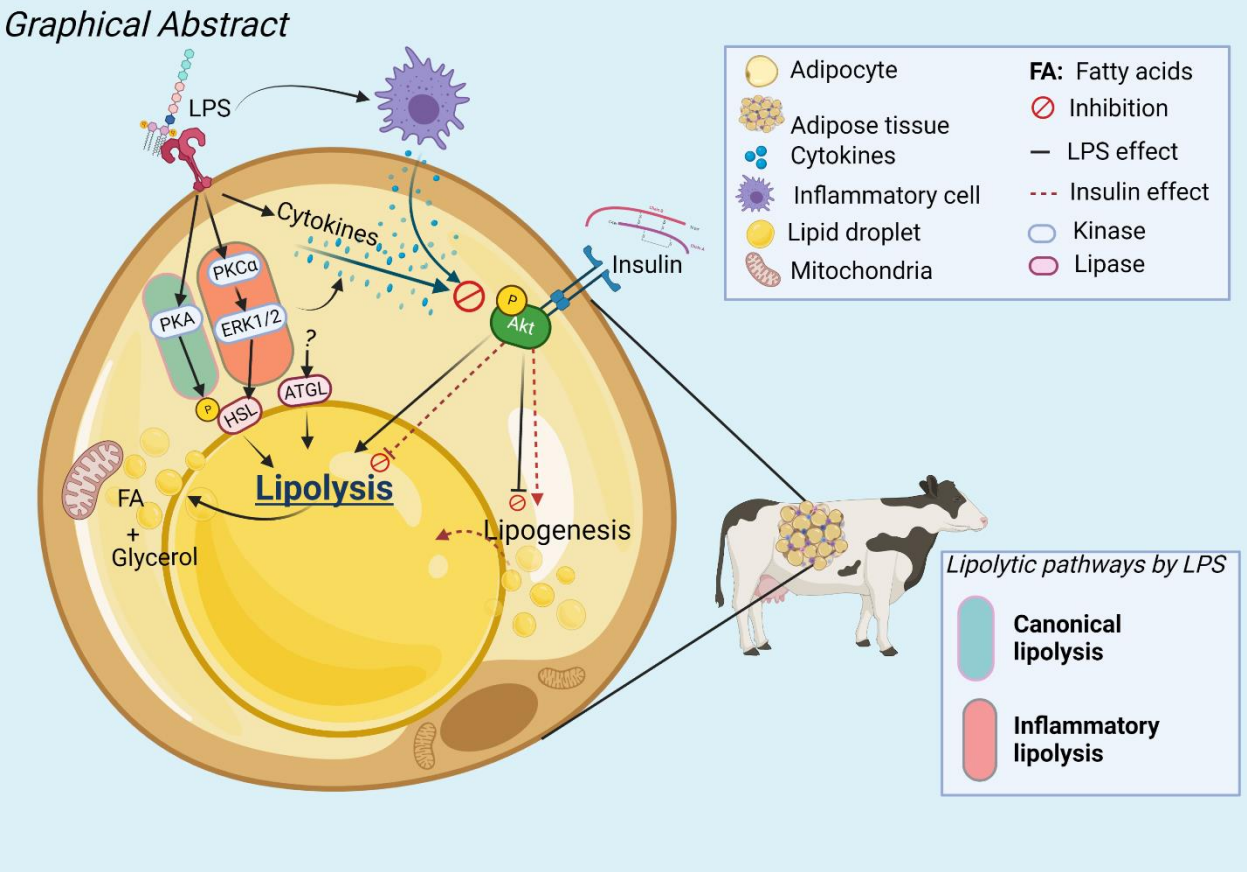

Figure 15. Graphical abstract. Lipopolysaccharide (LPS) activates lipolysis and induces insulin resistance in adipose tissue from dairy cows. LPS, an endotoxin, activates the canonical (blue square) through PKA (protein kinase A). Lipopolysaccharide also initiates the inflammatory lipolysis pathway (red square) by triggering ERK1/2 activity. At the same time, LPS inhibits the phosphorylation of the Akt protein, leading to decreased insulin action (lipogenesis and inhibition of lipolysis). Created with BioRender.com.

INTRODUCTION

The periparturient period is the lactation stage with the highest risk for metabolic and infectious diseases in dairy cows (Ospina et al., 2013). Around parturition, dairy cows mobilize fatty acids (**FA**) from adipose tissues (**AT**) through lipolysis to fulfill energy and nutrient demands that are not met by dietary intake (McNamara and Hillers, 1986). When lipolysis is active, adipose triglyceride lipase (**ATGL**) and hormone-sensitive lipase (**HSL**) hydrolyze triglycerides, releasing free fatty acids (**FFA**) into circulation. HSL is the main neutral lipase during demand lipolysis, and thus its activity is largely responsible for AT lipolytic responses during the periparturient period (De Koster et al., 2018b). Although insulin reduces AT lipolysis, around parturition low plasma insulin concentrations and the transient state of insulin resistance in AT limit the antilipolytic effects of the pancreatic peptide. This response is a homeorhetic adaptation that ensures sufficient glucose supply to the mammary gland by providing FFA as an energy substrate for other tissues (De Koster and Opsomer, 2013).

One significant risk factor for disease susceptibility around parturition is lipolysis dysregulation: defined as an impaired response of AT to the anti-lipolytic and pro-lipogenic effects of insulin (Contreras et al., 2017c). Lipolysis dysregulation and its consequent excessive fat mobilization are more common in dairy cows with high body condition scores, genetic predisposition to lipolysis, concurrent health disorders, or inflammatory conditions (Bobe et al., 2004, Drackley et al., 2005). In humans and rodents, endotoxin (**ET**) and especially lipopolysaccharide (**LPS**) may exacerbate lipolysis dysregulation (Zu et al., 2009a, Grisouard et al., 2012). This is because LPS induces triglyceride hydrolysis through canonical and inflammatory lipolytic pathways (Figure 15). In the canonical signaling pathway, LPS increases cAMP levels, triggering the phosphorylation of protein kinase A (**PKA**), which is the enzyme that

activates HSL. The inflammatory lipolytic pathways lead to the activation of HSL through mitogen-activated protein kinase/extracellular signal-regulated kinase (**MEK/ERK**) signaling (Shi et al., 2002) and other targets of the LPS sensor toll-like receptor 4 (Lu et al., 2008). The activation of MEK/ERK may exacerbate lipolysis dysregulation as inflammatory pathways impair protein kinase B (**Akt**) phosphorylation and thus insulin signaling (Figure 15) (Chen et al., 2015).

During the periparturient period, ET present in the uterine and gastrointestinal tract environments may translocate into systemic circulation especially during infectious and metabolic diseases (Eckel and Ametaj, 2016, 2020). Endotoxemia is also detected during coliform mastitis, digestive diseases, and infectious health events that occur during peak and late lactation (Andersen et al., 1996, Wenz et al., 2001). Experimental LPS exposure for 7 d in lactating cows appears to affect AT function. Horst et al. (2019b) showed enhanced FFA release during the first three days of LPS infusion that subsequently decreased from day 3 to 7. Therefore, endotoxemia may enhance lipolysis dysregulation in cows, yet the specific effects of LPS on bovine AT lipolysis and insulin signaling processes have not been examined. The present study determined how ET activates lipolytic response and affects insulin sensitivity in AT of dairy cows and provides evidence for the activation of the canonical and inflammatory lipolytic pathways by LPS.

MATERIALS AND METHODS

Animals and sample collection

All experimental procedures were approved by the Institutional Animal Care and Use Committee at Michigan State University (AUF#11-16-188-00).

Experiment 1

Twelve healthy periparturient (**PP**) multiparous Holstein cows from the Michigan State University Dairy Teaching and Research Center were used for this study. At the moment of

selection, cows were non-lactating and pregnant (210-240 days of gestation). Cows were blocked by body condition score (BCS) (by 0.5 point scale), assessed weekly by three trained investigators (Strieder-Barboza et al., 2015), only animals with a BCS of 3.0 to 4 were selected for the study, along with previous lactation 305-d mature-equivalent yield (MEq; within 5,700 kg), and parity (up to 1 lactation difference). The values (mean ± SEM) for BCS, MEq, and parity were 3.53±0.06, 14,597±170 kg, and 2.67±0.65, respectively. Cows were housed in tie stalls bedded with sawdust. All animals received close-up (-30 d relative to parturition) and fresh (1–15 d into lactation) diets that were formulated to meet or exceed their nutritional requirements defined by the National Research Council (Council, 2001). Subcutaneous AT (SCAT) samples were obtained from the right paralumbar fossa cranial to the tensor fascia latae muscle at 11±3.6 d before the expected calving date (**PreP**), and 6±1 d (**PP1**) and 13±1.4 d (**PP2**) after parturition, using the surgical procedure described by De Koster et al. (2018b). The site of the incision was moved ventrally 3–4 cm at each collection timepoint. This anatomic location offers a wider surgical area for repeated AT sampling, it is less likely to have fecal contamination, and it is seldom used as injection site. Five grams of SCAT were collected, and the biopsy incision was closed using a continuous interlocking suture with Braunamid (USP1, Aesculap, Center Valley, PA, 104 USA). Sutures were removed 12-14 d after each procedure.

Experiment 2

Twenty-four healthy non-gestating, non-lactating (**NL**) Holstein cows were selected at a local abattoir and assigned a BCS before slaughter by a trained veterinarian. Only animals with a BCS of 3.0 to 4.0 were selected for the study. Animals were euthanized by captive bolt, and internal organs were evaluated to exclude any cows with evidence of intra-abdominal, thoracic, or gastrointestinal disorders. Then, following skin removal, SCAT samples were collected from the

right paralumbar fossa.

In vitro lipolysis assays

AT lipolysis was assessed as described by De Koster et al. (2018b), with some modifications. Immediately after collection, AT was placed in 30 mL Krebs-Ringer Bicarbonate HEPES Buffer (KRBH, pH 7.4) and transported to the laboratory at 38°C. AT was minced into approximately 100 mg tissue fragments using sterile surgical scissors and transferred into 24-well plates containing 1mL KRBH supplemented with 3% FA-free bovine serum albumin (BSA, Millipore-Sigma, Burlington, MA, USA). Explant weight was determined precisely using an analytical scale (Mettler Toledo, Columbus, OH, USA). Culture plates with AT explants were pre-incubated at 38°C for 20 min on a shaker. Next, reagents were added to the culture plates as described below. All reagents were prepared fresh immediately before the lipolysis assay.

In both experiments, **Basal** lipolysis was established without the addition of any reagent. The beta-adrenergic agonist isoproterenol (**ISO**, I6504, Millipore-Sigma) at a concentration of 1μM was used as a positive control for lipolysis. ISO lipolytic responses are well characterized in AT from periparturient cows and bovine adipocytes including the activation of PKA and HSL (Faylon et al., 2015, De Koster et al., 2016)

To determine the lipolytic effects of LPS, SCAT from a subset of NL cows were treated with 0, 1, 10, 20, or 100 μg/mL of LPS from *Escherichia coli* O55:B5 (**LPS**, L6529, Sigma-Aldrich) for 3 h. Based on the lipolytic response observed and a previous report that characterized the inflammatory responses in AT from dairy cows (Mukesh et al., 2010), the 20 μg/mL dose was selected as the working concentration for experiments 1 and 2.

In experiment 1, the objective was to characterize AT lipolytic response to LPS during the PP period. SCAT explants from PP cows were treated with Basal, ISO, LPS (20 μg/mL), and

LPS+ISO. After 3 h of incubation, AT explants and media samples were collected, snap-frozen in liquid nitrogen (N_2), and stored at −80 °C until further analysis.

In experiment 2, the objective was to determine the mechanism that leads to the activation of lipolysis during an LPS challenge. To establish differences in the activation of the canonical and inflammatory pathways we included a 7 h incubation time. This selection is based on work by (Hoareau et al., 2010), demonstrating that complete activation of inflammatory pathways in adipocytes only occurs after 6 h of exposure to LPS. The lipolysis assay was performed in SCAT from NL cows. Explants were incubated for 3 and 7 h with Basal, LPS (20 µg/mL), ISO, and LPS+ISO. To assess insulin response, 1 µg/L of insulin from bovine pancreas (**INS**, I0516, Sigma-Aldrich) was included alone (**INS**) and in combination with LPS (**LPS+INS**), ISO (**ISO+INS**), and **LPS+ISO+INS**. In the 7 h treatments, culture media was collected, snap-frozen in liquid nitrogen, and stored at -80 °C after 3 h of incubation. Explants were then moved into a new 24-well plates with fresh treatments; this was required to avoid inhibition of lipolysis and reuptake of FA by the accumulation of glycerol and FFA in the medium (Schweiger et al., 2014). After 7 h, AT explants and sample media were collected and stored as described above until analysis. Glycerol release was determined at 3 h and then pooled with 7 h samples to quantify the cumulative lipolytic response.

Lipolysis was assessed by quantification of glycerol released in the culture medium, using free glycerol reagent (Millipore-Sigma, F6428). Media samples (67 µL), blank (KRBH+3% BSA), and standards (Glycerol standard solution, G7793, Sigma-Aldrich) were loaded into a 96-well plate, and 200 µL of free glycerol reagent was added. After 5 min of incubation at 38 °C, optical density was measured at 540 nm. The intra- and inter-assay coefficients of variation were 4.71% and 12.63%, respectively. All samples were run in duplicate. Glycerol released was normalized by

the weight of the AT explant (nmol/mg) and the results are expressed as a ratio of the basal release of glycerol in, nmol of glycerol per mg of AT, or nmol of glycerol per mg of AT per hour.

RNA extraction from adipose samples

SCAT samples were transferred into screwcap tubes containing 1mL of TRI Reagent (R2050-1 ZymoResearch, Irvine, CA, USA) and 2.3 mm zirconia/silica beads (Biospec, Bartlesville, OK, USA). The samples were placed on dry ice and homogenized at 3.4 m/s for 3x30 sec using a bead mill tissue homogenizer (FisherScientific, Waltham, MA, USA). Next, samples were centrifugated at 12,000 *g* for 10 min, and the liquid phase was collected carefully, avoiding the lipid layer on the top. Chloroform (200 µL) was added, and the samples were shaken for 15 sec and placed on ice for 3 min. Following 15 min of centrifugation, the aqueous phase was collected and transferred to the Quick-RNA Miniprep plus Kit (R1058 Zymo Research, Irvine, CA, USA) to extract total RNA according to the manufacturer's protocol. DNase I (E1010 Zymo research) was used to eliminate genomic DNA. RNA was stored at -80 °C, and the concentration and integrity of total RNA were evaluated using a NanoDrop 1000 spectrophotometer (Thermofisher Scientific, Waltham, MA, USA). All samples had a 260:280 nm ratio between 1.91 and 2.01 and an RNA integrity number >6. Reverse transcription was performed with 200 ng of RNA using 4 µL of the qScript cDNA SuperMix (95048 Quantabio, Beverly, MA, USA) for 5 minutes at 25 °C, 30 minutes at 42 °C, and 5 minutes at 85 °C. cDNA was stored at -20 °C.

Gene expression analysis

Transcriptional studies were performed using the Wafergen SmartChip Real-time PCR system as described in (De Koster et al., 2018b). SYBR gene expression primers were used for qPCR assays and were either commercially available or designed from bovine sequences and synthesized (Millipore-Sigma Aldrich). Samples were assayed in duplicate on the high-throughput

qPCR instrument Wafergen Smartchip (Takara Bio, Mountain View, CA, USA). Each 100 nL PCR reaction contained 1X of LightCycler 480 SYBR Green Master Mix (Roche), 200nM of primer assays (Appendix Table 14), and 1.5 ng/μL of sample cDNA. A non-template control and non-reverse-transcriptase control monitored contamination and primer-dimer formation that could produce false-positive results and validated the absence of genomic DNA. The following cycling conditions were used on the Wafergen SmartChip Real-time PCR system: Initial enzyme activation at 95 °C for 10 min, 45 cycles of denaturation at 95 °C for 10 sec, and annealing at 60 °C for 53 sec. The linear dynamic range was 0.99±0.0002. Housekeeping genes with the lowest pairwise variation value, including eukaryotic translation initiation factor 3 subunit K (*EIF3K*), ribosomal protein Lateral Stalk Subunit P0 (*RPLP0)*, and ribosomal protein S9 (*RPS9*) were selected from a pool of genes that also included *ACTB, GAPDH,* and *PPIA*. Expression of genes of interest was normalized against the geometric mean of selected housekeeping genes as described by Hellemans et al. (2007). Data are presented as fold changes relative to the Basal samples with the 95% confidence interval. These were calculated from least-squares mean differences according to the formula $2^{-\Delta\Delta Ct}$, where $\Delta\Delta Ct = \Delta Ct_{\text{Target Sample}} - \Delta Ct_{\text{Calibrator Sample (Basal)}}$.

Protein analysis

Proteins were extracted from ~100 mg of snap-frozen SCAT samples, with a bead mill homogenizer using RIPA buffer (Teknova, Hollister, CA, USA) supplemented with protease cOmplete™ mini EDTA-free protease inhibitor (Roche, San Francisco, CA, USA) and phosphatase inhibitors (Phosphatase inhibitor cocktail II J61022, Thermofisher Scientific). The concentration of protein was determined using the Pierce™ BCA protein assay kit (Thermo Scientific, 23225). The optimal protein concentration for the antibodies used in these experiments was 0.5 mg/mL as established in the 12–230 kDa Wes™ Separation Module capillary cartridges

of the Simple Protein Wes™ system [SM-W004, ProteinSimple, Santa Clara, CA, USA (Nelson et al., 2017)]. Antibodies and dilutions were as follows: rabbit monoclonal anti-HSL (1:25, #4107, Cell Signaling, Danvers, MA, USA), anti-phosphorylated HSL serine 563 (1:25, #PA5-17488, Thermo Fisher), anti-ATGL (1:25, #2138, Cell Signaling), anti-phosphorylated PKA threonine 147 (1:50, #5661, Cell Signaling), anti-PKCα (1:50, #2056, Cell Signaling), anti-PKCδ (1:50, #9616, Cell Signaling), anti-Akt (1:50, #9272, Cell Signaling) and anti-phosphorylated Akt serine 473 (1:10, #9271, Cell Signaling). Detection used the anti-rabbit module for the Wes™ (DM-001, ProteinSimple) kit that includes Luminol-S, Peroxide, Antibody Diluent 2, streptavidin-HRP, and anti-rabbit secondary antibody. Sample proteins were separated by microcapillary electrophoresis and the chemiluminescence signal peaks were generated for analysis. These signal peaks were transformed into digital images depicting bands as observed in Western blot analysis. Using Compass software (ProteinSimple), the peak areas of HSL, pHSL, ATGL, PKA, PKCα, PKCδ, Akt, and pAkt, proteins were estimated and normalized against the total protein detected with the Total Protein detection module kit (DM-TP01, ProteinSimple). The peak areas are directly proportional to the amount of the target protein quantified. The normalized data ATGL, PKA, and PKC are expressed as relative increase vs Basal, and ratios pHSL(Ser563):HSL and pAkt:Akt.

For ERK1/2 detection, Western blots were performed as described previously (Evaul and Hammes, 2008, Ma et al., 2016, Roy et al., 2018). Samples were separated on 4-20% sodium dodecyl sulfate-polyacrylamide gel, and the primary antibodies used were rabbit polyclonal p44/42-MAPK3/1(Erk1/2) (1:1000, #9102S, Cell Signaling) and phospho-p44/42-MAPK3/1(p-Erk1/2) (T202/Y204, 1:1000, # 9101S, Cell Signaling). Western blotting data were quantified by computer-aided densitometry analysis, normalized to total Erk1/2 levels, and expressed as relative increase vs Basal, as described previously (Ma et al., 2016, Roy et al., 2018).

Statistical analysis

Statistical analyses were performed using the Proc Mixed program from SAS version 9.4 (SAS Inst., Inc., Cary NC). The normality of the variables was checked using the Shapiro-Wilk Test ($P<0.05$). Residuals of the models were checked and found to be normally distributed. Non-significant ($P>0.05$) two-way interactions were removed from the model. Tukey's post hoc adjustment test was used for pairwise comparisons. In experiment 1, time relative to parturition (PreP, PP1, and PP2) was included as a repeated measure. The random effects included block and cows within block and time. The effect of the block was not significant in the model. In experiment 2, incubation time (3 h and 7 h) was included as a repeated measure within the random factor cow.

RESULTS

LPS Induces Lipolysis in AT From Dairy Cows

SCAT explants from 5 NL cows were treated with LPS at 1, 10, 20, and 100 µg/mL for 3 h. Compared to untreated samples (Basal), LPS at concentrations from 1 to 20 µg/mL increased glycerol release 1.7- to 2.10-fold (Figure 16A). This lipolytic response was similar to that induced by 1 µM of ISO (i.e., adrenergic stimulation; Figure 16A). Based on these results, we selected 20 µg/mL as the LPS dose for subsequent experiments. LPS at 100 µg/mL did not induce lipolysis in AT explants.

In experiment 1, we determined if LPS induced lipolysis in AT from PP cows and if the lipolytic response was affected by time relative to parturition (i.e., PreP, PP1, PP2). Treatment ($P<0.01$) and time relative to parturition ($P<0.05$) affected lipolytic responses. LPS increased glycerol release by 67±12% across all time points compared to Basal (Figure 16B). Lipolytic responses induced by LPS were lower than those induced by ISO (Figure 16B). Lipolysis induced by LPS was 41.9±15% higher in SCAT explants at PreP compared with those collected at PP2

(Figure 16C).

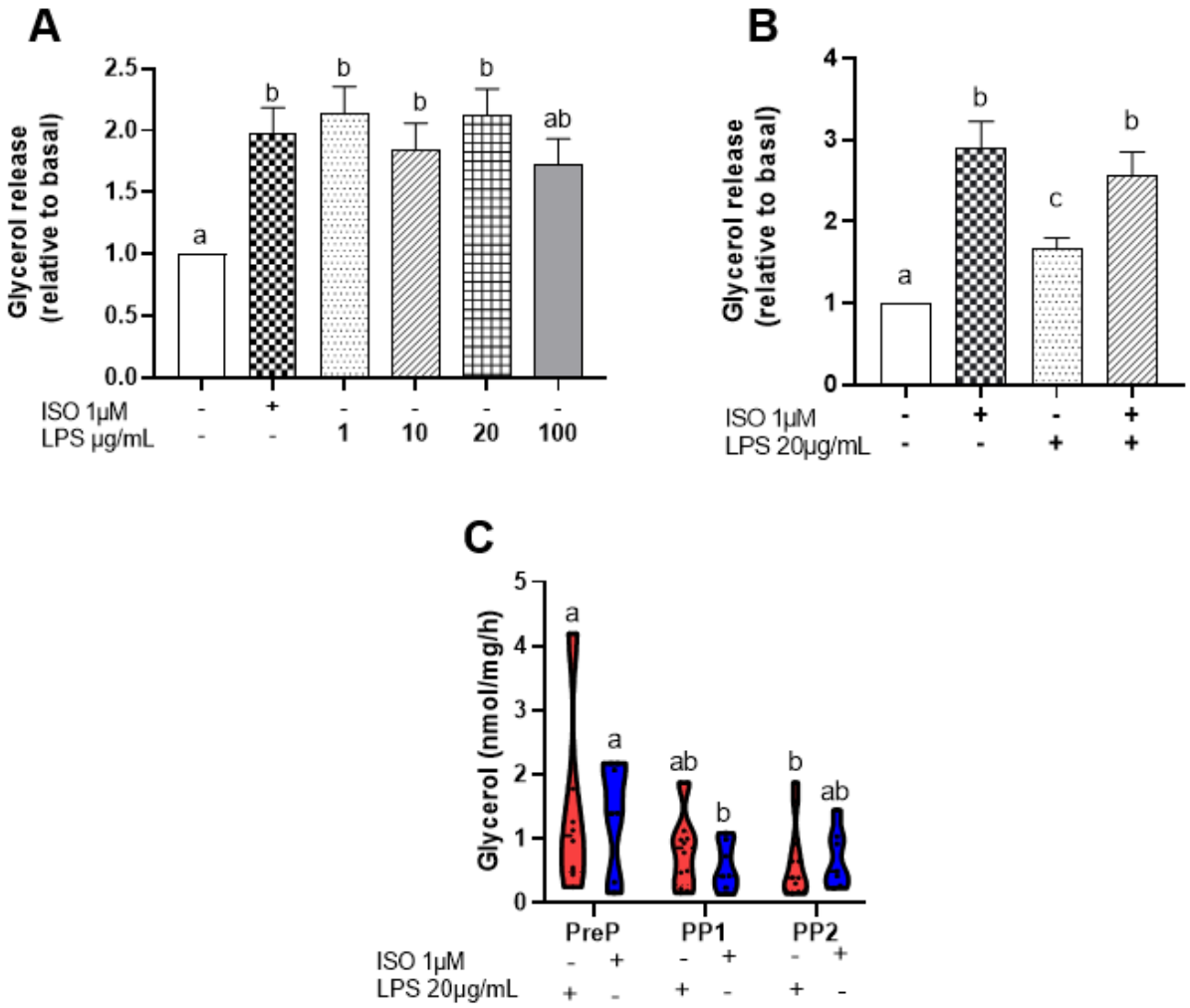

Figure 16. LPS induces lipolytic responses in dairy cows' adipose tissues (AT). (A) Glycerol release by subcutaneous adipose tissue (SCAT) explants from nonlactating cows exposed to no reagents (basal), isoproterenol (ISO; 1 μM), or LPS (at 1, 10, 20, or 100 μg/mL), for 3 h; n = 5. **(B)** Glycerol release across all time points from SCAT explants from periparturient (PP) dairy cows treated with basal, LPS (20 μg/mL), ISO, and LPS+ISO for 3 h; n = 12. Values in A and B are LSM of the ratio of glycerol relative to basal glycerol release (nmol/mg of adipose tissue; AT). (C) Glycerol release from SCAT collected from periparturient cows at 11 ± 3.6 d before expected calving date (PreP), and 6 ± 1 d (PP1) and 13 ± 1.4 d (PP2) after parturition treated with ISO and LPS, for 3 h; n = 12. Values are LSM of glycerol nmol/mg of AT. Error bars represent SEM. Bars with different letters (a–c) differ significantly ($P < 0.05$).

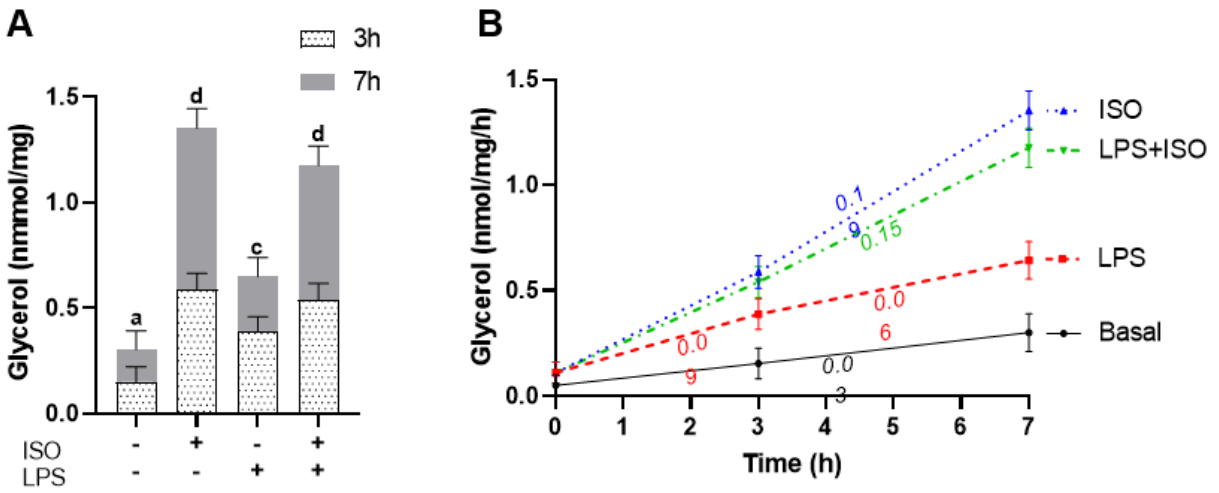

Figure 17. LPS induced lipolysis in dairy cows' adipose tissues (AT) is affected by stimulation time. (A) Glycerol release by subcutaneous AT (SCAT) explants from non-lactating (NL) cows exposed to: Basal (no reagents), isoproterenol (ISO=1µM), lipopolysaccharide (LPS=20µg/ml,) or LPS+ISO for 3 h and 7 h. Bars represent least-squares means ± SEM of glycerol release (nmol/mg of AT) at 3 h (light bars) or 7 h (grey bars); n=24. Statistical analysis was performed using the total glycerol release values after 7 h of culture. **(B)** Glycerol (nmol/mg of AT) release at 3 and 7 h in explants treated with Basal, ISO, LPS, or LPS+ISO for 7 h; calculated lipolytic rates (glycerol nmol/mg AT) are reported by each line for Basal, LPS, ISO, and LPS+ISO; n=24. Error bars represent the SEM. Bars or points with different letters differ significantly ($^{a, b, c}$, $P<0.001$).

In experiment 2, we determined the effect of LPS on AT lipolysis during 3 and 7 h incubation periods in NL cows. Basal lipolysis rate remained constant during both 3 and 7 h incubations at 0.034±0.0001 nmol/ mg of AT per hour (Figure 17A and B). Similarly, the ISO glycerol release rate was steady across both incubation periods 0.195±0.009 nmol/mg/h (Figure 17A and B). Compared to Basal, LPS increased lipolysis in explants by 115±18% at 3 h and 68.7±16% at 7 h of incubation (Figure 17A). The lipolytic rate during LPS incubation decreased from 0.099±0.001 at 0-3 h to 0.061±0.001 nmol of glycerol/mg/h between 4-7 h (Figure 17B). However, when adrenergic stimulation was included (LPS+ISO), the lipolysis rate was higher and constant at 0.152 ±0.004 nmol/mg/h (Figure 17B).

LPS Activates Adipose Triglyceride Lipase (ATGL) and Hormone Sensitive Lipase (HSL)

HSL is the main neutral lipase in AT demand lipolysis and the ratio pHSL(Ser563):HSL is a proxy for its activity. In NL cows, Basal pHSL(Ser563):HSL remained constant at 3 and 7 h

(Figure 18A). ISO increased pHSL(Ser563):HSL at 3 and 7 h (Figure 18A). Unexpectedly, and although LPS induced lipolysis at 3 h, pHSL(Ser563):HSL did not increase remaining similar to Basal (Figure 18A). However, at 7 h, LPS rose pHSL(Ser563):HSL compared to Basal (Figure 18A).

To further assess the mechanism of HSL activation at 3 h, we evaluated protein kinase A (PKA) and Cα (PKCα) abundance, as these two kinases phosphorylate HSL to trigger its triglyceride hydrolytic action. PKA abundance increased in explants treated with ISO by 2.48±0.39-fold change compared to Basal. Explants treated with LPS showed moderate activation of PKA that could drive limited HSL or ATGL activity (Figure 18B). ISO enhanced PKCα at 3 h by 3.48±0.76-fold change compared to Basal (Figure 18C). These findings confirmed that HSL activation through PKCα in SCAT explants only occurs after 3 h of LPS stimulation. To determine the lipase driving LPS induced lipolysis at 3 h, we evaluated ATGL activity by assessing its content using capillary electrophoresis. Compared to Basal and ISO, LPS increased ATGL expression at 3 h by 1.58±0.21-fold change (Figure 18D). These data suggest that ATGL drives lipolysis during the initial stages of AT exposure to LPS.

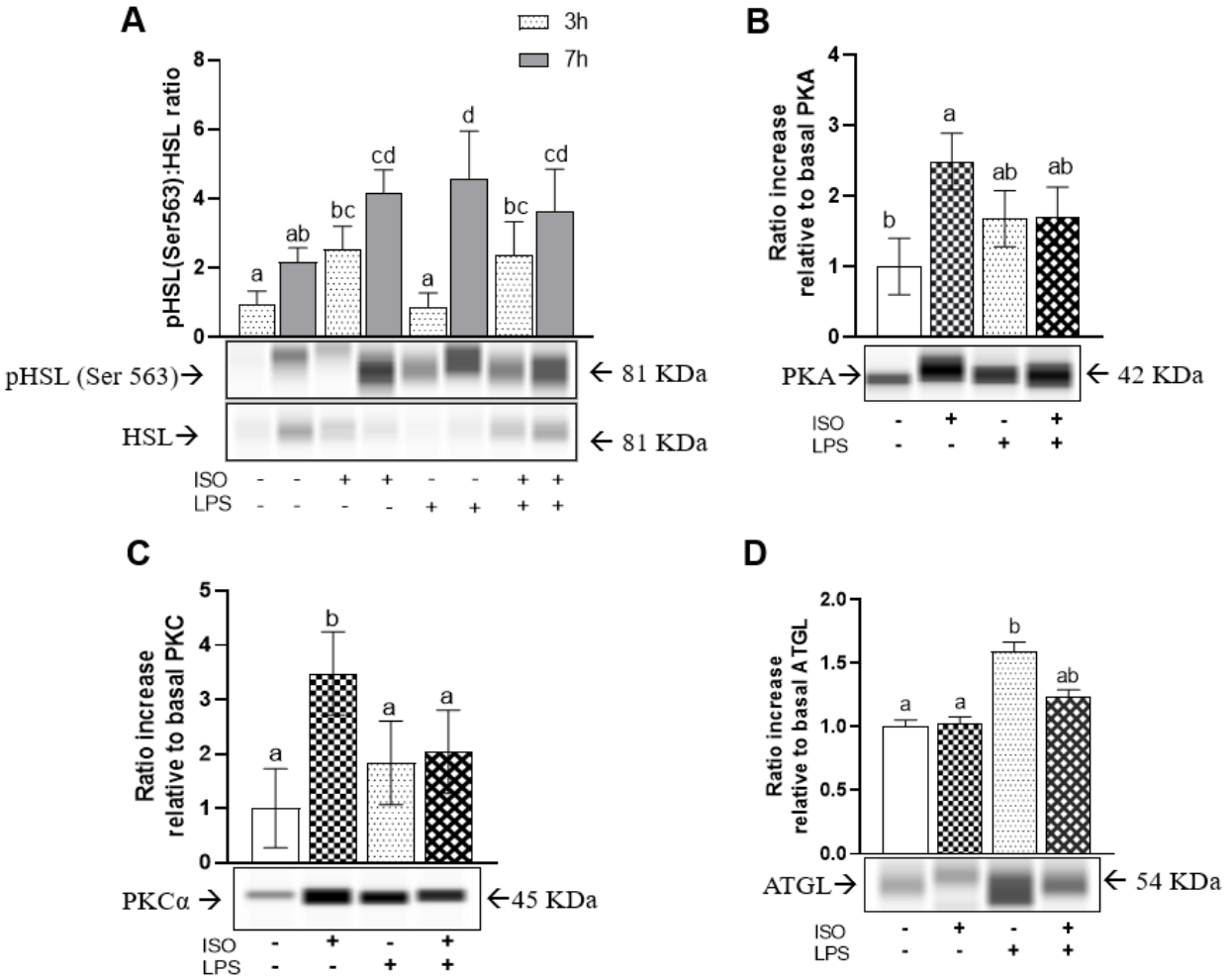

Figure 18. Hormone sensitive lipase (HSL) and adipose triglyceride lipase (ATGL) in dairy cows AT activity during an LPS challenge is affected by time. Subcutaneous AT (SCAT) explants from non-lactating (NL) cows were treated with isoproterenol (ISO=1µM), LPS (LPS=20 µg/ml, LPS+ISO or no reagents (Basal) for 3 h and 7 h. **(A)** HSL and pHSL (Ser 563) abundance. Bars are least-squares means of the ratio of pHSL:HSL ± SEM; n=8. **(B)** Protein kinase A (PKA) expression in SCAT from NL cows after treatment with Basal, ISO, LPS, or LPS+ISO for 3 h. Bars are the least-squares mean of total PKA expression relative to basal values ± SEM; n=12. **(C)** Protein kinase Cα (PKCα) expression in SCAT from NL cows after treatment with Basal, ISO, LPS, or LPS+ISO for 3 h. Bars are the least-squares mean of total PKCα expression relative to basal values ± SEM; n=12. **(D)** ATGL expression in SCAT from NL cows after treatment with Basal, ISO, LPS, or LPS+ISO for 3 h. Bars are the least-squares mean of total ATGL expression relative to basal values ± SEM; n=12. Protein bands in all panels are representative of capillary electrophoresis runs. Bars with different letters differ significantly (^{a,b,c,d} $P<0.05$).

LPS Alters AT Lipid Mobilization Gene Networks Expression in a Time-Dependent Manner

The lipid mobilization process in AT is controlled transcriptionally by the expression of lipolytic and lipogenic gene networks. In NL cows, ISO increased the expression of *LIPE*

(encoding HSL) and the lipoprotein lipase gene *LPL* at 3 h, but by 7 h their transcription was reduced (Table 9, $P<0.05$). Similar to the response observed after ISO exposure, LPS reduced the expression of *LIPE* at 7 h (Table 9, $P<0.0001$). Treatment (Basal, ISO, LPS, LPS+ISO) did not affect the expression of other lipolysis-related genes (*ABHD5, ADRB1*, *ADRB2*). However, the expression of lipogenic-related genes (*AGPAT1*, *LPIN1, PPARa*) was affected by the incubation time, and their expression was downregulated by LPS, ISO, and LPS+ISO at 7 h ($P<0.005$). Genes of the glycerol-3-phosphate pathway that are part of the triacylglycerol synthesis process were affected by time and treatment ($P<0.05$). Diacylglycerol O-acyltransferase-1 gene *(DGAT1)* was upregulated by LPS at 3 h, and then downregulated at 7 h (Table 9).

Table 9. Exposure to LPS modulates lipolytic, lipogenic, and inflammatory gene networks in AT from dairy cows.

Network	Trt	Basal		INS		ISO		ISO+INS		LPS		LPS+INS		LPS+ISO		LPS+ISO +INS		P value		
	Time h	*3*	*7*	*3*	*7*	*3*	*7*	*3*	*7*	*3*	*7*	*3*	*7*	*3*	*7*	*3*	*7*	Trt	Time	Trt × Time
Lipolysis	*LIPE*	1 ab	1 a	1.30 ab	1.03 a	2.46 c	1.05 a	1.54 bc	1.01 a	1.66 bc	1.00 a	1.02 ab	0.97 a	1.46 bc	0.89 a	1.34 ab	1.07 a	*0.04*	*<.0001*	*ns*
	LPL	1 a	1 a	1.18 a	0.91 a	1.75 b	0.85 a	1.16 ab	1.00 ab	1.37 ab	0.91 a	0.95 a	0.98 a	1.08 ab	0.82 a	1.17 a	0.97 a	*0.03*	*<.0001*	*ns*
Lipogenesis	*AGPAT2*	1 b	1 b	0.96 ab	1.00 ab	1.29 ab	0.95 ab	1.24 ab	0.81 ab	0.98 b	0.76 a	0.85 ab	0.99 ab	0.95 b	0.71 a	1.05 ab	0.85 ab	*ns*	*0.002*	*0.02*
	DGAT1	1 a	1 a	1.16 ab	0.89 a	1.47 b	0.98 ab	1.31 b	0.89 a	1.30 b	0.89 a	0.95 a	1.08 ab	1.20 b	0.89 ab	1.13 b	1.18 ab	*ns*	*<.005*	*0.02*
Insulin	*IRS*	1 ab	1 ab	0.94 ab	1.14 bc	1.17 bc	0.96 a	1.09 bc	1.05 ab	0.88 a	1.46 c	0.99 bc	1.09 ab	0.93 ab	1.15 bc	1.02 ab	1.21 bc	*0.06*	*ns*	*0.01*
Inflammation	CCL2	1 ab	1 a	0.94 ab	1.14 a	1.03 ab	1.05 a	0.97 ab	1.18 ab	1.51 c	1.43 b	1.49 c	1.41 b	1.17 b	1.43 b	1.25 b	1.68 c	*0.002*	*0.08*	*ns*
	CD204	1[a] b	1 a	1.18 ab	0.98 a	1.13 ab	0.93 a	1.34 b	0.85[a]	1.15 b	0.82 a	1.28 b	0.90 a	1.23 b	0.79 a	1.08 b	0.87 a	*0.98*	*<.0001*	*ns*
	IL6	1 a	1 a	1.20 ab	1.17 ab	1.34 ab	1.00 a	1.46 ab	1.51 b	1.96 bc	1.63 bc	2.49 bc	1.62 bc	1.87 bc	1.84 bc	2.99 bc	3.34 c	*<.001*	*0.11*	*ns*
	IL8	1 a	1 ab	1.07 ab	1.02 ab	1.05 ab	1.05 ab	1.32 ab	1.19 b	1.72 b	2.51 c	1.76 ab	2.60 c	1.48 ab	2.89 c	1.95 b	4.62 c	*<.01*	*<.0001*	*ns*
	IL10	1 bc	1 bc	0.89 bc	0.74 ab	0.90 bc	0.91 bc	1.21 bc	0.69 a	1.34 c	0.82 ab	1.17 bc	0.95 ab	1.07 b	0.88 bc	1.12 bc	0.96 bc	*0.04*	*0.032*	*ns*

Table 9 (cont'd)

SOCS1	1 ab	1 a	1.02 ab	1.02 a	1.06 ab	1.10 ab	1.08 ab	1.18 ab	1.10 b	1.33 bc	1.20 bc	1.41 c	1.04 ab	1.36 bc	1.29 bc	1.60 c	*0.01*	*ns*	*ns*

a–c Fold changes without a common superscript within a row represent differences determined by Tukey adjustments of the ΔCt values.

[1]non-lactating (NL) cows after short (3 h) and extended (7 h) lipolysis induced by isoproterenol (ISO=1 µM) LPS (LPS=20 µg/ml, LPS+ISO) or no reagents (Basal), and inhibition of lipolysis induced by insulin (INS=1 µg/L), (LPS+INS, ISO+INS, LPS+ISO+INS).

[2]Fold change = $2^{(-\Delta\Delta Ct)}$; $\Delta\Delta Ct = \Delta Ct_{\text{calibrator sample}} - \Delta Ct_{\text{target sample}}$.

[3]Gene expression values were calculated from LSM differences of the ΔCt values (ΔΔCt) normalized to the mean of EIF3K, *RPLPO,* and RPS9 housekeeping genes. The Basal sample was the calibrator for the calculation of ΔΔCt. 95% confidence intervals of the ΔΔCt values were transformed to fold changes.

[4]Trt= Treatment; ns= P > 0.10.

LPS Impairs the Anti-Lipolytic Effect of Insulin in AT

We assessed AT response to insulin by quantifying the reduction of lipolytic responses (glycerol release) in explants. In NL cows, ISO+INS reduced lipolysis in AT by 3 and 7 h compared to ISO (Figure 19A). When explants were treated with LPS+INS, lipolysis was reduced at 3 h compared to samples exposed only to LPS (Figure 19A). However, at 7 h, LPS+INS did not reduce the rate of lipolysis as opposed to LPS (Figure 19A). Glycerol release in LPS+ISO+INS explants was not reduced compared to LPS+ISO at 3 and 7 h (Figure 19A).

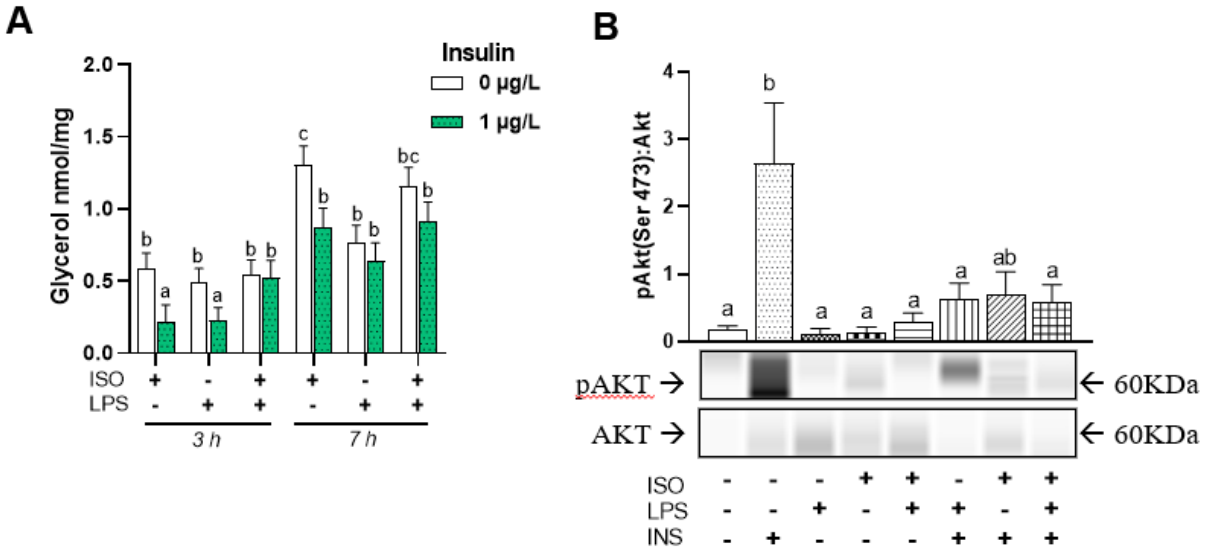

Figure 19. The anti-lipolytic effect of insulin in AT is affected by LPS. (A) Subcutaneous AT explants were harvested from non-lactating (NL) dairy cows and treated with Isoproterenol (ISO=1µM), LPS (20 µg/ml) and LPS+ISO in the presence of insulin (0µg/L, white bars; and 1µg/L, green bars) for 3 h and 7 h. Bars represent least-squares means ± SEM of glycerol release (nmol/mg of AT); n=12. **(B)** AKT and pAKT abundance in explants treated with isoproterenol (ISO=1µM), LPS (LPS=20 µg/ml, LPS+ISO or no reagents (Basal) for 7 h in the presence or absence of insulin (1µg/L). Bars are least-squares means of the ratio of pAKT:AKT ± SEM; n=8. Error bars represent the SEM. Bars with different letters differ significantly (^{a,b,c} $P<0.05$).

In NL cows, LPS affected the expression of insulin receptor substrate 1 gene (*IRS1)*, upregulating its transcription at 7 h compared to Basal and ISO, (Table 9, $P<0.001$). An important marker of insulin signaling cascade activation is the ratio pAkt:Akt. As expected, in explants from NL cows treated during 7 h with INS, pAkt:Akt increased compared to Basal (Figure 19B).

Similarly, insulin activated Akt in ISO+INS at 7 h (Figure 19B). The pAkt:Akt in ISO, LPS, and LPS+ISO was lower than INS at 7 h (Figure 19B). Insulin did not activate Akt in LPS+INS and LPS+ISO+INS treatments (Figure 19B).

Inflammatory Responses to LPS Support the Activation of Lipolysis in AT

LPS is a potent activator of the innate immune system, and, as expected, it enhanced the expression of proinflammatory gene networks (Table 9 and S5). In NL cows, genes involved in the initiation of inflammation such as *CCL2, IL6, and SOCS1 were upregulated* following LPS stimulation for 3 h (Table 9, $P<0.05$). At 7 h, genes encoding the proinflammatory cytokines *CD44* and *IL8* were also upregulated compared to 3 h exposure in treatments containing LPS (Table 9 and S5). At 7 h, anti-inflammatory cytokines were downregulated by LPS compared to 3 h, ($P<0.001$). Among these cytokines, *IL10* was significantly upregulated at 3 h and its expression was reduced after 7 h of exposure to LPS (Table 9, $P<0.0001$).

In rodent adipocytes, the activation of extracellular signal-regulated kinase 1 (ERK1) and ERK2 is one of the main components of the inflammatory lipolytic pathway (Zu et al., 2009a). To evaluate the activation of ERK1/2 in bovine AT after LPS stimulation, we quantified the abundance of pERK1 (Thr202) and pERK2 (Try204) in NL cows. At 3 h there were no changes in the pERK1/2:tERK1/2 (Figure 20A). At 7 h, ISO and LPS increased pERK1/2:tERK1/2 compared to Basal by 2.65±0.32 and 2.89±0.15-fold change respectively. LPS+ISO presented an additive effect in the phosphorylation of ERK1/2, as evidenced with higher pERK1/2:tERK1/2 vs. ISO or LPS (Figure 20B).

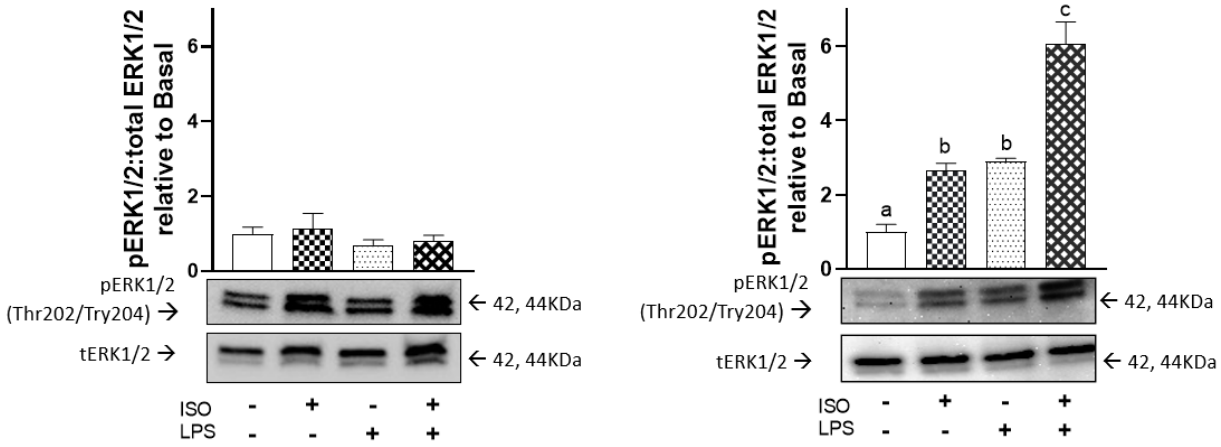

Figure 20. LPS activates the ERK1/2 inflammatory signaling pathway in AT. Extracellular signal-regulated kinases 1/2 (ERK1/2) abundance in subcutaneous AT (SCAT) explants from non-lactating (NL) cows treated with isoproterenol (ISO=1 µM), LPS (LPS=20 µg/ml, LPS+ISO or no reagents (Basal) for 3 h **(A)** and 7 h **(B)**. Bars represent least-squares means of the pERK1/2:total ERK1/2 ratio relative to Basal; n=4. Error bars represent the SEM. Protein bands in all panels are representative of capillary electrophoresis runs. Bars with different letters differ significantly (^{a,b,c,} $P<0.05$).

DISCUSSION

During the first weeks of lactation, health disturbances such as digestive (e.g., displaced abomasum) and reproductive diseases (e.g., retained placenta) often result in high plasma levels of bacterial remnants, including LPS (Andersen et al., 1996, Eckel and Ametaj, 2016, Dickson et al., 2019b). Although not all health disturbances in periparturient cows are related to ET exposure, the consequences of these endotoxemic periods are problematic as cows that suffer an illness early in the periparturient period are at a greater risk of developing a second disease later in lactation (Bradford et al., 2015, Probo et al., 2018). A mechanism involved in this increased susceptibility to disease is the development of lipolysis dysregulation that is known to predispose cows to ketosis and displaced abomasum (Ospina et al., 2010a, Contreras et al., 2015). However, a link between endotoxemia and lipolysis dysregulation in dairy cattle has not yet been established. In this study, we demonstrated that LPS triggers lipolysis in AT through the activation of canonical and inflammatory lipolytic pathways and concurrently impairs the response of adipocytes to insulin.

Although dairy cattle AT inflammatory responses to LPS have been described (Mukesh et al., 2010), to our knowledge, this is the first study to characterize AT lipolytic responses to ET in PP and NL cows. Similar to studies in rodents and humans, we demonstrated that LPS at doses ranging from 1 to 20 µg/ml induced lipolysis to levels comparable to those elicited by adrenergic stimulation (i.e., ISO). At higher doses (100 µg/ml), the lipolytic effect of LPS was blunted coinciding with the responses observed in AT from rodents when infused with ET at 100 ng/100 g body weight (Feingold et al., 1992). The intensity of the lipolytic response to LPS in bovine AT appears to be analogous to that in murine adipocytes, where LPS at doses from 0.1 µg/ml up to 10 µg/ml for 24 h induce lipolysis (Zu et al., 2009a). In contrast, human adipocytes are more sensitive to LPS lipolytic effects, as comparatively low doses ranging from 0.01 to 1 µg/ml trigger triglyceride hydrolysis (Grisouard et al., 2012). In mid-lactation Holstein cows, Horst et al. (2019b) demonstrated that LPS exerts a lipolytic stimulus during the first 3 days of a 7-day continuous intravenous infusion with doses ranging from 0.017 to 0.026 µg/kg. The present study confirms the lipolytic potential of LPS using an ex vivo model of lipolysis and provides data supporting the AT origin of the plasma FFA peaks described by Horst et al. (2019b) in vivo.

Lipolysis intensity in PP cows is affected by adipocyte size that is in turn reduced as lactation progresses (De Koster et al., 2016, Contreras et al., 2017a). Thus, upon activation of lipolysis, larger adipocytes release more glycerol and FFA compared to those with smaller volumes. The effect of adipocyte size on lipolysis has been observed in other species. The AT from rats with high adiposity is more sensitive to lipolysis after adrenergic stimulation compared to lean rats (Lanza-Jacoby et al., 1995). The intensity of LPS-induced lipolysis is also affected by adipocyte size with higher release of glycerol and FFA in cells from high adiposity compared to lean rats (Lanza-Jacoby et al., 1995). Similar to rodents, in the present study, LPS-induced lipolytic

activity was higher in AT explants from PreP compared to PP1 and PP2; this may be attributed to sampled adipocytes having larger volumes pre- vs. post-calving.

Since endotoxemic periods in PP cows often last several hours to days, we assessed LPS-induced lipolytic responses at 3 h and 7 h to mimic the peracute and acute stages of exposure to ET. During the initial 3 h, our results indicate that lipolysis in response to ET is dependent on the activity of ATGL. In rats, Zu et al. (2009a) demonstrated that LPS and its core component lipid A activate ATGL directly. Although PKA is the rate-limiting enzyme of lipolysis induced by β-adrenergic signaling (Pagnon et al., 2012), its phosphorylation was limited in the present study at 3 h. Furthermore, PKA phosphorylation is not necessary for ATGL activation (Zimmermann et al., 2004a). Possible PKA-independent mechanisms of ATGL activation in the context of an inflammatory challenge (e.g. LPS) include its phosphorylation by AMPK (Kim et al., 2016) and the activation of its co-activator CGI-58 by ETs (Lord et al., 2012). Based on our observations, ATGL breakdown of triglycerides appears to be part of the peracute phase response of endotoxemia that increases systemic energy availability.

After 7 h of stimulation with LPS, the phosphorylation of HSL increased, indicating lipolytic activity. Our study provides evidence for the activation of HSL through both the canonical and the inflammatory lipolytic pathways. In the classic pathway, catecholamines (e.g., norepinephrine, epinephrine) and peptide hormones (e.g., growth hormone, prolactin) activate adenyl cyclase, which converts ATP to cAMP (Londos et al., 1999, Moon et al., 2011). The latter ultimately phosphorylates PKA, whose substrates are perilipin (adipocyte's lipid droplet coating) and HSL (Londos et al., 1999). When LPS binds to TLR4, intracellular Ca^{2+} concentrations rise rapidly, leading to an increment in the levels of intracellular cAMP (Song et al., 2007, Moon et al., 2011), subsequent phosphorylation of PKA and, ultimately, HSL and perilipin activation. The

present study revealed a marked increase in PKA and HSL phosphorylation after 7 h of LPS stimulation, demonstrating the activation of the canonical lipolytic pathway by the ET.

Reports in rodents and humans demonstrate that LPS also triggers lipolysis through an inflammatory pathway that includes the activation of the mitogen-activated protein kinase /extracellular signal-regulated kinase (MEK/ERK) pathway upon TLR4 binding. The mechanism of activation of MEK/ERK involves the pro-inflammatory cytokines IL6, IL8, and TNFα (Ryden et al., 2002, Brown et al., 2004). The MEK/ERK pathway activates β-3 adrenergic receptors leading to HSL and perilipin phosphorylation in a PKA-dependent manner (Zu et al., 2009a, Hong et al., 2018). The β-3 adrenergic receptor is expressed in AT of cattle and in PP dairy cows its transcription is increased by 111% 30 d postpartum relative to pre-calving (-30 d) levels (Sumner and McNamara, 2007). Among adrenergic receptors, the activation of β-3 leads to the most robust lipolytic activity in bovine adipocytes (Casteilla et al., 1994). The present study demonstrated that activation of the MEK/ERK pathway occurred after 7 h of LPS stimulation. This activation was even more evident in the combination of LPS+ISO, possibly indicating an additive effect on β adrenergic receptor signaling. MEK/ERK activation coincided with marked transcription upregulation of the proinflammatory cytokines IL6 and IL8 in LPS and LPS+ISO treatments. Therefore, LPS has the capacity to activate the inflammatory lipolytic pathway in dairy cattle AT through MEK/ERK signaling.

LPS binding to TLR4 can also trigger the inflammatory lipolytic pathway through protein kinase C (**PKC**) signaling. Apart from being a key mediator of inflammatory responses induced by TLRs activation [extensively reviewed by Loegering and Lennartz (2011)], PKC has the capacity to phosphorylate HSL and perilipin in rodents and fish (Fricke et al., 2004, Bergan et al., 2013). Our results demonstrate that PKC was activated after 7 h of LPS stimulation and this

coincided with higher phosphorylation of HSL. PKC can also activate ERK and, therefore, trigger lipolytic activity through adrenergic receptor signaling as described above (Ueda et al., 1996).

Since insulin plays a central role in regulating lipolysis, we evaluated AT insulin sensitivity during LPS stimulation. During conditions favoring positive energy balance, insulin signaling inactivates PKA and its downstream target HSL, leading to the suppression of lipolysis (Yin et al., 2019). We determined that INS was effective in reducing the phosphorylation (i.e., activation) of HSL and, consequently, lipolysis at 3 and 7 h. Our results indicate that, when LPS was present for 7 h, AT develops insulin resistance, defined as the decreased biological response to normal concentrations of insulin in those tissues sensitive to its effects (Kahn, 1978). The resistance to insulin signaling was indicated by diminished Akt phosphorylation. In monogastric species, HSL activity is regulated directly by Akt signaling as it triggers the activity of phosphodiesterase 3b, the enzyme that degrades cAMP and, thus, limits PKA phosphorylation (Degerman et al., 1998). Diminished Akt activity results from aberrant phosphorylation of IRS-1 that is mediated by proinflammatory cytokines (Chen et al., 2015). IL6 and SOCS1, elevated in LPS treated explants in this study, directly inhibit IRS-1 signaling. SOCS1 blunts tyrosine phosphorylation of IRS-1 and IL6 activates the JAK-STAT signaling pathway that blocks its transcription and that of GLUT4 (Ueki et al., 2004, Chen et al., 2015). The robust proinflammatory response exhibited by SCAT explants in the present study coincides with previous transcriptional studies that evaluated immune responses to LPS in AT depots from Holstein cows (Mukesh et al., 2010). Our findings and those by Mukesh and colleagues provide mechanistic evidence that explains, at least in part, the systemic insulin resistance status found in dairy cows during and after intramammary and intravenous LPS infusions (Yin et al., 2019).

There are limitations to note from the present study. First, 7 h LPS stimulation experiments

were performed only in NL cows. Although AT inflammatory responses in healthy PP cows are similar to those observed in late lactation cows during feed restriction-induced negative energy balance (Contreras et al., 2016a), the AT responses to insulin in an LPS challenge during the first weeks, postpartum may differ given their limited insulin sensitivity. Our results, however, provide essential information for future studies on AT lipolytic and inflammatory responses to endotoxemia in PP cows. Second, this study only evaluated the responses to ET in SCAT. In non-lactating non-gestating human females, AT responses to LPS differ by site, with lower inflammatory responses and limited lipolysis in visceral AT compared to SCAT (Vatier et al., 2012). Future studies should determine if bovine visceral AT is also less sensitive to LPS-induced lipolysis and inflammation compared to SCAT. Finally, the ex-vivo model used in the present study does not consider variables that affect the AT response to ET in vivo. These variables may include the migration of circulating immune cells into AT and the removal of ET and lipolytic products from AT by blood.

CONCLUSION

LPS induces a lipolytic response in SCAT from both NL and PP dairy cows. This response is mediated by the activation of neutral lipases ATGL and HSL through the canonical and inflammatory lipolytic pathways (Figure 15). The inflammatory response induced by LPS is associated with the development of insulin resistance in SCAT. These results demonstrate that endotoxemia may enhance dairy cows' susceptibility to lipolysis dysregulation and metabolic diseases associated with dyslipidemia.

CHAPTER 5: TLR4 MODULATES LIPOPOLYSACCHARIDE-INDUCED LIPOLYSIS IN BOVINE ADIPOCYTES

ABSTRACT

Adipocytes are the primary cells responsible for lipid storage in dairy cows. During the postpartum period, adipocytes regulate energy balance by enhancing lipolysis when high energy is demanded. However, intense and extended lipolysis increases the risk for postpartum disease. Since lipolysis is activated by both canonical and inflammatory pathways, postpartum dairy cows with blood circulating levels of lipopolysaccharide (LPS) could have a greater risk of lipolysis dysregulation. LPS, a component of the outer membrane of Gram-negative bacteria, has been described as an inflammatory ligand through Toll-like receptor 4 (TLR4) pathway in different types of cells. Although LPS is recognized for activating lipolysis in adipose tissue (AT) explants, the mechanisms by which LPS activates lipolysis and effective strategies to mitigate its lipolytic response are still unknown. The objective of this study was to investigate the mechanisms of the lipolytic effect of LPS in isolated primary bovine adipocytes. Preadipocytes were obtained from subcutaneous AT of multiparous Holstein cows (n=9). Differentiated adipocytes with and without knockdown of TLR4 were incubated with LPS for up to 7 h. The antilipolytic effect of insulin was measured during LPS induced lipolysis, and inhibitors of the canonical [niacin (Nia)] and inflammatory [flunixin meglumine (FM)] pathway were used in the presence of LPS. Compared to basal media, LPS at 1 µg/mL was effective to activate lipolysis by 72.66±15%. When *TLR4* expression was blocked with siRNA (siTLR4), the lipolytic effect of LPS was prevented. Insulin reduced lipolytic effect of LPS during the short incubation (3 h), but not during the longer exposure (7 h). In adipocytes treated with FM, the lipolytic effect of LPS was inhibited. Similarly, in adipocytes preincubated with FM, the antilipolytic effect of insulin was recovered. These data

demonstrate that TLR4 activation in bovine adipocytes activates lipolysis mainly by inflammatory mechanisms and it provides initial evidence of possible targets for inhibiting lipolysis in dairy cows.

INTRODUCTION

The adipose tissue (**AT**) serves as the primary organ for energy storage in the form of triglycerides (**TG**). During the onset of lactation, dairy cows relay on lipolysis of TG's reserves within the adipocytes to fulfill their energy requirements (Contreras et al., 2018). However, excessive lipolysis is associated with increased risk for postpartum disease (Ospina et al., 2010b). One of the factors contributing to intense lipolysis, is the high abundance of inflammatory mediators in postpartum cows, we previously demonstrate that endotoxin triggers lipolysis in AT explants (Chirivi et al., 2022). However, the mechanisms by which inflammation affects lipid metabolism in adipocytes have been poorly studied in dairy cows. Therefore, the understanding of the adipocyte's molecular alterations induced by inflammation is of utmost importance in order to design therapeutics to reduce extended and intense lipolysis and the incidence of periparturient disease.

Hydrolysis of triglycerides (i.e., Lipolysis) is regulated by three major neutral lipases: adipose triglyceride lipase (**ATGL**), hormone-sensitive lipase (**HSL**), and monoglyceride lipase (**MGL**) (Vaughan et al., 1964, Zimmermann et al., 2004b, Taschler et al., 2011). Canonical lipolysis is mainly activated by catecholamines and natriuretic peptides. Once catecholamines bind to β-adrenergic receptors (**β-ARs**) in the adipocyte membrane, the intracellular levels of cyclic AMP (**cAMP**) are elevated by the activity of adenyl cyclase. The accumulation of cAMP promotes protein kinase (**PKA**) activation, which phosphorylates HSL and perilipin-1 (**PLIN-1**). The phosphorylation of PLIN-1 releases the coactivator α-β hydrolase domain containing 5 (**ABHD5**) from PLIN-1, which allows the activation of ATGL (Granneman et al., 2009). However, PKA is not the only kinase phosphorylating HSL. During inflammation, cytokines and bacterial components activate endoplasmic reticulum stress leading to the activation of inositol-requiring

protein 1 (**IREA1**). This protein is required for regulating extracellular signal-regulated kinase 1/2 (**ERK1/2**) (Foley et al., 2021). The activation of ERK1/2 results in phosphorylation of HSL and lipolysis (Greenberg et al., 2001). Furthermore, the activation of ERK1/2 signaling leads to the activation and synthesis of ciclooxinases 2 (**COX2**) and protaglandins (**PGs**). PGE2, in particular, activates lipolysis by enhancing HSL phosporylation and ATGL activity (Inazumi et al., 2020).

Adipocyte lipolysis is hormonally regulated by insulin. Upon binding to the insulin receptor, insulin triggers the phosphorylation of insulin receptor substrates 1 and 2 (**IRS-1/IRS-2**), leading to the activation of phosphatidylinositol 3-kinase (**PI3K**), phosphoinositide-dependent kinase 1 (**PDK1**), and protein kinase B (**Akt**) (Laviola et al., 2006). The phosphorlation of Akt leads to phosphodiesterase 3b (**PDE3B**) activity, which in turns degradates cAMP, and thus limits PKA phosphorylation and lipolysis (Degerman et al., 1998). However, AT inflamamtion including that triggered by endotoxin, induces aberrant IRS-1/2 phosphorylation, resulting in diminished anti-lipolitic effect of insulin (Hotamisligil et al., 1996, Chirivi et al., 2022).

To inhibit lipolysis, the canonical and the inflammatory pathway need to be targeted. The cannonical pathway of lipolysis could be inhibited in dairy cows with niacin (**NIA**), which is a supplemental inhibits PKA activation and consequently HSL phosphorylation (Tunaru et al., 2003). Flunixin meglumine, the only non-steroidal anti-inflammatory drug authorized in dairy cows, is a strong COX inhibitor that may reduce lipolysis by reducing the synthesis of pro-inflammatory molecules (Kovacevic et al., 2019, Inazumi et al., 2020). However, the antilipolytic effect of NIA and FM on endotoxin-induced lipolysis remains unknown.

The present study determined that endotoxin-induced lipolysis and dysfunction in bovine adipocytes are mediated by Toll-like receptor 4 (**TLR4**) activity. This study provides evidence for the first time of the potential contribution of COX inhibition as an approach to reduced excessive

lipolysis in dairy cows.

MATERIALS AND METHODS

Isolation of Preadipocytes

Subcutaneous adipose tissue samples were randomly collected from a group of healthy, no gestating, nonlactating adult Holstein cows (n = 9) in a local abattoir. Isolation of adipose tissue steam cells was performed by mincing AT in fragments of 5-10 mg approximately. Two fragments of explants were incubated in 12-well plates with MesenPRO RS™ (ThermoFisher, Cat N° 12746012) and growth culture medium was replenished with fresh medium three times per week. After 7 d of organ culture the outgrown cells were visible and AT fragments were removed. Cells were expanded as previously described (Thelen et al., 2018) using preadipocyte medium (PAM) containing 10% FBS, Dulbecco's Modified Eagle's Medium/F12, 44.05 mM sodium bicarbonate (Corning, Cat N° 61-065-RO), 100 µM ascorbic acid, (Sigma-Aldrich, Cat N° A4544-100G), 33 µM biotin (Sigma-Aldrich, B4501-1G), 17 µM pantothenate (Sigma-Aldrich, Cat N° P5155-100G), 1% L-glutamine (Gibco, Cat N° 25030-081), antibiotic antimycotic containing 10,000 units/mL of penicillin, 10,000 µg/mL of streptomycin, and 25 µg/mL of Amphotericin B (Gibco, Cat N° 15240, Waltham, MA USA) and 20 mM HEPES with replacement every 2 days.

TLR4 silencing

We inhibited the expression of TLR4 using small interference RNA (**siRNA**) to assess the effects of this receptor on LPS-induced lipolysis. As reported previously (Rendon et al., 2022) Preadipocytes were seeded in 6-well cell culture plates (Corning Costar Corp., Cambridge, MA, USA) at 20,000 cells/cm^2 and incubated overnight in αMEM (Corning, Cat N° 50-010-PB), 5% FBS, Hiperfect transfection reagent (Qiagen, Cat N° 301704), and 40 nM of three combined siRNA sequences targeting *TLR4* (si*TLR4*), or a non-coding siRNA (siNC) (Table10). Sequences

were designed by IDT Technologies (Coralville, IA). After incubation, the medium was replaced with preadipocyte media, and cells were allowed to proliferate until confluency for 48 h.

Table 10. siTLR4 primers.

Design ID	Forward	Reverse
CD.Ri.383506. 13.1	5'GAGCUUCAAUGAUGUCAUUAC CUTA3'	5'UAAGGUAAUGACAUCAUUGAAGC UCAG3'
CD.Ri.383506. 13.2	5'UGAGCUUCAAUGAUGUCAUUA CCT3'	5'AAGGUAAUGACAUCAUUGAAGCU CAGA3'
CD.Ri.383506. 13.4	5'CUGAGCUUCAAUGAUGUCAUU ACT3'	5'AGGUAAUGACAUCAUUGAAGCUC AGAU3'

Adipogenesis

Preadipocytes were seeded in 6-well cell culture plates (Corning Costar Corp., Cambridge, MA, USA) at 20,000 cells/cm^2 and allowed to proliferate until confluency and induced to differentiate as reported previously (Strieder-Barboza et al., 2019). Adipogenesis was evaluated after 7 d using Bodipy 493/503 (ThermoFisher Cat N° D3922), a neutral lipid staining, and the nuclear stain NucSpot® Live 650 (Biotium, Cat N° 40082) and reported as Bodipy fluorescence intensity/nuclei count using long-term live-cell imaging IncuCyte® S3 system (Sartorius). Quantification of cell images after 4 days was performed using IncuCyte ZOOM™ software.

Lipolysis Assays

(1) To determine the effect of LPS on lipolysis, mature adipocytes were FBS starved for 1 h and incubated during 3 h in lipolysis media [Krebs Ringer Bicarbonate-Buffered solution (KRBB) + 2% BSA] containing 0, 0.01, 0.1, 1 and 10 µg/mL of LPS from *Escherichia coli* O55:B5 (**LPS**; Cat N° L6529, Sigma-Aldrich, St. Louis, MO). The goal was to choose the LPS dose for oncoming experiments.

(2) To establish the role of TLR4 activation on lipolysis, 7-day si*TLR4* and siNC adipocytes were FBS starved for 1 h and incubated for 3 h in lipolysis media containing 1 µg/mL of LPS or the beta-adrenergic agonist isoproterenol at 1 µM (**ISO**; Cat N° I6504, Millipore-Sigma, Burlington, MA). ISO was used as a positive control for lipolysis and basal lipolysis was established without the addition of any reagent.

(3) To determine the effect of endotoxin on adipocyte's insulin sensitivity , 7-d mature adipocytes were FBS starved for 1 h and incubated 30 min with 1 µg/L of insulin from bovine pancreas (**INS**; Sigma-Aldrich, Cat N° I0516). Next, adipocytes were incubated for 7 h in lipolysis media treated with LPS (**LPS+INS**), or ISO (**ISO+INS**).

(4) To establish LPS' effect on the activation of canonical and inflammatory lipolytic pathways, 7-d adipocytes were pre-treated during 2h with 100 µM of niacin (**Nia**; Cat N° HY-B0143, MedChemExpress LLC, Monmouth Junction, NJ, USA), or 10 µM of flunixin meglumine (**FM;** Cat N° HY-B0386, MedChemExpress LLC,) or the combination **Nia+FM.** Then, adipocytes were treated with ISO and LPS as described above.

(5) To determine how activation of the canonical and inflammatory pathways affect adipocyte's insulin sensitivity, 7-d adipocytes were pre-treated for 2h with Nia and FM. Followed by a 30-min incubation with INS. Subsequently, adipocytes were incubated in lipolysis media with LPS and ISO.

Lipolysis quantification

After incubation times described above, culture media was collected, snap-frozen in liquid nitrogen, and stored at -80 °C. Lipolysis was assessed by quantification of glycerol released in the culture medium, using Glycerol-Glo^{TM} Assay (Cat N° J3151, Promega Corp., Madison, WI USA) following manufacturer recommendations. The intra- and inter-assay coefficients of variation were

4.71% and 12.63%, respectively. All samples were run in duplicate. Glycerol released was normalized by the content of protein and the results are expressed as a ratio of the basal release of glycerol.

RNA Extraction from Adipocytes

RNA was extracted using the Maxwell® RSC simplyRNA cells kit (AS1390, Promega Corp.,) following manufacturer protocol. Five µL of DNase I (Promega) was used to eliminate genomic DNA. Automated extraction of RNA was carried out using the Maxwell® RSC instrument (Promega Corp.). RNA was stored at -80°C, and the concentration and integrity of total RNA were evaluated using a NanoDrop One© spectrophotometer (Cat N° 840274200, Thermofisher Scientific, Waltham, MA, USA). All samples had a 260:280 nm ratio between 2.01 and 2.04 and RNA integrity value >9. Reverse transcription was performed with 500 ng of RNA using 4 µL of the qScript cDNA SuperMix (95048 Quantabio, Beverly, MA, USA) for 5 minutes at 25°C, 30 minutes at 42°C, and 5 minutes at 85°C. cDNA was stored at -20°C.

Gene expression analysis

Transcriptional studies were performed as previously described (Chirivi et al., 2022). Samples were assayed in duplicate, each 10 µL PCR reaction contained 1X (5 µL) of SYBR™ Green PCR Master Mix (4309155, Applied Biosystems), 400 nM of primer assays (Table 10), and 5 ng of sample cDNA. A non-template control and non-reverse-transcriptase control monitored contamination and primer-dimer formation that could produce false-positive results and validated the absence of genomic DNA. Housekeeping genes with the lowest pairwise variation values including eukaryotic translation initiation factor 3 subunit K (*EIF3K*), ribosomal protein lateral stalk subunit P0 (*RPLP0)*, and ribosomal protein S9 (*RPS9*) were used. Expression of genes of interest was normalized against the geometric mean of selected housekeeping genes' CT.

Quantification cycle values were extrapolated using the $2^{-\Delta\Delta CT}$ method. Gene expression data are presented as geometric means ± 95% CI.

Protein analysis

Cells were suspended in 200 µL of RIPA buffer (Teknova, Hollister, CA, USA) supplemented with protease cOmplete™ mini EDTA-free protease inhibitor (Roche, San Francisco, CA, USA) and phosphatase inhibitors (Phosphatase inhibitor cocktail II J61022, Thermofisher Scientific). The concentration of protein was determined as previously described (Chirivi et al., 2022). The optimal protein concentration for the antibodies used in these experiments was 0.75 mg/mL as established in the 12–230 kDa Wes™ Separation Module capillary cartridges of the Simple Protein Wes™ system [SM-W004, ProteinSimple, Santa Clara, CA, USA (Nelson et al., 2017)]. Antibodies and dilutions were as follows: rabbit monoclonal anti-HSL (1:25, #4107, Cell Signaling, Danvers, MA, USA), anti-phosphorylated HSL serine 563 (1:25, #PA5-17488, Thermo Fisher), anti-ERK1/1 p44/42-MAPK3/1(Erk1/2) (1:1000, #9102S, Cell Signaling) and anti-phosphorylated p44/42-MAPK3/1(p-Erk1/2) (T202/Y204, 1:1000, # 9101S, Cell Signaling). Protein expression was detected on the Protein Wes™ system (SM-W004, ProteinSimple) as previously reported (Chirivi et al., 2022). The normalized data are expressed as relative increase vs Basal, and ratios pHSL(Ser563):HSL and pERK:ERK.

Statistical analysis

Statistical analyses were performed using JMP Pro16 (SAS Inst., Inc., Cary NC). The normality of the variables was checked using the Shapiro-Wilk Test ($P<0.05$). Residuals of the models were checked and found to be normally distributed. The statistical significance was determined by one- or two-way ANOVA and Tukey's post hoc adjustment was used for pairwise comparisons. Results are presented as mean ± SEM unless stated otherwise. Significance was

declared at $P \leq 0.05$, and tendencies were declared at $0.05 < P \leq 0.15$.

RESULTS

Primary Bovine Adipocytes are Differentiated after 7 days

Compared to day 0, bovine adipocytes after 7 d of differentiation showed 63.33± 4.12% adipogenesis efficiency as evidenced by higher accumulation of lipid droplets stained with Bodipy 493/503 ($P < 0.0001$; Figure 21A-B).

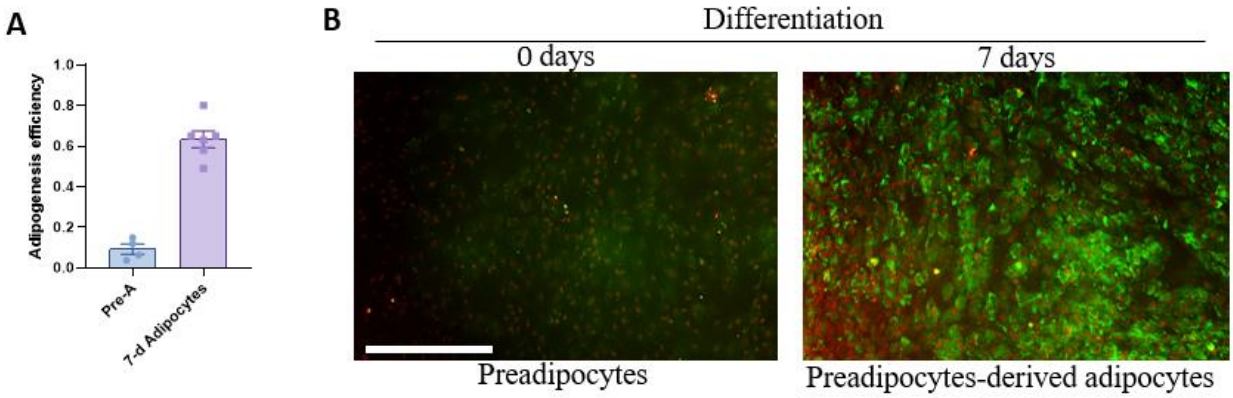

Figure 21. In vitro differentiation of bovine pre-adipocytes. (A) Adipogenesis efficiency as calculated by the IncuCyte zoom software (N° of cells with at least one lipid droplet over total # of cells in each well) n=4. **(B)** Representative images of cultured bovine cells. Triglycerides (green) were stained with Bodipy 493/503 and nuclei (red) were stained with NucSpot 650. Scale bar = 400 microns. Absorbance value is presented as mean ± SEM.

LPS Activates Lipolysis in a TLR4-dependent manner

Compared to basal conditions, LPS increased lipolysis in a quadratic response ($P < 0.0001$), reaching the effective lipolytic dose at 1 µg/mL with 72.66±15.1% more glycerol released (Figure 22A). This lipolytic response was comparable to the one activated by the canonical pathway (ISO 1 µM). To demonstrate the role of TLR4 during lipolysis, a subset of preadipocytes were pretreated with si*TLR4*. During a 7-day culture period, we observed a significant 82.31% decrease in *TLR4* mRNA expression compared to the siNC cells ($P < 0.01$; Figure 22B). Compared to basal, lipolysis was enhanced by 1.42- and 1.50-fold change when adipocytes were incubated with LPS and positive control ISO respectively ($P < 0.0001$; Figure 22C). In the presence of LPS,

the knockdown of *TLR4* inhibited lipolysis. As a proxy of lipolysis activation, LPS, and ISO enhanced the phosphorylation of HSL by 1.66 and 1.64-fold change ($P < 0.05$; Figure 22D). In contrast, the knockdown of TLR4 avoided the phosphorylation of HSL when adipocytes were exposed to LPS (Figure 22D). In the presence of LPS, a higher phosphorylation of ERK1/2 was observed, however, the knockdown of *TLR4* prevented ERK1/2 phosphorylation ($P < 0.0001$; Figure 22E).

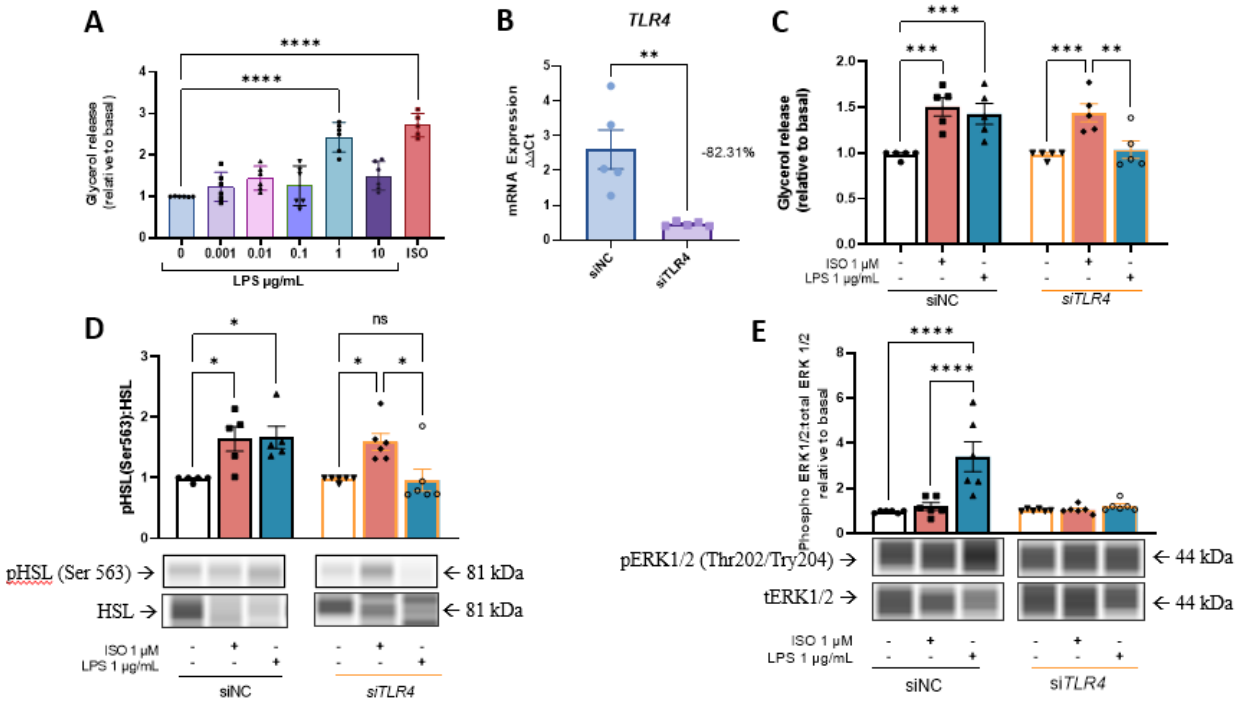

Figure 22. TLR4 mediates LPS-induced lipolysis in bovine adipocytes. Differentiated (7-d) bovine adipocytes were treated with LPS (LPS = 0, 0.001, 0.01, 0.1, 1, 10 µg/mL) or isoproterenol (ISO=1µM) for 3 h. **(A)** Glycerol release in cell culture media relative to no treated cells (0 µg/mL). **(B)** Fold change of *TLR4* gene expression relative to HC (2- ΔΔCT). Preadipocytes adipocytes were treated with non-coding siNC or si*TLR4* (siRNA *TLR4*). Gene expression was quantified 7 d after silencing and normalized with reference genes EIF3K, RPL19, and RPS9**. (C)** Glycerol release in 7d differentiated adipocytes treated with non-coding siNC or si*TLR4.* **(D)** Protein abundance of HSL and phosphorylated HSL (Ser 563) relative to basal. Bands were detected at 81 kDa. **(E)** Protein abundance of extracellular signal-regulated kinases 1/2 (ERK1/2) and phosphorylated ERK1/2 (pERK1/2) at Thr202/tyr204 relative to basal**.** Protein data are means of the ratio phosphorylated : total protein. Bands were detected at 44 kDa. Each dot represents a different set of cells. Error bars represent ± SEM. Bars with * differ ($P<0.05$) or ** ($P<0.01$) or *** ($P<0.001$) n = 6.

LPS Impairs the Anti-Lipolytic Effect of Insulin in bovine adipocytes

We assessed adipocyte response to insulin by quantifying the reduction of lipolytic responses (glycerol release) in the cell media. The inclusion of INS during ISO-induced lipolysis effectively reduced glycerol release at 3 h and 7 h by 20.55±7.93% and 46.5±5.16% respectively ($P < 0.05$; Figure 23A-B). IN reduced LPS-induced lipolysis at 3 h by 21.47±7.93 ($P < 0.05$; Figure 23A). However, IN did not inhibit lipolysis when cells are exposed to LPS for 7 h (-0.44±5.16%).

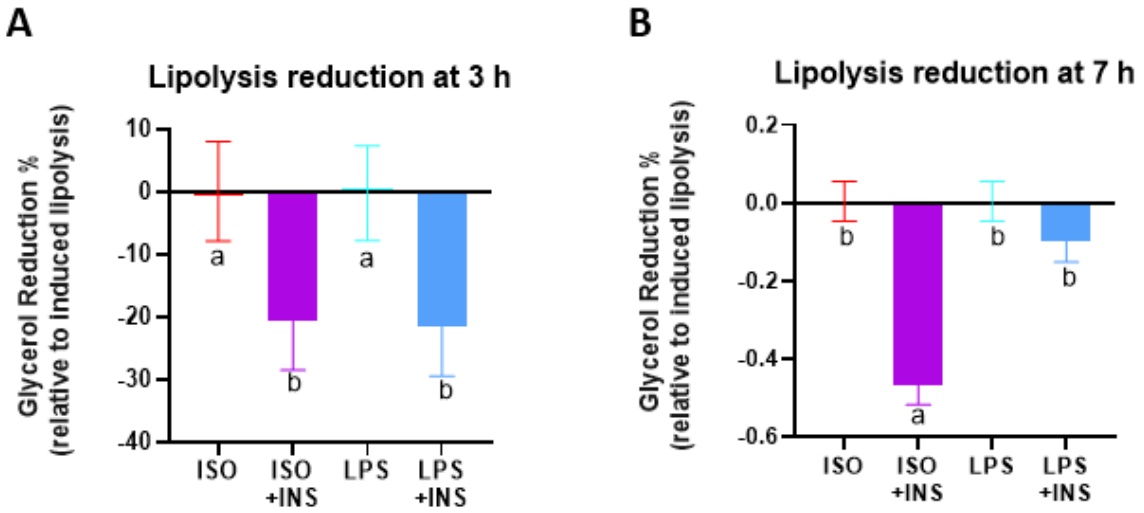

Figure 23. LPS impairs the anti-lipolytic effect of insulin. Differentiated (7-d) bovine adipocytes were pre-incubated with or without insulin (INS: 1 µg/L) for 30 min and treated with LPS (LPS = 1 µg/mL) or isoproterenol (ISO=1µM) for 3 h **(A)** and 7 h **(B).** Bars means ± SEM of percent of INS-mediated glycerol reduction compared to ISO and LPS alone. Bars with different letters differ significantly (^{a,b,c} $P<0.05$).

Cyclooxygenase inhibition reduced LPS-induced lipolysis

To assess the antilipolytic effect of Nia and FM, bovine adipocytes were pretreated with Nia, FM, or Nia+FM for 2 h. As expected, Nia effectively reduced ISO-induced lipolysis to baseline levels. Likewise, the combination of Nia and FM suppressed ISO-induced lipolysis ($P <$ 0.0001; Figure 24A). However, in the presence of LPS, Nia did not completely inhibit lipolysis. In contrast FM was effective in reducing LPS-induced lipolysis ($P < 0.001$; Figure 24B).

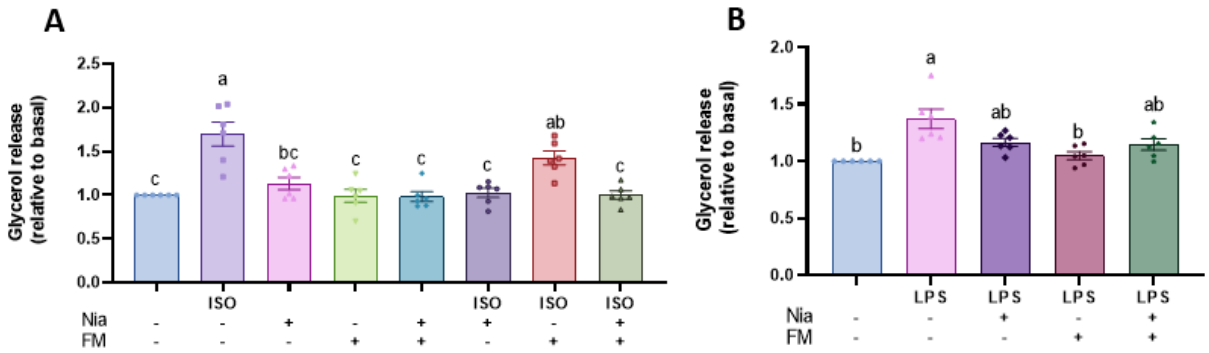

Figure 24. COX inhibition reduces LPS-induced lipolysis. Glycerol release in 7-d differentiated bovine adipocytes pre-treated with or without inhibitors of lipolysis niacin (Nia; 100 µM) and flunixin meglumine (FM 10 µM) for 2 h. Adipocytes were treated with (A) isoproterenol (ISO=1µM) or (B) LPS (LPS = 1 µg/mL) for 7 h. Bars means ± SEM glycerol release relative to basal Each dot represents a different set of cells.

Cyclooxygenase Inhibition Restores Adipocyte Insulin Sensitivity

We examined the impact of Nia and FM on adipocyte's insulin sensitivity during inflammation. Adipocytes differentiated for 7 d were incubated during 2 h with Nia, FM or both. After treating the cells with INS, lipolysis was stimulated using LPS. When adipocytes were pretreated with Nia, insulin did not effectively decrease lipolysis. However, adipocytes that were pretreated with FM exhibited responsiveness to the antilipolytic effect of insulin ($P < 0.05$); Figure 25A).

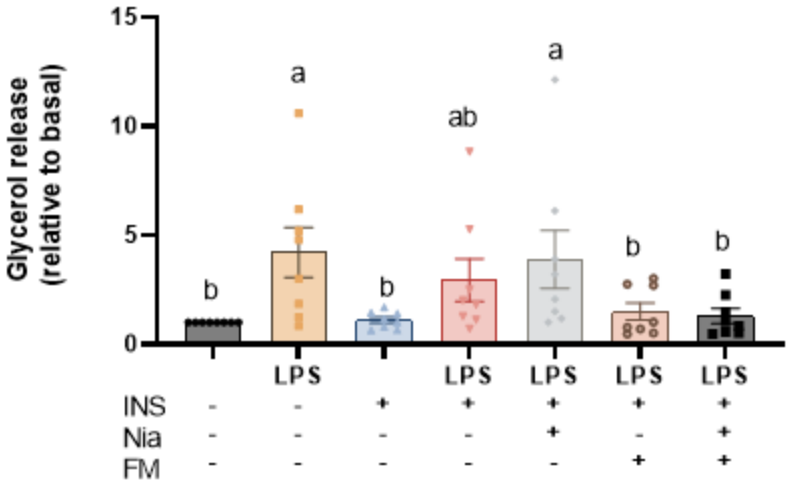

Figure 25. COX inhibition restores antilipolytic capacity of insulin. Glycerol release in 7-d differentiated bovine adipocytes pre-treated with or without inhibitors of lipolysis niacin (Nia; 100 µM) and flunixin meglumine (FM 10 µM) for 2 h. Adipocytes were pre-incubated with or without insulin (INS: 1 µg/L) and finally treated with LPS (LPS = 1 µg/mL) for 7 h. Bars means ± SEM glycerol release relative to basal Each dot represents a different set of cells.

DISCUSSION

The postpartum period in dairy cows is characterized by enhanced lipolysis within the AT to support energy requirements by the onset of lactation. However, when adipocytes become less responsive to insulin, it can lead to lipolysis dysregulation, which predisposes dairy cows to the development of metabolic diseases. One of the mechanisms involved in lipolysis dysregulation is the inflammatory effect of endotoxins. Endotoxins in the bloodstream (i.e., endotoxemia), are derived from leaky gut and infectious diseases especially during the postpartum period of dairy cows. Therefore, limiting the intensity of triglyceride hydrolysis during inflammation may reduce the negative impact of lipolysis dysregulation. Furthermore, understanding the interaction between endotoxin, lipolysis, and insulin is essential for comprehending the underlying mechanisms contributing to metabolic disorders such as ketosis and fatty liver in dairy cows. Hence, this study shows that endotoxin directly stimulates lipolysis in bovine adipocytes by TLR4 pathway. Endotoxin reduces insulin sensitivity and for the first time we demonstrated the modulatory roles

of COX inhibition during endotoxin-induced lipolysis.

The inflammatory and lipolytic effects of LPS have been previously characterized in AT explants from dairy cows by our research group (Chirivi et al., 2022). However, this study characterizes for the first time the lipolytic response and the underlying mechanism of LPS-induced lipolysis in bovine adipocytes. In line with previous studies in murine adipocytes, a concentration of 0.01 µg/mL of LPS is insufficient to initiate lipolysis. Instead, a minimum of 0.1 µg/mL is required for lipolysis activation over a 24 h period (Zu et al., 2009b). In the present study, we identified that a concentration of 1 µg/mL of LPS effectively induce lipolysis in a shorter period of time (3 h). Interestingly, humans adipocytes appear to be more sensitive to the lipolytic effect of LPS, since 0.01 µg/mL of LPS is effective to trigger a lipolytic response (Grisouard et al., 2010). The lipolytic responses induced by LPS observed in the current study are comparable to those produced by ISO.

TLR4 serves as the primary receptor for gram-negative bacteria endotoxins, playing a central role in immune signaling across many cell types, including adipocytes (Shi et al., 2006). Our model effectively achieved TLR4 knockdown using siRNA by reducing TLR4 mRNA expression by 82.31%. These findings align with a previously reported 78% reduction in TLR4 mRNA levels in 3T3-L1 adipocytes. However, this is a novel approach in bovine adipocytes that could potentially contribute to the understanding of endotoxin effects in dairy cows. In TLR4 knockdown adipocytes, LPS failed to induce lipolysis and activate HSL and ERK1/2. However, TLR4 knockdown adipocytes exhibited a normal lipolytic response when exposed to ISO. Therefore, TLR4 is a critical receptor for activating the lipolysis cascade triggered by LPS. Our results align with the observation is TLR4 mutant mice who presented reduced in vivo and in vitro lipolysis activation (Zu et al., 2009b).

Upstream regulation of lipolysis occurs by canonical and inflammatory pathways converging at the phosphorylation of HSL (Grisouard et al., 2010). In the canonical pathway, β-adrenergic stimulation, as the one induced with ISO in the current study, represents the most powerful activator of PKA, which in turn phosphorylates HSL. While, during inflammation, ERK1/2 has been reported as the key regulator of HSL-mediated adipocyte lipolysis in 3T3-L1 adipocytes (Foley et al., 2021). Therefore, the final proxy to quantify lipolysis activation is by the enhanced phosphorylation of HSL, the main neutral lipase responsible for the hydrolysis of triglycerides molecules (Grabner et al., 2021). The absence of glycerol release and reduced ERK1/2 and HSL phosphorylation observed in the present study in TLR4 knockdown adipocytes exposed to LPS, align with previous reports that suggest that lipolysis induced by LPS is ERK1/2 dependent (Zu et al., 2009b).

Insulin is the most potent physiological inhibitor of AT lipolysis. The pancreatic peptide inhibits lipolysis by triggering Akt and phosphodiesterase 3B (PDE3B) activation leading to HSL suppression (Rahn Landström et al., 2000). During the postpartum period cows are less sensitive to insulin, as part of the homeorhetic adaptations that allow lipolysis to fulfill the energy requirements during the early lactation. However, insulin resistance can have deleterious effects as it promotes excessive and protracted lipolysis, increasing the risk for metabolic diseases. In the present study, we determined insulin reduced canonical lipolysis. However, exposure to endotoxin LPS led to a reduction in the ability of insulin to inhibit lipolysis, indicating the development of insulin resistance (i.e., reduced biological effects of insulin). These findings align with previous observations in AT explants exposed to LPS by our group (Chirivi et al., 2022). Therefore, our results suggest that the paracrine effects of immune cells activated by LPS may not be necessary for the initiation of insulin resistance within the AT. Instead, direct exposure of adipocytes to LPS

appears to impair their insulin sensitivity. Although the mechanisms of insulin resistance were not investigated in the present study, there is extensive evidence suggesting that increased production of proinflammatory cytokines including TNF-α and IL6 during LPS exposure, are responsible for downregulation of PDE3B which results in reduced capacity to reduce lipolysis (Rahn Landström et al., 2000). Similarly, inflammatory factors such as TNF, JNK, and suppressor of cytokine signaling (SOCS), which are commonly activated by LPS, have been shown to exert a negative regulatory effect on insulin receptor substrate (**IRS**). This effect consists in aberrant phosphorylation of IRS which leads to reduced insulin signaling and contributes to the development of insulin resistance (Rui et al., 2002).

Niacin is a potent antilipolytic agent approved for use in lactating dairy cows. It inhibits the canonical lipolytic pathway after binding the G protein-coupled receptor 109A (GPR109A) and inhibiting PKA activation in adipocytes (Tunaru et al., 2003). As expected, we observed that niacin inhibited canonical lipolysis induced with ISO. However, it did not exhibit the same inhibitory effect on LPS-induced lipolysis. This specific finding may suggest that LPS-induced lipolysis is not primarily mediated by PKA activity.

In adipocytes treated with COX inhibitor, the lipolytic effect of LPS was abolished in the present study. These findings indicate that LPS appears to induce lipolysis through the inflammatory pathway rather than the canonical PKA pathway. To the best of our knowledge, this is the first study that investigates the effect of COX inhibition on inflammatory lipolysis in adipocytes. A recent study investigating the selective inhibition of COX2 activity with celecoxib in 3T3-L1 adipocytes found that COX2 inhibition did not diminish the ISO-induced canonical lipolysis (Gartung et al., 2016). These findings are consistent with our own results, where we also observed that FM did not reduce ISO-induced lipolysis. However, there is a lack of research on

the effects of COX inhibition specifically during inflammatory-induced lipolysis. Given that the administration of COX inhibitors is commonly associated with hypothermia, a recent study proposed that the mechanisms behind the induction of hypothermia by COX inhibitors may be attributed to reduced lipolysis in brown adipocytes (Bashir et al., 2020). The researchers found that acetaminophen reduced basal and ISO-induced lipolysis. FM is a potent inhibitor of COX enzymes, which are responsible for the synthesis of prostaglandins and tromboxaneA2. By inhibiting COX activity, FM effectively blocks the activation of lipolysis mediated by inflammatory products such as prostaglandin E2 (Inazumi et al., 2020). LPS is well known activator of inducible COX2 in different cell types including adipocytes (Chang et al., 2022). The activity of COX2 plays an important role in lipid mobilization. The overexpression of COX2 reduced triglyceride levels in adipocytes and hepatocytes by enhancing lipolysis (Banhos Danneskiold-Samsøe et al., 2019). While COX2 knockout mice presented increased size and number of adipocytes, suggesting that COX2 deficiency favors adipogenesis (Wang et al., 2022). Our observations could be explained by the potent inhibitory activity of FM on COX enzymes. However, more research is needed to elucidate the complete mechanisms of action for the anti-lipolytic effect of FM in bovine adipocytes.

As discussed above, the adipose tissue insulin resistance is mainly mediated by inflammatory products that attenuate insulin signaling. Additional evidence suggests that the activation COX2-PGE2 is crucially involved adipose tissue insulin resistance (Hsieh et al., 2009, Chan et al., 2019). We observed in the present study that adipocytes pretreated with FM were responsive to the antilipolytic effect of insulin. This effect could be explained by a lack of COX2 activity during FM treatment. Our observations align with previous study that observed improved insulin sensitivity in high fat diet mice treated with celecoxib, a selective COX2 inhibitor (Chan

et al., 2016). The improvement in the insulin sensitivity was achieved by reversing the AT inflammatory gene a protein expression. The results obtained from this study are important for potential interventions targeting excessive lipolysis in postpartum dairy cows, as they provide insights into the mechanisms of LPS-induced lipolysis.

CONCLUSION

The present study demonstrates that LPS mediates lipolysis and insulin resistance in bovine adipocytes through TLR4 signaling. Furthermore, results from this study show that treating adipocytes with FM reduced the lipolytic effect of LPS. This highlights the potential target of inhibiting COX enzymes to reduce excessive lipolysis and enhance adipocyte's insulin sensitivity in dairy cows.

CHAPTER 6: CONCLUSION

Lipolysis dysregulation in AT is an impaired response to the antilipolytic effect of insulin, which increases disease susceptibility. Dairy cows may have increased blood circulation of endotoxins during the periparturient period due to leaky gut, ruminal acidosis, heat stress, and infectious diseases including mastitis and endometritis. This dissertation helps to better understand the role of endotoxemia as an important mediator of lipolysis dysregulation in AT from dairy cows around parturition. We demonstrate that endotoxin-triggered inflammation mediates lipolysis dysregulation, thereby inflammation could potentially increase risk for metabolic disease by affecting AT function.

Our data demonstrate that during periparturient lipolysis dysregulation: 1) Cows presenting spontaneous clinical ketosis exhibit a systemic inflammatory response characterized by endotoxemia. However, when treated with COX inhibitors (e.g., Flunixin meglumine), those cows show a reduction of both blood ketone bodies and NEFA. 2)The AT exhibit an inflammatory phenotype characterized by macrophage trafficking and expression of proinflammatory cytokines 3) We demonstrate for the first time that inflammation derived from endotoxin is an activator of lipolysis dysregulation and contributes to the development of AT insulin resistance. 4) We prove that TLR4 is needed for the initiation of lipolysis dysregulation mediated by endotoxin in bovine adipocytes. 5) We provide evidence that pharmacological inhibition of COX activity resulted in reduced lipolysis dysregulation and improved endotoxin-mediated insulin sensitivity in vitro.

Endotoxemia in cows with clinical ketosis may be a contributing factor to the development of lipolysis dysregulation. This provides valuable insights into the potential impact of infectious diseases and endotoxemia on the development of metabolic disorders in dairy cows. Cows with clinical ketosis had reduced hyperketonemia and NEFA in blood following niacin administration

and COX inhibition with flunixin meglumine. This evidenced the central role of inflammation during metabolic disease and highlights the need for more research in the interventions utilized to treat and prevent metabolic disorders. The findings in this dissertation define new gaps in our knowledge of metabolic disorders. For example, there is a need to determine whether endotoxemia-associated metabolic disorders are initiated before calving or even during the previous lactations.

The AT function is impaired during lipolysis dysregulation-associated metabolic disease. The impaired insulin sensitivity and higher inflammatory profile observed in adipose tissues from cows suffering clinical ketosis provide evidence of the connection between inflammation and reduced antilipolytic effect of insulin. However, these findings provided new gaps in our knowledge of the trafficking of adipose tissue macrophages and the role of inflammation during lipolysis dysregulation. Further research is needed to understand the role of specific subtypes of immune cells including TREM2 macrophages, which remove cell debris and excessive lipids during lipolysis (Liebold et al., 2023). Finally, there is a big opportunity to understand how endotoxemia directly impacts adipose tissue function.

Endotoxin activates lipolysis and reduces insulin sensitivity in cultured adipose tissue explants. Our findings from this ex vivo model demonstrate the lipolytic effect of endotoxins and provide evidence of the potential development of adipose tissue insulin resistance in cows suffering endotoxemia. Evidence from humans and rodents suggests that the development of AT dysfunction and metabolic diseases is closely linked to low-grade chronic inflammation (Cani et al., 2007). However, it remains unknown whether a similar relationship exists in dairy cows. Considering that TLR4 is a determinant factor initiating endotoxin-induced lipolysis, the modulation of TLR4 expression could potentially mitigate the impact of endotoxemia on AT

dysfunction during the postpartum period. Additionally, our observations indicated a positive response following inhibition of COX activity in adipocytes and dairy cows with clinical ketosis. Further research is needed to fully understand the role of COX and prostaglandins in the activation and resolution of AT inflammation, as total inhibition of COX activity can also have detrimental effects on AT function. Therefore, it is essential to refine the optimal treatment approach to ensure that any interventions targeting COX and prostaglandins strike a delicate balance, preventing excessive inhibition that could harm AT function while effectively addressing AT inflammation. This refinement will help optimize potential therapeutic strategies in the future. Overall, these findings provide valuable insights that can guide the exploration and development of future nutritional or pharmaceutical interventions aimed at minimizing AT alterations and improving the well-being, lactation, and reproductive performance of periparturient dairy cows.

REFERENCES

Abou-Rjeileh, U., J. M. Dos Santos Neto, M. Chirivi, N. O'Boyle, D. Salcedo, C. Prom, J. Laguna, J. Parales-Giron, A. L. Lock, and G. A. Contreras. 2023. Oleic acid abomasal infusion limits lipolysis and improves insulin sensitivity in adipose tissue from periparturient dairy cows. J Dairy Sci.

Abuajamieh, M., S. K. Kvidera, M. V. S. Fernandez, A. Nayeri, N. C. Upah, E. A. Nolan, S. M. Lei, J. M. DeFrain, H. B. Green, K. M. Schoenberg, W. E. Trout, and L. H. Baumgard. 2016. Inflammatory biomarkers are associated with ketosis in periparturient Holstein cows. Research in veterinary science 109:81-85.

Abuajamieh, M. K. A. 2015. Effects of heat stress or ketosis on metabolism and inflammatory biomarkers in ruminants and monogastrics. Graduate Theses and Dissertations https://lib.dr.iastate.edu/etd/14762.

Aguirre, V., E. D. Werner, J. Giraud, Y. H. Lee, S. E. Shoelson, and M. F. White. 2002. Phosphorylation of Ser307 in insulin receptor substrate-1 blocks interactions with the insulin receptor and inhibits insulin action. The Journal of biological chemistry 277(2):1531-1537.

Aileen, W. C. Jason, and P.-Y. Robert. 2015. Effects of heat stress on the immune system , metabolism and nutrient partitioning : implications on reproductive success.

Akiba, Y., K. Maruta, T. Takajo, K. Narimatsu, H. Said, I. Kato, A. Kuwahara, and J. D. Kaunitz. 2020. Lipopolysaccharides transport during fat absorption in rodent small intestine. American Journal of Physiology-Gastrointestinal and Liver Physiology 318(6):G1070-G1087.

Alhusaini, S., K. McGee, B. Schisano, A. Harte, P. McTernan, S. Kumar, and G. Tripathi. 2010. Lipopolysaccharide, high glucose and saturated fatty acids induce endoplasmic reticulum stress in cultured primary human adipocytes: Salicylate alleviates this stress. Biochemical and Biophysical Research Communications 397(3):472-478.

Amar, J., R. Burcelin, J. B. Ruidavets, P. D. Cani, J. Fauvel, M. C. Alessi, B. Chamontin, and J. Ferriéres. 2008. Energy intake is associated with endotoxemia in apparently healthy men. Am J Clin Nutr 87(5):1219-1223.

Andersen, P. H., H. Houe, A. Fomsgaard, and R. Høier. 1996. Prevalence of antibodies to lipid A in Danish cattle. Zentralbl Veterinarmed A 43(5):271-279.

Atri, C., F. Z. Guerfali, and D. Laouini. 2018. Role of Human Macrophage Polarization in Inflammation during Infectious Diseases. Int J Mol Sci 19(6).

Babitt, J., B. Trigatti, A. Rigotti, E. J. Smart, R. G. Anderson, S. Xu, and M. Krieger. 1997. Murine SR-BI, a high density lipoprotein receptor that mediates selective lipid uptake, is N-glycosylated and fatty acylated and colocalizes with plasma membrane caveolae. The Journal of biological chemistry 272(20):13242-13249.

Bäckhed, F., H. Ding, T. Wang, L. V. Hooper, G. Y. Koh, A. Nagy, C. F. Semenkovich, and J. I. Gordon. 2004. The gut microbiota as an environmental factor that regulates fat storage. Proceedings of the National Academy of Sciences of the United States of America 101(44):15718-15723.

Bäckhed, F., J. K. Manchester, C. F. Semenkovich, and J. I. Gordon. 2007. Mechanisms underlying the resistance to diet-induced obesity in germ-free mice. Proceedings of the National Academy of Sciences of the United States of America 104(3):979-984.

Bae, J., C. J. Ricciardi, D. Esposito, S. Komarnytsky, P. Hu, B. J. Curry, P. L. Brown, Z. Gao, J. P. Biggerstaff, J. Chen, and L. Zhao. 2014. Activation of pattern recognition receptors in brown adipocytes induces inflammation and suppresses uncoupling protein 1 expression and mitochondrial respiration. American Journal of Physiology-Cell Physiology 306(10):C918-C930.

Banhos Danneskiold-Samsøe, N., S. B. Sonne, J. M. Larsen, A. N. Hansen, E. Fjære, M. S. Isidor, S. Petersen, J. Henningsen, I. Severi, L. Sartini, Y. Schober, J. Wolf, W. A. Nockher, C. Wolfrum, S. Cinti, C. Sina, J. B. Hansen, L. Madsen, S. Brix, and K. Kristiansen. 2019. Overexpression of cyclooxygenase-2 in adipocytes reduces fat accumulation in inguinal white adipose tissue and hepatic steatosis in high-fat fed mice. Scientific Reports 9(1):8979.

Bannerman, D. D. and S. E. Goldblum. 1999. Direct effects of endotoxin on the endothelium: barrier function and injury. Laboratory investigation; a journal of technical methods and pathology 79(10):1181-1199.

Barragan, A. A., J. M. Piñeiro, G. M. Schuenemann, P. J. Rajala-Schultz, D. E. Sanders, J. Lakritz, and S. Bas. 2018. Assessment of daily activity patterns and biomarkers of pain, inflammation, and stress in lactating dairy cows diagnosed with clinical metritis. Journal of Dairy Science 101(9):8248-8258.

Bashir, S., B. Elegunde, and W. A. Morgan. 2020. Inhibition of lipolysis: A novel explanation for the hypothermic actions of acetaminophen in non-febrile rodents. Biochemical Pharmacology 172:113774.

Bauman, D. E. and W. B. Currie. 1980. Partitioning of nutrients during pregnancy and lactation: a review of mechanisms involving homeostasis and homeorhesis. J Dairy Sci 63(9):1514-1529.

Beatty, W. L., S. Méresse, P. Gounon, J. Davoust, J. Mounier, P. J. Sansonetti, and J. P. Gorvel. 1999. Trafficking of Shigella lipopolysaccharide in polarized intestinal epithelial cells. The Journal of cell biology 145(4):689-698.

Bergan, H. E., J. D. Kittilson, and M. A. Sheridan. 2013. PKC and ERK mediate GH-stimulated lipolysis. J Mol Endocrinol 51(2):213-224.

Bhavsar, I., C. S. Miller, and M. Al-Sabbagh. Macrophage Inflammatory Protein-1 Alpha (MIP-1 alpha)/CCL3: As a Biomarker. General Methods in Biomarker Research and their Applications. 2015 Jun 1:223-49. doi: 10.1007/978-94-007-7696-8_27. eCollection 2015.

Birjmohun, R. S., S. I. v. Leuven, J. H. M. Levels, C. v. t. Veer, J. A. Kuivenhoven, J. C. M. Meijers, M. Levi, J. J. P. Kastelein, T. v. d. Poll, and E. S. G. Stroes. 2007. High-Density Lipoprotein Attenuates Inflammation and Coagulation Response on Endotoxin Challenge in Humans. Arteriosclerosis, Thrombosis, and Vascular Biology 27(5):1153-1158.

Bjerre-Harpøth, V., A. C. Storm, M. Eslamizad, B. Kuhla, and M. Larsen. 2015. Effect of propylene glycol on adipose tissue mobilization in postpartum over-conditioned Holstein cows. Journal of Dairy Science 98(12):8581-8596.

Bobe, G., J. W. Young, and D. C. Beitz. 2004. Invited Review: Pathology, Etiology, Prevention, and Treatment of Fatty Liver in Dairy Cows*. Journal of Dairy Science 87(10):3105-3124.
Boudina, S. and T. E. Graham. 2014. Mitochondrial function/dysfunction in white adipose tissue. Experimental Physiology 99(9):1168-1178.

Bradford, B. J., K. Yuan, J. K. Farney, L. K. Mamedova, and A. J. Carpenter. 2015. Invited review: Inflammation during the transition to lactation: New adventures with an old flame. J Dairy Sci 98(10):6631-6650.

Brockman, R. P. and B. Laarveld. 1986. Hormonal regulation of metabolism in ruminants; a review. Livestock Production Science 14(4):313-334.

Brodzki, P., J. Marczuk, U. Lisiecka, M. Szczubiał, A. Brodzki, H. Gorzkoś, and K. Kulpa. 2021. Comparative evaluation of cytokine and acute-phase protein concentrations in sera of dairy cows with subclinical and clinical ketosis as a different view of the causes of the disease. Veterinary world 14(6):1572-1578.

Brown, J. M., M. S. Boysen, S. Chung, O. Fabiyi, R. F. Morrison, S. Mandrup, and M. K. McIntosh. 2004. Conjugated linoleic acid induces human adipocyte delipidation: autocrine/paracrine regulation of MEK/ERK signaling by adipocytokines. The Journal of biological chemistry 279(25):26735-26747.

Brundert, M., J. Heeren, M. Merkel, A. Carambia, J. Herkel, P. Groitl, T. Dobner, R. Ramakrishnan, K. J. Moore, and F. Rinninger. 2011. Scavenger receptor CD36 mediates uptake of high density lipoproteins in mice and by cultured cells. Journal of lipid research 52(4):745-758.
Caesar, R., C. S. Reigstad, H. K. Bäckhed, C. Reinhardt, M. Ketonen, G. Östergren Lundén, P. D. Cani, and F. Bäckhed. 2012. Gut-derived lipopolysaccharide augments adipose macrophage accumulation but is not essential for impaired glucose or insulin tolerance in mice. Gut 61(12):1701-1707.

Camilleri, M. 2019. Leaky gut: mechanisms, measurement and clinical implications in humans. Gut 68(8):1516-1526.

Cani, P. D., J. Amar, M. A. Iglesias, M. Poggi, C. Knauf, D. Bastelica, A. M. Neyrinck, F. Fava, K. M. Tuohy, C. Chabo, A. Waget, E. Delmee, B. Cousin, T. Sulpice, B. Chamontin, J. Ferrieres, J. F. Tanti, G. R. Gibson, L. Casteilla, N. M. Delzenne, M. C. Alessi, and R. Burcelin. 2007. Metabolic Endotoxemia Initiates Obesity and Insulin Resistance. Diabetes 56(7):1761-1772.

Cao, Y. 2013. Angiogenesis and vascular functions in modulation of obesity, adipose metabolism, and insulin sensitivity. Cell metabolism 18(4):478-489.

Capel, M. B., K. D. Bach, S. Mann, and J. A. A. McArt. 2021. A randomized controlled trial to evaluate propylene glycol alone or in combination with dextrose as a treatment for hyperketonemia in dairy cows. Journal of Dairy Science 104(2):2185-2194.

Carlson, C. J., S. Koterski, R. J. Sciotti, G. B. Poccard, and C. M. Rondinone. 2003. Enhanced basal activation of mitogen-activated protein kinases in adipocytes from type 2 diabetes: potential role of p38 in the downregulation of GLUT4 expression. Diabetes 52(3):634-641.

Carneiro, L. A., L. H. Travassos, and D. J. Philpott. 2004. Innate immune recognition of microbes through Nod1 and Nod2: implications for disease. Microbes Infect 6(6):609-616.

Caslin, H. L., M. Bhanot, W. R. Bolus, and A. H. Hasty. 2020. Adipose tissue macrophages: Unique polarization and bioenergetics in obesity. Immunological reviews 295(1):101-113.

Casteilla, L., P. Muzzin, J. P. Revelli, D. Ricquier, and J. P. Giacobino. 1994. Expression of beta 1- and beta 3-adrenergic-receptor messages and adenylate cyclase beta-adrenergic response in bovine perirenal adipose tissue during its transformation from brown into white fat. The Biochemical journal 297 (Pt 1)(Pt 1):93-97.

Ceciliani, F., J. J. Ceron, P. D. Eckersall, and H. Sauerwein. 2012. Acute phase proteins in ruminants. J Proteomics 75(14):4207-4231.

Chan, P.-C., F.-C. Hsiao, H.-M. Chang, M. Wabitsch, and P. S. Hsieh. 2016. Importance of adipocyte cyclooxygenase-2 and prostaglandin E2-prostaglandin E receptor 3 signaling in the development of obesity-induced adipose tissue inflammation and insulin resistance. The FASEB Journal 30(6):2282-2297.

Chan, P.-C., M.-T. Liao, and P.-S. Hsieh. 2019. The Dualistic Effect of COX-2-Mediated Signaling in Obesity and Insulin Resistance. International journal of molecular sciences 20(13):3115.

Chang, C.-C., K.-C. Sia, J.-F. Chang, C.-M. Lin, C.-M. Yang, I.-T. Lee, T. T. T. Vo, K.-Y. Huang, and W.-N. Lin. 2022. Participation of lipopolysaccharide in hyperplasic adipose expansion: Involvement of NADPH oxidase/ROS/p42/p44 MAPK-dependent Cyclooxygenase-2. Journal of Cellular and Molecular Medicine 26(14):3850-3861.

Chang, C. C., K. C. Sia, J. F. Chang, C. M. Lin, C. M. Yang, K. Y. Huang, and W. N. Lin. 2019. Lipopolysaccharide promoted proliferation and adipogenesis of preadipocytes through JAK/STAT and AMPK-regulated cPLA2 expression. International journal of medical sciences 16(1):167-179.

Chen, L., R. Chen, H. Wang, and F. Liang. 2015. Mechanisms Linking Inflammation to Insulin Resistance. International Journal of Endocrinology 2015:508409.

Chen, Q., M. Lu, B. R. Monks, and M. J. Birnbaum. 2016. Insulin Is Required to Maintain Albumin Expression by Inhibiting Forkhead Box O1 Protein. The Journal of biological chemistry 291(5):2371-2378.

Chen, S., J. Wang, D. Peng, G. Li, J. Chen, and X. Gu. 2018. Exposure to heat-stress environment affects the physiology, circulation levels of cytokines, and microbiome in dairy cows. Scientific Reports 8(1):14606.

Chi, W., D. Dao, T. C. Lau, B. D. Henriksbo, J. F. Cavallari, K. P. Foley, and J. D. Schertzer. 2014. Bacterial peptidoglycan stimulates adipocyte lipolysis via NOD1. PloS one 9(5):e97675-e97675.

Chirivi, M., D. Cortes-Beltran, C. J. Rendon, and G. A. Contreras. 2023a. Supplemental Figure S1. https://doi.org/10.6084/m9.figshare.23705802.v1

Chirivi, M., D. Cortes, C. J. Rendon, and G. A. Contreras. 2023b. Lipolysis inhibition as a treatment of clinical ketosis in dairy cows, a randomized clinical trial J Dairy Sci, In Press.

Chirivi, M., C. J. Rendon, M. N. Myers, C. M. Prom, S. Roy, A. Sen, A. L. Lock, and G. A. Contreras. 2022. Lipopolysaccharide induces lipolysis and insulin resistance in adipose tissue from dairy cows. J Dairy Sci 105(1):842-855.

Chow, J. C., D. W. Young, D. T. Golenbock, W. J. Christ, and F. Gusovsky. 1999. Toll-like receptor-4 mediates lipopolysaccharide-induced signal transduction. J Biol Chem 274(16):10689-10692.

Ciaffi, J., D. Mitselman, L. Mancarella, V. Brusi, L. Lisi, P. Ruscitti, P. Cipriani, R. Meliconi, R. Giacomelli, C. Borghi, and F. Ursini. 2021. The Effect of Ketogenic Diet on Inflammatory Arthritis and Cardiovascular Health in Rheumatic Conditions: A Mini Review. Front Med (Lausanne) 8:792846.

Clemente-Postigo, M., W. Oliva-Olivera, L. Coin-Aragüez, B. Ramos-Molina, R. M. Giraldez-Perez, S. Lhamyani, J. Alcaide-Torres, P. Perez-Martinez, R. E. Bekay, F. Cardona, and F. J. Tinahones. 2019. Metabolic endotoxemia promotes adipose dysfunction and inflammation in human obesity. American Journal of Physiology-Endocrinology and Metabolism 316(2):E319-E332.

Coats, B. R., K. Q. Schoenfelt, V. C. Barbosa-Lorenzi, E. Peris, C. Cui, A. Hoffman, G. Zhou, S. Fernandez, L. Zhai, B. A. Hall, A. S. Haka, A. M. Shah, C. A. Reardon, M. J. Brady, C. J. Rhodes,

F. R. Maxfield, and L. Becker. 2017. Metabolically Activated Adipose Tissue Macrophages Perform Detrimental and Beneficial Functions during Diet-Induced Obesity. Cell Rep 20(13):3149-3161.

Contreras, G. A., J. De Koster, J. de Souza, J. Laguna, V. Mavangira, R. K. Nelli, J. Gandy, A. L. Lock, and L. M. Sordillo. 2020. Lipolysis modulates the biosynthesis of inflammatory lipid mediators derived from linoleic acid in adipose tissue of periparturient dairy cows. Journal of dairy science 103(2):1944-1955.

Contreras, G. A., E. Kabara, J. Brester, L. Neuder, and M. Kiupel. 2015. Macrophage infiltration in the omental and subcutaneous adipose tissues of dairy cows with displaced abomasum. J Dairy Sci 98(9):6176-6187.

Contreras, G. A., C. Strieder-Barboza, and J. De Koster. 2018. Symposium review: Modulating adipose tissue lipolysis and remodeling to improve immune function during the transition period and early lactation of dairy cows. Journal of Dairy Science 101(3):2737-2752.

Contreras, G. A., C. Strieder-Barboza, J. de Souza, J. Gandy, V. Mavangira, A. L. Lock, and L. M. Sordillo. 2017a. Periparturient lipolysis and oxylipid biosynthesis in bovine adipose tissues. PLoS One 12(12):e0188621.

Contreras, G. A., C. Strieder-Barboza, and W. Raphael. 2017b. Adipose tissue lipolysis and remodeling during the transition period of dairy cows. Journal of Animal Science and Biotechnology 8(1):41.

Contreras, G. A., C. Strieder-Barboza, and W. Raphael. 2017c. Adipose tissue lipolysis and remodeling during the transition period of dairy cows. J Anim Sci Biotechnol 8:41-41.

Contreras, G. A., K. Thelen, S. E. Schmidt, C. Strieder-Barboza, C. L. Preseault, W. Raphael, M. Kiupel, J. Caron, and A. L. Lock. 2016a. Adipose tissue remodeling in late-lactation dairy cows during feed-restriction-induced negative energy balance. J Dairy Sci 99(12):10009-10021.

Contreras, G. A., K. Thelen, S. E. Schmidt, C. Strieder-Barboza, C. L. Preseault, W. Raphael, M. Kiupel, J. Caron, and A. L. Lock. 2016b. Adipose tissue remodeling in late-lactation dairy cows during feed-restriction-induced negative energy balance. Journal of Dairy Science 99(12):10009-10021.

Cote, J. F. 1971. Bovine ketosis: principles of therapy. Can Vet J 12(1):19-20.

Council, N. R. 2001. Nutrient Requirements of Dairy Cattle: Seventh Revised Edition, 2001. The National Academies Press, Washington, DC.

Crowe, A. R. and W. Yue. 2019. Semi-quantitative Determination of Protein Expression using Immunohistochemistry Staining and Analysis: An Integrated Protocol. Bio Protoc 9(24):e3465.

da Cruz Nascimento, S. S., J. L. Carvalho de Queiroz, A. Fernandes de Medeiros, A. C. de França Nunes, G. Piuvezam, B. L. Lima Maciel, T. Souza Passos, and A. H. A. Morais. 2022. Anti-inflammatory agents as modulators of the inflammation in adipose tissue: A systematic review. PloS one 17(9):e0273942.

De Koster, J., R. K. Nelli, C. Strieder-Barboza, J. de Souza, A. L. Lock, and G. A. Contreras. 2018a. The contribution of hormone sensitive lipase to adipose tissue lipolysis and its regulation by insulin in periparturient dairy cows. Scientific Reports 8(1):13378.

De Koster, J., R. K. Nelli, C. Strieder-Barboza, J. de Souza, A. L. Lock, and G. A. Contreras. 2018b. The contribution of hormone sensitive lipase to adipose tissue lipolysis and its regulation by insulin in periparturient dairy cows. Scientific reports 8(1):13378.

De Koster, J., C. Strieder-Barboza, J. de Souza, A. L. Lock, and G. A. Contreras. 2018c. Short communication: Effects of body fat mobilization on macrophage infiltration in adipose tissue of early lactation dairy cows. Journal of Dairy Science 101(8):7608-7613.

De Koster, J., C. Urh, M. Hostens, W. Van den Broeck, H. Sauerwein, and G. Opsomer. 2017. Relationship between serum adiponectin concentration, body condition score, and peripheral tissue insulin response of dairy cows during the dry period. Domest Anim Endocrinol 59:100-104.

De Koster, J., W. Van den Broeck, L. Hulpio, E. Claeys, M. Van Eetvelde, K. Hermans, M. Hostens, V. Fievez, and G. Opsomer. 2016. Influence of adipocyte size and adipose depot on the in vitro lipolytic activity and insulin sensitivity of adipose tissue in dairy cows at the end of the dry period. J Dairy Sci 99(3):2319-2328.

De Koster, J. D. and G. Opsomer. 2013. Insulin resistance in dairy cows. Vet Clin North Am Food Anim Pract 29(2):299-322.

de Luca, C. and J. M. Olefsky. 2008. Inflammation and insulin resistance. FEBS letters 582(1):97-105.

de Souza, C. O., M. A. Kurauti, F. de Fatima Silva, H. de Morais, R. Curi, S. M. Hirabara, J. C. Rosa Neto, and H. M. de Souza. 2015. Celecoxib and Ibuprofen Restore the ATP Content and the Gluconeogenesis Activity in the Liver of Walker-256 Tumor-Bearing Rats. Cellular Physiology and Biochemistry 36(4):1659-1669.

Degerman, E., T. R. Landström, J. Wijkander, L. S. Holst, F. Ahmad, P. Belfrage, and V. Manganiello. 1998. Phosphorylation and Activation of Hormone-Sensitive Adipocyte Phosphodiesterase Type 3B. Methods 14(1):43-53.

Deng, J., S. Liu, L. Zou, C. Xu, B. Geng, and G. Xu. 2012. Lipolysis Response to Endoplasmic Reticulum Stress in Adipose Cells*. Journal of Biological Chemistry 287(9):6240-6249.

Dervishi, E., G. Plastow, B. Hoff, and M. Colazo. 2021. Common and specific mineral and metabolic features in dairy cows with clinical metritis, hypocalcaemia or ketosis. Research in veterinary science 135:335-342.

Deshmane, S. L., S. Kremlev, S. Amini, and B. E. Sawaya. 2009. Monocyte chemoattractant protein-1 (MCP-1): an overview. J Interferon Cytokine Res 29(6):313-326.

Dettlaff-Pokora, A., T. Sledzinski, and J. Swierczynski. 2016. Upregulation of Pnpla2 and Abhd5 and downregulation of G0s2 gene expression in mesenteric white adipose tissue as a potential reason for elevated concentration of circulating NEFA after removal of retroperitoneal, epididymal, and inguinal adipose tissue. Molecular and Cellular Biochemistry 422(1):21-29.

Dickson, M. J., S. K. Kvidera, E. A. Horst, C. E. Wiley, E. J. Mayorga, J. Ydstie, G. A. Perry, L. H. Baumgard, and A. F. Keating. 2019a. Impacts of chronic and increasing lipopolysaccharide exposure on production and reproductive parameters in lactating Holstein dairy cows. Journal of Dairy Science.

Dickson, M. J., S. K. Kvidera, E. A. Horst, C. E. Wiley, E. J. Mayorga, J. Ydstie, G. A. Perry, L. H. Baumgard, and A. F. Keating. 2019b. Impacts of chronic and increasing lipopolysaccharide exposure on production and reproductive parameters in lactating Holstein dairy cows. J Dairy Sci 102(4):3569-3583.

Djokovic, R., M. Cincovic, V. Kurćubić, M. Petrović, M. Lalović, B. Jašović, and Z. Stanimirović. 2014. Endocrine and Metabolic Status of Dairy Cows during Transition Period. Thai Journal of Veterinary Medicine 44:59-66.

Dosogne, H., E. Meyer, A. Sturk, J. van Loon, A. M. Massart-Leën, and C. Burvenich. 2002. Effect of enrofloxacin treatment on plasma endotoxin during bovine Escherichia coli mastitis. Inflammation Research 51(4):201-205.

Drackley, J. K., H. M. Dann, N. Douglas, N. A. J. Guretzky, N. B. Litherland, J. P. Underwood, and J. J. Loor. 2005. Physiological and pathological adaptations in dairy cows that may increase susceptibility to periparturient diseases and disorders. Italian Journal of Animal Science 4(4):323-344.

Drewe, J., C. Beglinger, and G. Fricker. 2001. Effect of ischemia on intestinal permeability of lipopolysaccharides. European Journal of Clinical Investigation 31(2):138-144.
Duffield, T. 2000. Subclinical Ketosis in Lactating Dairy Cattle. Veterinary Clinics of North America: Food Animal Practice 16(2):231-253.

Duran, M. J., J. Kannampuzha-Francis, D. Nydam, and E. Behling-Kelly. 2021. Characterization of Particle Size Distribution of Plasma Lipoproteins in Dairy Cattle Using High-Resolution Polyacrylamide Electrophoresis. Frontiers in Animal Science 2.

Eckel, E. F. and B. N. Ametaj. 2016. Invited review: Role of bacterial endotoxins in the etiopathogenesis of periparturient diseases of transition dairy cows. Journal of Dairy Science 99(8):5967-5990.

Eckel, E. F. and B. N. Ametaj. 2020. Bacterial Endotoxins and Their Role in Periparturient Diseases of Dairy Cows: Mucosal Vaccine Perspectives. Dairy 1(1):61-90.

Egan, J. J., A. S. Greenberg, M. K. Chang, S. A. Wek, M. C. Moos, Jr., and C. Londos. 1992. Mechanism of hormone-stimulated lipolysis in adipocytes: translocation of hormone-sensitive lipase to the lipid storage droplet. Proceedings of the National Academy of Sciences of the United States of America 89(18):8537-8541.

Elis, S., S. Coyral-Castel, S. Freret, J. Cognié, A. Desmarchais, A. Fatet, C. Rame, E. Briant, V. Maillard, and J. Dupont. 2013. Expression of adipokine and lipid metabolism genes in adipose tissue of dairy cows differing in a female fertility quantitative trait locus. Journal of Dairy Science 96(12):7591-7602.

Evaul, K. and S. R. Hammes. 2008. Cross-talk between G protein-coupled and epidermal growth factor receptors regulates gonadotropin-mediated steroidogenesis in Leydig cells. The Journal of biological chemistry 283(41):27525-27533.

Faylon, M. P., L. H. Baumgard, R. P. Rhoads, and D. M. Spurlock. 2015. Effects of acute heat stress on lipid metabolism of bovine primary adipocytes. Journal of Dairy Science 98(12):8732-8740.

Feingold, K. R., I. Staprans, R. A. Memon, A. H. Moser, J. K. Shigenaga, W. Doerrler, C. A. Dinarello, and C. Grunfeld. 1992. Endotoxin rapidly induces changes in lipid metabolism that produce hypertriglyceridemia: low doses stimulate hepatic triglyceride production while high doses inhibit clearance. Journal of lipid research 33(12):1765-1776.

Ferrante Jr, A. W. 2013. The immune cells in adipose tissue. Diabetes, Obesity and Metabolism 15(s3):34-38.

Foley, K. P., Y. Chen, N. G. Barra, M. Heal, K. Kwok, A. K. Tamrakar, W. Chi, B. M. Duggan, B. D. Henriksbo, Y. Liu, and J. D. Schertzer. 2021. Inflammation promotes adipocyte lipolysis via IRE1 kinase. The Journal of biological chemistry 296:100440.

Foreign Agriculture Service, U. d. 2011. Dairy: World Markets and Trade http://www.fas.usda.gov/psdonline/circulars/dairy.pdf2011 [cited 2017 10/12/2017]. Available from:http://www.fas.usda.gov/psdonline/circulars/dairy.pdf.

Förstermann, U., E. I. Closs, J. S. Pollock, M. Nakane, P. Schwarz, I. Gath, and H. Kleinert. 1994. Nitric oxide synthase isozymes. Characterization, purification, molecular cloning, and functions. Hypertension 23(6 Pt 2):1121-1131.

Fricke, K., A. Heitland, and E. Maronde. 2004. Cooperative activation of lipolysis by protein kinase A and protein kinase C pathways in 3T3-L1 adipocytes. Endocrinology 145(11):4940-4947.

Fujisaka, S. 2021. The role of adipose tissue M1/M2 macrophages in type 2 diabetes mellitus. Diabetol Int 12(1):74-79.

Fujisaka, S., I. Usui, A. Bukhari, M. Ikutani, T. Oya, Y. Kanatani, K. Tsuneyama, Y. Nagai, K. Takatsu, M. Urakaze, M. Kobayashi, and K. Tobe. 2009. Regulatory mechanisms for adipose tissue M1 and M2 macrophages in diet-induced obese mice. Diabetes 58(11):2574-2582.

Gartung, A., J. Zhao, S. Chen, E. Mottillo, G. C. VanHecke, Y. H. Ahn, K. R. Maddipati, A. Sorokin, J. Granneman, and M. J. Lee. 2016. Characterization of Eicosanoids Produced by Adipocyte Lipolysis: IMPLICATION OF CYCLOOXYGENASE-2 IN ADIPOSE INFLAMMATION. The Journal of biological chemistry 291(31):16001-16010.

Gasic, S., B. Tian, and A. Green. 1999. Tumor necrosis factor alpha stimulates lipolysis in adipocytes by decreasing Gi protein concentrations. The Journal of biological chemistry 274(10):6770-6775.

Ghoshal, S., J. Witta, J. Zhong, W. de Villiers, and E. Eckhardt. 2009. Chylomicrons promote intestinal absorption of lipopolysaccharides. J Lipid Res 50(1):90-97.

González, F. D., R. Muiño, V. Pereira, R. Campos, and J. L. Benedito. 2011. Relationship among blood indicators of lipomobilization and hepatic function during early lactation in high-yielding dairy cows. J Vet Sci 12(3):251-255.

Gordon, J. L., S. J. Leblanc, and T. F. Duffield. 2013. Ketosis treatment in lactating dairy cattle. Vet Clin North Am Food Anim Pract 29(2):433-445.

Gordon, J. L., S. J. LeBlanc, D. F. Kelton, T. H. Herdt, L. Neuder, and T. F. Duffield. 2017. Randomized clinical field trial on the effects of butaphosphan-cyanocobalamin and propylene glycol on ketosis resolution and milk production. J Dairy Sci 100(5):3912-3921.

Gozho, G. N., D. O. Krause, and J. C. Plaizier. 2007. Ruminal Lipopolysaccharide Concentration and Inflammatory Response During Grain-Induced Subacute Ruminal Acidosis in Dairy Cows. Journal of Dairy Science 90(2):856-866.

Graber, C. D., R. B. Reinhold, J. G. Breman, R. A. Harley, and G. R. Hennigar. 1971. Fatal Heat Stroke: Circulating Endotoxin and Gram-Negative Sepsis as Complications. JAMA 216(7):1195-1196.

Grabner, G. F., H. Xie, M. Schweiger, and R. Zechner. 2021. Lipolysis: cellular mechanisms for lipid mobilization from fat stores. Nature Metabolism 3(11):1445-1465.

Granneman, J. G., H.-P. H. Moore, R. Krishnamoorthy, and M. Rathod. 2009. Perilipin Controls Lipolysis by Regulating the Interactions of AB-hydrolase Containing 5 (Abhd5) and Adipose Triglyceride Lipase (Atgl). Journal of Biological Chemistry 284(50):34538-34544.

Green, A., S. B. Dobias, D. J. Walters, and A. R. Brasier. 1994. Tumor necrosis factor increases the rate of lipolysis in primary cultures of adipocytes without altering levels of hormone-sensitive lipase. Endocrinology 134(6):2581-2588.

Greenberg, A. S., W. J. Shen, K. Muliro, S. Patel, S. C. Souza, R. A. Roth, and F. B. Kraemer. 2001. Stimulation of lipolysis and hormone-sensitive lipase via the extracellular signal-regulated kinase pathway. The Journal of biological chemistry 276(48):45456-45461.

Griffin, C., L. Eter, N. Lanzetta, S. Abrishami, M. Varghese, K. McKernan, L. Muir, J. Lane, C. N. Lumeng, and K. Singer. 2018. TLR4, TRIF, and MyD88 are essential for myelopoiesis and CD11c+ adipose tissue macrophage production in obese mice. Journal of Biological Chemistry 293(23):8775-8786.

Grisouard, J., E. Bouillet, K. Timper, T. Radimerski, K. Dembinski, D. M. Frey, R. Peterli, H. Zulewski, U. Keller, B. Muller, and M. Christ-Crain. 2012. Both inflammatory and classical lipolytic pathways are involved in lipopolysaccharide-induced lipolysis in human adipocytes. Innate Immun 18(1):25-34.

Grisouard, J., E. Bouillet, K. Timper, T. Radimerski, K. Dembinski, D. M. Frey, R. Peterli, H. Zulewski, U. Keller, B. Müller, and M. Christ-Crain. 2010. Both inflammatory and classical lipolytic pathways are involved in lipopolysaccharide-induced lipolysis in human adipocytes. Innate Immunity 18(1):25-34.

Gu, F., S. Zhu, Y. Tang, X. Liu, M. Jia, N. Malmuthuge, T. G. Valencak, J. W. McFadden, J.-X. Liu, and H.-Z. Sun. 2023. Gut microbiome is linked to functions of peripheral immune cells in transition cows during excessive lipolysis. Microbiome 11(1):40.

Guo, W., W. Li, Y. Su, S. Liu, X. Kan, X. Ran, Y. Cao, S. Fu, and J. Liu. 2021. GPR109A alleviate mastitis and enhances the blood milk barrier by activating AMPK/Nrf2 and autophagy. Int J Biol Sci 17(15):4271-4284.

Ha, S., S. Kang, M. Han, J. Lee, H. Chung, S.-I. Oh, S. Kim, and J. Park. 2022. Predicting ketosis during the transition period in Holstein Friesian cows using hematological and serum biochemical parameters on the calving date. Scientific Reports 12(1):853.

Hakogi, E., H. Tamura, S. Tanaka, A. Kohata, Y. Shimada, and K. Tabuchi. 1989. Endotoxin levels in milk and plasma of mastitis-affected cows measured with a chromogenic limulus test. Vet Microbiol 20(3):267-274.

Hall, D. M., K. R. Baumgardner, T. D. Oberley, and C. V. Gisolfi. 1999. Splanchnic tissues undergo hypoxic stress during whole body hyperthermia. The American journal of physiology 276 5:G1195-1203.

Hellemans, J., G. Mortier, A. De Paepe, F. Speleman, and J. Vandesompele. 2007. qBase relative quantification framework and software for management and automated analysis of real-time quantitative PCR data. Genome Biology 8(2):R19-R19.

Herdt, T. H. and R. S. Emery. 1992. Therapy of diseases of ruminant intermediary metabolism. Vet Clin North Am Food Anim Pract 8(1):91-106.

Hikawyj-Yevich, I. and J. A. Spitzer. 1977. Endotoxin influence on lipolysis in isolated human and primate adipocytes. Journal of Surgical Research 23(2):106-113.

Hirosumi, J., G. Tuncman, L. Chang, C. Z. Görgün, K. T. Uysal, K. Maeda, M. Karin, and G. S. Hotamisligil. 2002. A central role for JNK in obesity and insulin resistance. Nature 420(6913):333-336.

Hoareau, L., K. Bencharif, P. Rondeau, R. Murumalla, P. Ravanan, F. Tallet, P. Delarue, M. Cesari, R. Roche, and F. Festy. 2010. Signaling pathways involved in LPS induced TNFalpha production in human adipocytes. Journal of inflammation (London, England) 7:1-1.

Holm, C. 2003. Molecular mechanisms regulating hormone-sensitive lipase and lipolysis. Biochem Soc Trans 31(Pt 6):1120-1124.

Hong, S., W. Song, P. H. Zushin, B. Liu, M. P. Jedrychowski, A. I. Mina, Z. Deng, D. Cabarkapa, J. A. Hall, C. J. Palmer, H. Aliakbarian, J. Szpyt, S. P. Gygi, A. Tavakkoli, L. Lynch, N. Perrimon, and A. S. Banks. 2018. Phosphorylation of Beta-3 adrenergic receptor at serine 247 by ERK MAP kinase drives lipolysis in obese adipocytes. Molecular metabolism 12:25-38.

Hoque, M. N., A. Istiaq, M. S. Rahman, M. R. Islam, A. Anwar, A. M. A. M. Z. Siddiki, M. Sultana, K. A. Crandall, and M. A. Hossain. 2020. Microbiome dynamics and genomic determinants of bovine mastitis. Genomics 112(6):5188-5203.

Horowitz, A., S. D. Chanez-Paredes, X. Haest, and J. R. Turner. 2023. Paracellular permeability and tight junction regulation in gut health and disease. Nature Reviews Gastroenterology & Hepatology.

Horst, E. A., S. K. Kvidera, M. J. Dickson, C. S. McCarthy, E. J. Mayorga, M. Al-Qaisi, H. A. Ramirez, A. F. Keating, and L. H. Baumgard. 2019a. Effects of continuous and increasing lipopolysaccharide infusion on basal and stimulated metabolism in lactating Holstein cows. J Dairy Sci 102(4):3584-3597.

Horst, E. A., S. K. Kvidera, M. J. Dickson, C. S. McCarthy, E. J. Mayorga, M. Al-Qaisi, H. A. Ramirez, A. F. Keating, and L. H. Baumgard. 2019b. Effects of continuous and increasing lipopolysaccharide infusion on basal and stimulated metabolism in lactating Holstein cows. Journal of Dairy Science.

Hotamisligil, G. S., P. Peraldi, A. Budavari, R. Ellis, M. F. White, and B. M. Spiegelman. 1996. IRS-1-mediated inhibition of insulin receptor tyrosine kinase activity in TNF-alpha- and obesity-induced insulin resistance. Science (New York, N.Y.) 271(5249):665-668.

Hristovska, T., M. R. Cincović, B. Belić, D. Stojanović, M. Jezdimirović, R. Đoković, and B. Toholj. 2017. Effects of niacin supplementation on the insulin resistance in Holstein cows during early lactation. Acta Veterinaria Brno 86(3):231-238.

Hruby, A. and F. B. Hu. 2015. The Epidemiology of Obesity: A Big Picture. Pharmacoeconomics 33(7):673-689.

Hsieh, P.-S., J.-S. Jin, C.-F. Chiang, P.-C. Chan, C.-H. Chen, and K.-C. Shih. 2009. COX-2-mediated Inflammation in Fat Is Crucial for Obe

Huang, C., J. Wang, H. Liu, R. Huang, X. Yan, M. Song, G. Tan, and F. Zhi. 2022. Ketone body β-hydroxybutyrate ameliorates colitis by promoting M2 macrophage polarization through the STAT6-dependent signaling pathway. BMC Medicine 20(1):148.

Hurley, J. C. 1995. Endotoxemia: methods of detection and clinical correlates. Clin Microbiol Rev 8(2):268-292.

Inazumi, T., K. Yamada, N. Shirata, H. Sato, Y. Taketomi, K. Morita, H. Hohjoh, S. Tsuchiya, K. Oniki, T. Watanabe, Y. Sasaki, Y. Oike, Y. Ogata, J. Saruwatari, M. Murakami, and Y. Sugimoto. 2020. Prostaglandin E(2)-EP4 Axis Promotes Lipolysis and Fibrosis in Adipose Tissue Leading to Ectopic Fat Deposition and Insulin Resistance. Cell Rep 33(2):108265.

Iwersen, M., U. Falkenberg, R. Voigtsberger, D. Forderung, and W. Heuwieser. 2009. Evaluation of an electronic cowside test to detect subclinical ketosis in dairy cows. J Dairy Sci 92(6):2618-2624.

Jaakson, H., P. Karis, K. Ling, A. Ilves-Luht, J. Samarütel, M. Henno, I. Jõudu, A. Waldmann, E. Reimann, P. Pärn, R. M. Bruckmaier, J. J. Gross, T. Kaart, M. Kass, and M. Ots. 2018. Adipose tissue insulin receptor and glucose transporter 4 expression, and blood glucose and insulin responses during glucose tolerance tests in transition Holstein cows with different body condition. Journal of Dairy Science 101(1):752-766.

Jackson, E., R. Shoemaker, N. Larian, and L. Cassis. 2017. Adipose Tissue as a Site of Toxin Accumulation. Comprehensive Physiology 7(4):1085-1135.

Ji, D., J.-y. Yin, D.-f. Li, C.-t. Zhu, J.-p. Ye, and Y.-q. Pan. 2020. Effects of inflammatory and anti-inflammatory environments on the macrophage mitochondrial function. Scientific Reports 10(1):20324.

Jo, J., J. Guo, T. Liu, S. Mullen, K. D. Hall, S. W. Cushman, and V. Periwal. 2010. Hypertrophy-driven adipocyte death overwhelms recruitment under prolonged weight gain. Biophysical journal 99(11):3535-3544.

Johnson, P. J., C. E. Wiedmeyer, N. T. Messer, and V. K. Ganjam. 2009. Medical implications of obesity in horses--lessons for human obesity. J Diabetes Sci Technol 3(1):163-174.

Jurga, L., v. H. Vanessa, A. N. Elisabet, D. Andrea, B. Lennart, N. Erik, L. Dominique, A. Peter, and R. Mikael. 2007. NF-κB is important for TNF-α-induced lipolysis in human adipocytes. Journal of lipid research 48(5):1069-1077.

Kahn, C. R. 1978. Insulin resistance, insulin insensitivity, and insulin unresponsiveness: a necessary distinction. Metabolism: clinical and experimental 27(12 Suppl 2):1893-1902.

Kawai, T., M. V. Autieri, and R. Scalia. 2021. Adipose tissue inflammation and metabolic dysfunction in obesity. Am J Physiol Cell Physiol 320(3):C375-c391.

Kenéz, A., L. Locher, J. Rehage, S. Dänicke, and K. Huber. 2014. Agonists of the G protein-coupled receptor 109A-mediated pathway promote antilipolysis by reducing serine residue 563 phosphorylation of hormone-sensitive lipase in bovine adipose tissue explants. J Dairy Sci 97(6):3626-3634.

Kessler, E. C., J. J. Gross, R. M. Bruckmaier, and C. Albrecht. 2014. Cholesterol metabolism, transport, and hepatic regulation in dairy cows during transition and early lactation. Journal of Dairy Science 97(9):5481-5490.

Khafipour, E., D. O. Krause, and J. C. Plaizier. 2009. A grain-based subacute ruminal acidosis challenge causes translocation of lipopolysaccharide and triggers inflammation. Journal of Dairy Science 92(3):1060-1070.

Khan, S. and C. H. Wang. 2014. ER stress in adipocytes and insulin resistance: mechanisms and significance (Review). Molecular medicine reports 10(5):2234-2240.

Kim, J. Y., E. van de Wall, M. Laplante, A. Azzara, M. E. Trujillo, S. M. Hofmann, T. Schraw, J. L. Durand, H. Li, G. Li, L. A. Jelicks, M. F. Mehler, D. Y. Hui, Y. Deshaies, G. I. Shulman, G. J. Schwartz, and P. E. Scherer. 2007. Obesity-associated improvements in metabolic profile through expansion of adipose tissue. The Journal of clinical investigation 117(9):2621-2637.

Kim, S. J., T. Tang, M. Abbott, J. A. Viscarra, Y. Wang, and H. S. Sul. 2016. AMPK Phosphorylates Desnutrin/ATGL and Hormone-Sensitive Lipase To Regulate Lipolysis and Fatty Acid Oxidation within Adipose Tissue. Molecular and cellular biology 36(14):1961-1976.

Kim, S. M., M. Lun, M. Wang, S. E. Senyo, C. Guillermier, P. Patwari, and M. L. Steinhauser. 2014. Loss of white adipose hyperplastic potential is associated with enhanced susceptibility to insulin resistance. Cell metabolism 20(6):1049-1058.

Kinoshita, A., Á. Kenéz, L. Locher, U. Meyer, S. Dänicke, J. Rehage, and K. Huber. 2016. Insulin Signaling in Liver and Adipose Tissues in Periparturient Dairy Cows Supplemented with Dietary Nicotinic Acid. PloS one 11(1):e0147028.

Kitchens, R. L., P. A. Thompson, R. S. Munford, and G. E. O'Keefe. 2003. Acute inflammation and infection maintain circulating phospholipid levels and enhance lipopolysaccharide binding to plasma lipoproteins. Journal of lipid research 44(12):2339-2348.

Koltes, D. A. and D. M. Spurlock. 2011. Coordination of lipid droplet-associated proteins during the transition period of Holstein dairy cows. Journal of Dairy Science 94(4):1839-1848.

Kosteli, A., E. Sugaru, G. Haemmerle, J. F. Martin, J. Lei, R. Zechner, and A. W. Ferrante, Jr. 2010. Weight loss and lipolysis promote a dynamic immune response in murine adipose tissue. The Journal of clinical investigation 120(10):3466-3479.

Kovacevic, Z., D. Stojanovic, M. Cincovic, B. Belic, I. Davidov, N. Stojanac, and A. Galfi. 2019. Effect of postpartum administration of ketoprofen on proinflammatory cytokine concentration and their correlation with lipogenesis and ketogenesis in Holstein dairy cows. Pol J Vet Sci 22(3):609-615.

Kramski, M., A. J. Gaeguta, G. F. Lichtfuss, R. Rajasuriar, S. M. Crowe, M. A. French, S. R. Lewin, R. J. Center, and D. F. Purcell. 2011. Novel sensitive real-time PCR for quantification of bacterial 16S rRNA genes in plasma of HIV-infected patients as a marker for microbial translocation. J Clin Microbiol 49(10):3691-3693.

Kremer, W. D. J., E. N. Noordhuizen-Stassen, F. J. Grommers, Y. H. Schukken, R. Heeringa, A. Brand, and C. Burvenich. 1993. Severity of Experimental Escherichia coli Mastitis in Ketonemic and Nonketonemic Dairy Cows. Journal of Dairy Science 76(11):3428-3436.

Krumm, C. S., S. L. Giesy, C. L. Orndorff, and Y. R. Boisclair. 2018. Variation in x-box binding protein 1 (XBP1) expression and its dependent endoplasmic reticulum chaperones does not regulate adiponectin secretion in dairy cows. J Dairy Sci 101(6):5559-5570.

Kunz, H. E., C. R. Hart, K. J. Gries, M. Parvizi, M. C. Laurenti, C. Dalla Man, N. J. Moore, X. Zhang, Z. C. Ryan, E. C. Polley, M. D. Jensen, A. Vella, and I. R. Lanza. 2021. Adipose tissue macrophage populations and inflammation are associated with systemic inflammation and insulin resistance in obesity. American journal of physiology. Endocrinology and metabolism.

Kusminski, C. M. and P. E. Scherer. 2012. Mitochondrial dysfunction in white adipose tissue. Trends in endocrinology and metabolism: TEM 23(9):435-443.

Kvidera, S. K., M. J. Dickson, M. Abuajamieh, D. B. Snider, M. V. S. Fernandez, J. S. Johnson, A. F. Keating, P. J. Gorden, H. B. Green, K. M. Schoenberg, and L. H. Baumgard. 2017. Intentionally induced intestinal barrier dysfunction causes inflammation, affects metabolism, and reduces productivity in lactating Holstein cows. Journal of Dairy Science 100(5):4113-4127.

Lange, K. H., B. Larsson, A. Flyvbjerg, R. Dall, M. Bennekou, M. H. Rasmussen, H. Ørskov, and M. Kjaer. 2002. Acute growth hormone administration causes exaggerated increases in plasma

lactate and glycerol during moderate to high intensity bicycling in trained young men. J Clin Endocrinol Metab 87(11):4966-4975.

Lanza-Jacoby, S., G. L. Rose, E. F. Rosato, N. Sedkova, and R. V. Considine. 1995. In vitro effect of endotoxin on lipolysis and lipoprotein lipase activity in adipocytes from lean, obese and obese diabetic Zucker rats. Journal of Endotoxin Research 2(6):449-454.

Lass, A., R. Zimmermann, G. Haemmerle, M. Riederer, G. Schoiswohl, M. Schweiger, P. Kienesberger, J. G. Strauss, G. Gorkiewicz, and R. Zechner. 2006. Adipose triglyceride lipase-mediated lipolysis of cellular fat stores is activated by CGI-58 and defective in Chanarin-Dorfman Syndrome. Cell metabolism 3(5):309-319.

Laubenthal, L., L. Ruda, N. Sultana, J. Winkler, J. Rehage, U. Meyer, S. Dänicke, H. Sauerwein, and S. Häussler. 2017. Effect of increasing body condition on oxidative stress and mitochondrial biogenesis in subcutaneous adipose tissue depot of nonlactating dairy cows. J Dairy Sci 100(6):4976-4986.

Laugerette, F., J.-P. Furet, C. Debard, P. Daira, E. Loizon, A. Géloën, C. O. Soulage, C. Simonet, J. Lefils-Lacourtablaise, N. Bernoud-Hubac, J. Bodennec, N. Peretti, H. Vidal, and M.-C. Michalski. 2012. Oil composition of high-fat diet affects metabolic inflammation differently in connection with endotoxin receptors in mice. American Journal of Physiology-Endocrinology and Metabolism 302(3):E374-E386.

Laviola, L., S. Perrini, A. Cignarelli, A. Natalicchio, A. Leonardini, F. De Stefano, M. Cuscito, M. De Fazio, V. Memeo, V. Neri, M. Cignarelli, R. Giorgino, and F. Giorgino. 2006. Insulin signaling in human visceral and subcutaneous adipose tissue in vivo. Diabetes 55(4):952-961.

LeBlanc, S. 2010. Monitoring metabolic health of dairy cattle in the transition period. J Reprod Dev 56 Suppl:S29-35.

Lemor, A., A. Hosseini, H. Sauerwein, and M. Mielenz. 2009. Transition period-related changes in the abundance of the mRNAs of adiponectin and its receptors, of visfatin, and of fatty acid binding receptors in adipose tissue of high-yielding dairy cows. Domest Anim Endocrinol 37(1):37-44.

Levels, J. H., P. R. Abraham, A. van den Ende, and S. J. van Deventer. 2001. Distribution and kinetics of lipoprotein-bound endotoxin. Infection and immunity 69(5):2821-2828.

Li, J., N. Zhang, B. Ye, W. Ju, B. Orser, J. E. Fox, M. B. Wheeler, Q. Wang, and W. Y. Lu. 2007. Non-steroidal anti-inflammatory drugs increase insulin release from beta cells by inhibiting ATP-sensitive potassium channels. Br J Pharmacol 151(4):483-493.

Li, M., X. Chi, Y. Wang, S. Setrerrahmane, W. Xie, and H. Xu. 2022. Trends in insulin resistance: insights into mechanisms and therapeutic strategy. Signal Transduction and Targeted Therapy 7(1):216.

Li, P., M. Lu, M. T. A. Nguyen, E. J. Bae, J. Chapman, D. Feng, M. Hawkins, J. E. Pessin, D. D. Sears, A. K. Nguyen, A. Amidi, S. M. Watkins, U. Nguyen, and J. M. Olefsky. 2010. Functional heterogeneity of CD11c-positive adipose tissue macrophages in diet-induced obese mice. Journal of Biological Chemistry 285(20):15333-15345.

Li, X. 2018. Endoplasmic reticulum stress regulates inflammation in adipocyte of obese rats via toll-like receptors 4 signaling. Iranian journal of basic medical sciences 21(5):502-507.

Liebold, I., S. Meyer, M. Heine, A. Kuhl, J. Witt, L. Eissing, A. W. Fischer, A. C. Koop, J. Kluwe, J. S. Z. Wiesch, M. Wehmeyer, U. Knippschild, L. Scheja, J. Heeren, L. Bosurgi, and A. Worthmann. 2023. TREM2 Regulates the Removal of Apoptotic Cells and Inflammatory Processes during the Progression of NAFLD. Cells 12(3).

Lim, C. L., G. Wilson, L. Brown, J. S. Coombes, and L. T. Mackinnon. 2007. Pre-existing inflammatory state compromises heat tolerance in rats exposed to heat stress. American Journal of Physiology-Regulatory, Integrative and Comparative Physiology 292(1):R186-R194.

Loegering, D. J. and M. R. Lennartz. 2011. Protein kinase C and toll-like receptor signaling. Enzyme Res 2011:537821-537821.

Loh, K., H. Deng, A. Fukushima, X. Cai, B. Boivin, S. Galic, C. Bruce, B. J. Shields, B. Skiba, L. M. Ooms, N. Stepto, B. Wu, C. A. Mitchell, N. K. Tonks, M. J. Watt, M. A. Febbraio, P. J. Crack, S. Andrikopoulos, and T. Tiganis. 2009. Reactive oxygen species enhance insulin sensitivity. Cell metabolism 10(4):260-272.

Londos, C., D. L. Brasaemle, C. J. Schultz, D. C. Adler-Wailes, D. M. Levin, A. R. Kimmel, and C. M. Rondinone. 1999. On the control of lipolysis in adipocytes. Ann N Y Acad Sci 892:155-168.

Lopes, R. L., T. J. Borges, R. F. Zanin, and C. Bonorino. 2016. IL-10 is required for polarization of macrophages to M2-like phenotype by mycobacterial DnaK (heat shock protein 70). Cytokine 85:123-129.

Lord, C. C., J. L. Betters, P. T. Ivanova, S. B. Milne, D. S. Myers, J. Madenspacher, G. Thomas, S. Chung, M. Liu, M. A. Davis, R. G. Lee, R. M. Crooke, M. J. Graham, J. S. Parks, D. L. Brasaemle, M. B. Fessler, H. A. Brown, and J. M. Brown. 2012. CGI-58/ABHD5-derived signaling lipids regulate systemic inflammation and insulin action. Diabetes 61(2):355-363.

Lu, M., A. W. Varley, S. Ohta, J. Hardwick, and R. S. Munford. 2008. Host inactivation of bacterial lipopolysaccharide prevents prolonged tolerance following gram-negative bacterial infection. Cell host & microbe 4(3):293-302.

Luche, E., B. Cousin, L. Garidou, M. Serino, A. Waget, C. Barreau, M. André, P. Valet, M. Courtney, L. Casteilla, and R. Burcelin. 2013. Metabolic endotoxemia directly increases the proliferation of adipocyte precursors at the onset of metabolic diseases through a CD14-dependent mechanism. Molecular metabolism 2(3):281-291.

Lumeng, C. N., J. L. Bodzin, and A. R. Saltiel. 2007. Obesity induces a phenotypic switch in adipose tissue macrophage polarization. The Journal of clinical investigation 117(1):175-184.

Ma, X., E. Hayes, H. Prizant, R. K. Srivastava, S. R. Hammes, and A. Sen. 2016. Leptin-Induced CART (Cocaine- and Amphetamine-Regulated Transcript) Is a Novel Intraovarian Mediator of Obesity-Related Infertility in Females. Endocrinology 157(3):1248-1257.

Magkos, F., G. Fraterrigo, J. Yoshino, C. Luecking, K. Kirbach, S. C. Kelly, L. de Las Fuentes, S. He, A. L. Okunade, B. W. Patterson, and S. Klein. 2016. Effects of Moderate and Subsequent Progressive Weight Loss on Metabolic Function and Adipose Tissue Biology in Humans with Obesity. Cell metabolism 23(4):591-601.

Mancuso, P. 2016. The role of adipokines in chronic inflammation. Immunotargets Ther 5:47-56.

Mani, V., T. E. Weber, and N. K. Gabler. 2017. Endotoxin, inflammation, and intestinal function in livestock.

Manimaran, A., A. Kumaresan, S. Jeyakumar, T. K. Mohanty, V. Sejian, N. Kumar, L. Sreela, M. A. Prakash, P. Mooventhan, A. Anantharaj, and D. N. Das. 2016. Potential of acute phase proteins as predictor of postpartum uterine infections during transition period and its regulatory mechanism in dairy cattle. Veterinary world 9(1):91-100.

Mann, S., F. A. L. Yepes, M. Duplessis, J. J. Wakshlag, T. R. Overton, B. P. Cummings, and D. V. Nydam. 2016. Dry period plane of energy: Effects on glucose tolerance in transition dairy cows. Journal of Dairy Science 99(1):701-717.

Mateus, L., L. Lopes da Costa, P. Diniz, and A. J. Ziecik. 2003. Relationship between endotoxin and prostaglandin (PGE2 and PGFM) concentrations and ovarian function in dairy cows with puerperal endometritis. Animal Reproduction Science 76(3):143-154.

Mathur, N., A. S. Andreasen, M. Pedersen, K. Møller, R. Berg, B. K. Pedersen, and M. J. Laye. 2012. Altered Subcutaneous Adipose Tissue Response to Systemic LPS Administration in Patients with Type 2 Diabetes. Journal of Diabetes & Metabolism 3(8).

McArt, J. A. A., D. V. Nydam, and G. R. Oetzel. 2012. Epidemiology of subclinical ketosis in early lactation dairy cattle. J Dairy Sci 95(9):5056-5066.

McArt, J. A. A., D. V. Nydam, and M. W. Overton. 2015. Hyperketonemia in early lactation dairy cattle: A deterministic estimate of component and total cost per case. Journal of Dairy Science 98(3):2043-2054.

McCann, J. C., S. Luan, F. C. Cardoso, H. Derakhshani, E. Khafipour, and J. J. Loor. 2016. Induction of Subacute Ruminal Acidosis Affects the Ruminal Microbiome and Epithelium. Front Microbiol 7:701.

McKernan, K., M. Varghese, R. Patel, and K. Singer. 2020. Role of TLR4 in the induction of inflammatory changes in adipocytes and macrophages. Adipocyte 9(1):212-222.

McNamara, J. P. 1991. Regulation of adipose tissue metabolism in support of lactation. J Dairy Sci 74(2):706-719.

McNamara, J. P. and J. K. Hillers. 1986. Adaptations in lipid metabolism of bovine adipose tissue in lactogenesis and lactation. Journal of lipid research 27(2):150-157.

Mehta, N. N., F. C. McGillicuddy, P. D. Anderson, C. C. Hinkle, R. Shah, L. Pruscino, J. Tabita-Martinez, K. F. Sellers, M. R. Rickels, and M. P. Reilly. 2010. Experimental endotoxemia induces adipose inflammation and insulin resistance in humans. Diabetes 59(1):172-181.

Mielenz, M. 2016. Invited review: nutrient-sensing receptors for free fatty acids and hydroxycarboxylic acids in farm animals. animal 11(6):1008-1016.

Miranda, M., X. Escoté, M. J. Alcaide, E. Solano, V. Ceperuelo-Mallafré, P. Hernández, M. Wabitsch, and J. Vendrell. 2010. Lpin1 in human visceral and subcutaneous adipose tissue: similar levels but different associations with lipogenic and lipolytic genes. American Journal of Physiology-Endocrinology and Metabolism 299(2):E308-E317.

Montgomery, S. R., L. K. Mamedova, M. Zachut, G. Kra, S. Häussler, M. Vaughn, J. Gonzalez, and B. J. Bradford. 2019. Effects of sodium salicylate on glucose kinetics and insulin signaling in postpartum dairy cows. Journal of Dairy Science 102(2):1617-1629.

Moon, E. Y., Y. S. Lee, W. S. Choi, and M. H. Lee. 2011. Toll-like receptor 4-mediated cAMP production up-regulates B-cell activating factor expression in Raw264.7 macrophages. Exp Cell Res 317(17):2447-2455.

Moreira, A. P. B., T. F. S. Texeira, A. B. Ferreira, M. do Carmo Gouveia Peluzio, and R. de Cássia Gonçalves Alfenas. 2012. Influence of a high-fat diet on gut microbiota, intestinal permeability and metabolic endotoxaemia. British Journal of Nutrition 108(5):801-809.

Morrow, D. A. 1976. Fat cow syndrome. J Dairy Sci 59(9):1625-1629.

Moshage, H. J., J. A. Janssen, J. H. Franssen, J. C. Hafkenscheid, and S. H. Yap. 1987. Study of the molecular mechanism of decreased liver synthesis of albumin in inflammation. The Journal of clinical investigation 79(6):1635-1641.

Mottillo, E. P., A. E. Bloch, T. Leff, and J. G. Granneman. 2012. Lipolytic Products Activate Peroxisome Proliferator-activated Receptor (PPAR) α and δ in Brown Adipocytes to Match Fatty Acid Oxidation with Supply. Journal of Biological Chemistry 287(30):25038-25048.

Mukesh, M., M. Bionaz, D. E. Graugnard, J. K. Drackley, and J. J. Loor. 2010. Adipose tissue depots of Holstein cows are immune responsive: Inflammatory gene expression in vitro. Domestic Animal Endocrinology 38(3):168-178.

Munford, R. S. 2016. Endotoxemia-menace, marker, or mistake? J Leukoc Biol 100(4):687-698.

Murano, I., G. Barbatelli, V. Parisani, C. Latini, G. Muzzonigro, M. Castellucci, and S. Cinti. 2008. Dead adipocytes, detected as crown-like structures, are prevalent in visceral fat depots of genetically obese mice. Journal of lipid research 49(7):1562-1568.

Neal, M. D., C. Leaphart, R. Levy, J. Prince, T. R. Billiar, S. Watkins, J. Li, S. Cetin, H. Ford, A. Schreiber, and D. J. Hackam. 2006. Enterocyte TLR4 mediates phagocytosis and translocation of bacteria across the intestinal barrier. Journal of immunology (Baltimore, Md. : 1950) 176(5):3070-3079.

Nelson, G. M., J. M. Guynn, and B. N. Chorley. 2017. Procedure and Key Optimization Strategies for an Automated Capillary Electrophoretic-based Immunoassay Method. Journal of visualized experiments : JoVE (127).

Ning, M., Y. Zhao, Z. Li, and J. Cao. 2022. Ketosis Alters Transcriptional Adaptations of Subcutaneous White Adipose Tissue in Holstein Cows during the Transition Period. Animals (Basel) 12(17).

Nishi, Y., K. Tsukano, M. Otsuka, M. Tsuchiya, and K. Suzuki. 2019. Relationship between bronchoalveolar lavage fluid and plasma endotoxin activity in calves with bronchopneumonia. The Journal of veterinary medical science 81(7):1043-1046.

Nolan, J. P., D. K. Hare, J. J. McDevitt, and M. V. Ali. 1977. In vitro studies of intestinal endotoxin absorption. I. Kinetics of absorption in the isolated everted gut sac. Gastroenterology 72(3):434-439.

Nordestgaard, B. G., E. Hjelms, S. Stender, and K. Kjeldsen. 1990. Different efflux pathways for high and low density lipoproteins from porcine aortic intima. Arteriosclerosis: An Official Journal of the American Heart Association, Inc. 10(3):477-485.

Oliveira, B. M., A. Pinto, A. Correia, P. G. Ferreira, M. Vilanova, and L. Teixeira. 2020. Characterization of Myeloid Cellular Populations in Mesenteric and Subcutaneous Adipose Tissue of Holstein-Friesian Cows. Scientific Reports 10(1):1771.

Ordovas, J. M. and D. Corella. 2008. Metabolic syndrome pathophysiology: the role of adipose tissue. Kidney Int Suppl (111):S10-S14.

Ospina, P. A., J. A. McArt, T. R. Overton, T. Stokol, and D. V. Nydam. 2013. Using Nonesterified Fatty Acids and β-Hydroxybutyrate Concentrations During the Transition Period for Herd-Level Monitoring of Increased Risk of Disease and Decreased Reproductive and Milking Performance. Veterinary Clinics: Food Animal Practice 29(2):387-412.

Ospina, P. A., D. V. Nydam, T. Stokol, and T. R. Overton. 2010a. Association between the proportion of sampled transition cows with increased nonesterified fatty acids and beta-hydroxybutyrate and disease incidence, pregnancy rate, and milk production at the herd level. J Dairy Sci 93(8):3595-3601.

Ospina, P. A., D. V. Nydam, T. Stokol, and T. R. Overton. 2010b. Associations of elevated nonesterified fatty acids and β-hydroxybutyrate concentrations with early lactation reproductive performance and milk production in transition dairy cattle in the northeastern United States. Journal of Dairy Science 93(4):1596-1603.

Ospina, P. A., D. V. Nydam, T. Stokol, and T. R. Overton. 2010c. Evaluation of nonesterified fatty acids and β-hydroxybutyrate in transition dairy cattle in the northeastern United States: Critical thresholds for prediction of clinical diseases. Journal of Dairy Science 93(2):546-554.

Ozcan, U., Q. Cao, E. Yilmaz, A.-H. Lee, N. N. Iwakoshi, E. Ozdelen, G. Tuncman, C. Gorgun, L. H. Glimcher, and G. S. Hotamisligil. 2004. Endoplasmic reticulum stress links obesity, insulin action, and type 2 diabetes. Science (New York, N.Y.) 306:457+.

Pagnon, J., M. Matzaris, R. Stark, R. C. Meex, S. L. Macaulay, W. Brown, P. E. O'Brien, T. Tiganis, and M. J. Watt. 2012. Identification and functional characterization of protein kinase A phosphorylation sites in the major lipolytic protein, adipose triglyceride lipase. Endocrinology 153(9):4278-4289.

Parton, R. G. and M. A. del Pozo. 2013. Caveolae as plasma membrane sensors, protectors and organizers. Nature Reviews Molecular Cell Biology 14(2):98-112.

Penfornis, P. and A. Marette. 2005. Inducible nitric oxide synthase modulates lipolysis in adipocytes. Journal of lipid research 46(1):135-142.

Perreault, M. and A. Marette. 2001. Targeted disruption of inducible nitric oxide synthase protects against obesity-linked insulin resistance in muscle. Nature medicine 7(10):1138-1143.

Pescara, J. B., J. A. A. Pires, and R. R. Grummer. 2010. Antilipolytic and lipolytic effects of administering free or ruminally protected nicotinic acid to feed-restricted Holstein cows. Journal of Dairy Science 93(11):5385-5396.

Peter, A. T., W. T. K. Bosu, and R. O. Gilbert. 1990. Absorption of Escherichiacoli endotoxin (lipopolysaccharide) from the uteri of postpartum dairy cows. Theriogenology 33(5):1011-1014.

Petersen, M. C. and G. I. Shulman. 2018. Mechanisms of Insulin Action and Insulin Resistance. Physiological reviews 98(4):2133-2223.

Pinto, A., A. Bonucci, E. Maggi, M. Corsi, and R. Businaro. 2018. Anti-Oxidant and Anti-Inflammatory Activity of Ketogenic Diet: New Perspectives for Neuroprotection in Alzheimer's Disease. Antioxidants (Basel) 7(5).

Pires, J. A., J. B. Pescara, and R. R. Grummer. 2007. Reduction of plasma NEFA concentration by nicotinic acid enhances the response to insulin in feed-restricted Holstein cows. J Dairy Sci 90(10):4635-4642.

Piya, M. K., P. G. McTernan, and S. Kumar. 2013. Adipokine inflammation and insulin resistance: the role of glucose, lipids and endotoxin. Journal of Endocrinology 216(1):T1-T15.

Plaizier, J. C., P. Azevedo, B. L. Schurmann, P. Górka, G. B. Penner, and E. Khafipour. 2020. The Duration of Increased Grain Feeding Affects the Microbiota throughout the Digestive Tract of Yearling Holstein Steers. Microorganisms 8(12).

Pond, C. M. and C. A. Mattacks. 1995. Interactions between adipose tissue around lymph nodes and lymphoid cells in vitro. Journal of lipid research 36(10):2219-2231.

Pond, C. M. and C. A. Mattacks. 1998. In vivo evidence for the involvement of the adipose tissue surrounding lymph nodes in immune responses. Immunology Letters 63(3):159-167.

Porter, P., D. E. Noakes, and W. D. Allen. 1972. Intestinal secretion of immunoglobulins in the preruminant calf. Immunology 23(3):299-312.

Pravettoni, D., K. Doll, M. Hummel, E. Cavallone, M. Re, and A. G. Belloli. 2004. Insulin resistance and abomasal motility disorders in cows detected by use of abomasoduodenal electromyography after surgical correction of left displaced abomasum. Am J Vet Res 65(10):1319-1324.

Probo, M., O. B. Pascottini, S. LeBlanc, G. Opsomer, and M. Hostens. 2018. Association between metabolic diseases and the culling risk of high-yielding dairy cows in a transition management facility using survival and decision tree analysis. J Dairy Sci 101(10):9419-9429.

Prodanović, R., D. Kirovski, I. Vujanac, A. Djordjevic, S. Romić, M. Pantelić, and G. Korićanac. 2022. Obesity-related prepartal insulin resistance in dairy cows is associated with increased lipin 1 and decreased FATP 1 expression in skeletal muscle. Research in veterinary science 150:189-194.

Queen, D., C. Ediriweera, and L. Liu. 2019. Function and Regulation of IL-36 Signaling in Inflammatory Diseases and Cancer Development. Front Cell Dev Biol 7:317.

Rahn Landström, T., J. Mei, M. Karlsson, V. Manganiello, and E. Degerman. 2000. Down-regulation of cyclic-nucleotide phosphodiesterase 3B in 3T3-L1 adipocytes induced by tumour necrosis factor alpha and cAMP. Biochem J 346 Pt 2(Pt 2):337-343.

Ramírez, M. a. J., Á. Ibáñez, M. Navasa, E. Casals, M. Morales-Ruiz, W. Jiménez, V. Arroyo, and J. Rodés. 2004. High-density lipoproteins reduce the effect of endotoxin on cytokine production and systemic hemodynamics in cirrhotic rats with ascites. Journal of Hepatology 40(3):424-430.

Rendon, C. J., E. Flood, J. M. Thompson, M. Chirivi, S. W. Watts, and G. A. Contreras. 2022. PIEZO1 mechanoreceptor activation reduces adipogenesis in perivascular adipose tissue preadipocytes. Frontiers in Endocrinology 13.

Ribiere, C., A. M. Jaubert, N. Gaudiot, D. Sabourault, M. L. Marcus, J. L. Boucher, D. Denis-Henriot, and Y. Giudicelli. 1996. White adipose tissue nitric oxide synthase: A potential source for NO production. Biochemical and Biophysical Research Communications 222(3):706-712.

Richter, C., J. W. Park, and B. N. Ames. 1988. Normal oxidative damage to mitochondrial and nuclear DNA is extensive. Proc Natl Acad Sci U S A 85(17):6465-6467.

Roche, J. R., N. C. Friggens, J. K. Kay, M. W. Fisher, K. J. Stafford, and D. P. Berry. 2009. Invited review: Body condition score and its association with dairy cow productivity, health, and welfare. Journal of Dairy Science 92(12):5769-5801.

Rodriguez, A. R., D. E. Herzberg, M. P. Werner, H. Y. Müller, and H. A. Bustamante. 2018. Plasma Concentration of Norepinephrine, β-endorphin, and Substance P in Lame Dairy Cows. J Vet Res 62(2):193-197.

Rogero, M. M. and P. C. Calder. 2018. Obesity, Inflammation, Toll-Like Receptor 4 and Fatty Acids. Nutrients 10(4):432.

Rohrer, L., P. M. Ohnsorg, M. Lehner, F. Landolt, F. Rinninger, and A. von Eckardstein. 2009. High-density lipoprotein transport through aortic endothelial cells involves scavenger receptor BI and ATP-binding cassette transporter G1. Circulation research 104(10):1142-1150.

Ronald Kahn, C. 1978. Insulin resistance, insulin insensitivity, and insulin unresponsiveness: A necessary distinction. Metabolism 27(12, Supplement 2):1893-1902.

Roy, S., D. Gandra, C. Seger, A. Biswas, V. A. Kushnir, N. Gleicher, T. R. Kumar, and A. Sen. 2018. Oocyte-Derived Factors (GDF9 and BMP15) and FSH Regulate AMH Expression Via Modulation of H3K27AC in Granulosa Cells. Endocrinology 159(9):3433-3445.

Ruegsegger, G. J. and L. H. Schultz. 1986. Use of a combination of propylene glycol and niacin for subclinical ketosis. J Dairy Sci 69(5):1411-1415.

Rui, L., M. Yuan, D. Frantz, S. Shoelson, and M. F. White. 2002. SOCS-1 and SOCS-3 block insulin signaling by ubiquitin-mediated degradation of IRS1 and IRS2. The Journal of biological chemistry 277(44):42394-42398.

Ryan, K. A., M. F. Smith, Jr., M. K. Sanders, and P. B. Ernst. 2004. Reactive oxygen and nitrogen species differentially regulate Toll-like receptor 4-mediated activation of NF-kappa B and interleukin-8 expression. Infection and immunity 72(4):2123-2130.

Rydén, M., E. Arvidsson, L. Blomqvist, L. Perbeck, A. Dicker, and P. Arner. 2004. Targets for TNF-alpha-induced lipolysis in human adipocytes. Biochem Biophys Res Commun 318(1):168-175.

Ryden, M., A. Dicker, V. van Harmelen, H. Hauner, M. Brunnberg, L. Perbeck, F. Lonnqvist, and P. Arner. 2002. Mapping of early signaling events in tumor necrosis factor-alpha -mediated lipolysis in human fat cells. The Journal of biological chemistry 277(2):1085-1091.

Saponaro, C., M. Gaggini, F. Carli, and A. Gastaldelli. 2015. The Subtle Balance between Lipolysis and Lipogenesis: A Critical Point in Metabolic Homeostasis. Nutrients 7(11):9453-9474.

Sargeant, J. M., A. M. O'Connor, I. A. Gardner, J. S. Dickson, M. E. Torrence, I. R. Dohoo, S. L. Lefebvre, P. S. Morley, A. Ramirez, and K. Snedeker. 2010. The REFLECT statement: reporting guidelines for randomized controlled trials in livestock and food safety: explanation and elaboration. J Food Prot 73(3):579-603.

Schmitt, R., L. Pieper, S. Borchardt, J. M. Swinkels, C. C. Gelfert, and R. Staufenbiel. 2022. Effects of a single transdermal administration of flunixin meglumine in early postpartum Holstein Friesian dairy cows: Part 1. Inflammatory and metabolic markers, uterine health, and indicators of pain. Journal of Dairy Science.

Schweiger, M., T. O. Eichmann, U. Taschler, R. Zimmermann, R. Zechner, and A. Lass. 2014. Measurement of lipolysis. Methods Enzymol 538:171-193.

Sharma, A., C. K. Maurya, D. Arha, A. K. Rai, S. Singh, S. Varshney, J. D. Schertzer, and A. K. Tamrakar. 2019. Nod1-mediated lipolysis promotes diacylglycerol accumulation and successive inflammation via PKCδ-IRAK axis in adipocytes. Biochimica et Biophysica Acta (BBA) - Molecular Basis of Disease 1865(1):136-146.

Shi, H., M. V. Kokoeva, K. Inouye, I. Tzameli, H. Yin, and J. S. Flier. 2006. TLR4 links innate immunity and fatty acid-induced insulin resistance. Journal of Clinical Investigation 116(11):3015-3025.

Shi, L., R. Kishore, M. R. McMullen, and L. E. Nagy. 2002. Lipopolysaccharide stimulation of ERK1/2 increases TNF-alpha production via Egr-1. American journal of physiology. Cell physiology 282(6):C1205-1211.

Shi, Z., Y. Song, X. Gao, J. J. Loor, A. Aboragah, H. Yu, Z. Fang, Y. Zhu, X. Du, X. Li, W. Gao, and G. Liu. 2021. Disruption of endoplasmic reticulum homeostasis exacerbates liver injury in clinically ketotic cows. Journal of Dairy Science.

Shwartz, G., K. L. Hill, M. J. VanBaale, and L. H. Baumgard. 2009. Effects of flunixin meglumine on pyrexia and bioenergetic variables in postparturient dairy cows. J Dairy Sci 92(5):1963-1970.

Siddiqui, R. A. and J. F. Williams. 1989. The regulation of fatty acid and branched-chain amino acid oxidation in cancer cachectic rats: a proposed role for a cytokine, eicosanoid, and hormone trilogy. Biochem Med Metab Biol 42(1):71-86.

Song, J., M. J. Duncan, G. Li, C. Chan, R. Grady, A. Stapleton, and S. N. Abraham. 2007. A novel TLR4-mediated signaling pathway leading to IL-6 responses in human bladder epithelial cells. PLoS Pathog 3(4):e60.

Song, L., D. S. Kim, W. Gou, J. Wang, P. Wang, Z. Wei, B. Liu, Z. Li, K. Gou, and H. Wang. 2020. GRP94 regulates M1 macrophage polarization and insulin resistance. American journal of physiology. Endocrinology and metabolism 318(6):E1004-e1013.

Stevens, I., N. Ogura, M. Kelley, R. L. D'Ordine, H. Mizumura, T. Oda, J. Akiyoshi, and E. G. Jahngen. 2022. Advanced Recombinant Cascade Reagent PyroSmart NextGen® for Bacterial Endotoxins Test as Described in the Pharmacopeias. BPB Reports 5(5):105-114.

Strieder-Barboza, C., E. Thompson, K. Thelen, and G. A. Contreras. 2019. Technical note: Bovine adipocyte and preadipocyte co-culture as an efficient adipogenic model. Journal of Dairy Science 102(4):3622-3629.

Strieder-Barboza, C., A. Zondlak, J. Kayitsinga, A. F. A. Pires, and G. A. Contreras. 2015. Lipid mobilization assessment in transition dairy cattle using ultrasound image biomarkers. Livestock Science 177:159-164.

Sumner, J. M. and J. P. McNamara. 2007. Expression of lipolytic genes in the adipose tissue of pregnant and lactating Holstein dairy cattle. J Dairy Sci 90(11):5237-5246.

Szewczenko-Pawlikowski, M. and W. Kozak. 2000. Accumulation of unsaturated lipids in monocytes during early phase pyrogen tolerance. Biochimica et Biophysica Acta (BBA) - Molecular and Cell Biology of Lipids 1484(2):183-194.

Taggart, A. K., J. Kero, X. Gan, T. Q. Cai, K. Cheng, M. Ippolito, N. Ren, R. Kaplan, K. Wu, T. J. Wu, L. Jin, C. Liaw, R. Chen, J. Richman, D. Connolly, S. Offermanns, S. D. Wright, and M. G. Waters. 2005. (D)-beta-Hydroxybutyrate inhibits adipocyte lipolysis via the nicotinic acid receptor PUMA-G. The Journal of biological chemistry 280(29):26649-26652.

Tang, D., R. Kang, C. B. Coyne, H. J. Zeh, and M. T. Lotze. 2012. PAMPs and DAMPs: signal 0s that spur autophagy and immunity. Immunological reviews 249(1):158-175.

Taniguchi, C. M., B. Emanuelli, and C. R. Kahn. 2006. Critical nodes in signalling pathways: insights into insulin action. Nature reviews. Molecular cell biology 7(2):85-96.

Taschler, U., F. P. W. Radner, C. Heier, R. Schreiber, M. Schweiger, G. Schoiswohl, K. Preiss-Landl, D. Jaeger, B. Reiter, H. C. Koefeler, J. Wojciechowski, C. Theussl, J. M. Penninger, A. Lass, G. Haemmerle, R. Zechner, and R. Zimmermann. 2011. Monoglyceride Lipase Deficiency

in Mice Impairs Lipolysis and Attenuates Diet-induced Insulin Resistance. Journal of Biological Chemistry 286(20):17467-17477.

Tatone, E. H., T. F. Duffield, M. B. Capel, T. J. DeVries, S. J. LeBlanc, and J. L. Gordon. 2016. A randomized controlled trial of dexamethasone as an adjunctive therapy to propylene glycol for treatment of hyperketonemia in postpartum dairy cattle. J Dairy Sci 99(11):8991-9000.

Thelen, K., S. W. Watts, and G. A. Contreras. 2018. Adipogenic potential of perivascular adipose tissue preadipocytes is improved by coculture with primary adipocytes. Cytotechnology 70(5):1435-1445.

Torre-Villalvazo, I., A. E. Bunt, G. Alemán, C. C. Marquez-Mota, A. Diaz-Villaseñor, L. G. Noriega, I. Estrada, E. Figueroa-Juárez, C. Tovar-Palacio, L. A. Rodriguez-López, P. López-Romero, N. Torres, and A. R. Tovar. 2018. Adiponectin synthesis and secretion by subcutaneous adipose tissue is impaired during obesity by endoplasmic reticulum stress. Journal of Cellular Biochemistry 119(7):5970-5984.

Toshchakov, V., B. W. Jones, P. Y. Perera, K. Thomas, M. J. Cody, S. Zhang, B. R. Williams, J. Major, T. A. Hamilton, M. J. Fenton, and S. N. Vogel. 2002. TLR4, but not TLR2, mediates IFN-beta-induced STAT1alpha/beta-dependent gene expression in macrophages. Nat Immunol 3(4):392-398.

Trojnar, M., J. Patro-Małysza, Ż. Kimber-Trojnar, B. Leszczyńska-Gorzelak, and J. Mosiewicz. 2019. Associations between Fatty Acid-Binding Protein 4–A Proinflammatory Adipokine and Insulin Resistance, Gestational and Type 2 Diabetes Mellitus. Cells 8(3).

Tschoner, T. and M. Feist. 2022. Substance P concentrations in the blood plasma and serum of adult cattle and calves during different painful procedures and conditions - a systematic review. BMC Vet Res 18(1):232.

Tuma, P. L. and A. L. Hubbard. 2003. Transcytosis: Crossing Cellular Barriers. Physiological reviews 83(3):871-932.

Tunaru, S., J. Kero, A. Schaub, C. Wufka, A. Blaukat, K. Pfeffer, and S. Offermanns. 2003. PUMA-G and HM74 are receptors for nicotinic acid and mediate its anti-lipolytic effect. Nature medicine 9(3):352-355.

Tvarijonaviciute, A., J. J. Ceron, S. L. Holden, D. J. Cuthbertson, V. Biourge, P. J. Morris, and A. J. German. 2012. Obesity-related metabolic dysfunction in dogs: a comparison with human metabolic syndrome. BMC Vet Res 8:147-147.

Ueda, Y., S. Hirai, S. Osada, A. Suzuki, K. Mizuno, and S. Ohno. 1996. Protein kinase C activates the MEK-ERK pathway in a manner independent of Ras and dependent on Raf. The Journal of biological chemistry 271(38):23512-23519.

Ueki, K., T. Kondo, and C. R. Kahn. 2004. Suppressor of cytokine signaling 1 (SOCS-1) and SOCS-3 cause insulin resistance through inhibition of tyrosine phosphorylation of insulin receptor substrate proteins by discrete mechanisms. Molecular and cellular biology 24(12):5434-5446.

Uhlar, C. M. and A. S. Whitehead. 1999. Serum amyloid A, the major vertebrate acute-phase reactant. Eur J Biochem 265(2):501-523.

Umpierrez, G. and A. X. Freire. 2002. Abdominal pain in patients with hyperglycemic crises. J Crit Care 17(1):63-67.

Vailati Riboni, M., S. Meier, N. V. Priest, C. R. Burke, J. K. Kay, S. McDougall, M. D. Mitchell, C. G. Walker, M. Crookenden, A. Heiser, J. R. Roche, and J. J. Loor. 2015. Adipose and liver gene expression profiles in response to treatment with a nonsteroidal antiinflammatory drug after calving in grazing dairy cows. Journal of Dairy Science 98(5):3079-3085.

Vanholder, T., J. Papen, R. Bemers, G. Vertenten, and A. C. B. Berge. 2015. Risk factors for subclinical and clinical ketosis and association with production parameters in dairy cows in the Netherlands. Journal of Dairy Science 98(2):880-888.

Vatier, C., S. Kadiri, A. Muscat, C. Chapron, J. Capeau, and B. Antoine. 2012. Visceral and subcutaneous adipose tissue from lean women respond differently to lipopolysaccharide-induced alteration of inflammation and glyceroneogenesis. Nutrition & diabetes 2(12):e51.

Vaughan, M., J. E. Berger, and D. Steinberg. 1964. HORMONE-SENSITIVE LIPASE AND MONOGLYCERIDE LIPASE ACTIVITIES IN ADIPOSE TISSUE. The Journal of biological chemistry 239:401-409.

Vishnyakova, T. G., A. V. Bocharov, I. N. Baranova, Z. Chen, A. T. Remaley, G. Csako, T. L. Eggerman, and A. P. Patterson. 2003. Binding and internalization of lipopolysaccharide by Cla-1, a human orthologue of rodent scavenger receptor B1. The Journal of biological chemistry 278(25):22771-22780.

Vrakas, S., K. C. Mountzouris, G. Michalopoulos, G. Karamanolis, G. Papatheodoridis, C. Tzathas, and M. Gazouli. 2017. Intestinal Bacteria Composition and Translocation of Bacteria in Inflammatory Bowel Disease. PloS one 12(1):e0170034.

Wahrenberg, H., F. Lönnqvist, and P. Arner. 1989. Mechanisms underlying regional differences in lipolysis in human adipose tissue. The Journal of clinical investigation 84(2):458-467.

Waldron, M. R., T. Nishida, B. J. Nonnecke, and T. R. Overton. 2003. Effect of lipopolysaccharide on indices of peripheral and hepatic metabolism in lactating cows. J Dairy Sci 86(11):3447-3459.

Wang, C., X. Zhang, L. Luo, Y. Luo, D. Wu, D. Spilca, Q. Le, X. Yang, K. Alvarez, W. C. Hines, X. O. Yang, and M. Liu. 2022. COX-2 Deficiency Promotes White Adipogenesis via PGE2-Mediated Paracrine Mechanism and Exacerbates Diet-Induced Obesity. Cells 11(11):1819.

Wang, J., X. Gu, J. Yang, Y. Wei, and Y. Zhao. 2019. Gut Microbiota Dysbiosis and Increased Plasma LPS and TMAO Levels in Patients With Preeclampsia. Frontiers in cellular and infection microbiology 9:409.

Wang, L., L. Li, X. Ran, M. Long, M. Zhang, Y. Tao, X. Luo, Y. Wang, Y. Jiao, X. Mao, and J. Ren. 2013. Lipopolysaccharides Reduce Adipogenesis in 3T3-L1 Adipocytes Through Activation of NF-κB Pathway and Downregulation of AMPK Expression. Cardiovascular Toxicology 13(4):338-346.

Wang, X.-J., B.-Y. Chen, B.-W. Yang, T.-L. Yue, and C.-F. Guo. 2021. Short communication: Chemical structure, concentration, and pH are key factors influencing antimicrobial activity of conjugated bile acids against lactobacilli. Journal of Dairy Science 104(2):1524-1530.

Weisberg, S. P., D. McCann, M. Desai, M. Rosenbaum, R. L. Leibel, and A. W. Ferrante, Jr. 2003. Obesity is associated with macrophage accumulation in adipose tissue. The Journal of clinical investigation 112(12):1796-1808.

Wenz, J. R., G. M. Barrington, F. B. Garry, K. D. McSweeney, R. P. Dinsmore, G. Goodell, and R. J. Callan. 2001. Bacteremia associated with naturally occuring acute coliform mastitis in dairy cows. Journal of the American Veterinary Medical Association 219(7):976-981.

Whitfield-Cargile, C. M., M. C. Coleman, N. D. Cohen, A. M. Chamoun-Emanuelli, C. N. DeSolis, T. Tetrault, R. Sowinski, A. Bradbery, and M. Much. 2021. Effects of phenylbutazone alone or in combination with a nutritional therapeutic on gastric ulcers, intestinal permeability, and fecal microbiota in horses. J Vet Intern Med 35(2):1121-1130.

Wisse, B. E. 2004. The inflammatory syndrome: the role of adipose tissue cytokines in metabolic disorders linked to obesity. Journal of the American Society of Nephrology : JASN 15 11:2792-2800.

Wittek, T., M. Fürll, and P. D. Constable. 2004. Prevalence of endotoxemia in healthy postparturient dairy cows and cows with abomasal volvulus or left displaced abomasum. J Vet Intern Med 18(4):574-580.

Wu, Z. L., S. Y. Chen, S. Hu, X. Jia, J. Wang, and S. J. Lai. 2020. Metabolomic and Proteomic Profiles Associated With Ketosis in Dairy Cows. Front Genet 11:551587.

Yamamoto, M., S. Sato, H. Hemmi, K. Hoshino, T. Kaisho, H. Sanjo, O. Takeuchi, M. Sugiyama, M. Okabe, K. Takeda, and S. Akira. 2003. Role of Adaptor TRIF in the MyD88-Independent Toll-Like Receptor Signaling Pathway. Science (New York, N.Y.) 301(5633):640.

Yao, Z., J. M. Mates, A. M. Cheplowitz, L. P. Hammer, A. Maiseyeu, G. S. Phillips, M. D. Wewers, M. V. Rajaram, J. M. Robinson, C. L. Anderson, and L. P. Ganesan. 2016. Blood-Borne Lipopolysaccharide Is Rapidly Eliminated by Liver Sinusoidal Endothelial Cells via High-Density Lipoprotein. Journal of immunology (Baltimore, Md. : 1950) 197(6):2390-2399.

Yasukawa, T., E. Tokunaga, H. Ota, H. Sugita, J. A. Martyn, and M. Kaneki. 2005. S-nitrosylation-dependent inactivation of Akt/protein kinase B in insulin resistance. The Journal of biological chemistry 280(9):7511-7518.

Yin, C., W. H. Liu, Y. Liu, L. Wang, and Y. Xiao. 2019. PID1 alters the antilipolytic action of insulin and increases lipolysis via inhibition of AKT/PKA pathway activation. PloS one 14(4):e0214606-e0214606.

Zachut, M. 2015. Defining the Adipose Tissue Proteome of Dairy Cows to Reveal Biomarkers Related to Peripartum Insulin Resistance and Metabolic Status. Journal of Proteome Research 14(7):2863-2871.

Zachut, M. and G. A. Contreras. 2022. Symposium review: Mechanistic insights into adipose tissue inflammation and oxidative stress in periparturient dairy cows. J Dairy Sci 105(4):3670-3686.

Zarrin, M., L. De Matteis, M. C. M. B. Vernay, O. Wellnitz, H. A. van Dorland, and R. M. Bruckmaier. 2013. Long-term elevation of β-hydroxybutyrate in dairy cows through infusion: Effects on feed intake, milk production, and metabolism. Journal of Dairy Science 96(5):2960-2972.

Zhang, F., D. Li, Q. Wu, J. Sun, W. Guan, Y. Hou, Y. Zhu, and J. Wang. 2019. Prepartum body conditions affect insulin signaling pathways in postpartum adipose tissues in transition dairy cows. Journal of Animal Science and Biotechnology 10(1):38.

Zhang, G. and B. N. Ametaj. 2020. Ketosis an Old Story Under a New Approach. Dairy 1(1):42-60.

Zhang, G., D. Hailemariam, E. Dervishi, S. A. Goldansaz, Q. Deng, S. M. Dunn, and B. N. Ametaj. 2016. Dairy cows affected by ketosis show alterations in innate immunity and lipid and carbohydrate metabolism during the dry off period and postpartum. Research in veterinary science 107:246-256.

Zhang, H., L. Wu, C. Xu, C. Xia, L. Sun, and S. Shu. 2013. Plasma metabolomic profiling of dairy cows affected with ketosis using gas chromatography/mass spectrometry. BMC Vet Res 9:186.

Zhang, J. M. and J. An. 2007. Cytokines, inflammation, and pain. Int Anesthesiol Clin 45(2):27-37.

Zhang, L., J. Shi, D. Du, N. Niu, S. Liu, X. Yang, P. Lu, X. Shen, N. Shi, L. Yao, R. Zhang, G. Hu, G. Lu, Q. Zhu, T. Zeng, T. Liu, Q. Xia, W. Huang, and J. Xue. 2022. Ketogenesis acts as an endogenous protective programme to restrain inflammatory macrophage activation during acute pancreatitis. eBioMedicine 78.

Zhao, L., P. Hu, Y. Zhou, J. Purohit, and D. Hwang. 2011. NOD1 activation induces proinflammatory gene expression and insulin resistance in 3T3-L1 adipocytes. American journal of physiology. Endocrinology and metabolism 301(4):E587-598.

Zhao, M. and X. Chen. 2015. Effect of lipopolysaccharides on adipogenic potential and premature senescence of adipocyte progenitors. American journal of physiology. Endocrinology and metabolism 309(4):E334-344.

Zhong, B. 2009. How to calculate sample size in randomized controlled trial? Journal of thoracic disease 1(1):51-54.

Zhu, J., H. Yamane, and W. E. Paul. 2010. Differentiation of effector CD4 T cell populations (*). Annu Rev Immunol 28:445-489.

Zhu, Y., Y. Guan, J. J. Loor, X. Sha, D. N. Coleman, C. Zhang, X. Du, Z. Shi, X. Li, Z. Wang, G. Liu, and X. Li. 2019. Fatty acid-induced endoplasmic reticulum stress promoted lipid accumulation in calf hepatocytes, and endoplasmic reticulum stress existed in the liver of severe fatty liver cows. Journal of Dairy Science 102(8):7359-7370.

Zimmermann, R., J. G. Strauss, G. Haemmerle, G. Schoiswohl, R. Birner-Gruenberger, M. Riederer, A. Lass, G. Neuberger, F. Eisenhaber, A. Hermetter, and R. Zechner. 2004a. Fat mobilization in adipose tissue is promoted by adipose triglyceride lipase. Science (New York, N.Y.) 306(5700):1383-1386.

Zimmermann, R., J. G. Strauss, G. Haemmerle, G. Schoiswohl, R. Birner-Gruenberger, M. Riederer, A. Lass, G. Neuberger, F. Eisenhaber, A. Hermetter, and R. Zechner. 2004b. Fat Mobilization in Adipose Tissue Is Promoted by Adipose Triglyceride Lipase. Science (New York, N.Y.) 306(5700):1383-1386.

Zinicola, M., F. Lima, S. Lima, V. Machado, M. Gomez, D. Döpfer, C. Guard, and R. Bicalho. 2015. Altered Microbiomes in Bovine Digital Dermatitis Lesions, and the Gut as a Pathogen Reservoir. PLOS ONE 10(3):e0120504.

Zu, L., J. He, H. Jiang, C. Xu, S. Pu, and G. Xu. 2009a. Bacterial endotoxin stimulates adipose lipolysis via toll-like receptor 4 and extracellular signal-regulated kinase pathway. J Biol Chem 284(9):5915-5926.

Zu, L., J. He, H. Jiang, C. Xu, S. Pu, and G. Xu. 2009b. Bacterial Endotoxin Stimulates Adipose Lipolysis via Toll-Like Receptor 4 and Extracellular Signal-regulated Kinase Pathway*. Journal of Biological Chemistry 284(9):5915-5926.

APPENDIX

Table 11. Blood metabolites were positively influenced by PGNIAFM in dairy cows with ketosis.

Metabolite	Treatment Group[1]	Mean			SEM	*P*[2]		
		d3	d7	d14		Treatment	Day	Treatment × Day
Albumin g/dL	PG	4.06	4.14	4.15	0.14	<0.0001	0.09	0.10
	PGNIA	4.22	4.02	4.02	0.14			
	PGNIAFM	3.96	3.95	3.85	0.14			
	HC	4.23	4.47	4.57	0.13			
BHB mmol/L	PG	1.39^{a}	1.29^{a}	1.26^{a}	0.16	<0.0001	<0.0001	<0.0001
	PGNIA	1.29^{a}	1.25^{a}	1.12^{ab}	0.16			
	PGNIAFM	0.92^{b}	0.94^{b}	0.94^{b}	0.16			
	HC	0.63^{b}	0.62^{b}	0.61^{b}	0.15			
BUN mg/dL	PG	9.33	9.30	9.88	0.74	0.43	0.02	0.67
	PGNIA	9.22	10.42	10.42	0.74			
	PGNIAFM	8.94	9.04	9.22	0.74			
	HC	9.89	10.16	11.52	0.69			
Calcium mg/dL	PG	9.04	9.11	9.02	0.28	0.52	0.92	0.72
	PGNIA	9.02	9.26	9.26	0.28			
	PGNIAFM	9.23	8.90	9.22	0.28			
	HC	8.98	9.21	9.19	0.27			
Cholesterol mg/dL	PG	70.083^{h}	79.20^{efg}	98.70^{bcd}	5.43	<0.001	<0.0001	<0.01
	PGNIA	73.83^{fgh}	88.62^{cde}	104.38^{b}	5.43			
	PGNIAFM	60.29^{h}	69.00^{gh}	86.29^{edf}	5.43			
	HC	85.79^{edf}	103.09^{bc}	129.39^{a}	5.12			
Glucose mg/dL	PG	60.95^{b}	60.37^{b}	61.04^{b}	2.32	<0.0001	0.002	<0.05
	PGNIA	59.87^{b}	60.37^{b}	60.37^{b}	2.32			
	PGNIAFM	71.20^{a}	64.04^{ab}	62.95^{b}	2.3			
	HC	71.318^{a}	72.53^{a}	70.11^{a}	2.19			
Magnesium mg/dL	PG	3.02	3.06	3.11	0.11	0.2459	<0.0001	0.534
	PGNIA	2.89	2.97	2.97	0.11			
	PGNIAFM	2.75	2.94	2.97	0.11			
	HC	2.78	2.78	2.75	0.10			
NEFA mmol/L	PG	0.53^{ab}	0.51^{bc}	0.54^{ab}	0.04	0.05	<.0001	0.06
	PGNIA	0.53^{ab}	0.59^{a}	0.59^{a}	0.04			
	PGNIAFM	0.51^{bc}	0.51^{bc}	0.46^{c}	0.04			
	HC	0.37^{c}	0.38^{c}	0.38^{c}	0.03			

Table 11 (cont'd)

Total Protein g/dL	PG	6.49	6.75	7.01	0.17	0.002	<0.0001	0.45
	PGNIA	6.84	7.01	7.01	0.17			
	PGNIAFM	6.79	7.09	7.27	0.17			
	HC	7.47	7.80	8.00	0.16			
Triglycerides mg/dL	PG	8.00	8.87	9.75	1.04	0.82	0.001	0.85
	PGNIA	9.12	9.79	9.79	1.04			
	PGNIAFM	8.79	6.45	8.41	1.04			
	HC	8.00	8.37	9.53	0.98			

[1]Treatments for clinical ketosis (CK) cows with BHB>1.2 mmol/L at d0: PG = Propylene Glycol, PGNIA = PG + Niacin, PGNIAFM = PGNIA + flunixin meglumine, and HC = Healthy cows, with no sign of disease and BHB<1.2 at d0 no treatment

[2]*P* values are from to $\log_{10}$ transformed data analysis in albumin, BHB, NEFA, and total protein.

[a-h]Probability of the interaction treatment × Day: Mean values in the same row with different superscripts differ ($P<0.05$) adjusted by Tukey. CK n=24, HC = 27

Table 12. Primer sequences for gene expression analysis.

Gene	Sequence number	Primer Sequences (5'-3')
ABHD5	NM_001076063.2	F: CTGCAGATGATGTGGGAAAGC
		R: GACTGCCTGGTTCTCGTGTCA
CCL2	NM_174006.2	F: TCAACAGTAAGAAGATCTCCATGCA
		R: CAGGACGGTCTTGAAAATCACA
CPT1A	NM_001304989	F: TCCTGGTGGGCTACCAATTA
		R: TGCGTCTGTAAAGCAGGATG
FABP4	NM_174314.2	F: ACAAGTACAAAACTGGGATGGAA
		R: TGACACCATTCATGACACATTC
GLUT4	NM_174604.1	F: CAGGACGGTCTTGAAAATCACA
		R: CCT GTG TGG ACC CTC AGT CA
IL10	NM_174088.1	F: AGCCTTGTCGGAAATGATCCAGTTTTA
		R: TCTCCACCGCCTTGCTCTTGT
IL6	NM_173923.2	F: CCAGAGAAAACCGAAGCTCTCAT
		R: CCTTGCTGCTTTCACACTCATC
IL8	NM_173925.2	F: CTGCCTAAACCCCAAGGAA
		R: AACCCTACACCAGACCCACA
IRS1	XM_003585773.5	F: TGTTGACTGAACTGCACGTTCT
		R: CATGTGGCCAGCTAAGTCCTT
LIPE	NM_001080220.1	F: GAGTTTGAGCGGATCATTCA
		R: TGAGGCCATGTTTGCTAGAG
LIPIN1	NM_001206156.2	F: TCGTGGTGAAGATCGGAAAT
		R: GTTTCTGGAAGGCCTGCAT
LOCS527744	XM_015475510.1	F: ACATCACCCTCAGCTTCACC
		R: GCGGTTGTTATCCGACTCAT
LPL	NM_001075120.1	F: GACAGGATGTGGCCAAGTTT
		R: TTGCCCAGGGGATAGTTAAA
PPARA	NM_001034036.1	F: AATAACGCGATTCGTTTTGG
		R: TCCATGTCGTGGATGAGAAA
PPARG	NM_181024.2	F: GCGACTTAGCAATATTTATAGCTGTC
		R: AGGCTTGCAGCAGATTGTCT
SIRPA	NM_175788.1	F: TGGACCAGCATCTTCATCGT
		R: TCTGTCTGATTCGGAGGAGGT
SPP1	NM_174187.2	F: TCTGGATGGCATTTGGGTTCA
		R: AAGAACAGGCGAGGAACTGA
TLR4	NM_174198.6	F: GCCATGTACCAAGCATTGTG
		R: TCACAGAGGCCCAGTCTCTT
TNF	NM_173966.3	F: CTTCTGCCTGCTGCACTTCG
		R: GAGTTGATGTCGGCTACAACG
EIF3K	NM_001034489.2	F: CTTCTGGCAAGCCCTGGATG
		R: TAGCTGGCTGTCTGTCAGATCCC
RPLP0	NM_001012682.1	F: AATCGCCAATGCCAACTC
		R: CCCTTTCGCTTACCTATACC
RPS9	NM_001101152.2	F: GGAGACCCTTCGAGAAGTCC
		R: GGGCATTACCTTCGAACAGA

Table 13. Antibody information for flow cytometry in adipose tissue.

Antibody	Catalog #	Conjugation Kit	Final Antibody Dilution
CD11b	Clone MM12A, Washington State University	Mix-n-Stain FITC antibody labeling Kit (Biotium Cat 92295)	1:100
CD14	Clone CAM36A, Washington State University	Lightning-Link PE-Cy7® tandem conjugation kit (Novus Cat 762-0010)	1:50
CD45	Clone CACTB51A, Washington State University	Dylight® 405 conjugation kit (fast) – lightning link (Abcam Cat ab201798)	1:100
CD172a	clone DH59B, Washington State University	Mix-n-stain PerCP antibody labeling kit (Biotium Cat 92308)	1:100
MHCII	Clone CAT82A, Washington State University	Mix-n-stain APC antibody labeling kit (Biotium Cat 92307)	1:100
TREM	R&D systems FAB17291U	AlexaFluor 350 R&D systems FAB17291U	1:50

Table 14. Genes used for qPCR in adipose tissue from dairy cows.

GENE	RefSeq
ABHD5	NM_001076063.2
ADIPOQ	NM_174742.2
ADRB1	NM_194266.1
ADRB2	NM_174231.1
AGPAT1	NM_177518.1
AGPAT2	NM_001080264.1
CCL2	NM_174006.2
CD14	NM_174008.1
CD163	NM_001163413.1
CD204	NM_001113240.1
CD206	XM_003586772.5
CD44	NM_174013.3
CD68	NM_001045902.1
CPT1A	NM_001304989
DGAT1	NM_174693.2
FABP4	NM_174314.2
IL10	NM_174088.1
IL6	NM_173923.2
IL8	NM_173925.2
IRAK	NM_001040555.1
IRS	XM_003585773.5
LIPE	NM_001080220.1
LIPIN1	NM_001206156.2
LPL	NM_001075120.1
MRC1	XM_003586772.5
PPARa	NM_001034036.1
RNASE6	NM_174594.2
SOCS1	XM_002697964.5
STAT1	NM_001077900.1
STAT3	NM_001012671.2
EIF3K	NM_001034489.2
RPLP0	NM_001012682.1
RPS9	NM_001101152.2